Università Politecnica delle Marche
Scuola di Dottorato di Ricerca in Scienze agrarie, alimentari e ambientali

Organo-mineral interactions from field to molecular scale

Advisor:

Prof. Costantino Vischetti

Co-advisor:

Dr. César Plaza

Ph.D. Dissertation of:

Beatrice Giannetta

XXXI edition-17º cycle

"Our challenge for the next decade is to use the best science to balance the increased demand for growing food with the consequences of climate change."

Susan Trumbore

"Sublime è quell'oggetto nella cui rappresentazione la nostra natura sensibile riconosce i propri limiti, mentre la nostra natura razionale avverte la propria superiorità, la propria libertà da ogni limite; un oggetto, dunque, contro cui soccombiamo fisicamente, ma su cui ci eleviamo moralmente, vale a dire in virtù delle idee"

Friedrich Schiller, *Del Sublime*

Abstract

Soil organic carbon (SOC) represents the largest carbon (C) stock on the Earth's surface and plays a pivotal role in regulating the global C cycle. A clear understanding of the mechanisms controlling the persistence of C in soil organic matter (SOM) across different ecosystems has never been more needed.

This thesis is focused on the chemical reactions regulating organo-mineral interactions (sorption, precipitation, aggregation), aiming to understand the effects of different environmental conditions and land uses on fundamental ecological mechanisms that control the fate of essential elements, metals, and, most importantly, the cycling and storage of C.

The investigated ecosystems included a variety of natural soils (broadleaved and coniferous forest soils, grassland soils), technosols and agricultural soils amended with biochar and organic fertilizers. Using elemental and thermal analyses, changes in the quantity and quality of physically-fractionated SOM pools characterized by different mechanisms of protection from decomposition have been examined. A common mechanism dominates SOM dynamics; microbial by-products, largely independent of ecosystem type, govern SOM accumulation in the mineral-associated organic matter.

In a second step, organo-mineral interactions in soils under different land uses, widely differing in their SOM content, were studied by a double approach: (i) a size fractionation by wet sieving after sonication, to isolate the particulate organic matter (POM, >20 μm) from the organo-mineral complex (OMC, <20 μm), and (ii) a characterization of the OMC by sequential extractions with different chemicals, each one disrupting a specific kind of bond between SOM and active mineral surfaces. The main pool of the OMC occurred by far in the final residue remaining after removing all the active mineral components causing insolubility, suggesting that the biochemical evolution from plant-derived material towards insoluble microbial forms is a relevant path for SOM stabilization.

Iron (Fe) (hydr)oxide minerals have been suggested as an important phase for the stabilization of SOC. Using state-of the-art synchrotron-based techniques, numerous studies focused on model metal (hydr)oxide systems (pure Fe (hydr)oxides) and Fe(III) complexation with different types of organic matter, including dissolved organic matter (DOM), peats, humic substances, small organic acids. Fe speciation in soils is highly dependent on environmental conditions and chemical interactions with SOM. However, it is less clear how stabilization mechanisms in natural systems (rather than model systems)

protect SOM from decomposition under different land uses. Thus, chemical interactions between soil Fe species and physically-fractionated SOM pools have been investigated.

By sorption/desorption experiments in which Fe was added to the system, the mechanisms controlling Fe(III)-mediated OC stabilization illustrated that carbohydrates are associated to Fe(III) oxides by surface complexation, possibly by an inner sphere ligand exchange mechanism. The irreversible nature of this complexation was confirmed by the reaction with Fe(III), where increasing added Fe(III) correlated to a decrease in organic C desorbed. These results demonstrated that the binding of labile SOM compounds to Fe(III) contributes to its preservation, and that the mechanisms involved (flocculation *vs*. coating) depend on the size fractions.

Moreover, the products of these batch experiments were analyzed by Fe K-edge extended X-ray absorption fine structure (EXAFS). This approach helps reveal the mechanisms by which SOM pools can control Fe(III) speciation and to elucidate how both Fe(III)-OM complexes and Fe(III) polymerization can affect SOM reactivity.

In order to provide additional information about the environmental factors that control transformation rates and products, Fe EXAFS has been applied to the fine silt/clay and fine sand fractions obtained from a variety of natural soils and agricultural soils amended with biochar alone and combined with organic fertilizers. The role of SOM amount and quality on the hindrance of Fe hydrolysis, crystallization and transformation processes has been unraveled.

Considered the research gap between model and natural systems in understanding the possible SOM stabilization mechanisms as a function of ecosystems, physical fractionation methods coupled with synchrotron-based characterization provide unique information relevant to regulation of global terrestrial SOC cycling.

Table of Contents

List of Figures

List of Tables

1. Introduction

1.1. The role of organic matter in the global C cycle

Soil organic matter (SOM) is the most intriguing feature of soils and one of the most fascinating properties of terrestrial ecosystems. It is the integrating parameter of soil fertility and stability of both natural and agricultural ecosystems, due to the important role that plays in all physical, chemical and biological processes occurring in the edaphic system (Stevenson 1994; Kaiser 2004).

The amount of SOM present in the soil is a function of input and output fluxes (Davidson and Janssens, 2006). SOM is often considered as a single, homogeneous reservoir; actually, it is a heterogeneous mixture consisting of plant, animal tissues, and microbial materials and the byproducts of microbial processes in different stages of decomposition and with different levels of complexity, having mean residence times ranging from weeks to millennia (Pulleman, 2002, Miltner et al., 2012; Paul, 2016; Lal, 2018). The heterogeneous and complex nature of SOM implies that its different fractions and constituents have a multifunctional role in soil. In brief, SOM helps to maintain soil structure by forming stable, larger aggregates that hold plant-available water, thus improving soil permeability, aeration and drainage. Relationships between the quality and quantity of SOM fractions and soil physical properties and function are often insufficient, but urgently desirable for SOM management for its agronomic, environmental or ecological services, facing major global issues, such as food security, desertification, land degradation and climate change (Schmidt et al., 2011; Plaza et al., 2018b).

The primary constituent of SOM is soil organic carbon (SOC) and the amount of organic matter (OM) stored in soils represents one of the largest reservoirs of organic carbon (OC) on a global scale (Schlesinger, 1995). Globally, soils and surface litter store 2-3 times the amount of C present in atmospheric carbon dioxide (CO_2). Soil carbon (C) reservoir estimated to 1-m depth are of 1,462-1,548 Pg, about 3 times the biotic (560 Pg) and 2 times the atmospheric (876 Pg) stocks (Lal, 2018). Consequently, changes in the size and the turnover rate of soil C pools may potentially alter the atmospheric CO_2 concentration and the global climate. Managing soils to increase their C storage capacity has been proposed as a means to reduce the rise of CO_2 concentrations in the atmosphere.

Creating a positive soil/ecosystem C budget through a smart land uses management and

the adoption of best management practices represents a crucial step in SOC sequestration. Among the ecosystems where a potential C sequestration could be feasible, the rate of SOC sequestration is 0.25-1.0 Mg C ha^{-1} $year^{-1}$ in croplands, 0.10-0.175 in pastures, 0.5-1-0 in permanent crops and urban lands (Lal, 2018). Achieving this challenging objective requires a clear and generalizable understanding, across different soils and land uses, of the primary drivers and mechanisms responsible for the buildup and long-persistence of SOM.

1.1.1. Organic C stabilization at a land use ecosystem level

The effect of climate and land use changes on the vulnerability of SOM pools is studied via the quantification of abundance and strength of organo-mineral/metal stabilization mechanisms. Soil C stock and sink capacity and, in general, soil biogeochemical cycling and productivity, are sharply affected by land use (*e.g.*, undisturbed *versus* agricultural soils subjected to aggressive human imprints) (Amundson et al., 2015). Vegetation and parent material are main drivers of soil formation (Jenny, 1941), affecting SOC storage controlling the input and decomposition and their role in SOM stocks and persistence has been investigated in different ecosystems, spanning from spruce and deciduous forests to grasses and arable soils (Guggenberger et al., 1994, 1995; Simpson et al., 2007; Clemente et al., 2011; Weismeier et al., 2012; Denef et al., 2013; Catoni et al., 2016).

The storage of SOC increases in the order cropland < forest < grassland (Martin et al., 2011; Meersmans et al., 2008). A large number of studies and meta-analyses found strong evidence for a large SOC decline 30 to 80% when forests or grasslands were converted to cropland (Guo and Gifford, 2002; Poeplau et al., 2011; Wei et al., 2014). Contrasting with these losses, land use extensification, particularly the conversion of cropland to grasslands or forests, often leads SOC increases (Post and Kwon, 2000; Schulp and Veldkamp, 2008).

Moreover, considering land uses, only few attempts to understand SOM stabilization dynamics in technosols are reported in literature (Chaudhuri et al., 2013; Rodríguez-Vila et al., 2016; Moreno-Barriga et al., 2017), pointing to the need of including these soils within other land uses, for a generalizable understanding of the characteristic of SOM pools protected by different mechanisms.

Although physical, chemical, microbial, biochemical and ecological mechanisms can be responsible for SOC stabilization, the role of recalcitrance and the molecular structure has been questioned, considering SOC an ecosystem property (Schmidt et al., 2011). A judicious management of natural and agroecosystems represent the only valid solution to

climate changes.

1.1.2. Organo-mineral interactions

SOM physiochemical stabilization mechanisms with metal phases or soil minerals range from occlusion of organics within aggregates, sorption of organics to minerals and co-precipitation of organics with dissolved metals.

The SOM is often divided into different pools based on its chemistry and/or rates of decomposition. Briefly, SOM encompasses all biologically derived organic material located within or on the surface of soil colloids. According to widely accepted concepts, mechanisms of SOM stabilization include:

- occlusion within soil aggregates (physical protection) which is due to the spatial inaccessibility for decomposers, limited microbial turnover due to soil microbiota protection from predation, reduced diffusion of enzymes, and limited O_2 diffusion; physical protection mechanisms refer to the occlusion of SOM within macroaggregates, which forms a physical barrier that limits the accessibility of decomposers and enzymes to the organic substrates and the diffusion of O_2; physical protection depends on the level of aggregation and has been shown to be much greater within microaggregates than within macroaggregates (Pulleman and Marinissen, 2004);
- intimate interaction with mineral particles (chemical protection), which leads to reduced capacity of microorganisms to decompose bound substrates and to conformational changes of organic molecules which make them unavailable for soil enzymes;
- selective preservation and formation of SOM compounds with structural rearrangements and molecular association more resistant to decomposition (biochemical protection) (Jastrow et al., 1996; Piccolo, 2001; Six et al., 2002; von Lützow et al., 2006; Schnitzer and Monreal, 2011).

The turnover of different SOM pools depends not only on its quality and biochemical recalcitrance, but also on its accessibility to decomposers. SOM associated with clay particles can be less accessible to microbial decomposition and physically protected by incorporation into soil aggregates (Oades, 1988; Christensen, 2001). SOM binds with primary mineral particles into aggregates of different size-hierarchy (Tisdall and Oades, 1982) and, in turn, stable soil aggregation may provide a mechanism for physical protection of otherwise mineralizable SOM. As Golchin et al. (1994) described in their study, fresh plant material entering the soil is colonised by microorganisms and encrusted by primary

particles through the binding action of microbial agents (*e.g.*, mucilage and polysaccharides), thus forming stable macroaggregates. With time, the fresh plant material within macroaggregates is decomposed, leaving more chemically recalcitrant plant structural material, which are coated with microbial metabolites and mineral particles to form stable microaggregates (Golchin et al., 1994).

In detail, organo-mineral associations increase the mean residence time (MRT) of SOC and numerous studies reporting that SOC content correlates well with the soil clay-size fraction content (*i.e.,* with that of particles smaller than 2 μm) (Christensen, 2001; Barré et al., 2014). Soil clay-size fractions can contain six main types of minerals: phyllosilicates (known as clay minerals), metallic oxides and hydroxides (ferrihydrite, goethite ...), primary minerals (quartz, feldspars ...), and in some soils carbonates, gypsum or short-range order alumina-silicate minerals (allophane, imogolite). The interaction between small mineral particles and OM is likely affected by the soil mineralogy due to the different specific surface areas (SSAs) and the surface charge of the various minerals in soils (Six et al., 2002; Feng et al., 2013).

Considering that the content of clay-size mineral particles is an acceptable proxy to describe the protection that these minerals can provide, means that the influence of the surface properties (surface area and surface chemistry) and that of the microstructure of these minerals on SOC dynamics needs to be further discussed. The mechanisms for C stabilization in soils are still not well understood and the ultimate potential for C stabilization in soils is unknown. Therefore, advanced techniques operating at the appropriate spatial scale are required for a better understanding of the relationship between organic compounds and minerals.

1.2. Fe as a stabilization agent in C cycle

Iron (Fe) is the major component of many soil parent materials and represents the 5.1 percent of the Earth's crust (Prietzel et al., 2007). As the most abundant transition metal on the Earth's surface, Fe plays a particularly important role in environmental biogeochemistry. Fe may be present as soluble complexes (including hydrated Fe ions), as adsorbed surface complexes, or as solids. The limited solubility of Fe(III) causes a widespread occurrence of Fe minerals in oxic environments. The oxidized form of Fe (Fe(III)) is soluble under extremely acidic conditions but Fe(III) precipitates as Fe(III) (hydr)oxides in near-neutral pH environments. An array of Fe phases, ranging from Fe(II)/Fe(III) phyllosilicates to

poorly and highly crystalline Fe(III) oxides, hydroxides, and oxyhydroxides coexists in the soil system. Ferrihydrite, goethite and lepidocrocite are some examples of common Fe minerals. These are characterized by various degrees of crystallinity and density of surface groups. Ferrihydrite is frequently referred to as an amorphous ferric mineral and is the solid Fe phases initially formed in oxic environments. They dynamically evolve in response to environmental and geochemical conditions that drive Fe precipitation and reductive dissolution, with a consequent technical difficulty in analyzing mechanisms dictating OC sequestration.

Many nutrients, trace elements, and organic compounds strongly sorb to these Fe(III) oxides. Physicochemical condition, as pH, redox potential and activity of organic ligands can influence Fe minerals distribution along a soil profile or in aggregates. Fe minerals can be subjected to sorption, coprecipitation, (de)protonation and redox reactions with both inorganic and organic constituents, thus influencing soil physiochemical conditions. In detail, Fe-organic coprecipitation mechanisms include complexation of Fe(III) by OM, precipitation of insoluble Fe-organic complexes, adsorption of OM to ferrihydrite and occlusion of OM precipitated into newly formed ferrihydrite aggregates (Kleber et al., 2015). SOM can suppress hydrolysis of Fe(III), which not only affects bioavailability of Fe, but can also have a great impact on Fe speciation in larger water bodies since the Fe(III)-SOM complexes are highly mobile in comparison with precipitated Fe(III) (hydr)oxides, which may aggregate and sediment. Since SOM strongly influences Fe speciation, it exerts a significant impact on many biogeochemical cycles. Knowledge about Fe speciation in natural systems is important for predicting and/or understanding the fate and bioavailability of Fe, nutrients, contaminants, and other elements associated with Fe.

1.3. Methods to disentangle the complexity of organo-mineral associations

1.3.1. Fractionation methods

Chemical extraction and fractionation of SOM to quantify and characterize non-humic *vs.* humic constituents have been by far the dominant approaches to investigate transformation and stabilization processes of SOM in conventionally amended soils (Senesi and Plaza, 2007; Senesi et al., 2007). More recently, driven by growing evidence that the stability of SOM may not depend on its molecular structure alone (Schmidt et al., 2011), physical

fractionation techniques have been increasingly used to capture the influence of the soil mineral matrix on SOM dynamics. However, physically fractionated OM pools still need to be better resolved especially at the molecular level to achieve a more complete understanding of the biochemical, physical, and chemical mechanisms that together control the dynamics of SOM turnover.

The diverse physical and chemical characteristics of SOM enable it to influence soil biological, physical and chemical properties, so that each SOM pool will contribute differently to the various functions identified. To ensure optimum plant productivity on mineral soils, it is not only essential that adequate levels of SOM are maintained, but also that adequate levels of the correct types of SOM are present.

Experimental works have demonstrated that physically fractionated SOM pools are more meaningful with respect of turnover than chemically fractionated SOM pools (Hassink, 1995; Christensen, 2001). The research on physical fractionation received a great contribution with Tisdall and Oades (1982). In this work three different physical soil fractions were obtained through physical fractionation, in association with three classes of SOM (persistent, transient and temporary): macroaggregates (>250 μm), microaggregates (53-250 μm), silt and clay (<53 μm). Moreover, the analysis of SOM has benefited tremendously from physical fractionation according to size and/or density (Baldock and Skjemstad, 2000). Although there is not a single fractionation procedure that is applicable to all soils and gives a complete separation of SOM with different turnover times, a combination of methods is available to obtain proximate fractions. They are supposed to disperse soils into different types of substructures, that have been designed primary (organo-mineral associates) and secondary organo-mineral compounds, *i.e.*, soil aggregates. In this simplified conception of the soil structural arrangements, primary organo-mineral associates are formed by adsorption of SOM to mineral surfaces, mainly clay minerals and iron and aluminium oxides (Kögel-Knabner, 2000). They are isolated after complete dispersion of the soil. The primary particles, in turn, are held together in larger aggregates. These secondary organo-mineral associates are obtained after limited dispersion, and consist of aggregates of smaller primary organo-mineral compounds and particulate SOM. The physical fractionation procedures as described above mostly rely on different types of ultrasonic treatments for dispersion.

The lack of standardization of isolation procedures and ultrasonic energies used for dispersion is the major concern found, with high discrepancies between different ultrasonic isolation procedures. The amount of ultrasonic energy input applied to soils has to be

calibrated and cannot be compared between different laboratories without calibration. Another problem associated with this type of fractionation is redistribution of SOM between fractions during isolation procedure.

There are also several works in literature demonstrating that physical protection of SOM depends on the level of aggregation. Some authors have proposed physical fractionation procedures that are based on an initial density separation, which yields free light SOM, and a second density separation after ultrasonic disruption, which gives light intra-aggregate SOM freed from the soil mineral matrix. The method used in this thesis is a comprehensive and innovative approach allowing to isolate functionally-different SOM fractions (Plaza et al., 2012, 2013), *i.e.*, free SOM located between aggregates (unprotected C pool), SOM occluded within both macroaggregates and microaggregates (C pool weakly and strongly protected by physical mechanisms, respectively) freed from the soil mineral matrix, and the mineral-associated SOM pool (C pool protected by chemical mechanisms).

The longest turnover times have been usually measured for the OM associated to the silt and clay-sized fractions (von Lützow et al., 2006; Basile-Doelsch et al., 2007). However, an in-depth characterization of SOM in the finest fractions must follow, because these fractions usually account for most SOM (Rovira et al., 2010). It is in the finest fractions where chemical interactions between OM and active mineral surfaces mostly occur. These interactions are of several kinds: slight electrostatic adsorptions, association to clay surfaces through metal bonding, strong adsorptions to fine silt and especially clay surfaces, or association to Fe and aluminium (Al) free forms (Kögel-Knabner et al., 2008). In order to pursuit in the understanding of SOM stabilization, we need to go beyond the simple fact of its association to mineral particles (*i.e.,* generation of the organo-mineral complex), and investigate the relevance of each kind of association between the organic and the mineral component of such a complex.

1.3.2. Syncrotron-based and spectroscopic techniques applied to natural systems

X-ray absorption spectroscopy (XAS) is based on absorption of X-rays. During data acquisition, the sample is scanned over a specific energy range, *e.g.,* ca: 6880-7800 eV for Fe K-edge. When the energy of an X-ray equals the binding energy of a core electron, then there is a sharp increase in absorption; this is called the absorption edge. The binding energy

of the core level electrons varies for the elements, and it is possible to study electrons in different shells, *e.g.,* 1s (K-edge) and 2s/2p (L-edge). The pre-edge and the edge (+ some additional 50 eV after the edge) comprise the X-ray absorption near edge structure (XANES) region which can reveal key features including oxidation state and coordination environment. The oscillating structures near and after the edge are caused by backscattered photoelectrons. The region after the edge is called the extended X-ray absorption fine-structure (EXAFS) region. The photoelectrons are ejected when the energy of the incoming X-rays is higher than the binding energy of the core electron. Excess energy is then released kinetically in the form of an ejected photoelectron. The photoelectron may then scatter on neighboring atoms and depending on the distance, number and identity to/of the backscattering atoms, the interference between ejected and backscattered photoelectrons may differ. Therefore, EXAFS analysis provides information about the identity of the neighboring atoms, coordination number (CN), as well as the distances at which they occur. XAS is element specific and could be applied to solids, liquids, and gaseous samples. In contrast to techniques such as X-ray diffraction, XAS can be applied to both amorphous and crystalline samples, making it a very versatile technique.

Attempts to describe Fe speciation in natural systems frequently involve simplified model systems consisting of pure minerals or systems with natural organic matter (NOM). These model systems represent the two pools of Fe previously described by Karlsson and Persson (2012). They suggested the existence of Fe(III)-NOM complexes and polymeric Fe(III) (hydr)oxides. The partitioning between solid and soluble Fe is largely controlled by total Fe concentration, pH and NOM. NOM can suppress hydrolysis of Fe(III), which not only affects bioavailability of Fe, but can also have a great impact on Fe speciation in larger water bodies since the Fe(III)-NOM complexes are highly mobile in comparison with precipitated Fe(III) (hydr)oxides, which may aggregate and sediment.

Moreover, Fourier-transform infrared spectroscopy (FTIR) spectroscopy is used to gain information about bonding modes of organic functional groups by examining variations in their vibrational response to the absorption of infrared radiation.

It represents a spectroscopic probe complementary to EXAFS and its application to mineral-organo associations (MOAs) is useful in understanding the detailed mechanisms of bonding between OM and mineral surfaces as a function of pH and ionic strength. Since the reactivity of the organic molecules is modified by the mineral surface, the structure and reactivity of surfaces can also be modified by the organics, a full conceptual model of the interactions requires giving equal weight to studying both reaction partners.

1.4. Objectives

Recent studies stressed the importance of physical protection and mineral association as one of the most significant mechanisms responsible for SOM persistence on the long term (Kögel-Knabner et al., 2008; Marschner et al., 2008; Kleber, 2010; Schmidt et al., 2011; Lehmann and Kleber, 2015). Moreover, considering the central role played by organo-mineral interactions in C sequestration process, further studies are needed to directly investigate the specific binding mechanisms found in organo-mineral associations. Physical fractionation methods need to be combined with high-resolution spectroscopic techniques, and molecular characterization, in order to identify both SOM types and mineral components.

A clear understanding of the mechanisms controlling the persistence of C in SOM, and how they are affected by land use will provide information relevant to global terrestrial SOC cycling. Achieving this challenge requires a clear and generalizable understanding, across different soils and land uses, of the mechanisms responsible for the buildup and persistence of SOM.

Fe (hydr)oxide minerals have been suggested as an important phase for the stabilization of SOC (Lalonde et al., 2012; Chen et al., 2014, 2017). Being soil systems characterized by a broad of Fe mineral species (in ubiquitous clay minerals, as Fe-SOM complexes and polymeric Fe (hydr)oxydes, the possibility to quantify species fractions using advanced spectroscopic techniques can constitute a rapid and nondestructive alternative to sequential extraction methods. Although the relationship between Fe and C abundance is well-known, limited research has been performed to clarify the complex interdependence between Fe phases and amount and chemical composition of SOM (Hall et al., 2018) at an atomic scale using advanced spectroscopic techniques.

Considering the knowledge and research gap between model and natural systems in understanding the possible SOM stabilization mechanisms as a function of ecosystems, synchrotron-based characterization of representative fractionated soils from these systems will help to unravel the processes implicated in soil C sequestration.

Using state-of-the-art synchrotron-based techniques, numerous studies focused on model metal (hydr)oxide systems (pure Fe (hydr)oxides) and Fe(III) complexation with different types of OM including dissolved organic matter (DOM), peats, humic substances, small organic acids. Fe speciation in soils is highly dependent on environmental conditions and chemical interactions with SOM. However, it is less clear how stabilization mechanisms

in natural systems (rather than model systems) protect SOM from decomposition under different land uses. For this reason, this research was focused on understanding C reactions in different SOM pools. Regarding Fe association with NOM, it found its main application to characterize Fe(III) in organic soils under different pH ranges and with varying natural Fe content (*i.e.,* Gustafsson et al., 2007, Karlsson et al., 2008). Moreover, the application of Fe EXAFS in structurally and elementally complex soils and fractions can represent a challenging step, although this method should allow Fe speciation in soil particles and aggregates (Prietzel et al., 2007).

Considering these motivations, the main objective of this research was to investigate the physical and chemical interactions occurring between SOM and mineral (clay, oxides) colloids, in order to provide some new insights about the SOM stabilization and persistence. Studies about SOM physical and chemical stabilization mechanisms under a variety of land uses (*i.e.,* coniferous and broadleaved forest soils, grassland soils, technosols and agricultural soils) were performed. In detail, five coniferous forests (CF), five broadleaved forests (BF), five grassland soils (GL) and five technosols (TS) were sampled between May and June 2016 in different sites of the Marche Region (Italy). Four agricultural soil samples (AG), whose main characteristics were examined elsewhere (Plaza et al., 2016), were also included in this study.

In detail, this research had multiple specific objectives:

a) SOM distribution among primary fractions characterized by different mechanisms of protection, in a variety of soils under different land uses, and investigate if these SOM fractions thermal fingerprint (and, therefore, their "inherent recalcitrance") is dependent on different land uses and SOM source (Chapter 2).

b) Quantifying the different modes through which organic compounds are bound to the mineral matrix, using size fractionation by wet sieving after sonication, followed by a sequential extraction with chemical reagents (Chapter 3).

c) To comparatively investigate the effects of the heavy liquid, sodium polytungstate (SPT) *versus* sodium iodide (NaI), on the distribution of organic C and total N in free, intra-aggregate, and mineral-associated pools separated by common density-based procedures, determining the effects of washing the heavy mineral-associated SOM fraction on its organic C and total N contents; and evaluating the influence of soil properties on the potential effects of the heavy liquid and washing. (Appendix A).

d) To study, by coprecipitation and desorption experiments, how stabilization mechanisms promoted by Fe(III)in natural systems (rather than model systems) protect from decomposition differently stabilized SOM pools under different land uses (Chapter 4).

e) To use synchrotron-based techniques for a direct assessment of coprecipitation reactions, clarifying how Fe-SOM complexes and precipitated Fe (hydr)oxide form in natural environments and in soils with different pedoclimatic conditions and land uses (Chapter 5).

f) To test the effect of different amendments (*i.e.,* biochar, compost, and the simultaneous application of both) and of size fractions (*i.e.,* fine sand and fine silt plus clay) on the quantity and composition of Fe minerals (Chapter 6).

References

Amundson, R., Berhe, A.A., Hopmans, J.W., Olson, C., Sztein, A.E., Sparks, D.L., 2015. Soil and human security in the 21st century. Science 348, 647-653.

Barré, P., Fernandez-Ugalde, O., Virto, I., Velde, B., Chenu, C., 2014. Impact of phyllosilicate mineralogy on organic carbon stabilization in soils: incomplete knowlwdge and exciting prospects. Geoderma 235-236, 382-395.

Basile-Doelsch, I., Brun, T., Borschneck, D., Masion, A., Marol, C., Balesdent, J., 2009. Effect of landuse on organic matter stabilized in organomineral complexes: A study combining density fractionation, mineralogy and δ13C. Geoderma 151, 77–86.

Catoni, M., D'Amico, M.E., Zanini, E., Bonifacio, E., 2016. Effect of pedogenic processes and formation factors on organic matter stabilization in alpine forest soils. Geoderma 263, 151-160.

Chaudhuri, S., McDonald, L.M., Pena-Yewtukhiw, E.M., Skousen, J., Roy, M., 2013. Chemically stabilized soil organic carbon fractions in a reclaimed minesoil chronosequence: implications for soil carbon sequestration. Environmental Earth Sciences 70,1689-1698.

Chen C., Kukkadapu, R.K., Lazareva, O., Sparks, D.L., 2017. Solid-Phase Fe Speciation along the Vertical Redox Gradients in Floodplains using XAS and Mössbauer Spectroscopies. Environmental Science and Technology 51, 7903−7912.

Chen, C., Dynes, J.J., Wang, J., Sparks, D.L., 2014. Properties of Fe-organic matter associations via coprecipitation versus adsorption. Environmental Science and Technology 48, 13751-13759.

Christensen, B.T., 2001. Physical fractionation of soil structural and functional complexity in organic matter turnover. European Journal of Soil Science 52, 345-353

Clemente, J.S., Simpson, A.J., Simpson, M.J., 2011. Association of specific organic matter compounds in size fractions of soils under different environmental controls. Organic Geochemistry 42, 1169-1180.

Davidson, E.A., Janssens, I.A., 2006. Temperature sensitivity of soil carbon decomposition and feedbacks to climate change. Nature 144, 165-173.

Denef, K., Del Galdo, I., Venturi, A., Cotrufo, M.F., 2013. Assessment of Soil C and N Stocks and Fractions across 11 European Soils under Varying Land Uses. Open Journal of Soil Science 3, 297-313.

Feng, W., Plante, A.F., Six, J., 2013. Improving estimates of maximal organic carbon

stabilization by fine soil particles. Biogeochemistry 112, 81-93.

Golchin, A., Oades, J.M., Skjemstad, J.O., Clarke, P., 1994. Study of free and occluded particulate organic matter in soils by solid state 13C CP/MAS NMR spectroscopy and scanning electron microscopy. Australian Journal of Soil Research 32, 285-309.

Guggenberger, G., Christensen, B.T., Zech, W., 1994. Land-use effects on the composition of organic matter in particle-size separates of soil: I. Lignin and carbohydrate signature. European Journal of Soil Science 45, 449-458.

Guggenberger, G., Zech, W., Thomas, R.J., 1995. Lignin and carbohydrate alteration in particle-size separates of an Oxisol under tropical pastures following native savanna. Soil Biology & Biochemistry 27, 1629-1638.

Guo, L.B., Gifford, R.M., 2002. Soil carbon stocks and land use change: a meta analysis. Global Change Biology 8, 345-360.

Gustafsson, J.P., Persson, I., Kleja, D.B., Van Schaik, J.W.J., 2007. Binding of iron(III) to organic soils: EXAFS spectroscopy and chemical equilibrium modeling. Environmental. Science and Technology 41, 1232–1237.

Hall, S.J., Berhe, A.A., 2018. Thompson, A. Order from disorder: do soil organic matter composition and turnover co-vary with iron phase crystallinity? Biogeochemistry, 4.

Hassink, J., 1995. Density fractions of soil macroorganic matter and microbial biomass as predictors of C and N mineralization. Soil Biology and Biochemistry 27, 1099-1108.

Jastrow, J.D., Boutton, T.W., Miller, R.M., 1996. Carbon dynamics of aggregate-associated Organic Matter estimated by Carbon-13 natural abundance. Soil Science Society of America Journal 60, 801-807.

Jenny, H., 1941. Factors of soil formation. New York & London, McGraw-Hill Book Company.

Kaiser, J., 2004. Wounding earth's fragile skin. Science 304, 1616-1618.

Karlsson, T., Persson, P., 2012. Complexes with organic matter suppress hydrolysis and precipitation of Fe(III). Chemical Geology, 322-323, 19-27.

Karlsson, T., Persson, P., Skyllberg, U., Mörth, C.-M., Giesler, R., 2008. Characterization of Iron(III) in Organic Soils Using Extended X-ray Absorption Fine Structure Spectroscopy. Environmental Science and Technology 42, 5449–5454.

Kleber, M., 2010. What is recalcitrance soil organic matter? Environmental Chemistry 7, 320-332.

Kleber, M., Eusterhues, K., Keiluweit, M., Mikutta, C., Mikutta, R., Nico, P.S., 2015. Mineral-organic associations: formation, properties, and relevance in soil environments.

Advances in Agronomy 130, 1-140.

Kögel-Knabner, I., 2000. Analytical approaches for characterizing soil organic matter. Organic Geochemistry 31, 609-625.

Kögel-Knabner, I., Guggenberger, G., Kleber, M., Kandeler, E., Kalbitz, K., Scheu, S., Eusterhues, K., Leiweber, P., 2008. Organo-mineral associations in temperate soils: integrating biology, mineralogy, and organic matter chemistry. Journal of Plant Nutrition and Soil Science 171, 61-82.

Kölbl A., Kögel-Knabner I. 2004. Content and composition of free and occluded particulate organic matter in a differently textured Cambisolas revealed by Solid-State 13C-NMR spectroscopy. Journal of Plant Nutrition of Soil Science 167, 45-53.

Lal, R., 2018. Digging deeper: A holistic perspective of factors affecting soil organic carbon sequestration in agroecosystems. Global Change Biology 24, 3285-3301.

Lalonde, K., Mucci, A., Ouellet, A., Gélinas, Y., 2012. Preservation of organic matter in sediments promoted by iron. Nature 483, 198–200.

Lehmann, J., Kleber, M., 2015. The contentious nature of soil organic matter. Nature 528, 60-80.

Marschner, B., Brodowski, S., Dreves, A., Gleixner, G., Gude, A., Grootes, P.M., Hamer, U., Heim, A., Jandl, G., Ji, R., Kaiser, K., Kalbitz, K., Kramer, C., Leinweber, P., Rethemeyer, J., Schäffer, A., Schmidt, M.W.I., Schwark, L., Wiesenberg, G.L.B., 2008. How relevant is recalcitrance for the stabilization of organic matter in soils? Journal of Plant Nutrition and Soil Science 171, 91-110.

Martin, M.P., et al., 2011. Spatial distribution of soil organic carbon stocks in France. Biogeosciences 8, 1053-1065.

Meersmans, J., De Ridder, F., Canters, F., De Baets, S., Van Molle, M., 2008. A multiple regression approach to assess the spatial distribution of soil organic carbon (SOC) at the regional scale (Flanders, Belgium). Geoderma 143, 1-13.

Miltner, A., Bombach, P., Schmidt-Brücken, B., Kästner, M., 2012. SOM genesis: microbial biomass as a significant source. Biogeochemistry 111, 41-55.

Moreno-Barriga F, Díaz V, Acosta JA, Muñoz MÁ, Faz Á, Zornoza R (2017) Organic matter dynamics, soil aggregation and microbial biomass and activity in Technosols created with metalliferous mine residues, biochar and marble waste. Geoderma 301:19-29.

Oades, J.M., 1988. The retention of organic matter in soils. Biogeochemistry 5, 35-70.

Paul, E.A., 2016. The nature and dynamics of soil organic matter: plant inputs, microbial

transformations, and organic matter stabilization. Soil Biology and Biochemistry 98, 109-126.

Piccolo, A., 2001. The supramolecular structure of humic substances. Soil Science 166, 810-832.

Plaza C., Fernández, J.M., Pereira E.I.P., Polo A., 2012. A comprehensive method for fractionating soil organic matter not protected and protected from decomposition by physical and chemical mechanisms. CLEAN-Soil Air Water 40, 134-139.

Plaza, C., Courtier-Murias, D., Fernández, J.M., Polo, A., Simpson, A.J., 2013. Physical, chemical, and biochemical mechanisms of soil organic matter stabilization under conservation tillage systems: a central role for microbes and microbial by-products in C sequestration. Soil Biology and Biochemistry 57, 124–134.

Plaza, C., Courtier-Murias, D., Fernández, J.M., Polo, A., Simpson, A.J., 2013. Physical, chemical, and biochemical mechanisms of soil organic matter stabilization under conservation tillage systems: A central role for microbes and microbial by-products in C sequestration. Soil Biology and Biochemistry 57, 124-134.

Plaza, C., Giannetta, B., Fernández, J.M., López-de-Sá, E.G., Polo, A., Gascó, G., Méndez, A., Zaccone, C., 2016. Response of different soil organic matter pools to biochar and organic fertilizers. Agrciulture. Ecosystems and Environment 225, 150–159.

Plaza, C., Zaccone, C., Sawicka, K., Méndez, A.M., Tarquis, A., Gascó, G., Heuvelink, G.B.M., Schuur, E.A.G., Maestre, F.T., 2018b. Soil resources and element stocks in drylands to face global issues. Scientific Reports 8, 13788.

Poeplau, C., et al., 2011. Temporal dynamics of soil organic carbon after land-use change in the temperate zone - carbon response functions as a model approach. Global Change Biology 17, 2415-2427.

Post, W.M., Kwon, K.C., 2000. Soil carbon sequestration and land-use change: processes and potential. Global Change Biology 6, 317-327.

Prietzel, J., Thieme, J., Eusterhues, K., Eichert, D., 2007. Iron speciation in soils and soil aggregates by synchrotron-based X-ray microspectroscopy (XANES, μ-XANES). European Journal of Soil Science 58, 1027–1041.

Pulleman, M.M., 2002. Interactions between soil organic matter dynamics and soil structure as affected by farm management. The Netherlands: Thesis Wageningen University. 146 p.

Pulleman, M.M., Marinissen, J.C.Y., 2004. Physical protection of mineralizable C in aggregates from long-term pasture and arable soil. Geoderma 120, 273-282.

Rodríguez-Vila, A., Asensio, V., Forján, R., Covelo, E.F., 2016. Carbon fractionation in a mine soil amended with compost and biochar and vegetated with Brassica juncea L. Journal of Geochemical Exploration 169,137-143.

Schlesinger, W.H., 1995. An overview of the C cycle. In: Soils and Global Change (eds R. Lal, J. Kimble, J. Levin, B.A. Stewart), Lewis Publishers, Boca Raton, FL, 9-26.

Schmidt, M.W.I., Torn, M.S., Abiven, S., Dittmar, T., Guggenberger, G., Janssens I.A., Kleber, M., Kögel-Knabner, I., Lehmann, J., Manning, D.A.C., Nannipieri, P., Rasse, D.P., Weiner, S., Trumbore, S.E., 2011. Persistence of soil organic matter as an ecosystem property. Nature 478, 49-56.

Schnitzer, M., Monreal, C.M. 2011. Chapter tree - Quo Vadis soil organic matter research? A biological link to the chemistry of humification. In: Sparks, D.L. editor. Advances in Agronomy. Academic Press. 143-217 p.

Schulp, C.J.E., Veldkamp, A., 2008. Long-term landscape - land use interactions as explaining factor for soil organic matter variability in Dutch agricultural landscapes. Geoderma 146, 457-465.

Senesi, N., Plaza C., 2007. Role of humification processes in recycling organic wastes of various natureand sources as soil amendments. CLEAN: Soil Air Water 35, 26-41.

Senesi, N., Plaza, C., Brunetti G., Polo A., 2007. A comparative survey of recent results on humic-like fractions in organic amendments and effect of native soil humic substances. Soil Biology and Biochemistry 39,1244-1262.

Simpson, A.J., Simpson, M.J., Smith, E., Kelleher, B.P., 2007. Microbially derived inputs to soil organic matter: are current estimates too low? Environmental Science and Technology 41, 8070-8076.

Six, J., Conant, R.T., Paul, E.A., Paustian K., 2002. Stabilization mechanisms of soil organic matter: implications for C-saturation of soils. Plant and Soil 241, 155-176.

Sohi S.P., Mahieu N., Arah J.R.M., Powlson D.S., Madari B., Gaunt J.L. 2001. A procedure for isolating soil organic matter fractions suitable for modeling. Soil Science Society of America Journal 65, 1121-1128.

Stevenson, F.J., 1994. Humus Chemistry: Genesis, Composition, Reactions. New York, NY: Wiley- Interscience. 512 p.

Tisdall, J.M., Oades, J.M., 1982. Organic matter and water -stable aggregates in soils. Journal of Soil Science 33, 141-163.

Von Lützow, M., Kögel-Knabner, I., Ekschmitt, K., Matzner, E., Guggenberger, G., Marschner, B., Flessa, H., 2006. Stabilization of organic matter in temperate soils:

mechanisms and their relevance under different soil conditions-a review. European Journal of Soil Science 57, 426-445.

Wei, X., Shao, M., Gale, W., Li, L., 2014. Global pattern of soil carbon losses due to the conversion of forests to agricultural land. Scientific Reports 4, 4062.

Wiesmeier, M., Spörlein, P., Geuß, U., Hangen, E., Haug, S., Reischl, A., Schilling, B., von Lützow, M., Kögel-Knabner I., 2012. Soil organic carbon stocks in southeast Germany (Bavaria) as affected by land use, soil type and sampling depth. Global Change Biology 18, 2233-2245.

2. Distribution and thermal stability of physically and chemically protected organic matter fractions in soils cross different ecosystems

(Giannetta, B., Plaza, C., Vischetti, C., Cotrufo, M.F., Zaccone, C., 2018. Biology and Fertility of Soils *54, 671-681)*

Abstract

Accrual of carbon (C) and nitrogen (N) in soil is a significant and realizable management option to mitigate climate change; thus, a clear understanding of the mechanisms controlling the persistence of C and N in soil organic matter (SOM) across different ecosystems has never been more needed. Here, we investigated SOM distribution between physically and chemically stabilized fractions in soils from a variety of ecosystems (*i.e.,* coniferous and broadleaved forest soils, grassland soils, technosols, and agricultural soils). Using elemental and thermal analyses, we examined changes in the quantity and quality of physically fractionated SOM pools characterized by different mechanisms of protection from decomposition. Independently of the ecosystem type, most of the organic C and total N were found in the mineral-associated SOM pool, known to be protected mainly by chemical mechanisms. Indexes of thermal stability and C/N ratio of this heavy SOM fraction were lower (especially in agricultural soils) compared to light SOM fractions found free or occluded in aggregates, and suggested a marked presence of inherently labile compounds. Our results confirm that the association of labile organic molecules with soil minerals is a major stabilization mechanism of SOM, and demonstrate that this is a generalizable finding occurring across different mineral soils and ecosystems.

2.1. Introduction

Soils represent the largest terrestrial organic carbon (C) reservoir (Jobbágy and Jackson 2000) with the potential to accrue enough additional C to halt the increase in atmospheric CO_2, as proposed by the recently launched 4 per mil initiative (Chabbi et al. 2017). Achieving this challenging objective requires a clear and generalizable understanding, across different soils and ecosystem types, of the mechanisms responsible for the buildup and persistence of soil organic matter (SOM).

The notion of recalcitrance as a key factor controlling SOM stability has been questioned during the last decades. More specifically, biochemical recalcitrance, an inherent molecular property of resistance to decomposition, has been usually associated with humified SOM or complex aromatic structures, such as lignin, cutin, and pyrogenic organic matter (Stevenson 1994; Sollins et al. 1996; Krull et al. 2003). However, recent works presented evidence against this concept and stressed the importance of physical protection and mineral association as one of the most significant mechanisms responsible for SOM persistence on the long term in mineral soils (Kögel-Knabner et al. 2008; Marschner et al. 2008; Kleber 2010; Schmidt et al. 2011; Dungait et al. 2012; Lehmann and Kleber 2015). Thus, SOM in particulate form, such as the light fraction (LF), is generally prone to fast decomposition unless physically protected in soil aggregates. Aggregates are composite secondary SOM structures (Christensen 2001) and therefore are not clearly distinguished by turnover times (Poeplau et al. 2018). Yet the organic matter protected within aggregates, and in particular within microaggregates (< 250 μm), is considered among the most persistent form of SOM (Six et al. 2000), although the longest turnover times are assigned to heavy, fine organic matter associated with minerals (von Lützow et al. 2006; Poeplau et al. 2018).

Microbial biomass is considered to be turned over much faster than plant residues (Kästner 2000), thus suggesting that the molecular imprint of SOM by molecules and fragments derived from microbial biomass is probably much more important than previously considered (Miltner et al. 2012). When microorganisms degrade plant residues, they use low molecular- weight compounds from the plant biomass to build their own biomass, and the majority of this material is then incorporated into non-living SOM (Kindler et al. 2006; Miltner et al. 2012, and ref. therein). Cotrufo et al. (2013) hypothesized that labile plant constituents are the main source of microbial by-products, and these in turn are the main precursors of SOM stabilized by the soil matrix, through the formation of physically or chemically realized organo-mineral associations (Vogel et al. 2014). For example, McGill and Paul (1976) and Turchenek and Oades (1979) observed that microbial cell wall materials were a major component of SOM accumulated in the coarse clay fraction, while Ladd et al. (1996, and ref. therein) reported that clay-size fractions were enriched of organic nitrogen (N) of microbial origin. Moreover, particle size fractionation after ultrasonic dispersion and subsequent dating showed young radiocarbon ages of the fine clay-associated organic C, indicating that this organic C was more active than that associated with the coarse clay (Anderson and Paul 1984).

Several other studies have suggested that thermally labile, microbial-derived materials and easily metabolizable compounds (*e.g.,* carbohydrates and amino acids) are dominant inthe mineral-associated organic matter (MAOM) pool, whereas the LF free (LF_free) or occluded within macro- (LF_M) and especially microaggregates (LF_m) are believed to be mainly of plant origin and characterized by an increasing degree of persistence (Kleber et al. 2011; Hatton et al. 2012; Keiluweit et al. 2012; Plaza et al. 2013, 2016). Given its chemical nature, the MAOM pool is also the richest in N among SOM pools, i.e., with the lowest C/N (Christensen 2001), pointing to the need of a better understanding of N distribution in the soil. In fact, despite the importance of N sequestration to ecosystem functioning, to date there has not been a comprehensive examination of the implications of SOM stabilization in ecologically meaningful fractions for long-term N sequestration in different soils and ecosystems (Bingham and Cotrufo 2016).

Soil C stock and sink capacity were recently described as ecosystem properties (Schmidt et al. 2011), sharply affected by several factors including land use (*e.g.,* undisturbed versus agricultural soils subjected to aggressive human imprints) (Amundson et al. 2015). Besides climate, vegetation and parent material are main drivers of soil formation (Jenny 1941), and their role in SOM stocks and persistence has been investigated in different ecosystems, spanning from spruce and deciduous forests to grasses and arable soils (Guggenberger et al. 1994, 1995; Leifeld and Kögel-Knabner 2005; Simpson et al. 2007; Clemente et al. 2011; Wiesmeier et al. 2012; Denef et al. 2013; Catoni et al. 2016). Despite all these research efforts, an accurate assessment of soil organic C and total N distribution across pools with different mechanisms of physical and chemical protection is still needed to improve our knowledge of the response of soil properties, including C stocks, to land management and/or changes in land use and cover (Guo and Gifford 2002; Wiesmeier et al. 2012; Wei et al. 2017). This would help better understand if SOM persistence, and therefore the distribution among fractions, is an ecosystem property rather than the main common denominator across different soils and ecosystems. In addition, technosols, *i.e.,* man-made soils, are widely distributed throughout the world as they are found where human activity has led to the construction of artificial soils, sealing of natural soil, or extraction of material normallynot affected by surface processes (*e.g.,* mines, dumps, oil spills, earth movements, coal fly ash deposits) (IUSS Working Group WRB 2006). Many technosols, in particular those in dumps, are originated covering man-made substrate with a layer of natural soil in order to permit revegetation. Although technosols have been recently included in soil classifications, often associated with other soil groups in a complex pattern, here they are considered as a

modern form of soil in anthropogenic ecosystems. Only few attempts to understand SOM stabilization dynamics in technosols are reported in literature (Chaudhuri et al. 2013; Rodríguez-Vila et al. 2016; Moreno- Barriga et al. 2017), pointing to the need of including them when contrasting different ecosystems, for a generalizable understanding of the characteristic of SOM pools protected by different mechanisms of stabilization.

In this study, we measured (1) the organic C and total N contents of bulk soils from five different ecosystems, including coniferous and broadleaved forests, grasslands, and technosols in anthropogenic systems and agroecosystems, and (2) their distribution in ecologically meaningful SOMfractions, namely a light fraction (LF < 1.85 g cm−3), found free or occluded in macro- (2000–250 μm), and microaggregates (> 250 μm), thus stabilized by either inherent recalcitrance and/or an increasing strength of physical protection, and the heavy (>1.85 g cm^{-3}) MAOM fraction, mostly stabilized by chemical association to minerals. The main objectives of this work were to (a) elucidate SOM distribution among primary fractions characterized by different mechanisms of protection, in a variety of soils from different ecosystems, and (b) investigate if the thermal fingerprint of SOM fractions (possibly mirroring their inherent recalcitrance) is an ecosystem property or can be generalized across different soils and ecosystems. While the different mechanisms of SOM stabilization have been investigated since a long time, only few works focused on their generalizability across different mineral soils and ecosystems.

Finally, including technosols in this study would improve our knowledge of the kind and rate of stabilization mechanisms taking place during the initial phases of pedogenetic processes (Zaccone et al. 2014), being technosols young soils that develop in technogenic man-made parent materials.

2.2. Materials and methods

2.2.1. Study sites and soil sampling

Five ecosystem types, known to have contrasting climatic and edaphic conditions, were considered in this study. To achieve a broad range of soils, we collected samples from four to five different sites for each of the five ecosystem types. Five coniferous forests (CF), five broadleaved forests (BF), five grassland soils (GL), and five technosols (TS) were sampled between May and June 2016 in different sites of the Marche Region (Italy). The coniferous forests consisted mainly of Pinus nigra woodlands occurring between 350 and 1400 m a.s.l.,

the broadleaved woodlands in stands of different species (*e.g., Fagus sylvatica*, *Ostrya carpinifolia*, *Quercus pubescens*) growing between 320 and 1300 m a.s.l., and the grassland soils in meadows and pastures characterized bymeso- to xerophilous species (e.g., *Bromus erectus*) and *Medicago sativa* and developing between 890 and 1700 m a.s.l. The technosols included two open-pit mines, filled and then reclaimed with *Helianthus annuus* (since 2010) and with *Triticum* (since 2000), respectively, two dumps, reclaimed in 2000 and in 2011, respectively, and a site of disposal of compost and other non-hazardous waste materials (all TS sites < 300 m a.s.l.). Mean annual temperature of sampling sites ranged from 7.3 and 15.0 °C, whereas mean annual precipitation ranged between 810 and 1570 mm. Four agricultural soils (AG) cropped with barley and collected in Arganda del Rey (Madrid, Spain) were also included in this study; these soils were located at 530 m a.s.l. and characterized by a mean annual precipitation of about 440 mm and a mean annual temperature of 14 °C (Plaza et al. 2016). More details about the sampling sites are reported in Table 2.1.

At each location, 3 to 10 soil samples were collected randomly from several points, depending on site surface and homogeneity, using a soil auger and mixed to obtain a composite sample. The depth of sampling varied from 10 to 25 cm, and corresponded to the top soil horizon (Table 2.1).

2.2.2. Bulk soil characterization

Prior to analysis, soil samples were gently crushed and passed through a 2-mm sieve. Soil reaction (pH) was measured on suspensions of 1:2.5 sample:water and sample:KCl (1 M) (Thomas 1996), whereas electrical conductivity (EC) was measured on water extracts obtained at a sample-to-water ratio of 1:5 (Rhoades 1996). All soils were also analyzed for texture by the pipette method, whereas C and N elemental composition was determined as described in section below. Soil properties averaged by ecosystem type are reported in Table 2.2.

2.2.3. Physical fractionation of SOM

The physical fractionation of SOM was carried out using the method described by Plaza et al. (2013), with the aim to separate the heavy MAOM fraction from the light particulate

organic matter (LF) fraction, and distinguish the latter into free LF and LF occluded in aggregates of different sizes. Specifically, we separated four fractions: (a) free LF, located between aggregates (unprotected C pool; LF_free); (b) LF occluded within macroaggregates (SOM pool weakly protected by physical mechanisms; LF_M); (c) LF occluded within microaggregates (SOM pool strongly protected by physical mechanisms; LF_m); and (d) a heavy SOM pool associated with the minerals (highly persistent mostly chemically protected; MAOM). This method is based on the densimetric procedure by Golchin et al. (1994) and Sohi et al. (2001) for the fractionation of free and occluded LF, and on the method by Six et al. (2000, 2002) for the breakup of macroaggregates preserving microaggregates. First, 148 g of NaI at a density of 1.85 g mL^{-1} were added to 10 g of 2-mm sieved, air-dried soil in a 100-mL polycarbonate centrifuge tube. Free LF was separated from the heavy fraction by density flotation in the NaI solution and subsequent suction, filtration through a glass fiber filter, and scrupulous washings with deionized water. Macroaggregates remaining in the heavy fraction were broken up, using the microaggregate isolator device designed by Six et al. (2000, 2002), into stable microaggregates, MAOM and LF_M, which were collected after a second density separation. Another density separation after an ultrasonic disruption at an energy input of 1500 J g^{-1} allowed the LF_m isolation from the MAOM. The recovered LF_free, LF_M, LF_m, and MAOM fractions were oven-dried at 60 °C, weighed, and ground with a ball mill for further analyses.

2.2.4. Organic C and total N analysis

Organic C and total N contents of both bulk soil samples and SOM fractions were determined by dry combustion using a Thermo Flash 2000 NC Soil Analyzer. For organic C determination, the whole soil samples and mineral-associated SOM fractions were subject to acid fumigation before analysis to remove carbonates (Harris et al. 2001). All analyses were carried out in triplicate.

2.2.5. Thermogravimetric analysis

Thermogravimetric analysis (TGA) was carried out on all SOM fractions using a Perkin Elmer Thermogravimetric Analyzer TGA 4000. An aliquot (ca. 20 mg) of each sample was placed in a ceramic crucible and heated from 30 to 850 °C at 20 °C min^{-1} under an oxidizing atmosphere of air at a flow rate of 30 mL min^{-1}. Two indexes of overall thermal stability

were calculated: T50 (°C), representing the temperature at which 50% of the SOM mass is lost, and the thermal stability index (H), here defined as the ratio between the weight losses within 400–550 and 250–400 °C temperature ranges. These thermal indexes are reported on a moisture- and ash-free basis.

2.2.6. Data analysis

Data were analyzed with the Kruskal-Wallis test, with ecosystem type or SOM fraction as factors. The Dunn's test at the 0.05 level was used for multiple mean comparison. All statistical analyses were performed using R, version 3.4.1 (R Core Team 2017).

2.3. Results and discussion

2.3.1 Organic C and total N concentration in soils

Organic C and total N contents of examined soils span a broad range, as expected (Table 2.2). Grassland soils show the highest average values for both organic C (86 g kg^{-1}) and total N (9 g kg^{-1}), whereas the lowest are found in AG (11.8 g C $kg^{-1}$and 1.1 g N kg^{-1}) (Table 2.2). In particular, both the organic C and total N average contents rank as GL > CF > BF > TS > AG (Table 2.2), thus mirroring the link between organic C and total N dynamics. As a result, C/N across land uses vary in the order CF>BF~AG>GL~TS (Table 2.2).

The conversion of grassland or forest soils to agricultural soils is well known to cause reductions of SOM contents, due to decreased inputs of plant-derived materials and increased decomposition rates through tillage (Matson et al. 1997; Post and Kwon 2000). Wiesmeier et al. (2012) reported that grassland and forest ecosystems showed ca. 40% higher SOC content compared to croplands depending on soil properties. Some studies have found that SOM increases with the clay content (*e.g.,* Magdoff and Weil 2004). However, in our work, neither organic C nor total N are significantly correlated with clay or clay + silt contents.

2.3.2. Organic C and total N distribution

Independently of ecosystem, most soil organic C is accumulated in the MAOM fraction, with average concentrations ranging from 6.1 g kg^{-1} in AG up to 49.3 g kg^{-1} in GL (Table

2.3). While the MAOM pool size is highly different between ecosystems, reflecting differences in total SOC stocks, the percentage of organic C accumulated in MAOM ranges between 44% for CF and 64% for TS, although these values are not significantly different from each other (Table 3). This finding suggests that different ecosystems, and thus SOM inputs do not significantly affect this pool. Nonetheless, it is particularly noteworthy that TS exhibit the highest percentage of organic C in the MAOM fraction (Table 2.3), in spite of their low SOM contents (Table 2.2).

The second most abundant organic C pool is LF_free, with mean concentration values ranging from 1.8 g kg^{-1} in AG up to 26.2 g kg^{-1} in GL (Table 2.3). The LF occluded in macro- (LF_M) and microaggregates (LF_m) represent comparatively minor soil C pools, with no significant differences between them. The highest percentage of C stabilized in LF_free is found in CF (38%), followed by GL (30%), BF (25%), TS (19%), and AG (16%) (Table 2.3). An opposite trend is observed for the LF_M and LF_m fractions, where the relatively highest C accumulation in LF_M and LF_m is found in AG (8.8 and 9.0%, respectively) and TS (8.2 and 11.5%, respectively) (Table 2.3).

Total N relative distribution among SOM fractions also follows the trend MAOM> LF_free ≥LF_m~LF_M (Table 2.3). In particular, up to 5.3 and 2.1 g N kg^{-1} of soil are found in the MAOM and LF_free pools of GL, respectively, whereas contents detected in the LF_M and LF_m fractions are much lower (always ≤0.2 g kg^{-1}). As for organic C, no significant differences among ecosystem types are found for the percentage of N stabilized in the MAOM (58% in CF to 69% in AG) and LF_free pools (9% in AG to 23% in GL). On the opposite, significant differences among land uses are observed in the LF_M and LF_m fractions, with relatively highest N accumulation in LF_M and LF_m found in AG (6 and 7%, respectively) and TS (4 and 8%, respectively) (Table 2.3).

Plant litter decomposability is thought to strongly affect the accumulation of organic matter in soils within different ecosystems. According to Castellano et al. (2015), recalcitrant C compounds, characteristic of coniferous needles, may confer to litter a low decomposition rate and microbial use efficiency (Kooch et al. 2012; Cotrufo et al. 2013), leading to a relatively higher C accumulation in LF_free. We thus hypothesized a different distribution of organic C and total N among SOM pools under forests and grasses as compared to the more heavily managed agricultural soils and technosols, due to different mineralization rates of surface litter and roots. In agricultural soils and especially in technosols, an increased aggregate disruption and aeration might have been expected to lead to SOM accumulation mainly in MAOM. As a whole, however, our results indicate that,

although soils under different ecosystems exhibit markedly different total organic C and N contents, the relative distribution of organic C and total N among SOM pools is pretty consistent, in spite of their different vulnerability to anthropogenic management.

2.3.3. C/N ratio of SOM fractions

Organic matter in bulk soils shows C/N ratios ranging from 9 in TS to 14 in CF (Table 2.2). The C/N ratios of all the fractions are significantly higher for CF that for the other ecosystems (Table 2.4), consistently with the relatively lower decomposition degree of SOM in CF compared to the other ecosystems (Castellano et al. 2015). On the opposite, AG soils generally show the lowest C/N ratios for all fractions, with the exception of LF_free (Table 2.4).

For all ecosystems, the C/N ratio of the MAOM pool is significantly lower than those of the other fractions (Table 2.4). A number of studies have reported a decrease in the C/N ratio from coarse to fine fractions suggesting both an increase of the decomposition degree of the SOM and a relative accumulation of microbial-derived materials (Kiem et al. 2002; Chen et al. 2014). Thus, the low C/N ratio of MAOM fractions is probably indicative of a depletion in lignin and plant-derived components and of an enrichment in materials of prevailing microbial origin (Paul and Clark 1989; Golchin et al. 1994; Guggenberger et al. 1995; Kögel-Knabner et al. 2008; Cotrufo et al. 2013; Courtier- Murias et al. 2013; Plaza et al. 2013, 2016). In a parallel work, Zaccone et al. (2018) reported the MAOM fraction to be characterized by high total DNA contents and very low C/N ratios at the same time. According to the Microbial Efficiency Mineral Stabilization framework, high quality N litter may lead to greater accumulation of microbial products and concomitant formation of MAOM in soils with a high soil matrix capacity (Cotrufo et al. 2013). Moreno-Barriga et al. (2017), studying the evolution of C and N pools following the addition of different materials to mine tailings, concluded that easily available organic compounds triggered microbial growth during the first days of incubation and enhanced the formation of aggregates. This phenomenon probably occurred in TS, mirroring the early stage of pedogenic evolution, and suggested that aggregate stability may increase following a decrease of labile C forms, being then either used as fuel by microorganisms or stabilized by association with mineral particles. The accumulation of organic C and total N in the MAOM fraction confirms that these pools are less susceptible to further mineralization and offer a longer-term storage (Courtier-Murias et al. 2013).

The low C/N of MAOM recorded for all the land uses is also consistent with the adsorption of nitrogenous compounds (*e.g.,* amino acids, amino sugars, proteins, cell wall constituents), possibly of microbial origin (Stevenson 1994; Ladd et al. 1996; Knicker 2004; Sollins et al. 2006; Nannipieri and Paul, 2009), onto mineral surfaces.

Clay minerals strongly affect the stabilization of organic N directly (Ladd et al. 1996; Nielsen et al. 2006; Sollins et al. 2006) and through the formation of aggregate-protected particulate and non-particulate organic matter (*e.g.,* Yoo and Wander 2008), although most of these studies have been carried out in vitro using purified clay particles and purified proteins (Nannipieri and Paul 2009). The large majority (> 80%) of this organic N was found to be in the form of amides, in peptides and proteins of microbial origin (DiCosty et al. 2003; Simpson et al. 2007). By contrast, the high C/N ratio found in LF_free and occluded LF fractions suggests a relatively high occurrence of slightly-to-partially decomposed plant materials in these fractions (Christensen 2001; Rasmussen et al. 2005).

2.3.4. Thermal stability of SOM pools

Being the thermal stability of any material related to its chemistry and surface properties, the thermal stability of SOM may serve as a proxy for biogeochemical stability and provide insight about the energy of interaction between SOM and soil minerals (Plante et al. 2009). At the same time, thermal analysis does not provide information at molecular level and is affected by several operational parameters, including arrangement and type of sample holder, packing density and grain size of sample, heating rate, initial sample mass, crucible material, and furnace atmosphere (Plante et al. 2009 and ref. therein).

Thermogravimetric (TG) curves of all SOM fractions generally show two main steps of weight loss in the range of temperature 100–550 °C. The first, between 250 and 350 °C, is associated with more easily oxidizable compounds, including polysaccharides (e.g., cellulosic material) and aliphatic structures (Plante et al. 2009). The second, between 350 and 550 °C, due to the thermal degradation of recalcitrant, aromatic structures including lignin and non-hydrolyzable compounds (Schnitzer and Hoffman 1966; Lopez-Capel et al. 2005) (Fig. 2.1). Therefore, the ratio between these two weight losses, here defined as H, as well as the T50 value, i.e., the temperature at which 50%of the SOM mass is lost, can be used to describe SOM stability and/or recalcitrance (*e.g.,* Rovira and Vallejo 2000). In fact, within each fraction, the H and T50 values found are significantly correlated to each other ($R = 0.666–0.981$, $p \leq 0.001$, $n = 24$), independently of the land use.

Differences in H and T50 among pools in CF, BF, and GL soils are not statistically significant, while in TS and AG the LF_free and MAOM fractions usually showed lower values of both thermal indexes compared to LF_M and LF_m (Table 2.4), being these latter fractions the result of residual plant material depleted in labile compounds. Technosols generally show the highest values of both H and T50 in all SOM fractions (Table 2.4). Moreover, TS is the only soil group in which a significant correlation was found between C/N ratios and both H ($R = 0.463$, $p = 0.040$, $n = 20$) and T50 ($R = 0.630$, $p = 0.003$, $n = 20$).

When the weight loss (%) between 150 and 250 °C is considered (Fig. 2.2), the occurrence of more labile molecules in the MAOM fraction becomes evident, in accordance with the low C/N ratios characterizing this pool. In fact, the percentage of weight loss in the MAOM fraction is always higher than in the other fractions (Fig. 2.2). The interaction of labile molecules (e.g., sugars, amino acids, proteins) with mineral surfaces has been reported to be a key mechanism for the long-term stabilization of organic C (Lynch and Cotnoir 1956; Baldock and Skjemstad 2000; Kiem and Kögel-Knabner 2003), allowing low-molecular-weight metabolic compounds to be stored in relatively passive pools for up to millennia (Paustian et al. 1992). For example, Schulten and Leinweber (1999), analyzing the Ah horizon of a Gleysol, found pyrolysis-field ionization mass spectra and thermograms of the light SOM fraction (< 2.0 g cm^{-3}) to be similar to those of primary plant materials while the corresponding heavy fraction (> 2.0 g cm^{-3}) characterized by larger abundances of carbohydrates, lignin decomposition products, N-containing compounds, and peptides.

Finally, the comparatively small variation in both H and T50 values characterizing the MAOM fraction (< 16% and < 3%, respectively) regardless of the ecosystem from which it is derived (Table 2.4) is indicative of new molecules resulting from a common microbial transformation process rather than highly degraded litter inputs. This finding is in agreement with Kallenbach et al. (2016) who provided evidences about the influence of substrate–microbe interactions on the synthesis of novel SOM constituents that become stabilized by clay minerals.

2.4. Conclusions

We provide evidence that physical fractionation coupled with thermal analysis and C/N ratios allow obtaining new insights about SOM sequestration in mineral soils across different ecosystems. We found that MAOM, followed by the LF_free fraction, represents the major pool of both organic C (44–64% of the whole SOC stock) and total N (58–70%

of the whole N stock) independently of ecosystem type. The lowest C/N ratio and the highest percentage of weight loss recorded between 150 and 250 °C, both characterizing the MAOM fraction, indicate that this pool is comparatively richer in labile compounds.

At the same time, the very small variability observed for these proxies (H, T50, and C/N), independently of land use and SOM inputs, is indicative of new molecules resulting from a common microbial transformation process. Technosols store two third of the whole organic C and TN in the MAOM fraction, and show the highest values of both H and T50 in all SOM fractions. Moreover, the significant correlation found between C/N ratio and both H and T50 exclusively in TS underlines how, in these young, man-made soils, mechanisms of SOM sequestration probably mirror processes taking place during the first phases of the pedogenetic processes. As a whole, different ecosystems may differ in terms of absolute SOM content among fractions; however, our results suggest a common mechanism of SOM dynamics, where plant input and their inherent recalcitrance control LF quality and distribution, while microbial by-products, largely independent of ecosystem type, govern SOM accumulation in the MAOM fraction. Further studies are needed to better understand not only the mechanisms of SOM stabilization at the molecular lever by state-of the-art tools currently available but also the implications of the molecular mechanisms at larger scales and the ecological functions of the different SOM pools in the environment.

References

Amundson, R., Berhe, A.A., Hopmans, J.W., Olson, C., Sztein, A.E., Sparks, D.L., 2015. Soil and human security in the 21st century. Science 348, 647-653.

Anderson, D.W., Paul, E.A., 1984. Organo-mineral complexes and their study by radiocarbon dating. Soil Science Society of America Journal 48, 298-301.

Baldock, J.A., Skjemstad, J.O., 2000. Role of the soil matrix and minerals in protecting natural organic materials against biological attack. Organic Geochemistry 31, 697-710.

Bingham, A.H., Cotrufo, M.F., 2016. Organic nitrogen storage in mineral soil: implications for policy and management. Science of the Total Environment 551-552, 116-126.

Castellano, M.J., Mueller, K.E., Olk, D.C., Sawyer, J.E., Six, J., 2015. Integrating Plant Litter Quality, Soil Organic Matter Stabilization and the Carbon Saturation Concept. Global Change Biology 21, 3200-3209.

Catoni, M., D'Amico, M.E., Zanini, E., Bonifacio, E., 2016. Effect of pedogenic processes and formation factors on organic matter stabilization in alpine forest soils. Geoderma

263, 151-160.

Chabbi, A., Lehmann, J., Ciais, P., Loescher, H., Cotrufo, M.F., Don, A., SanClements, M., Schipper, L., Six, J., Smith, P., Rumpel, C., 2017. Aligning agriculture and climate policy. Nature Climate Change 7, 307-309.

Chaudhuri, S., McDonald, L.M., Pena-Yewtukhiw, E.M., Skousen, J., Roy, M., 2013. Chemically stabilized soil organic carbon fractions in a reclaimed minesoil chronosequence: implications for soil carbon sequestration. Environmental Earth Sciences 70,1689-1698.

Chen, C., Dynes, J.J., Wang, J., Sparks, D.L., 2014. Properties of Fe-organic matter associations via coprecipitation versus adsorption. Environmental Science and Technology 48, 13751-13759.

Christensen, B.T., 2001. Physical fractionation of soil and structural and functional complexity in organic matter turnover. European Journal of Soil Science 52, 345-353.

Clemente, J.S., Simpson, A.J., Simpson, M.J., 2011. Association of specific organic matter compounds in size fractions of soils under different environmental controls. Organic Geochemistry 42, 1169-1180.

Cotrufo, M.F., Wallenstein, M.D., Boot, C.M., Denef, K., Paul, E., 2013. The Microbial Efficiency-Matrix Stabilization (MEMS) framework integrates plant litter decomposition with soil organic matter stabilization: do labile plant inputs form stable soil organic matter? Global Change Biology 19, 988-995.

Courtier-Murias, D., Simpson, A.J., Marzadori, C., Baldoni, G., Ciavatta, C., Fernández, J.M., López-de-Sá, E.G., Plaza, C., 2013. Unraveling the long-term stabilization mechanisms of organic materials in soils by physical fractionation and NMR spectroscopy. Agricultue Ecosystems and Environment 171, 9-18.

Denef, K., Del Galdo, I., Venturi, A., Cotrufo, M.F., 2013. Assessment of Soil C and N Stocks and Fractions across 11 European Soils under Varying Land Uses. Open Journal of Soil Science 3, 297-313.

DiCosty, RJ, Weliky DP, Anderson SJ, Paul EA (2003) 15N-CPMAS nuclear magnetic resonance spectroscopy and biological stability of soil organic nitrogen in whole soil and particle-size fractions. Org Geochem 34:1635-1650.

Dungait, J.A.J., Hopkins, D.W., Gregory, A.S., Whitmore, A.P., 2012. Soil organic matter turnover is governed by accessibility not recalcitrance. Global Change Biology 18, 1781-1796.

Golchin, A., Oades, J.M., Skjemstad, J.O., Clarke, P., 1994. Study of Free and Occluded

Particulate Organic Matter in Soils by Solid state 13C CP/MAS NMR Spectroscopy and Scanning Electron Microscopy. Australian Journal of Soil Research 32, 285–309.

Guggenberger, G., Christensen, B.T., Zech, W., 1994. Land-use effects on the composition of organic matter in particle-size separates of soil: I. Lignin and carbohydrate signature. European Journal of Soil Science 45, 449-458.

Guggenberger, G., Zech, W., Thomas, R.J., 1995. Lignin and carbohydrate alteration in particle-size separates of an Oxisol under tropical pastures following native savanna. Soil Biol and Biochemistry 27, 1629–1638.

Guo, L.B., Gifford, R.M., 2002. Soil carbon stocks and land use change: a meta analysis. Global Chang Biology 8, 345-360.

Harris, D., Horwath, W.R., van Kessel, C., 2001. Acid fumigation of soils to remove carbonates prior to total organic carbon or carbon-13 isotopic analysis. Soil Science Society of America Journal 65, 1853–1856.

Hatton, P.-J., Kleber, M., Zeller, B., Moni, C., Plante, A.F., Townsend, K., Gelhaye, L., Lajtha, K., Derrien, D., 2012. Transfer of litter-derived N to soil mineral–organic associations: Evidence from decadal ^{15}N tracer experiments. Organic Geochemistry 42, 1489-1501.

IUSS Working Group WRB, 2006. World Reference Base for Soil Resources 2006: a Framework for International Classification, Correlation and Communication, 2nd edition. Food and Agriculture Organization of the United Nations, Rome.

Jenny, H., 1941. Factors of soil formation. New York & London, McGraw-Hill Book Company.

Jobbágy, E.G., Jackson, R.B., 2000. The vertical distribution of soil organic carbon and its relation to climate and vegetation. Ecological Applications 10, 423-436.

Kallenbach, C.M., Frey, S.D., Grandy, A.S., 2016. Direct evidence for microbial-derived soil organic matter formation and its ecophysiological controls. Nature Communications 7, 13630.

Kästner, M., 2000. "Humification" process or formation of refractory soil organic matter. In: Klein J (ed) Environmental processes II, vol 11b. Biotechnology, 2nd edn. Wiley-VCH, Weinheim, pp 89-125.

Keiluweit, M., Bougoure, J.J., Zeglin, L., Myrold, D.D., Weber, P.K., Pett-Ridge, J., Kleber, M., Nico, P.S., 2012. Nano-scale investigation of the association of microbial nitrogen residues with iron (hydr)oxides in a forest soil O-horizon. Geochimica et Cosmochimica Acta 95, 213-226.

Kiem, R., Knicker, H., Kögel-Knabner, I., 2002. Refractory organic carbon in particle-size fractions of arable soils I: distribution of refractory carbon between the size fractions. Organic Geochemistry 33, 1638-1697.

Kiem, R., Kögel-Knabner, I., 2003. Contribution of lignin and polysaccharides to the refractory carbon pool in C-depleted arable soils. Soil Biology and Biochemistry 35, 101-118.

Kindler, R., Miltner, A., Richnow, H.-H., Kästner, M., 2006. Fate of gram-negative bacterial biomass in soil-mineralization and contribution to SOM. Soil Biology and Biochemistry 38, 2860-2870.

Kleber, M., 2010. What is recalcitrance soil organic matter? Environmental Chemistry 7, 320-332.

Kleber, M., Nico, P.S., Plante, A., Filley, T., Kramer, M., Swanston, C., Sollins, P., 2011. Old and stable soil organic matter is not necessarily chemically recalcitrant: implication for modeling concepts and temperature sensitivity. Global Change Biology 17, 1097-1107.

Knicker, H., 2004. Stabilization of N-compounds in soil and organic-matter-rich sediments– what is the difference? Marine Chemistry 92, 167-195.

Kögel-Knabner, I., Guggenberger, G., Kleber, M., Kandeler, E., Kalbitz, K., Scheu, S., Eusterhues, K., Leiweber, P., 2008. Organo-mineral associations in temperate soils: integrating biology, mineralogy, and organic matter chemistry. Journal of Plant Nutrition and Soil Science 171, 61-82.

Kooch, Y., Hosseini, S.M., Zaccone, C., Jalilvand, H., Hojjati, S.M., 2012. Soil organic carbon sequestration as affected by afforestation: the Darab Kola forest (north of Iran) case study. Journal of Environmental Monitoring 14, 2438-2446.

Krull, E.S., Baldock, J.A., Skjemstad, J.O., 2003. Importance of mechanisms and processes of the stabilisation of soil organic matter for modelling carbon turnover. Functional Plant Biology 30, 207–222.

Ladd, J.N., Foster, R.C., Nannipieri, P., Oades, J.M., 1996. Soil structure and biological activity. In: Stotzky G, Bollag J-M (eds) Soil Biochemistry, vol 9. Marcel Dekker, New York, pp 23-78.

Lehmann, J., Kleber, M., 2015. The contentious nature of soil organic matter. Nature 528, 60-80.

Leifeld, J., Kögel-Knabner, I., 2005. Soil organic matter as early indicators for carbon stock changes under different land-use? Geoderma 124,143-155.

Lopez-Capel, E., Sohi, S.P., Gaunt, J.L., Manning, D.A.C., 2005. Use of thermogravimetry-differential scanning calorimetry to characterize modelable soil organic matter fractions. Soil Science Society of America Journal 69, 136-140.

Lynch, D.L., Cotnoir, L.J., 1956. The influence of clay minerals on the breakdown of certain organic substances. Soil Science Society of America Journal 20, 367–370.

Magdoff, F., Weil, R.R., 2004. Soil Organic Matter in Sustainable Agriculture. CRC Press, Boca Raton, FL.

Marschner, B., Brodowski, S., Dreves, A., Gleixner, G., Gude, A., Grootes, P.M., Hamer, U., Heim, A., Jandl, G., Ji, R., Kaiser, K., Kalbitz, K., Kramer, C., Leinweber, P., Rethemeyer, J., Schäffer, A., Schmidt, M.W.I., Schwark, L., Wiesenberg, G.L.B., 2008. How relevant is recalcitrance for the stabilization of organic matter in soils? Journal of Plant Nutrition and Soil Science 171, 91-110.

Matson, P.A., Parton, W.J., Power, A.G., Swift, M.J., 1997. Agricultural intensification and ecosystem properties. Science 277, 504-509.

McGill, W.B., Paul, E.A., 1976. Fractionation of soil and 15N nitrogen to separate the organic and clay interactions of immobilized N. Canadian J Soil Science 56, 203-212.

Miltner, A., Bombach, P., Schmidt-Brücken, B., Kästner, M., 2012. SOM genesis: microbial biomass as a significant source. Biogeochemistry 111, 41-55.

Moreno-Barriga, F., Díaz, V., Acosta, J.A., Muñoz, M.Á., Faz, Á., Zornoza, R., 2017. Organic matter dynamics, soil aggregation and microbial biomass and activity in Technosols created with metalliferous mine residues, biochar and marble waste. Geoderma 301, 19-29.

Nannipieri, P., Paul, E.A., 2009. The chemical and functional characterization of soil N and its biotic components. Soil Biology and Biochemistry 41, 2357-2369.

Nielsen, K.M., Calamai, L., Pietramellara, G., 2006. Stabilization of extracellular DNA by transient binding to various soil surfaces. In: Nannipieri P, Smalla K (eds) Nucleic acids and proteins in soil (soil biology). vol. 8. Springer, Berlin Germany, pp 141-158.

Paul, E.A., Clark, F.E., 1989. Soil Microbiology and Biochemistry, Academic Press, San Diego.

Paustian, K., Parton., W.J., Persson, J., 1992. Modeling soil organic-matter in organic-amended and nitrogen-fertilized long-term plots. Soil Science Society of America Journal 56, 476-488.

Plante, A.F., Fernández, J.M., Leifeld, J., 2009. Application of thermal analysis techniques in soil science. Geoderma 153, 1–10.

Plaza, C., Courtier-Murias, D., Fernández, J.M., Polo, A., Simpson, A.J., 2013. Physical, chemical, and biochemical mechanisms of soil organic matter stabilization under conservation tillage systems: A central role for microbes and microbial by-products in C sequestration. Soil Biology and Biochemistry 57, 124–134.

Plaza, C., Giannetta, B., Fernández, J.M., López-de-Sá, E.G., Polo, A., Gascó, G., Méndez, A., Zaccone, C., 2016. Response of different soil organic matter pools to biochar and organic fertilizers. Agricultura, Ecosystems and Environment 225,150-159.

Poeplau C, et al., 2018. Isolating soil organic carbon fractions with varying turnover rates in temperate agricultural soils – A comprehensive method comparison. Soil Biology and Biochemistry 125, 10-26.

Post, W.M., Kwon, K.C., 2000. Soil carbon sequestration and land-use change: processes and potential. Global Change Biology 6, 317-327.

R Core Team, 2017. R: A language and environment for statistical computing. R Foundation for Statistical Computing, Vienna, Austria. URL: https://www.R-project.org/.

Rasmussen, C., Torn, M.S., Southard, R.J., 2005. Mineral Assemblage and Aggregates Control Carbon Dynamics in a California Conifer Forest. Soil Science Society of America Journal 69, 1711–1721.

Rhoades, J.D., 1996. Salinity: Electrical Conductivity and Total Dissolved Solids. In: Sparks DL (ed) Methods of Soil Analysis, Part 3-Chemical methods. SSSA Book Series 5.3 SSSA-ASA, Madison, WI, pp 417-435.

Rodríguez-Vila, A., Asensio, V., Forján, R., Covelo, E.F., 2016. Carbon fractionation in a mine soil amended with compost and biochar and vegetated with Brassica juncea L. Journal of Geochemical Exploration 169,137-143.

Rovira, P., Vallejo, R.V., 2000. Examination of thermal and acid hydrolysis procedures in characterization of soil organic matter. Communications in Soil Science and Plant Analysis 31, 81-100.

Schmidt, M.W.I., Torn, M.S., Abiven, S., Dittmar, T., Guggenberger, G., Janssens, I.A., Kleber, M., Kögel-Knabner, I., Lehmann, J., Manning, D.A.C., Nannipieri, P., Rasse, D.P., Weiner, S., Trumbore, S.E., 2011. Persistence of soil organic matter as an ecosystem property. Nature 478, 49-56.

Schnitzer, M., Hoffman, J., 1966. A thermogravimetric approach to the classification of organic soils. Soil Science Society of America Journal 30, 63–66.

Schulten, H.-R., Leinweber, P., 1999. Thermal stability and composition of mineral-bound organic matter in density fractions of soil. European Journal of Soil Science 50, 237-

248.

Simpson, A.J., Simpson, M.J., Smith, E., Kelleher, B.P., 2007. Microbially derived inputs to soil organic matter: are current estimates too low? Environmental Science and Technology 41, 8070-8076.

Six, J., Callewaert, P., Lenders, S., De Gryze, S., Morris, S.J., Gregorich, E.G., Paul, E.A., Paustian, K., 2002. Measuring and Understanding Carbon Storage in Afforested Soils by Physical Fractionation. Soil Science Society of America Journal 66, 1981-1987.

Six, J., Elliott, E.T., Paustian, K., 2000. Soil macroaggregate turnover and microaggregate formation: a mechanism for C sequestration under no-tillage agriculture. Soil Biology and Biochemistry 32, 2099-2103.

Sohi, S.P., Mahieu, N., Arah, J.R.M., Powlson, D.S., Madari, B., Gaunt, J.L., 2001. A procedure for Isolating Soil Organic Matter Fractions Suitable for Modeling. Soil Science Society of America Journal 65, 1121–1128.

Soil Survey Staff, 2014. Keys to Soil Taxonomy, 12th ed. USDA-Natural Resources Conservation Service, Washington, DC.

Sollins, P., Homann, P., Caldwell, B.A., 1996. Stabilization and destabilization of soil organic matter: mechanisms and controls. Geoderma 74, 65–105.

Sollins, P., Swanston, C., Kleber, M., Filley, T., Kramer, M., Crow, S., Caldwell, B.A., Lajtha, K., Bowden, R., 2006. Organic C and N stabilization in a forest soil: Evidence from sequential density fractionation. Soil Biology and Biochemistry 38, 3313-3324.

Stevenson, F.J., 1994. Humus Chemistry. Genesis, Composition, Reactions, 2nd edition. Wiley & Sons, New York.

Thomas, G.W., 1996. Soil pH and Soil Acidity. In: Sparks DL (ed) Methods of Soil Analysis, Part 3-Chemical methods. SSSA Book Series 5.3 SSSA-ASA, Madison, WI, pp 475-490.

Turchenek, L.W., Oades, J.M., 1979. Fractionation of organomineral complexes by sedimentation and density techniques. Geoderma 21, 311-343.

Vogel, C., Mueller, C.W., Höschen, C., Buegger, F., Heister, K., Schulz, S., Schloter, M., Kögel-Knabner, I., 2014. Submicron structures provide preferential spots for carbon and nitrogen sequestration in soils. Nature Communications 5, 2947.

von Lützow, M., Kögel-Knabner, I., Ekschmitt, K., Matzner, E., Guggenberger, G., Marschner, B., Flessa, H., 2006. Stabilization of organic matter in temperate soils: mechanisms and their relevance under different soil conditions-a review. European Journal of Soil Science 57, 426-445.

Wei, X., Wang, X., Ma, T., Huang, L., Pu, Q., Hao, M., Zhang, X., 2017. Distribution and mineralization of organic carbon and nitrogen in forest soils of the southern Tibetan Plateau. Catena 156, 298-304.

Wiesmeier, M., Spörlein, P., Geuß, U., Hangen, E., Haug, S., Reischl, A., Schilling, B., von Lützow, M., Kögel-Knabner, I., 2012. Soil organic carbon stocks in southeast Germany (Bavaria) as affected by land use, soil type and sampling depth. Global Change Biology 18, 2233-2245.

Yoo, G., Wander, M.M., 2008. Tillage effects on aggregate turnover and sequestration of particulate and humified soil organic carbon. Soil Science Society of America Journal 72, 670–676.

Zaccone, C., Quideau, S., Sauer, D., 2014. Soils and paleosols as archives of natural and anthropogenic environmental changes. European Journal of Soil Science 65, 403-405.

Zaccone, C., Beneduce, L., Lotti, C., Martino, G., Plaza, C., 2018. DNA occurrence in organic matter fractions isolated from amended, agricultural soils. Applied Soil Ecology 130, 134-142.

Table 2.1 Site details, sampling depth and classification of the coniferous forest (CF), broadleaved forest (BF), grassland (GL), technosols (TS) and agricultural (AG) soils included in this study.

Soil	Site	Coordinates		Depth (cm)	Soil Taxonomy †	Land use
CF 1	Frontignano (Castelsantangelo sul Nera, Italy)	13°09'52" E	42°54'44" N	0-20	Lithic Hapludoll	Reforestation with *Pinus nigra* (dominant species); age: 50 years
CF 2	Chiaserna (Cantiano, Italy)	12°40'08" E	43°27'34" N	0-20	Lithic Rendoll	Reforestation with *Pinus nigra* (dominant species); age: 50-60 years
CF 3	Foresta Cesane (Fossombrone, Italy)	12°47'47" E	43°41'41" N	0-10	Typic Udorthent	Reforestation with *Pinus nigra* (dominant species); age: 50-60 years
CF 4	Colle San Marco (Ascoli Piceno, Italy)	13°34'30" E	42°49'16" N	0-10	-	Reforestation with *Pinus nigra* (dominant species); age: 40 years
CF 5	San Lorenzo (San Severino Marche, Italy)	13°14'03" E	43°18'05" N	0-25	Lithic Rendoll	Reforestation with *Pinus nigra* (dominant species); age: 60 years
BF 1	Castelluccio (Castelsantangelo sul Nera, Italy)	13°10'27" E	42°52'59" N	0-20	Typic Haplustept	*Fagus sylvatica* stand (age: 50 years)
BF 2	Monte Catria (Cantiano, Italy)	12°41'57" E	43°27'51" N	0-10	Typic Udorthent	*Fagus sylvatica* coppiced stand (age: 50 years)
BF 3	Monte Montiego (Piobbico, Italy)	12°33'29" E	43°36'31" N	0-20	Entic Rendoll	Coppiced stand of *Quercus pubescens* with *Ostrya carpinifolia* (age: 20 years)
BF 4	Pozza (Acquasanta Terme, Italy)	13°24'53" E	42°44'21" N	0-15	-	*Castanea sativa* coppiced stand (age: 50 years)
BF 5	Frontale (Apiro, Italy)	13°05'56" E	43°21'01" N	0-20	Lithic Xerorthent	Orno-Ostryetum associations with *Quercus pubescens* (age: 30-40)

GL 1	Cacciano (Fabriano, Italy)	12°51'29" E	43°17'04" N	0-20	Lithic Haploxeroll	Natural or semi-natural meadows and pastures
GL 2	Forcatura (Fiuminata, Italy)	12°53'49" E	43°08'51" N	0-15	Typic Haplustoll	Natural or semi-natural meadows and pastures
GL 3	Acquosi (Gagliole, Italy)	13°05'09" E	43°15'49" N	0-10	Lithic Haploxeroll	Natural or semi-natural meadows and pastures
GL 4	Cacciano (Fabriano, Italy)	12°51'24" E	43°17'04" N	0-20	Lithic Haploxeroll	Natural or semi-natural meadows and pastures
GL 5	Monte Amandola (Sarnano, Italy)	13°16'13" E	42°58'20" N	0-20	Lithic Ustorthent	Natural or semi-natural meadows and pastures
TS 1	Botontano (Treia, Italy)	13°18'52" E	43°21'45" N	0-25	-	Open-pit mine filled and then reclaimed with *Helianthus annuus* (since 2010)
TS 2	Botontano (Treia, Italy)	13°18'55" E	43°21'39" N	0-25	-	Open-pit mine filled and then reclaimed with *Triticum* (since 2000)
TS 3	Asola (Potenza Picena, Italy)	13°14'49" E	43°13'34" N	0-20	-	Dump reclaimed in 2000
TS 4	Pollenza Scalo (Tolentino, Italy)	13°37'52" E	43°20'49" N	0-20	Typic or Oxyacquic Calcixerept	Site of disposal of compost and other non-hazardous waste materials
TS 5	Santa Lucia (Tolentino, Italy)	13°23'22" E	43°14'16" N	0-20	-	Dump reclaimed in 2011
AG 1	Arganda del Rey (Madrid, Spain)	3°29'06" W	40°18'58" N	0-15	Xerofluvent	Unamended, agricultural soil, planted with *Hordeum vulgare*
AG 2	Arganda del Rey (Madrid, Spain)	3°29'06" W	40°18'58" N	0-15	Xerofluvent	Unamended, agricultural soil, planted with *Hordeum vulgare*
AG 3	Arganda del Rey (Madrid, Spain)	3°29'06" W	40°18'58" N	0-15	Xerofluvent	Unamended, agricultural soil, planted with *Hordeum vulgare*

AG 4	Arganda del Rey (Madrid, Spain)	3°29'06" W	40°18'58" N	0-15	Xerofluvent	Unamended, agricultural soil, planted with *Hordeum vulgare*

† Soil Survey Staff (2014)

Table 2.2 Main physical and chemical properties (mean ± st. dev.) of coniferous forest soils (CF), broadleaved forest soils (BF), grassland soils (GL), technosols (TS) and agricultural soils (AG).

Land use	EC ($\mu S \cdot cm^{-1}$)	Reaction (pH units)	Sand ($g \cdot kg^{-1}$)	Silt ($g \cdot kg^{-1}$)	Clay ($g \cdot kg^{-1}$)	Organic C ($g \cdot kg^{-1}$)	Total N ($g \cdot kg^{-1}$)	C/N
CF	67±28 a	8.1±0.2 bc	455±87 ac	279±114 bc	246±91 ac	52.3±19.0 ac	3.7±1.0 ab	13.9±2.8 a
BF	61±29 a	8.1±0.3 ab	490±181 ac	328±91 abc	182±141 ab	35.9±28.2 ab	3.3±2.4 a	11.2±3.3 ab
GL	101±37 a	6.2±0.9 c	642±65 c	234±37 b	124±53 b	86.0±7.6 c	9.0±1.0 b	9.6±1.4 bc
TS	131±144 a	8.4±0.1 ab	187±69 b	445±33 ac	367±71 c	12.6±9.3 b	1.5±1.1 a	8.6±0.5 c
AG	103±16 a	8.4±0.1 a	339±23 ab	471±25 a	190±8 abc	11.8±0.6 ab	1.1±0.1 a	10.7±0.1 abc

Within the same column, different lowercase letters indicate statistically significant differences among land uses according to the Dunn's test at the 0.05 level.

Table 2.3 Organic C and N concentrations (mean ± st. dev.) of free Light fraction (LF_free), intra-macroaggregate light fraction (LF_M), intra-microaggregate light fraction (LF_m) and mineral-associated organic matter (MAOM) pools of coniferous forest soils (CF), broadleaved forest soils (BF), grassland soils (GL), technosols (TS) and agricultural soils (AG). Values expressed as % of total are reported in italic.

		Organic C				**Total N**			
		LF_free	**LF_M**	**LF_m**	**MAOM**	**LF_free**	**LF_M**	**LF_m**	**MAOM**
CF	($g \cdot kg_{soil}^{-1}$)	19.0±7.0 b A	2.9±1.5 a B	3.8±1.8 b B	22.6±7.2 ac A	0.76±0.26 bc AB	0.12±0.06 a C	0.20±0.11 a AC	2.15±0.60 ab B
	(%)	*38.4±12.8 b A*	*5.6±1.4 ab B*	*7.4±2.4 ab B*	*44.2±7.1 a A*	*20.6±6.5 a AB*	*3.2±1.1 ab C*	*5.5±2.4 abc AC*	*58.1±3.1 a B*
BF	($g \cdot kg_{soil}^{-1}$)	10.8±12.9 ab AB	2.4±2.1 ab A	2.6±1.8 ab A	17.4±7.8 ab B	0.58±0.83 ab AB	0.13±0.15 a A	0.16±0.13 a A	1.89±0.95 a B
	(%)	*24.6±10.6 ab AB*	*6.6±2.1 a C*	*7.8±3.0 ab AC*	*57.7±19.7 ab B*	*13.0±8.9 a AB*	*3.6±1.7 a C*	*4.6±1.3 bc AC*	*63.3±17.1 a B*
GL	($g \cdot kg_{soil}^{-1}$)	26.2±14.7 b AB	2.0±0.6 ab C	4.0±0.9 b AC	49.3±9.1 c B	2.10±1.18 c AB	0.12±0.03 a C	0.24±0.05 a AC	5.29±1.09 b B
	(%)	*30.3±16.1 ab AB*	*2.4±0.8 b C*	*4.7±1.1 b AC*	*57.8±12.1 ab B*	*23.3±11.9 a AB*	*1.3±0.4 b C*	*2.8±0.8 b AC*	*58.5±9.5 a B*
TS	($g \cdot kg_{soil}^{-1}$)	2.6±2.9 a AB	1.1±1.0 a A	1.8±2.2 a A	7.1±4.4 b B	0.20±0.26 a A	0.07±0.08 a A	0.15±0.22 a A	0.84±0.52 a B
	(%)	*18.6±16.6 a AB*	*8.2±1.8 a A*	*11.5±5.0 a A*	*63.7±18.4 b B*	*11.6±13.9 a A*	*3.9±1.6 a A*	*7.7±4.7 ac A*	*63.7±15.3 a B*
AG	($g \cdot kg_{soil}^{-1}$)	1.8±0.2 a AB	1.0±0.1 a A	1.1±0.1 a A	6.1±0.6 ab B	0.10±0.01 a AB	0.06±0.01 a C	0.08±0.01 a AC	0.77±0.15 a B
	(%)	*15.6±1.1 a AB*	*8.8±1.1 a C*	*9.0±1.1 a AC*	*51.5±2.8 ab B*	*8.7±0.9 a AB*	*5.7±0.9 a C*	*7.4±1.0 a AC*	*69.3±11.2 a B*

Within the same column, different lowercase letters indicate statistically significant differences according to the Dunn's test at the 0.05 level. Within the same row (land use), different uppercase letters indicate statistically significant differences according to the Dunn's test at the 0.05 level.

Table 2.4 Thermal stability index (*H*), T_{50} and C/N ratio values (mean ± st. dev.) of free (LF_free), intra-macroaggregate (LF_M), intra-microaggregate (LF_m) and mineral-associated (MAOM) organic matter pools of coniferous forest soils (CF), broadleaved forest soils (BF), grassland soils (GL), technosols (TS) and agricultural soils (AG).

	LF_free			**LF_M**			**LF_m**			**MAOM**		
	H	**T_{50} (ºC)**	**C/N**	***H***	**T_{50} (ºC)**	**C/N**	***H***	**T_{50} (ºC)**	**C/N**	***H***	**T_{50} (ºC)**	**C/N**
CF	0.74±0.14 ab A	347±12 ab A	25.8±6.1 a A	0.95±0.36 a A	367±33 a A	24.6±4.0 a A	0.77±0.43 a A	354±36 a A	19.4±3.2 b AB	0.88±0.06 ac A	367±9 a A	10.4±1.1 b B
BF	0.57±0.31 à A	340±23 a A	22.4±4.2 a A	1.08±0.54 a A	379±46 a A	21.7±5.5 a A	1.03±0.50 a A	368±42 a A	18.2±3.6 bc A	0.80±0.06 ab A	357±10 a A	9.9±2.3 bc B
GL	0.59±0.08 a A	345±5 a A	12.4±1.2 b AB	0.95±0.59 a A	371±42 a A	17.2±1.9 a C	1.00±0.68 a A	374±44 a A	16.4±1.3 abc AC	0.68±0.06 b A	342±8 b A	9.4±0.7 abc B
TS	1.29±0.42 b A	395±31 b AB	17.3±4.7 ab A	2.00±0.80 a A	415±28 a A	19.2±3.9 a A	1.99±0.97 a A	419±38 a A	14.1±4.2 ac AB	1.04±0.17 c A	360±11 a B	8.4±0.8 ac B
AG	0.41±0.01 a C	332±3 a A	19.4±1.3 ab A	0.71±0.01 a B	357±1 a A	16.8±2.2 a AB	0.79±0.02 a A	349±0 a A	13.0±0.7 a BC	0.73±0.02 ab B	353±0 ab A	8.1±1.1 a C

Within the same column, different lowercase letters indicate statistically significant differences according to the Dunn's test at the 0.05 level. Within the same row (land use), different uppercase letters indicate statistically significant differences according to the Dunn's test at the 0.05 level.

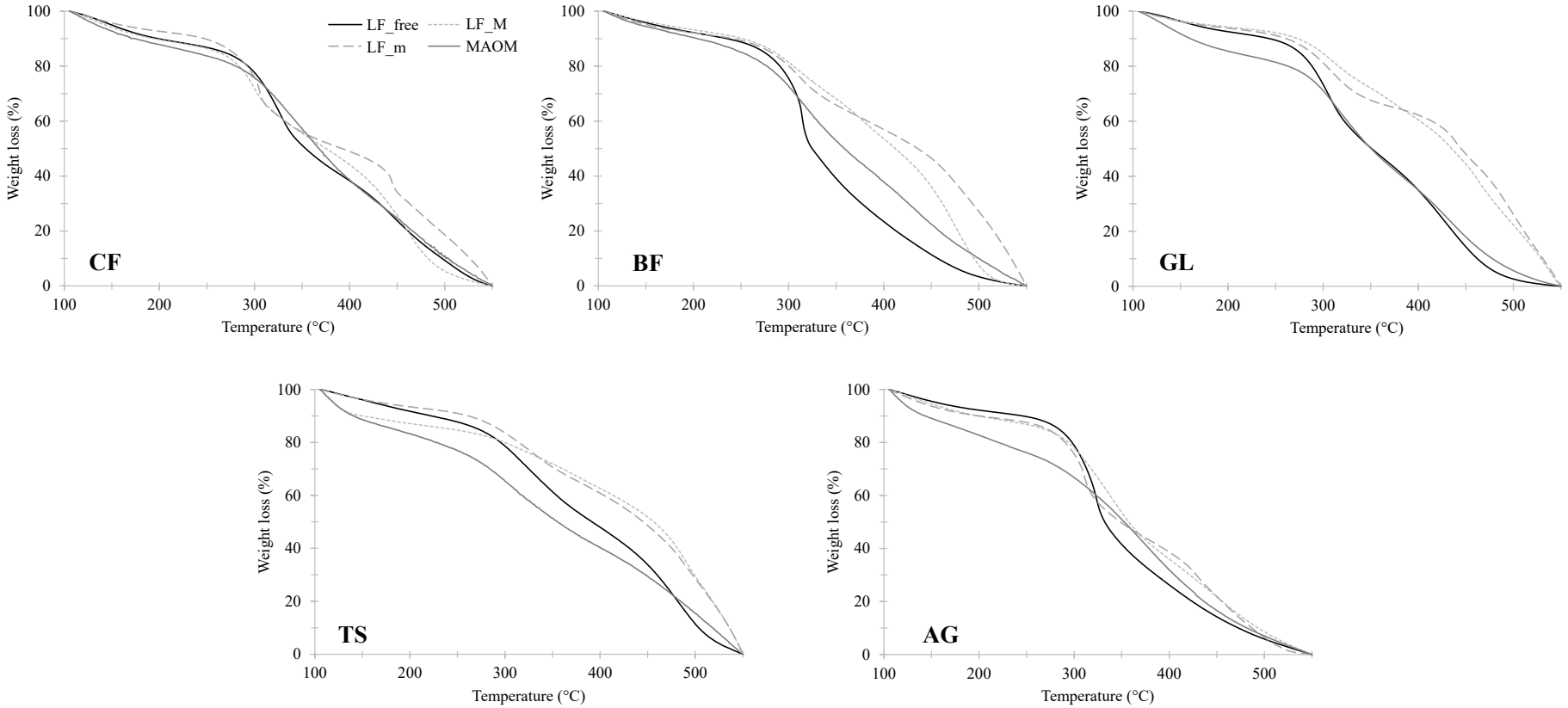

Figure 2.1 Thermogravimetric curves of free light fraction (LF_free), intra-macroaggregate light fraction (LF_M), intra-microaggregate light fraction (LF_m) and mineral-associated organic matter fraction (MAOM) of a representative sample for each soil group (coniferous forest soils, CF; broadleaved forest soils, BF; grassland soils, GL; technosols, TS; agricultural soils, AG).

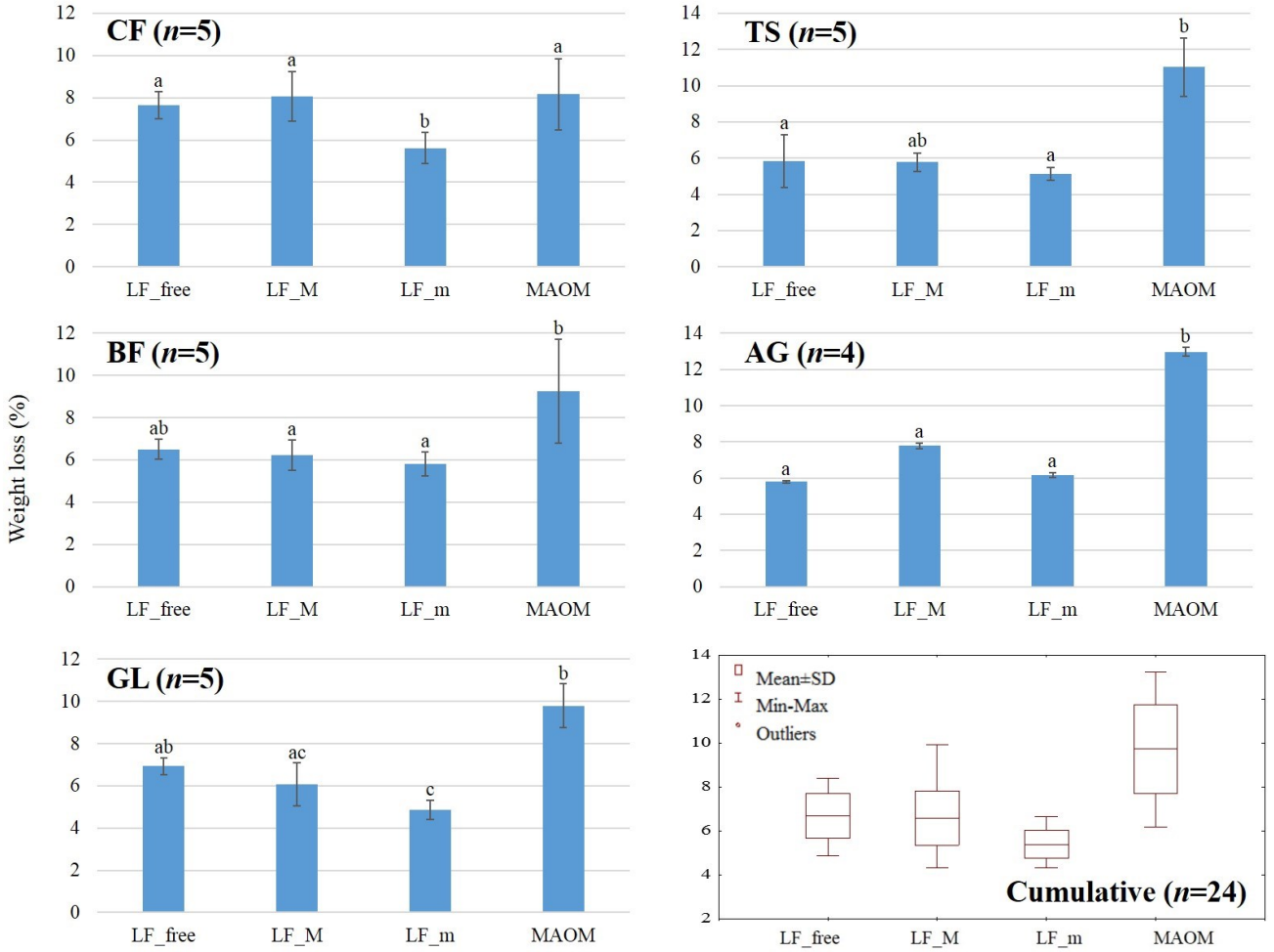

Figure 2.2 Percentage of weight loss (mean ± st. dev.) occurring in the temperature range 150-250 °C for each SOM fraction and within each ecosystem type (coniferous forest soils, CF; broadleaved forest soils, BF; grassland soils, GL; technosols, TS; agricultural soils, AG).

3. Land use effects on the stabilization of organic matter in soils: combining size fractionation with sequential chemical extractions

(Giannetta, B., Plaza, C., Zaccone, C., Vischetti, C., Rovira, P., Under review. Geoderma*)*

Abstract

The long-term stabilization of organic matter in mineral soils is now widely believed to be mainly driven by its interaction with the mineral matrix rather than by its recalcitrance. This interaction involves several processes, and the relative relevance of each one may vary according to land use. Here we study organo-mineral interactions in soils under different land uses (coniferous and broadleaved forest, grasslands, and technosols), widely differing in their soil organic matter (SOM) content, by a double approach: (i) a size fractionation by wet sieving after sonication, to isolate the particulate organic matter (POM, >20 μm) from the organo-mineral complex (OMC, <20 μm), and (ii) a characterization of the OMC by sequential extractions with different chemicals, each one disrupting a specific kind of bond between SOM and active mineral surfaces. More than 60% of total organic C (TOC) and >75% of total N were found in the OMC. Differences in land uses affected the total amount of SOM, but barely its distribution between POM and OMC. The sequential extractions showed that a substantial amount of the organic matter in the OMC (20-30%) was weakly bound to minerals. However, the main pool of the OMC occurred by far in the final residue remaining after removing all the active mineral components causing insolubility. Because the unextractability of the final residue can be due only to its own chemical characteristics (*i.e.,* solubility), and because this residue accounts for 34-48% of the TOC in OMC, 38-69% of the total N in the OMC and has a low C/N ratio, we suggest that the biochemical evolution from plant-derived material towards insoluble microbial forms is a relevant path for SOM stabilization.

3.1. Introduction

Soils represent the largest terrestrial organic carbon (OC) reservoir (Jobbágy and Jackson, 2000; Schmidt et al., 2011), and one of the main challenges for soil scientists is to clarify

its dynamics in the current climate change context (Davidson et al., 2000; Amundson et al., 2015; Doetterl et al., 2018). Due to the heterogeneity of soil organic matter (SOM), clarifying and modelling primary drivers and mechanisms of OC stability requires a clear understanding of the mechanisms responsible for SOM physical-chemical features, its build-up, its location within the mineral matrix, and its long-term persistence across different soils and ecosystem types.

The physical protection of SOM and its association to active minerals are widely recognized as the main driver for its long-term persistence in mineral soils (Kaiser and Guggenberger, 2000; Kögel-Knabner et al., 2008; Schmidt et al., 2011; Lehmann and Kleber, 2015). Physical fractionations based on particle-size, density or a combination of both have been widely used to isolate functional and meaningful SOM pools (*e.g.,* Cambardella and Elliott, 1993; Golchin et al., 1994; Amelung et al., 1998; Christensen, 2001; Plaza et al., 2013). The size fractions (sand, silt and clay-sized, all them containing both mineral particles and organic matter) represent the primary organo-mineral units; the secondary structures are the aggregates formed from the former (Christensen, 2001). Being primary structures, SOM in particle-size fractions is more clearly diverse as to their turnover than SOM in aggregates. In particular, the longest turnover times have been usually measured for the organic matter associated to the silt and clay-sized fractions (von Lützow et al., 2006; Basile-Doelsch et al., 2007).

The diversity of rationale, goals and mechanistic theories about SOM formation, stabilization and turnover has led to the application of different fractionation protocols, which have in turn hampered comparisons among studies (Poeplau et al., 2018). However, it seems clear that the distribution of SOM among the several size fractions reflects its stability. As shown in laboratory incubation experiments, the higher the proportion of total SOM in the finest fractions (particularly the <20 µm: fine silt and clay), the higher its overall stability (Rovira et al., 2010).

The size fractionation of SOM seems, therefore, a first and obvious step to study its stabilization. However, an in-depth characterization of SOM in the finest fractions must follow, because these fractions usually account for most SOM, particularly in soil layers below 15-cm depth (Rovira et al., 2010). It is in the finest fractions where chemical interactions between organic matter and active mineral surfaces mostly occur. These interactions are of several kinds: slight electrostatic adsorptions, association to clay surfaces through metal bonding, strong adsorptions to fine silt and especially clay surfaces, or association to iron (Fe) and aluminium (Al) free forms (Kögel-Knabner et al., 2008). In

order to pursuit in the understanding of SOM stabilization, we need to go beyond the simple fact of its association to mineral particles (i.e., generation of the organo-mineral complex), and investigate the relevance of each kind of association between the organic and the mineral component of such a complex.

The 'perfect' chemical extractant for SOM should perform a complete, massive, non-selective SOM extraction, without any generation of chemical artefacts (Stevenson, 1994). Of course, such an extractant does not exist. To date, sodium hydroxide (NaOH) extraction under inert atmosphere (Ar or N_2) is the closest available proxy. Well on the contrary, 'imperfect', non-massive, selective extractants are of particular interest for our work. Sodium tetraborate (NaTB henceforth) or sodium pyrophosphate (NaPP) have been used as mild extractors to obtain specific SOM fractions, associated to silt and clay surfaces by mild bonds or metal bridges (Bruckert, 1979; Schnitzer and Schuppli 1989), and the sequence NaTB - NaPP - NaOH was proposed for SOM fractionation in the organo-mineral complex (Bruckert and Kilbertus, 1980). González-Prieto et al. (1989) described an extended version of that method, which involved a further extraction with NaOH after reduction of Fe oxides with dithionite, and another after destruction of silicates with hydrofluoric acid (HF). The soil organo-mineral fractionation (SOF) method (Lopez-Sangil and Rovira, 2013) still introduced two steps, a preliminary extraction with a neutral saline solution of potassium sulfate to extract soluble or easily solubilizable compounds, and a mild attack with acid to destroy carbonate coatings, an essential step for carbonate-rich soils, common in the Mediterranean basin. In such a way, a quite extensive characterization of the organo-mineral complex can be achieved.

The aim of this paper was to attain a panoramic view of SOM stabilization in representative Mediterranean soils. To do so, we applied the approach described above: (i) a size fractionation, to isolate and quantify the POM and the organo-mineral complex, plus (ii) the detailed fractionation of organic matter in the organo-mineral complex by sequential extractions. To attain such a panoramic view, we took into account that the roles of vegetation, litter inputs and parent material in SOM stocks formation and persistence have shown to be crucial (*e.g.,* Guggenberger et al., 1994, 1995; Leifeld and Kögel-Knabner, 2005; Clemente et al., 2011; Catoni et al., 2016), and thus we used a set of soil samples under a variety of land uses and over a variety of geological substrates.

3.2. Materials and methods

3.2.1. Site selection and soil samples collection

Four land uses were compared in this study: coniferous forests (CF), broadleaved forests (BF), grassland soils (GL) and technosols (TS), all of them located in the Marche region (Italy). The coniferous forests were *Pinus nigra* woodlands occurring between 350 and 1400 m a.s.l. The broadleaved forests were Orno-Ostryetum associations with *Quercus pubescens* growing between 320 and 1300 m a.s.l. Grassland soils were under meadows and pastures covered by meso- to xerophilous species (e.g., *Bromus erectus*) and *Medicago sativa*, placed between 890 and 1700 m a.s.l. Finally, technosols were all placed below 300 m a.s.l., and included (i) two open-pit mines, filled and then reclaimed, one with *Helianthus annuus* since 2010, the other with *Triticum* sp. since 2000; (ii) two dumps, reclaimed in 2000 and in 2011; and (iii) a site of disposal of compost and other non-hazardous waste materials. Mean annual temperature of sampled sites ranged from 7.3 and 15.0 °C, and mean annual precipitation between 810 and 1570 mm. More details about these sites are reported elsewhere (Giannetta et al., 2018).

Five different sites for each land use were sampled between May and June 2016. At each site, 3-10 topsoil samples (10-25 cm depth) were collected randomly from several points separated 50 to 100 cm apart using a soil auger, and mixed to obtain a composite sample. Soil properties averaged by ecosystem type are reported in Table 3.1.

3.2.2. Physical fractionation of SOM

Size fractionation was performed by wet sieving, splitting soil particles into four different size fractions: coarse sand (CSa: 2000-200 µm), fine sand (FSa: 200-50 µm), coarse silt (CSi: 50-20 µm), and fine silt plus clay (FSCL: <20 µm) (Lopez-Sangil and Rovira, 2013). Each sample (15 g) was put into 50 mL vials and filled with deionized water to 3/4 of their volume. Samples were then subjected to rotatory agitation (20 rpm) for 60 minutes, and to further ultrasonic dispersion for 10 minutes (100 W output) using a Branson 45 sonifier.

The derived suspensions were immediately wet-sieved through a set of three sieves (200 µm, 50 µm and 20 µm mesh), thus splitting particles into four different size fractions. The fractions retained by sieves were directly recovered from them, quantitatively transferred to pre-weighted flasks and dried at 60 ºC to constant weight. The particles passing through the

last sieve (<20 µm: FSCL) were brought to about 1 L with water. Two mL of saturated solution of potassium alum were added, and the suspension was left to stand refrigerated for 2 days, until complete sedimentation of the solid particles. The overlying water was siphoned off and discarded. The sediment was recovered by centrifugation (15 min at 2500 g), transferred to a pre-weighed flask and dried at 60 ºC to constant weight.

While in the coarse fractions (>20 µm) organic matter occurs in the form of dark particles, clearly distinguishable from mineral ones, below the 20 µm threshold both components, organic and mineral, are no longer visually distinguishable. Following Lopez-Sangil and Rovira (2013), SOM in fractions >20 µm was taken as particulate organic matter (POM), whereas the <20 µm fraction was taken as the organo-mineral complex (OMC). The OMC was subjected to the SOF fractionation procedure, as described below.

3.2.3. Chemical fractionation of the organo-mineral complex

The method has been thoroughly described by Lopez-Sangil and Rovira (2013), and thus only the essential details are given here (Fig. 3.1). Briefly, the OMC was submitted to the following sequence of extractions:

1) 0.5 M potassium sulfate (K_2SO_4), to extract water-soluble compounds;

2) 0.1 M NaTB ($Na_2B_4O_7$), at pH 9.7, to extract compounds adsorbed to mineral surfaces by Van der Waals- or weak electrostatic bonds;

3) 0.1 M NaPP ($Na_4P_2O_7$), at pH 9.8, to extract compounds precipitated or stabilized by coordination complexes with metals (Ca, Mg, Fe, Al);

4) 0.1 M NaOH, at pH >12, to extract compounds strongly associated to mineral surfaces;

5) mild attack with 0.33 M sulfuric acid (H_2SO_4) at 5 ºC, followed by 0.1 M NaOH, to extract compounds occluded by carbonate coatings;

6) reduction with 20 mL 0.1 M sodium dithionite ($Na_2S_2O_4$), followed by 0.1 M NaOH, to extract compounds stabilized by free Fe^{3+} forms, previously made soluble through their reduction to Fe^{2+};

7) attack with cold 8 M hydrofluoric acid (HF), followed by 0.1 M NaOH, to extract compounds associated to clays by strong bonds, resistant to all the previous steps.

The remaining pellet after all previous steps was taken as humin.

All SOF extracts were brought up to a fixed volume, and stored at 4 ºC until OC and N analyses. The remaining residue (humin) was dried, weighed, and stored at room temperature until OC and N analyses.

3.2.4. Organic C and total N analyses

Total C and N contents of SOM fractions obtained after physical fractionation were determined by dry combustion using a Thermo Flash 2000 NC Analyzer. Before analysis, an aliquot of each sample was ground with a ball mill. For OC determination, the aliquots were subjected to acid fumigation before the analysis (Harris et al., 2001) to remove carbonates.

Steps 5-7 involved two parts. First, the extract obtained with the pre-treatment (sulfuric acid, dithionite, hydrofluoric acid); next, that obtained with 0.1 M NaOH. While the second one was analyzed for OC and N in all cases, in step 5 the first extract (H_2SO_4) could not be analyzed for total N, and in step 7 the first extract (HF) was discarded and thus could not be analyzed neither for OC nor for total N. Thus, extracted OC in step 7, and extracted N in steps 5 and 7, are underestimated. Leaving aside these exceptions, in the SOF extracts OC was quantified colorimetrically by dichromate oxidation (Nelson and Sommers, 1996), and total N in a ThermoQuest CHN analyzer, by evaporation of an aliquot of each extract into tin capsules over a hot plate at 60 ºC. In the first extract of step 6 (dithionite) OC was quantified in the CHN analyzer, because of the interference of dithionite, a strong reductor, with the dichromate oxidation.

In each of the steps 5-7 two consecutive extracts were obtained, and the analyses of OC and N were performed for each one separately. Nevertheless, here we consider both extracts altogether, for it is the sum of both extracts what covers the whole organic matter that becomes soluble after the blocking obstacle (carbonates, oxyhydroxydes, the clay herself) has been removed by the pre-treatment.

3.2.5. Statistical analysis

The amounts of OC and N of the whole soils, in the size fractions, and in the SOF fractions were compared by ANOVA, taking land use as a factor. For such analyses, data were previously log-transformed. Within a given ANOVA, differences between the several land uses were tested by the Duncan's test. Effects were deemed as significant when $p \leq 0.05$.

In order to understand how the fractions become replenished as the soil accumulates

OC or N, we studied by linear regression the relationships between (i) the OC and N content of each size fraction, *versus* that of the whole soil sample, and (ii) the OC and N content of each SOF fraction, *versus* that of the whole OMC. Polynomial equations of either 1st or 2nd order without intercept (*i.e.,* $Y = b_1X + b_2X^2$) were fitted using SigmaPlot v.10.

3.3. *Results*

3.3.1. Carbon and nitrogen in bulk soils

The OC and N contents of the studied soils span a broad range (Table 3.1). Briefly, GL have the highest average contents of OC (8.6%) and total N (0.9%), and TS the lowest (1.3 and 0.2%, respectively). Both OC and N average contents rank as GL > CF > BF > TS, thus mirroring the link between OC and N dynamics, also evidenced by the close linear relationship between OC and N contents (Fig. 3.2). Specific land use effects are also visible in the OC/N ratios, which rank as CF > BF > GL > TS (Table 3.2).

3.3.2. Carbon and nitrogen in the size fractions

The recovery of OC in the size fractions averaged around 96% of total OC in the whole sample, and that of N around 80%.

Both OC and N contents in each fraction depend on soil type. They are highest in GL soils (for all fractions), whereas tend to be lowest in TS, except for the coarsest fraction (2000-200 µm) (Table 3.2). Overall, OC and N contents follow this trend: GL > CF > BF > TS.

The OC and N contents of the fractions and those of the whole soil samples are positively and significantly correlated (Fig 3.3). The significance of these correlations is higher the smaller the size of the fraction, and is comparatively higher for N than for OC (Fig. 3.3). This suggests that the differences in OC and N content in the fractions merely reflect the richness in OC and N in the whole soil sample, rather than a specific effect of the land use.

The OMC accounts for 63 (in CF) to 77% (in GL) of total OC, and for 80% of total N (Table 3.3). Whereas in all coarse fractions (>20 µm: POM) the total OC content is higher than that of total N, in the <20 µm fraction (OMC) the opposite is found. The OMC is by

far the main sink for N-rich compounds; this role is the underlying reason for their OC/N ratios, the lowest among all (Table 3.3).

3.3.3. Organic C in the organo-mineral complex: SOF fractionation

The recovery of OC in the SOF fractions (sum of OC in all fractions, as % of the initial OC in the OMC) was on average 89.2%. The HF hydrolysate, which was not analyzed for OC, partly explains this loss; however, C losses may also be attributed to the repeated NaOH extractions, which may result in decarboxylations in spite of being all carried out under N_2.

For all land uses the highest OC amounts are found in the humin, which accounts for 34 to 48% of total OC in the OMC. Thus, in all cases a substantial part of SOM in the OMC remains insoluble even after clay minerals, bond-making metals, carbonates, Fe and Al oxides (precipitating factors) have been removed.

When translated to percentages over the total OC in the OMC (Table 3.4), some of the differences between land uses disappear, while significant differences are still found for most SOF fractions. This means that the differences can be attributed not only to contrasting SOM amounts, but also to specific land-use effects. Thus, in GL the OC associated to mineral matter through weak bonds (NaTB fraction) is highly relevant, while the soluble fraction (K_2SO_4 extract) and especially the fraction directly associated to clays through very strong bonds (HF-NaOH) are scarcely relevant. We note that in GL such a low relevance is due to the abundance of the other fractions; the absolute amount of OC in this fraction is actually similar to that of other land uses (Table 3.4). Moreover, another specific land-use effect is the relevance of the first NaOH extract in TS, about 4% of total OC, thus much lower than that of other land uses.

Values in Table 3.4 are affected by the total richness of the soils in OC. The amount of OC in most SOF fractions increases with the total OC in the OMC, and the increase is not homogeneous in all fractions (Fig. 3.3). Two fractions, the K_2SO_4 extract and the humin, seem to have an upper limit. In two fractions (Dithionite-NaOH and HF-NaOH) the amount of OC does not seem related to that of the whole OMC. In the HF-NaOH fraction the OC remains consistently low for all samples, always below 3 mg OC per gram OMC.

For four SOC fractions (NaTB, NaPP, NaOH, and H_2SO_4-NaOH) the OC content consistently increases with the total OC in the OMC. For NaTB-extracted, NaPP-extracted, and NaOH SOM fractions the relationships are strong and best described by growing curves, meaning that the relative relevance of these fractions increases with the total OC in the

OMC. In contrast, for the H_2SO_4-NaOH fraction data dispersion is high, likely because the accumulation of OC in this fraction depends on the amount of carbonates in fine silt and clays, thus making OC in the fraction and in the OMC less directly related.

3.3.4. Nitrogen in the organo-mineral complex

The recovery of N in the SOF fractions was 66.5% of the total initial N in the OMC.

Humin accounts for more than 60% of the OMC total N, and thus its dominance is higher than for OC. The N extractable after HF treatment is irrelevant, <1% of total N on average. In the sequence NaTB – NaPP – NaOH, the amount of OC extracted was roughly similar or tended to increase; in contrast, the amount of extracted N clearly tends to decrease, being lowest in the first NaOH extract. The NaOH extract contains always <10% of the total N on average, and in most cases <5%. Thus, while this fraction is one of the most important for OC, it is not for N. Another difference is that the extract obtained after dithionite treatment is more relevant for N than for OC; in soils under grasslands and broadleaved forests, it accounts for about 10% of total N.

As observed for OC, the amount of N in each SOF fraction relates to the total amount of N in the OMC. The relationships are somewhat different for each SOF fraction (Fig. 3.5). Only in one case, the humin, an uppermost limit appears. It is noteworthy that while such an uppermost limit was observed for OC in the K_2SO_4 extract, it is not observed for K_2SO_4-extractable N. It is also noteworthy the extremely low amount of N in the HF-NaOH fraction, apparently independent from the total N in the OMC.

For the first four fractions the relations are close, as shown by the high R^2 values. For the H_2SO_4-NaOH and the dithionite-NaOH fractions R^2 values were low, thus reflecting great data dispersion: as previously mentioned for OC, the amount of N in these fractions may be not too directly related to total N in the OMC because it depends also on variables such as the amount of carbonates and the amount of Fe oxides in fine silt and/or clay.

3.4. Discussion

3.4.1. Methodological constraints

The recovery of N after both sieving and SOF fractionation was much lower than that of OC. Therefore, the results for N, both in size fractions and in SOF extracts, are prone to larger biases than those for OC.

In the size fractionation, the ultrasonic treatment plus the extensive water leaching during sieving are obvious reasons for both OC and N losses, for they imply that soluble or easily solubilizable compounds are extracted massively. Nitrogen-rich compounds, including amino acids, peptides, proteins, alkaloids, nucleotides, are more likely to be part of these labile pool, whereas macromolecules such as lignin, suberin, cutins, lipid compounds, rich in C and poor in N, remain largely insoluble and are likely to resist much better the ultrasonic plus sieving treatment.

For the SOF method, the reasons for the low recovery of N compounds are a bit different. In the SOF method, all extractions are done quantitatively, without any losses of material. On the other hand, we were not able to analyse some extract for OC, N or both, and thus their OC or N could not be accounted for in the recovery calculations. In addition to these underestimations, the repeated NaOH extractions are likely to affect the characteristics of the obtained fractions. The pH of a 0.1 M NaOH solution is extremely alkaline (>12) and deamination may occur under these conditions, even when the extraction is carried out under N_2 atmosphere (as in our experiment). In Bremner's classical N fractionation method (Pansu and Gautheyrou, 2006), the N of amino sugars and amino acids is obtained by steam distillation after deamination by an alkaline reagent as phosphate-borate buffer at pH 11.2, either directly (amino sugars) or after boiling with NaOH at low concentration (amino acids). The SOF method does not include boiling with NaOH, but it includes a NaOH extraction overnight repeated four times (steps 4, 5, 6 and 7), and therefore deamination events are likely. This may explain why the relatively amount of N recovered in the first NaOH extract was low (Table 3.5), whereas the OC extracted was relevant, one of the main fractions actually (Table 3.4).

3.4.2. Distribution of organic matter among the size fractions: land use effects

A main result of our size fractionation work (summarized in Table 3.3) is the clear dominance of the OMC in all land uses. This agrees with the results obtained by Giannetta et al. (2018) using the same soils but with a different approach, i.e., based on density- rather than on size fractionation (Plaza et al., 2013). It has been often claimed that the organic matter in coarse fractions (particulate organic matter: POM) is more sensitive to differences in ecosystem types and land use changes (Poeplau and Don, 2013). Since the organic matter accrual in large size fractions is mainly determined by organic inputs and not by texture (Hassink, 1997), a change in land use from a low C-input ecosystem to a high C-input one should logically affect mainly the coarse SOM fractions.

Our results do not perfectly match this view. We found that the amount of organic matter in fractions >20 μm (POM) is higher in forest- and grassland soils than in technosols in absolute amounts, but not in relative terms (*i.e.,* as % of the total organic matter). As shown in Table 3, the distribution of organic matter between the four size fractions is substantially similar in TS, GL and BF. Only in CF soils, the coarsest POM fraction (2000-200 μm) is enriched in OC, whereas the organo-mineral complex is depleted. We must stress that, except for CF, the effects of land use were significant on the total amount of SOM but not on the distribution of organic matter among fractions.

In our work, CF become thus a well distinguishable group. Coniferous needles are rich in recalcitrant compounds (lignin, suberin, lipidic polymers) which confer to litter a low decomposition rate and microbial use efficiency (Kooch et al., 2012; Cotrufo et al., 2013), thus leading to a relatively higher OC accumulation in coarse POM fractions (Castellano et al., 2015). The OC/N ratios of all size fractions are higher for CF that for the other ecosystems (Table 3.2), consistently with previous reports (Guggenberger et al., 1994), and also with the relatively low decomposition degree of SOM in coniferous forests compared to other ecosystems (Castellano et al., 2015).

The results obtained for TS are noteworthy, in the sense that their behaviour is surprisingly similar to that of highly mature ecosystems. In the current paradigm about the filling of the several fractions, the accumulation of organic matter in soils involves its transfer between fractions, in which fresh inputs predominantly accumulate in the coarsest fraction (coarse sand size), pass both fine sand and coarse silt pools during the degradation continuum, and eventually accrue in the organo-mineral complex (Baldock et al., 1992). According to this paradigm, we should expect substantial differences between young and

poorly evolved soils (such as technosols) and more complex, SOM-rich and evolved systems, such as soils under mature forests. Instead, in our TS, the distribution of OC and N between particulate organic matter and the organo-mineral complex does not differ from that of GL or BF (Table 3.3). Moreno-Barriga et al. (2017) studied the evolution of OC and N pools following the addition of different materials to mine tailings, and concluded that easily-available organic compounds triggered microbial growth during the first days of incubation and enhanced the formation of aggregates, which in turn stabilize coarse debris. This phenomenon, which could occur in most technosols, mimics early stages of pedogenesis (Giannetta et al., 2018) and could make the SOM in technosols similar to that of much more evolved soil systems.

Coarse fractions are mainly similar to plant litter (Guggenberger et al., 1994) and are mainly plant debris in large pieces, not associated with minerals (Ladd et al., 1996). In contrast, fine fractions, in particular clay, accumulate more evolved materials, depleted in lignin and plant-derived components, and enriched in products of microbial origin (Paul and Clark, 1989; Golchin et al., 1994; Kögel-Knabner et al., 2008; Plaza et al., 2013, 2016; Zaccone et al., 2018). The decrease in OC/N ratios from coarse to fine fractions thus reflects a change from a chemistry dominated by plant materials to the chemistry of microbial biomass and metabolites.

Of particular relevance is the behaviour of nitrogenous compounds. The decrease in the OC/N ratio is an indicator of humification, well described in classical books (Duchaufour, 1977); but in addition to this explanation for the low OC/N ratio of the organo-mineral complex, observed in our dataset (Table 3.3), specific processes must also be accounted for. As shown in a previous work by Rovira and Vallejo (2002), the split of plant-derived debris between N-poor in the coarse fractions and N-rich in the fine fractions occurs from the very beginning of the mixing of plant debris with a mineral, organic matter-depleted soil. Clay surfaces, together with active mineral components such as Fe and Al oxyhydroxydes, establish bonds with soluble organic matter, including nitrogenous compounds such as amino acids, amino sugars, peptides or proteins, nucleic acids, partly plant-derived but also from microbial origin (Ladd et al., 1996; Knicker, 2004; Sollins et al., 2006; Nannipieri and Paul, 2009; Paul, 2016; Zaccone et al., 2018). The huge capacity of clays for stabilizing proteins has been known for many years (Pinck et al., 1954; Harter and Stotzky, 1971; Kleber et al., 2007). The effect of clays may be either through a direct stabilization of organic N (Ladd et al., 1996; Nielsen et al., 2006; Sollins et al., 2006) and through the formation of aggregate-protected particulate and non-particulate organic matter (*e.g.,* Yoo

and Wander, 2008), with most of this organic N (>80%) being in the form of amides, peptides and proteins of microbial origin (Simpson et al., 2007a). By contrast, the high OC/N ratio found in the POM fractions suggests a relatively high occurrence of slightly-to-partially decomposed plant materials in these fractions (Rasmussen et al., 2005).

3.4.3. Organic matter in the organo-mineral complex

In his review on organo-mineral complexes, Bruckert (1979) already noted that tetraborate often extracted more OC than NaOH, in agreement with our previous results, at least for acid soils (Lopez-Sangil and Rovira, 2013). The results of the current study agree with the previous ones only partially. In forest and grassland soils tetraborate extracts on average less OC than NaOH (Table 3.4), but in all land uses the sum of OC extracted by K_2SO_4, NaTB and NaPP – *i.e.,* all extractants before NaOH – is higher than that extracted by NaOH, thus showing that a substantial portion of organic matter in the organo-mineral complex is rather loosely associated to the mineral surfaces, through electrostatic, van der Waals, or metallic bonds. González-Prieto et al. (1989) obtained similar results for a dystric cambisol and two eutric fluvisols, in an estuarine zone of Galicia (NW Spain). There is an obvious need of experimental data to verify whether these mild bonds do really give relatively labile OC pools, more prone to become released from the OMC than other pools associated to minerals by strong bonds, breakable only by highly alkaline solutions (NaOH) or by harder treatments.

We must stress here that, while in the SOF procedure the word 'humin' is reserved for the last unextractable residue, the classical concept of humin would include all fractions after the first NaOH extraction, *i.e.,* the four last fractions in Table 3.4. The great importance of the humin (in its classical concept) was stressed by Duchaufour (1977), and our results agree with this view. In Table 3.4, the sum of the last four fractions accounts for a substantial part of the organo-mineral complex. However, the four components of the 'classical' humin in the SOF protocol do not have the same relevance. By far, the last residue (humin *stricto sensu*, in our fractionation) is the most important pool: in CF, it approaches 50% of the total OC in the organo-mineral complex. Slightly lower values, always <35%, have been obtained by Lopez-Sangil and Rovira (2013), but the humin was still a highly relevant pool. This pool remains insoluble after the long set of treatments and extractions, and in particular after the substantial destruction of the mineral matrix by HF; therefore, its strong insolubility is not due to any association with the mineral matter, but to its own biochemical composition.

Future work should aim at investigating the molecular composition of this fraction. In this regard, Simpson et al. (2007b) found that peptides, aliphatic species, carbohydrates, peptidoglycan, and lignin, as macromolecules or aggregate species, are major contributors of humin. They also found that microbial biomass may account for ~45% of the humin fraction in some soils (Simpson et al., 2007a).

In comparison with this last residue, other components of the 'classical' humin are much less relevant, on a quantitative basis. Thus, in spite of the presence of carbonates in many of our soils (median: 27%), the proportion of OC extracted after the cold acid attack (H_2SO_4-NaOH fraction) is low, in agreement with Lopez-Sangil and Rovira (2013). This suggests that in the soils under study carbonate coatings do not play a substantial role in protecting organic compounds, in contrast with previous claims (Alonso et al., 2004; Gocke et al., 2011).

It is also noteworthy the relatively low relevance of the dithionite-NaOH fraction, on average <5% of the total OC in the OMC, a somewhat unexpected result in the framework of current paradigms that give to Fe and Al oxyhydroxydes a pivotal role in the long-term stabilization of SOM (Mikutta et al., 2006; Kögel-Knabner et al., 2008). Finally, the amount of organic matter extracted after HF treatment is very low in absolute terms (1-2 mg OC g OMC^{-1}), in agreement with previous studies (Lopez-Sangil and Rovira, 2013).

3.5. Conclusions

We provide evidence that size fractionation coupled with an extensive set of chemical extractions allow obtaining new insights about SOM sequestration in mineral soils characterized by different land use. The distribution of OC and N among the obtained size fractions is little affected by land use. The only significant effects of land use on the distribution of SOM among fractions occurs in CF. Interestingly, TS behavior is similar to that of highly mature ecosystems.

Irrespective of land use, the OMC accounts for the very most of total OC and N. The sequential extractions show that the organic matter of the OMC can be split in several pools according to the way it is bound to the active mineral surfaces. A substantial part of the organic matter in the OMC is bound loosely through electrostatic, van der Waals-, or metallic bonds. For all land uses, the highest OC amounts are found in the humin, which remains insoluble after all the active mineral components causing precipitation have been removed. This strongly underlies the importance of biochemical transformation on SOM

stability and suggests that the relevance of the biochemical evolution from plant-derived material towards insoluble microbial forms as a path for SOM stabilization may have been underestimated.

References

Alonso, P., Dorronsoro, C., Egido, J.A., 2004. Carbonatation in palaeosols formed on terraces of the Tormes river basin (Salamanca, Spain). Geoderma 118, 261-276.

Amelung, W., Zech, W., Zhang, X., Follett, R.F., Tiessen, H., Knox, E., Flach, K.W., 1998. Carbon, nitrogen, and sulfur pools in particle-size fractions as influenced by climate. Soil Science Society of America Journal 62, 172-181.

Amundson, R., Berhe, A.A., Hopmans, J.W., Olson, C., Sztein, A.E., Sparks, D.L., 2015. Soil and human security in the 21st century. Science 348, 647–653.

Baldock, A.J.A., Oades, J.M., Waters, A.G., Peng, X., Vassallo, A.M., Wilson, M.A., 1992. Aspects of the chemical structure of soil organic materials as revealed by solid-state 13C NMR spectroscopy. Biogeochemistry 16, 1-42.

Basile-Doelsch, I., Amundson, R., Stone, W.E.E., Borschneck, D., Bottero, J.Y., Moustier, S., Masin, F., Colin, F., 2007. Mineral control of carbon pools in a volcanic soil horizon. Geoderma 137, 477-489.

Bruckert, S., 1979. Analyse des complexes organo-minéraux des sols. In: Bonneau, M., Souchier, B. (Eds.), Pédologie. Constituants et propriétés du sol, vol. 2. Masson, Paris, pp. 187-209.

Bruckert, S., Kilbertus, G., 1980. Fractionnement et analyse des complexes organominéraux de sols bruns et de chernozems. Plant and Soil 57, 271-295.

Cambardella, C.A., Elliott, E.T., 1993. Methods for physical separation and characterization of soil organic matter fractions. Geoderma 56, 449-457.

Castellano, M.J., Mueller, K.E., Olk, D.C., Sawyer, J.E., Six, J., 2015. Integrating plant litter quality, soil organic matter stabilization, and the carbon saturation concept. Global Change Biology 21, 3200-3209.

Catoni, M., D'Amico, M.E., Zanini, E., Bonifacio, E., 2016. Effect of pedogenic processes and formation factors on organic matter stabilization in alpine forest soils. Geoderma 263, 151-160.

Christensen, B.T., 2001. Physical fractionation of soil and structural and functional complexity in organic matter turnover. European Journal of Soil Science 52, 345-353.

Clemente, J.S., Simpson, A.J., Simpson, M.J., 2011. Association of specific organic matter compounds in size fractions of soils under different environmental controls. Organic Geochemistry 42, 1169-1180.

Cotrufo, M.F., Wallenstein, M.D., Boot, C.M., Denef, K., Paul, E., 2013. The Microbial Efficiency-Matrix Stabilization (MEMS) framework integrates plant litter decomposition with soil organic matter stabilization: Do labile plant inputs form stable soil organic matter? Global Change Biology 19, 988-995.

Davidson, E.A., Trumbore, S.E., Amundson, R., 2000. Soil warming and organic carbon content. Nature 408, 789-790.

Doetterl, S., Berhe, A.A., Arnold, C., Bodé, S., Fiener, P., Finke, P., Fuchslueger, L., Griepentrog, M., Harden, J.W., Nadeu, E., Schnecker, J., Six, J., Trumbore, S., Van Oost, K., Vogel, C., Boeckx, P., 2018. Links among warming, carbon and microbial dynamics mediated by soil mineral weathering. Nature Geoscience 11, 589-593.

Duchaufour, P., 1977. Dynamique de la matière organique. In: Duchaufour P., Pédologie, Vol. I: Pédogenèse et classification. Masson, Paris. pp. 28-69.

Giannetta, B., Plaza, C., Vischetti, C., Cotrufo, M.F., Zaccone, C., 2018. Distribution and thermal stability of physically and chemically protected organic matter fractions in soils across different ecosystems. Biology and Fertility of Soils 54, 671-681.

Gocke, M., Pustovoytov, K., Kuzyakov, Y., 2011. Carbonate recrystallization in root-free soil and rhizosphere of Triticum aestivum and Lolium perenne estimated by 14C labeling. Biogeochemistry 103, 209-222.

Golchin, A., Oades, J.M., Skjemstad, J.O., Clarke, P., 1994. Study of free and occluded particulate organic matter in soils by solid state 13C CP/MAS NMR spectroscopy and scanning electron microscopy. Australian Journal of Soil Research 32, 285-309.

Gonzalez-Prieto, S.J., Lista, M.A., Carballas, M., Carballas, T., 1989. Humic substances in a catena of estuarine soils: distribution of organic nitrogen and carbon. The Science of the Total Environment 81, 363-372.

Guggenberger, G., Christensen, B.T., Zech, W., 1994. Land-use effects on the composition of organic matter in particle-size separates of soil: I. Lignin and carbohydrate signature. European Journal of Soil Science 45, 449-458.

Guggenberger, G., Zech, W., Haumaier, L., Christensen, B.T., 1995. Land-use effects on the composition of organic matter in particle-size separates of soils: II. CPMAS and solution 13C NMR analysis 147-158.

Harris, D., Horwáth, W.R., van Kessel, C., 2001. Acid fumigation of soils to remove

carbonates prior to total organic carbon or Carbon-13 isotopic analysis. Soil Science Society of America Journal 65, 1853-1856.

Harter, R.D., Stotzky, G., 1971. Formation of clay-protein complexes. Soil Science Society of America Proceedings 35, 383-389.

Hassink, J., 1997. The capacity of soils to preserve organic C and N by their association with silt and clay particles. Plant and Soil 191, 77-87.

Jobbágy, E.G., Jackson, R.B., 2000. The vertical distribution of soil organic carbon and its relation to climate and vegetation. Ecological Applications 10, 423-436.

Kaiser, K., Guggenberger, G., 2000. The role of DOM sorption to mineral surfaces in the preservation of organic matter in soils. Organic Geochemistry 31, 711-725.

Kleber, M., Sollins, P., Sutton, R., 2007. A conceptual model of organo-mineral interactions in soils: self-assembly of organic molecular fragments into zonal structures on mineral surfaces. Biogeochemistry 85, 9-24.

Knicker, H., 2004. Stabilization of N-compounds in soil and organic-matter-rich sediments - What is the difference? Marine Chemistry 92, 167-195.

Kögel-Knabner, I., Guggenberger, G., Kleber, M., Kandeler, E., Kalbitz, K., Scheu, S., Eusterhues, K., Leinweber, P., 2008. Organo-mineral associations in temperate soils: Integrating biology, mineralogy, and organic matter chemistry. Journal of Plant Nutrition and Soil Science 171, 61-82.

Kooch, Y., Hosseini, S.M., Zaccone, C., Jalilvand, H., Hojjati, S.M., 2012. Soil organic carbon sequestration as affected by afforestation: The Darab Kola forest (north of Iran) case study. Journal of Environmental Monitoring 14, 2438-2446.

Ladd J.N., Foster R.C., Nannipieri, P., Oades, J.M., 1996. Soil structure and biological activity. In: Stotzky, G., Bollag, J.-M. (Eds) Soil biochemistry, vol 9. Marcel Dekker, New York, pp 23–78.

Lehmann, J., Kleber, M., 2015. The contentious nature of soil organic matter. Nature 528, 60-68.

Leifeld, J., Kögel-Knabner, I., 2005. Soil organic matter fractions as early indicators for carbon stock changes under different land-use? Geoderma 124, 143-155.

Lopez-Sangil, L., Rovira, P., 2013. Sequential chemical extractions of the mineral-associated soil organic matter: An integrated approach for the fractionation of organo-mineral complexes. Soil Biology & Biochemistry 62, 57-67.

Mikutta, R., Kleber, M., Torn, M.S., Jahn, R., 2006. Stabilization of soil organic matter: association with minerals or chemical recalcitrance? Biogeochemistry 77, 25-56.

Moreno-Barriga, F., Díaz, V., Acosta, J.A., Muñoz, M.Á., Faz, Á., Zornoza, R., 2017. Organic matter dynamics, soil aggregation and microbial biomass and activity in Technosols created with metalliferous mine residues, biochar and marble waste. Geoderma 301, 19-29.

Nannipieri, P., Paul, E.A., 2009. The chemical and functional characterization of soil N and its biotic components. Soil Biology & Biochemistry 41, 2357-2369.

Nielsen, K.M., Calamai, L., Pietramellara, G., 2006. Stabilization of extracellular DNA by transient binding to various soil surfaces. In: Nannipieri, P., Smalla K. (Eds), Nucleic acids and proteins in soil (soil biology), vol 8. Springer, Berlin, pp. 141–158.

Pansu, M., Gautheyrou, J., 2006. Handbook of Soil Analysis. Mineralogical, Organic and Inorganic Methods. Springer, Berlin.

Paul, E.A., Clark, F.E., 1989. Soil microbiology and biochemistry. Academic Press, San Diego.

Paul, E.A., 2016. The nature and dynamics of soil organic matter: Plant inputs, microbial transformations, and organic matter stabilization. Soil Biology & Biochemistry 98, 109-126.

Plaza, C., Courtier-Murias, D., Fernández, J.M., Polo, A., Simpson, A.J., 2013. Physical, chemical, and biochemical mechanisms of soil organic matter stabilization under conservation tillage systems? A central role for microbes and microbial by-products in C sequestration. Soil Biology & Biochemistry 57, 124-134.

Plaza, C., Giannetta, B., Fernández, J.M., López-de-Sá, E.G., Polo, A., Gascó, G., Méndez, A., Zaccone, C., 2016. Response of different soil organic matter pools to biochar and organic fertilizers. Agriculture, Ecosystems & Environment 225, 150–159.

Pinck, L.A., Dyal, R.S., Allison, F.E., 1954. Protein-montmorillonite complexes, their preparation and the effects of soil microorganisms on their decomposition. Soil Science 78, 109-118.

Poeplau, C., Don, A., 2013. Sensitivity of soil organic carbon stocks and fractions to different land-use changes across Europe. Geoderma 192, 189-201.

Poeplau, C., Don, A., Six, J., Kaiser, M., Benbi, D., Chenu, C., Cotrufo, M.F., Derrien, D., Gioacchini, P., Grand, S., Gregorich, E., Griepentrog, M., Gunina, A., Haddix, M., Kuzyakov, Y., Kühnel, A., Macdonald, L.M., Soong, J., Trigalet, S., Vermeire, M.-L., Rovira, P., van Wesemael, B., Wiesmeier, M., Yeasmin, S., Yevdokimov, I., Nieder, R., 2018. Isolating organic carbon fractions with varying turnover rates in temperate agricultural soils - A comprehensive method comparison. Soil Biology & Biochemistry

125, 10-26.

Rovira, P., Jorba, M., Romanyà, J., 2010. Active and passive organic matter fractions in Mediterranean forest soils. Biology and Fertility of Soils 46, 355-369.

Rovira, P., Vallejo V.R., 2002. Mineralization of carbon and nitrogen from plant debris, as affected by debris size and depth of burial. Soil Biology & Biochemistry 34, 327-339.

Schmidt, M.W.I., Torn, M.S., Abiven, S., Dittmar, T., Guggenberger, G., Janssens, I.A., Kleber, M., Kögel-Knabner, I., Lehmann, J., Manning, D.A.C., Nannipieri, P., Rasse, D.P., Weiner, S., Trumbore, S.E., 2011. Persistence of soil organic matter as an ecosystem property. Nature 478, 49-56.

Simpson, A.J., Simpson, M.J., Smith, E., Kelleher, B.P., 2007a. Microbially derived inputs to soil organic matter: Are current estimates too low? Environmental Science and Technology 41, 8070-8076.

Simpson, A.J., Song, G., Smith, E., Lam, B., Novotny, E.H., Hayes, M.H.B., 2007b. Unraveling the structural components of soil humin by use of solution-state nuclear magnetic resonance spectroscopy. Environmental Science & Technology 41, 876-883.

Sollins, P., Swanston, C., Kleber, M., Filley, T., Kramer, M., Crow, S., Caldwell, B.A., Lajtha, K., Bowden, R., 2006. Organic C and N stabilization in a forest soil: Evidence from sequential density fractionation. Soil Biology & Biochemistry 38, 3313-3324.

Stevenson F.J., 1994. Humus chemistry: genesis, composition, reactions. 2nd. ed. Wiley & Sons, New York, USA.

Tisdall, J.M., Oades, J.M., 1982. Organic matter and water stable aggregates in soil. Soil Science 33, 141-163.

von Lützow, M., Kögel-Knabner, I., Ekschmitt, K., Matzner, E., Guggenberger, G., Marschner, B., Flessa, H., 2006. Stabilization of organic matter in temperate soils: mechanisms and their relevance under different soil conditions - a review. European Journal of Soil Science 57, 426-445.

Wei, X., Wang, X., Ma, T., Huang, L., Pu, Q., Hao, M., Zhang, X., 2017. Distribution and mineralization of organic carbon and nitrogen in forest soils of the southern Tibetan Plateau. Catena 156, 298-304.

Yoo, G., Wander, M.M., 2008. Tillage effects on aggregate turnover and sequestration of particulate and humified soil organic carbon. Soil Science Society of America Journal 72, 670-676.

Zaccone, C., Beneduce, L., Lotti, C., Martino, G., Plaza, C., 2018. DNA occurrence in organic matter fractions isolated from amended, agricultural soils. Applied Soil Ecology

130, 134-142.

Table 3.1 Main properties of the studied soils (CF = coniferous forest soils; BF = broadleaved forest soils; GL = grassland soils; TS = technosols). Numeric data are averages ± standard deviations (n = 5). Data were log-transformed for ANOVAs and Duncan's test. Within a row, data followed by the same lowercase letter do not differ at p = 0.05. Raw data from Giannetta et al. (2018).

	CF	**BF**	**GL**	**TS**
Sand (%)	45.5 ± 8.7 ab	49.0 ± 18.1 ab	64.2 ± 6.5 a	18.7 ± 6.9 c
Silt (%)	27.9 ± 11.4 b	32.8 ± 9.1 ab	23.4 ± 3.7 b	44.5 ± 3.3 a
Clay (%)	24.6 ± 9.1 ab	18.2 ± 141 b	12.4 ± 5.3 b	367 ± 7.1 a
pH_{H2O}	8.1 ± 0.2 a	8.1 ± 0.3 a	6.2 ± 0.9 b	8.4 ± 0.1 a
EC ($\mu S \cdot cm^{-1}$)	67 ± 28 a	61 ± 29 a	101 ± 37 a	131 ± 144 a
OC (%)	5.23 ± 1.90 bc	3.59 ± 2.82 b	8.60 ± 0.76 c	1.26 ± 0.93 a
N (%)	0.37 ± 0.10 b	0.33 ± 0.24 b	0.90 ± 0.10 c	0.15 ± 0.11 a
OC / N	13.91 ± 2.79 b	11.22 ± 3.32 ab	9.59 ± 1.37 a	8.56 ± 0.45 a

Table 3.2 Content of organic carbon (OC) and total nitrogen (N) in the size fractions, in g 100 g fraction^{-1}, isolated from the studied soils (CF = coniferous forest soils; BF = broadleaved forest soils; GL = grassland soils; TS = technosols). Data are averages ± standard deviations (n = 5). Data were log-transformed for ANOVAs and Duncan's test. Within a row, data followed by the same lowercase letter do not differ, at p = 0.05.

Size fraction	CF	BF	GL	TS
		a) Organic carbon (OC)		
2000-200 µm	8.61 ± 5.54 ab	1.76 ± 1.78 a	15.67 ± 11.08 b	5.59 ± 6.97 a
200-50 µm	6.71 ± 4.77 ab	4.41 ± 4.70 a	11.93 ± 4.08 b	1.64 ± 2.05 a
50-20 µm	8.99 ± 5.41 b	5.91 ± 6.20 ab	16.36 ± 2.86 c	1.50 ± 1.15 a
< 20 µm	4.73 ± 1.49 b	4.48 ± 2.93 b	9.17 ± 1.16 c	1.37 ± 0.84 a
		b) Total nitrogen (N)		
2000-200 µm	0.24 ± 0.12 a	0.06 ± 0.04 a	0.77 ± 0.61 b	0.34 ± 0.44 ab
200-50 µm	0.29 ± 0.21 a	0.24 ± 0.25 a	0.79 ± 0.22 b	0.15 ± 0.18 a
50-20 µm	0.33 ± 0.21 a	0.31 ± 0.35 a	1.08 ± 0.16 b	0.11 ± 0.08 a
< 20 µm	0.38 ± 0.12 b	0.40 ± 0.26 b	0.86 ± 0.13 c	0.14 ± 0.10 a
		c) OC / N ratio		
2000-200 µm	37.8 ± 11.8 b	24.6 ± 10.2 ab	20.8 ± 5.8 a	20.1 ± 6.7 a
200-50 µm	22.7 ± 7.8 b	15.9 ± 5.4 ab	15.0 ± 3.1 ab	12.2 ± 3.2 a
50-20 µm	27.5 ± 6.3 c	20.3 ± 5.7 b	15.3 ± 2.0 ab	14.5 ± 2.3 a
< 20 µm	12.4 ± 1.9 b	11.1 ± 0.9 ab	10.7 ± 0.5 a	10.2 ± 0.8 a

Table 3.3 Organic carbon (OC) and total nitrogen (N) in the fractions, as % of the total OC and N in the studied soils (CF = coniferous forest soils; BF = broadleaved forest soils; GL = grassland soils; TS = technosols). Data are averages ± standard deviations (n = 5). Data were log-transformed for ANOVAs and Duncan's test. Within a row, data followed by the same lowercase letter do not differ, at p = 0.05. No letters are given when no significant differences were detected.

Size fraction	CF	BF	GL	TS
a) Organic carbon (OC)				
2000-200 µm	17.71 ± 4.82 b	8.67 ± 5.97 a	3.28 ± 2.46 a	6.78 ± 2.54 a
200-50 µm	8.88 ± 1.83	8.84 ± 5.82	7.23 ± 1.46	6.99 ± 2.66
50-20 µm	10.66 ± 3.40	9.52 ± 3.86	12.04 ± 1.44	10.33 ± 4.05
< 20 µm	62.75 ± 3.03 a	72.97 ± 14.04 ab	77.45 ± 3.04 b	75.91 ± 8.08 b
b) Total nitrogen (N)				
2000-200 µm	7.62 ± 1.71 c	4.43 ± 2.14 b	1.71 ± 0.92 a	4.05 ± 2.15 ab
200-50 µm	6.48 ± 1.86	7.03 ± 3.82	5.62 ± 0.99	6.71 ± 3.33
50-20 µm	6.07 ± 1.30	6.21 ± 3.06	9.21 ± 1.62	7.81 ± 2.67
< 20 µm	79.82 ± 2.13	82.32 ± 7.99	83.47 ± 2.02	81.42 ± 8.02

Table 3.4 Amounts of organic carbon (OC) in the several SOF fractions isolated from the studied soils (CF = coniferous forest soils; BF = broadleaved forest soils; GL = grassland soils; TS = technosols), (a) as mg OC per g of OMC, and (b) as % of the total OC in the OMC. Data are averages ± standard deviations (n = 5). Data were log-transformed for ANOVAs and Duncan's test. Data in the same row followed by the same lowercase letter do not differ, at p = 0.05. If no letters are given, no significant differences were detected.

Fraction	CF	BF	GL	TS
		a) *Absolute amounts*		
K_2SO_4	1.50 ± 0.21 b	1.18 ± 0.77 b	1.70 ± 0.33 b	0.43 ± 0.38 a
Na-TB	2.46 ± 1.39 a	2.58 ± 1.69 a	11.07 ± 6.39 b	0.89 ± 0.23 a
Na-PP	6.05 ± 3.68 ab	5.11 ± 6.17 a	11.42 ± 3.94 b	1.92 ± 0.88 a
NaOH	5.55 ± 1.91 b	7.43 ± 5.77 b	17.75 ± 8.47 c	0.86 ± 1.40 a
H_2SO_4 + NaOH	1.77 ± 0.94 a	1.96 ± 1.82 a	4.72 ± 1.82 b	1.10 ± 0.52 a
Dith + NaOH	1.39 ± 0.83 ab	1.73 ± 1.68 ab	3.27 ± 2.39 b	0.54 ± 0.10 a
HF + NaOH	1.56 ± 0.80	1.15 ± 0.68	1.58 ± 0.69	1.88 ± 0.38
Humin	18.39 ± 5.83 b	17.34 ± 10.77 b	25.52 ± 5.37 b	5.84 ± 3.74 a
		b) *% of total recovered OC*		
K_2SO_4	4.06 ± 0.88 b	3.10 ± 1.13 ab	2.29 ± 0.62 a	2.90 ± 1.66 ab
Na-TB	5.79 ± 2.83 a	6.80 ± 3.08 ab	13.82 ± 6.70 b	7.02 ± 1.18 ab
Na-PP	14.22 ± 9.11	10.98 ± 8.10	14.54 ± 2.74	14.39 ± 2.83
NaOH	14.30 ± 2.28 b	19.36 ± 8.39 b	22.22 ± 5.89 b	4.18 ± 6.12 a
H_2SO_4 + NaOH	5.16 ± 3.32	5.01 ± 3.73	6.11 ± 2.07	8.80 ± 4.13
Dith + NaOH	3.88 ± 2.40	6.05 ± 7.09	4.65 ± 3.59	4.42 ± 1.11
HF + NaOH	4.60 ± 2.95 a	4.05 ± 3.31 a	2.00 ± 0.68 a	16.91 ± 8.24 b
Humin	48.00 ± 8.05 b	44.65 ± 9.71 ab	34.37 ± 11.03 a	41.38 ± 7.54 ab

Table 3.5 Amounts of nitrogen (N) in the several SOF fractions isolated from the studied soils (CF = coniferous forest soils; BF = broadleaved forest soils; GL = grassland soils; TS = technosols), (a) as µg N per 100 g of OMC, and (b) as % of the total N in the OMC. Data were log-transformed for ANOVAs and Duncan's test. Data in the same row followed by the same lowercase letter do not differ, at p = 0.05. If no letters are given, no significant differences were detected.

Fraction	CF	BF	GL	TS
		a) *Absolute amounts*		
K_2SO_4	7.13 ± 2.77 a	7.45 ± 5.90 a	27.77 ± 6.02 b	5.37 ± 7.27 a
Na-TB	26.71 ± 17.18 a	32.16 ± 29.07 a	165.0 ± 77.76 b	7.95 ± 3.53 a
Na-PP	13.18 ± 7.25 a	28.08 ± 36.91 a	76.77 ± 42.03 b	5.12 ± 7.14 a
NaOH	9.09 ± 5.54 a	19.91 ± 35.56 a	47.88 ± 18.07 b	0.48 ± 1.07 a
H_2SO_4 + NaOH	10.86 ± 20.25 a	0.50 ± 0.73 a	38.01 ± 20.75 b	0.71 ± 1.02 a
Dith + NaOH	14.67 ± 8.67 a	12.82 ± 22.47 a	64.25 ± 35.77 b	3.23 ± 4.45 a
HF + NaOH	0.41 ± 0.47	1.27 ± 1.65	1.92 ± 3.97	0.33 ± 0.50
Humin	161.4 ± 49.9 b	171.2 ± 124.4 b	242.3 ± 65.4 b	54.1 ± 40.1 a
		b) *% of total recovered N*		
K_2SO_4	2.92 ± 0.46	2.67 ± 0.76	4.20 ± 0.64	5.10 ± 3.35
Na-TB	10.33 ± 6.08 a	11.94 ± 4.55 ab	24.06 ± 8.20 b	11.85 ± 5.31 ab
Na-PP	5.15 ± 1.59 ab	7.86 ± 4.52 ab	11.17 ± 4.58 b	4.98 ± 3.69 a
NaOH	3.78 ± 2.27 b	4.14 ± 5.29 b	7.12 ± 2.08 b	0.26 ± 0.59 a
H_2SO_4 + NaOH	4.23 ± 7.62 ab	0.20 ± 0.33 a	5.52 ± 2.61 b	0.66 ± 0.95 a
Dith + NaOH	5.65 ± 2.53	10.40 ± 18.57	9.55 ± 5.19	6.41 ± 9.08
HF + NaOH	0.15 ± 0.15	0.97 ± 1.75	0.23 ± 0.46	0.36 ± 0.52
Humin	67.79 ± 14.16 b	61.51 ± 18.96 b	38.15 ± 15.46 a	68.72 ± 3.43 b

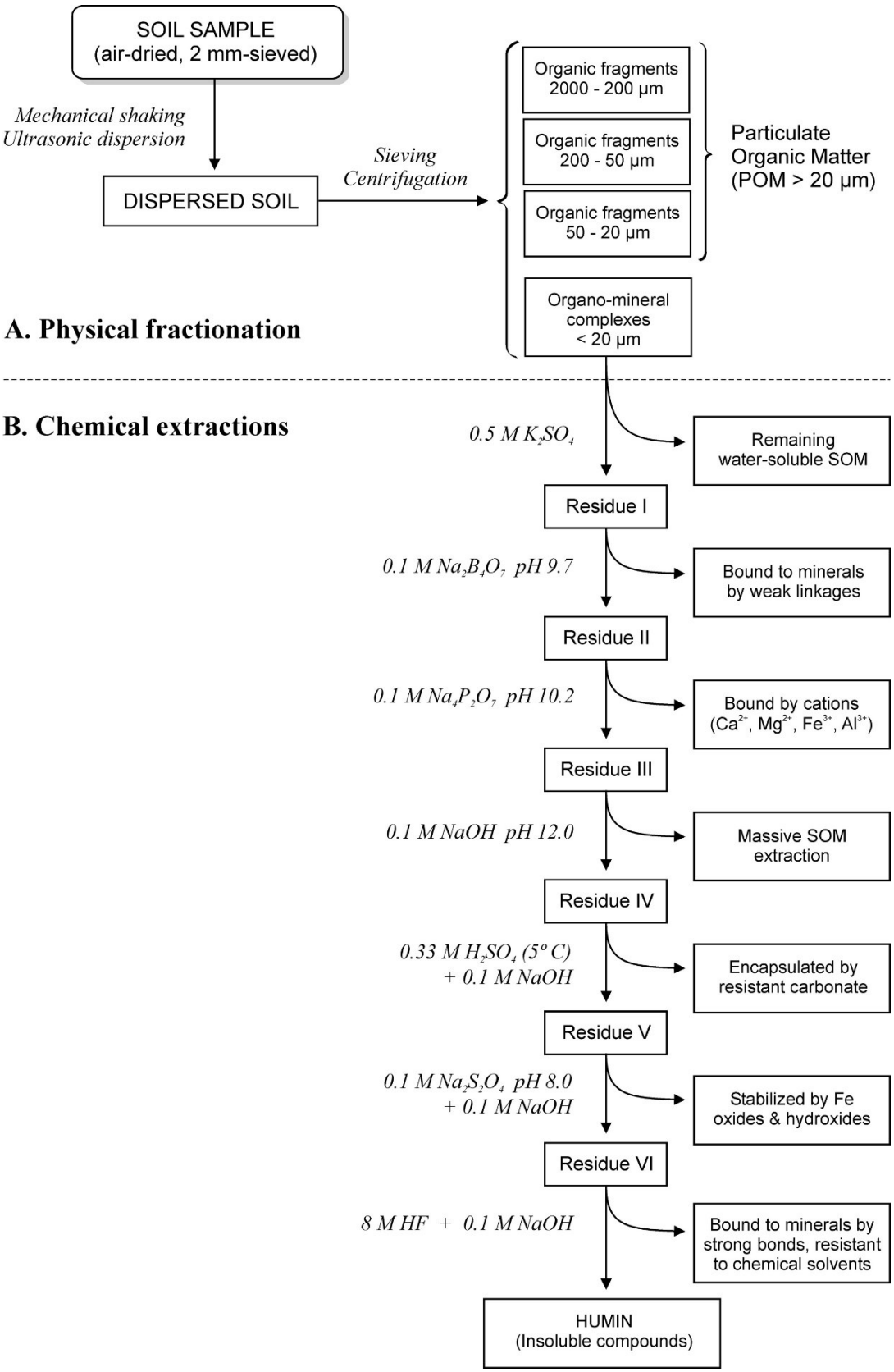

Figure 3.1 Flow diagram of the SOF method. Taken from Lopez-Sangil and Rovira (2013).

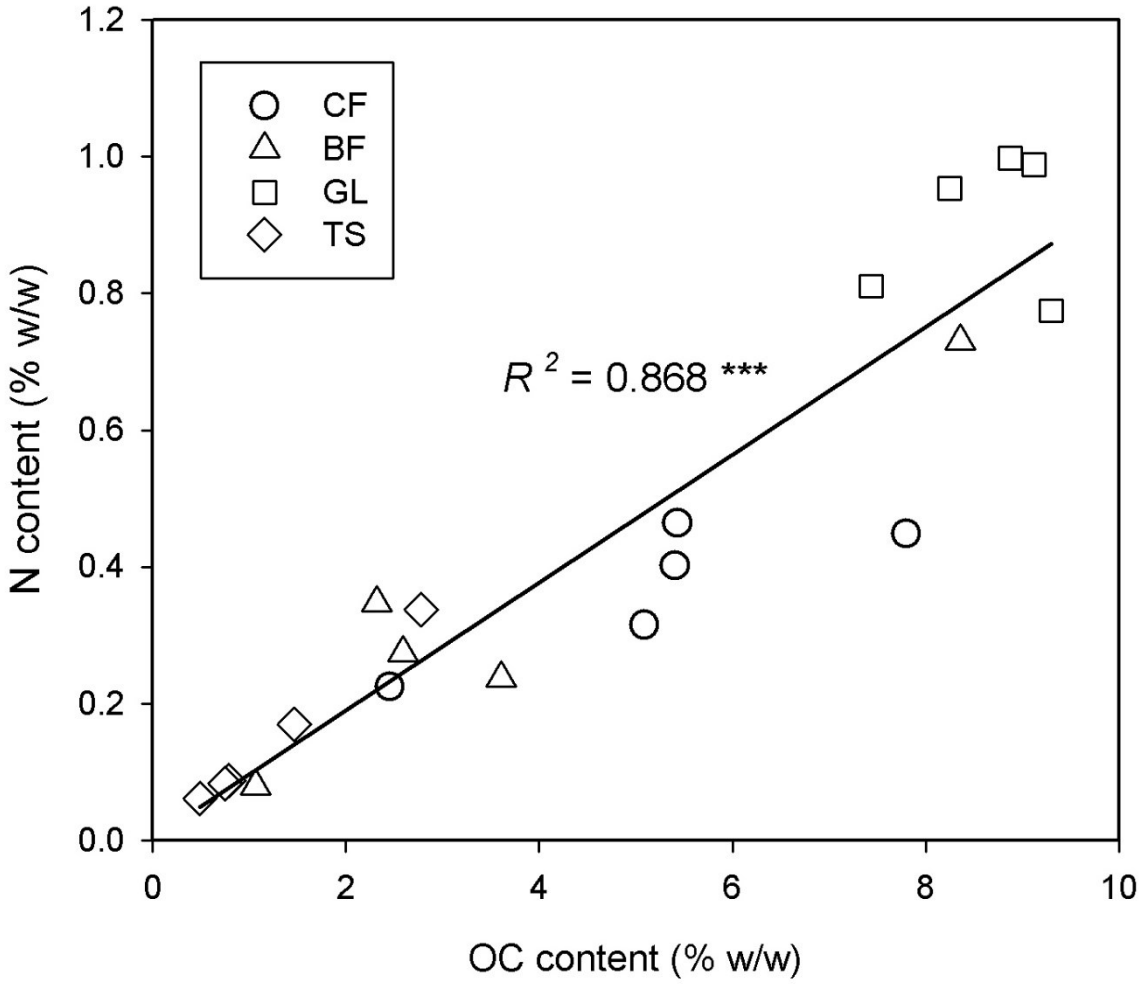

Figure 3.2 Relationships between OC and N in the studied soils. A: Linear correlation between OC and N content. B: Relationships between total OC in soil and OC/N ratio.

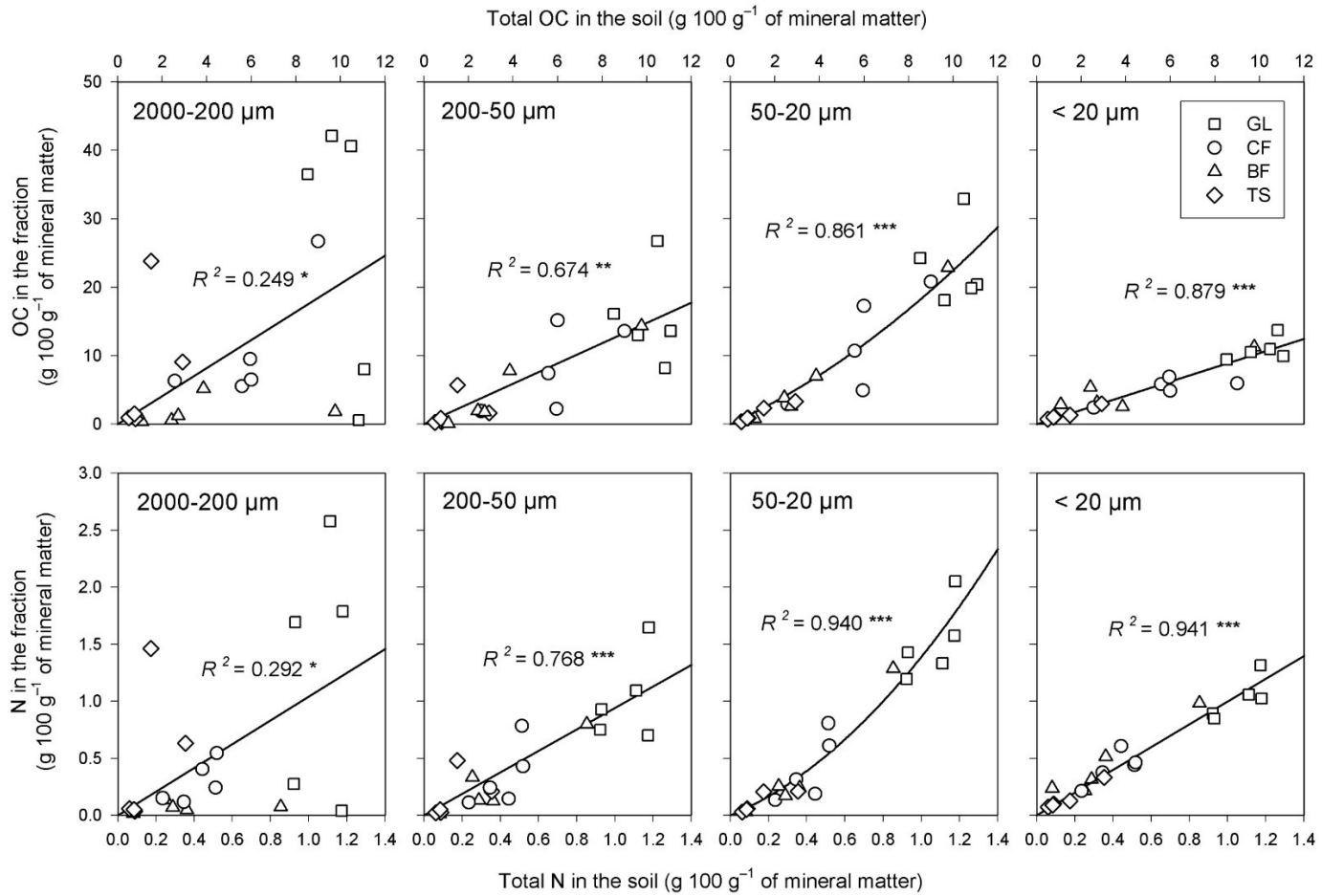

Figure 3.3 Relationships between total OC in the horizon and OC in each size fraction, and between total N in the horizon and N in the size fraction. Data have been fitted to polynomial equations of grade 1 or 2 (quadratic), of the type $Y = b_1X + b_2X^2$, in which b_2 may be zero. There is no b_0 value, and therefore the regression lines pass through the origin of coordinates (0,0). The signification of correlations is given: (*) at p = 0.05; (**) at p = 0.01; (***) at p = 0.001.

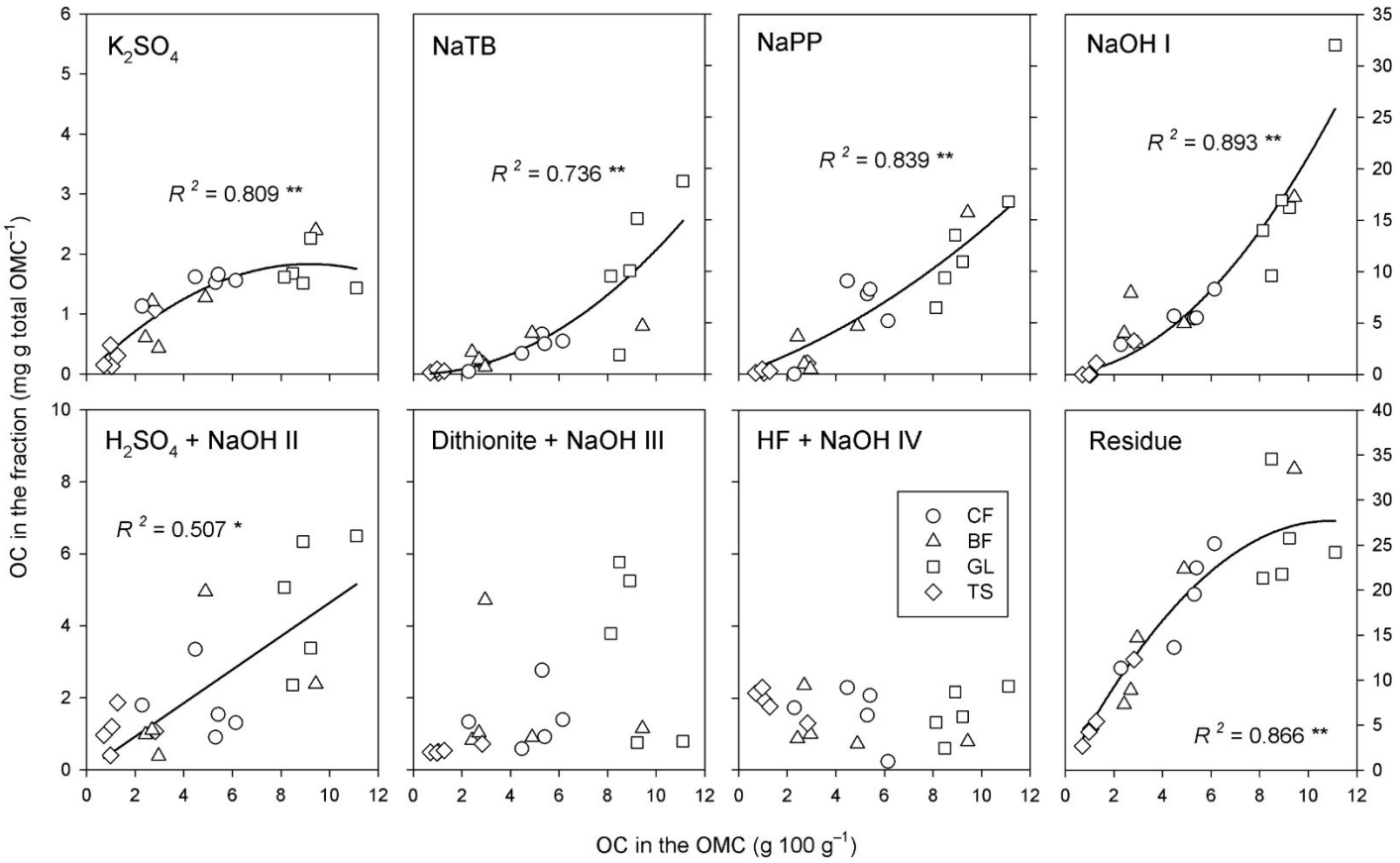

Figure 3.4 Relationships between total OC in the organomineral complex and OC in each SOF fraction. Data have been fitted to polynomial equations of grade 1 or 2 (quadratic), of the type $Y = b_1X + b_2X^2$, in which b_2 may be zero. There is no b_0 value, and therefore the regression lines pass through the origin of coordinates (0,0). The signification of correlations is given: (*) at p = 0.05; (**) at p = 0.01; (***) at p = 0.001.

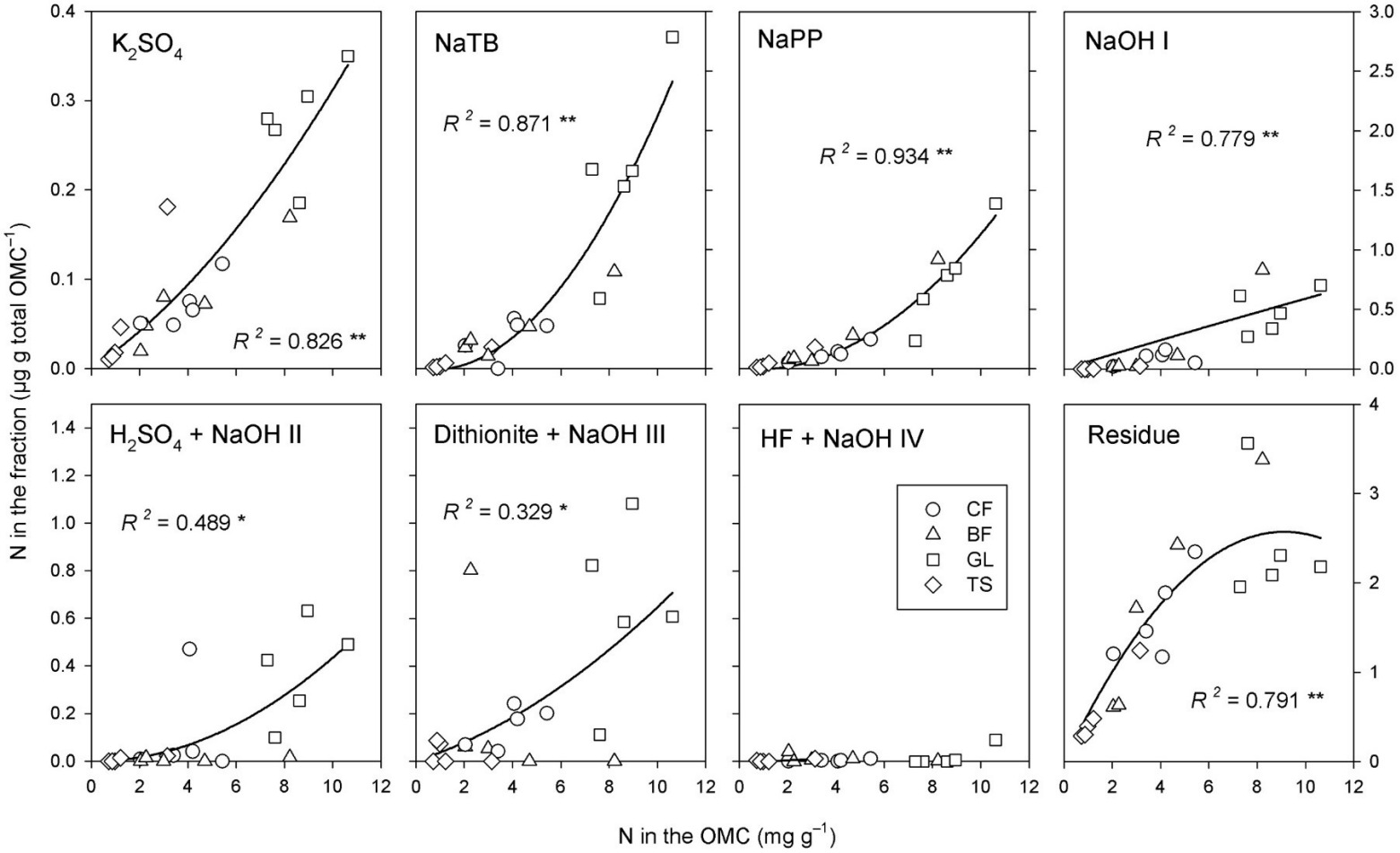

Figure 3.5 Relationships between total N in the organomineral complex and N in each SOF fraction. Data have been fitted to polynomial equations of grade 1 or 2 (quadratic), of the type $Y = b_1X + b_2X^2$, in which b_2 may be zero. There is no b_0 value, and therefore the regression lines pass through the origin of coordinates (0,0). The signification of correlations is given: (*) at p = 0.05; (**) at p = 0.01; (***) at p = 0.001.

4. The role of Fe(III) in soil organic matter stabilization in two size fractions having opposite features

(Giannetta, B., Zaccone, C., Plaza, C., Siebecker, M.G., Rovira, P., Vischetti, C., Sparks, D.L., 2019. Science of the Total Environment *653, 667-674)*

Abstract

Soil organic matter (SOM) protection, stability and long-term accumulation are controlled by several factors, including sorption onto mineral surfaces. Iron (Fe) has been suggested as a key regulator of SOM stability, both in acidic conditions, where Fe(III) is soluble, and in near neutral pH environments, where it precipitates as Fe(III) (hydr)oxides. The present study aimed to probe, by sorption/desorption experiments in which Fe was added to the system, the mechanisms controlling Fe(III)-mediated organic carbon (C) stabilization; fine silt and clay (FSi+Cl) and fine sand (FSa) SOM fractions of three soils under different land uses were tested. Fe(III) addition caused a decrease in the organic C remaining in solution after reaction, indicating an Fe-mediated organic C stabilization effect. This effect was two times larger for FSa than for FSi+Cl, the former fraction being characterized by both low specific surface area and high organic C content. The organic C retained in the solid phase after Fe-mediated stabilization has relatively low sensitivity to desorption. Moreover, attenuated total reflectance-Fourier transform infrared (ATR-FTIR) spectroscopy indicated that Fe-mediated organic C stabilization can be mainly ascribed to the formation of complexes between carbohydrate OH functional groups and Fe oxides. These results demonstrate that the binding of labile SOM compounds to Fe(III) contributes to its preservation, and that the mechanisms involved (flocculation *vs.* coating) depend on the size fractions.

4.1. Introduction

Soil organic matter (SOM) is widely known to be among the main factors affecting the quality of soils and their ability to provide essential ecosystem services. The decline of SOM has been highlighted as one of the main types of soil degradation, which is a major global issue with significant societal, economic and environmental impacts (FAO and ITPS, 2015). In fact, SOM has a role in virtually all physical, chemical and biological soil properties and is one of the largest carbon (C) stocks on the Earth's surface; consequently, soil organic carbon (SOC) plays a pivotal role in regulating the global C cycle (Amundson, 2001). The magnitude of the historic SOC loss due to inappropriate land management practices underlines the urgent need to develop strategies to restore or preserve organic matter in soils to help bolster productivity, prevent erosion and degradation, and mitigate climate change (Plaza et al., 2018a,b). Therefore, understanding the mechanisms of C sequestration in soils becomes fundamental to predict the response of SOC to climate change (Schmidt et al., 2011).

Carbon sequestration potential in soils has been mainly related to the size of mineral surface area (Feng et al., 2013) and to the clay content (Mayer, 1994; Hassink, 1997; Six et al., 2002; Kögel-Knabner et al., 2008). Representing an abundant constituent of the clay-size fraction, iron (Fe) (hydr)oxides have been suggested as an important phase forthe stabilization of SOC (Eusterhues et al., 2005; Lalonde et al., 2012; Sparks and Chen,2013; Chen et al., 2014, 2015, 2017). Fe(III) is ubiquitous in soils (range: 50-200 mmol kg^{-1}; Kappler and Straub, 2005); it is soluble under extremely acidic conditions, while it precipitates as Fe(III) (hydr)oxides in near-neutral pH environments.

The coprecipitation of Fe and soil organic matter (SOM) is therefore partly responsible for long-term C sequestration and affects both the mineral surface properties (e.g., specific surface area, surface charge, particle aggregation/dispersion) and the reactivity and structure of Fe (hydr)oxydes (von Lützow et al., 2006; Eusterhues et al., 2008). For example, Schwertmann (1966) demonstrated that the coprecipitation of SOM with Fe oxides affects Fe oxides crystal structure and inhibits the transformation into more stable forms (*e.g.,* ferrihydrite to goethite). Wagai and Mayer (2007) showed that the simple sorption of SOM onto metal oxide surfaces does not fully explain the critical role of Fe oxides for C storage; organo-metal precipitates and ternary SOM-Fe oxides-clay associations should be also responsible for C sequestration in soil.

Several studies have used model metal (hydr)oxide systems including pure Fe (hydr)oxides and Fe(III) complexation with dissolved organic matter (DOM) (Nierop et al., 2002; Eusterhues et al., 2008, 2011; Henneberry et al., 2012, Chen et al., 2014), peats (Karlsson and Persson, 2010), humic substances (Mikutta and Kretzschmar, 2011; Shimizu et al., 2013) and small organic acids (Yang et al., 2017) to investigate the role of SOM coprecipitation with Fe in terms of C storage (Lalonde et al., 2012; Chen et al., 2014). However, the molecular structure, species, and hydrolysis of Fe(III) in association with the functionally different fractions that comprise SOM, as well as the stability of SOM precipitated with Fe(III), have not been extensively examined.

According to Lopez-Sangil and Rovira (2013), the soil fraction <20 μm (*i.e.,* the fine silt and clay fraction; FSi+Cl) is involved in the protection of SOM from decomposer organisms. In this fraction, often referred to as organo-mineral complexes, SOM is stabilized by weak electrostatic interactions with clays, hydrogen bonds, precipitation by polyvalent cations (metal bridges) and association with Al and Fe oxides (Stevenson, 1994). On the other hand, the coarse fractions (i.e., sand and coarse silt) have low surface area and charge and thus are expected to be less relevant for organic C partitioning in soils. Nevertheless, it has been shown that also sand particles can be coated with Fe oxides through electrostatic forces, Van der Waals interactions, and Fe-O-Si bonds (Scheidegger et al., 1993), with consequences on adsorption phenomena and cation exchange capacity.

The main objective of this work was to fill this gap in the scientific literature and examine the chemical interactions between Fe species and physically-fractionated SOM pools linked to different conceptual stabilization mechanisms. For this purpose, two SOM fractions (*i.e.,* FSi+Cl and fine sand) extracted from three different soils under different land uses were tested in sorption/desorption experiments in which Fe was added to the system. In particular, FSi+Cl (<20 μm) represents the fraction with highest specific surface area (SSA) and is expected to be the most active fraction with respect to organic C and Fe(III) sorption, whereas the FSa (200-50 μm) is much coarser and was chosen as representative of soil particles with a much lower SSA but still potentially reactive with Fe(III) added in the sorption experiments. In this study, we (1) investigate the mechanisms of organic C sorption and stabilization promoted by Fe(III); (2) compare changes in N_2 accessible SSA in unreacted and reacted samples; (3) assess the main functional groups involved in organic C complexation and desorption experiments by means of attenuated total reflectance Fourier transform infrared (ATR-FTIR) spectroscopy.

4.2. Materials and methods

4.2.1. Soils and chemical analysis

Samples were collected from a coniferous forest (CF) soil, a grassland (GL) soil and an agricultural (AG) soil. The coniferous forest consisted mainly of *Pinus nigra* woodlands occurring at 630 m a.s.l., whereas the pasture, grown around 1000 m a.s.l., was dominated by meso- to xerophilous species (*e.g., Bromus erectus*). Mean annual temperatures at the sampling sites ranged from 9.7±6.1 to 13.7±6.7 °C, and mean annual precipitation was between 878 and 980 mm. The AG soil was located at 530 m a.s.l. in an area with a mean annual precipitation of 440 mm and a mean annual temperature of 14 ºC (Plaza et al., 2016). More information about these sites is given elsewhere (Giannetta et al., 2018).

Prior to analysis, soil samples were gently crushed and passed through a 2-mm sieve. Soil pH was measured on suspensions of 1:2.5 sample:water (Thomas, 1996), whereas electrical conductivity (EC) was measured on water extracts obtained at a sample-to water ratio of 1:5 (Rhoades, 1996). Soil texture was analyzed by the pipette method (Campbell et al., 1986). Organic C and total N contents were determined by dry combustion using a Thermo Flash 2000 NC Soil Analyzer. For organic C determination, soils were subjected to acid fumigation before the analysis to remove carbonates (Harris et al., 2001). Main soil properties are summarized in Table 4.1.

4.2.2. Physical fractionation of soil organic matter

Physical size fractionation by ultrasonic dispersion and wet sieving was performed, allowing for splitting particles into four different size fractions: coarse sand (CSa: 2000-200 µm diameter), fine sand (FSa: 200-50 µm), coarse silt (CSi: 50-20 µm) and fine silt and clay (FSi+Cl: <20 µm) (Lopez Sangil and Rovira, 2013). Ten g of each sample were put into 50 mL vials and filled with deionized water to 3/4 of their volume. Samples were then subjected to vertical agitation (20 rpm) for 60 minutes and to ultrasonic dispersion of the soil particles for 10 minutes at 60% of the total amplitude (100 W output) using a Branson 45 sonifier. The derived suspensions were then wet-sieved through a set of three sieves (200 µm, 50 µm and 20 µm hole) splitting particles into four different size fractions. The fractions retained by sieves (CSa, FSa, CSi) were directly recovered, quantitatively

transferred to pre-weighted vials and dried at 60 ºC to constant weight. The particles passing through the last sieve (<20 µm: FSi+Cl) were brought to ca. 1 L and left to stand refrigerated for 2 days; overlying water was then carefully siphoned off and discarded. The sediment was transferred into 250 mL polypropylene vials and centrifuged for 15 min at 2500 rpm. In the present research, we used and compared the FSi+Cl and FSa fractions. The organic C content of the isolated SOM fractions (OC_s) was determined as described above.

4.2.3. Sorption and desorption experiments

Fe(III)-SOM complexation was conducted following the methods proposed by Karlsson and Persson (2010) and Mikutta and Kretzschmar (2011). An aliquot (200 mg) of each fraction was weighted into a 50 mL polypropylene vial; acidified Fe(III) nitrate stock solution (12.15 mM) was added to each sample to reach a loading of 200 mg Fe /g OCs. The pH was monitored during the whole experiment and adjusted to 7±0.5 with 0.1 M KOH. The suspensions were shaken at 60 rpm for 24 hours and then centrifuged at 10,000 rpm for 20 minutes. The supernatant was removed and pressure filtered through a 0.2 µm polysulfone membrane filter. Filtrates were analyzed for both dissolved organic C (DOC), using a Vario TOC cube analyzer, and Fe concentration, by inductively coupled plasma mass spectrometry (ICP-MS) (Agilent 7500 Series). The amount of organic C remaining in solution after sorption (OC_{aq}) was obtained reporting DOC concentration as percentage of OCs. Sorption experiments were conducted in duplicate and at room temperature. SOM desorption from reacted samples was conducted 24 hours after sorption by adding 10 mL of 0.1 M NaH_2PO_4. The suspensions were shaken at room temperature for 24 hours at 60 rpm and then centrifuged at 10,000 rpm for 20 minutes. The supernatant was recovered, filtered through 0.2 µm membrane filter and then analyzed for DOC content (to calculate the organic C amount desorbed) and Fe concentration as described above. The desorption step was then repeated. The total amount of desorbed organic C (OC_{des}) was obtained by summing desorbed C concentrations resulting from both replicates, and data were expressed as percentage of the organic C remaining in the solid phase after sorption experiment (*i.e.,* OC_s-OC_{aq}). At the end of the sequence, the settled material was washed twice with deionized water and freeze-dried.

4.2.4. Specific surface area

The SSA of unreacted and reacted samples was determined by adsorption and desorption isotherms of N_2 at 77 K with a Micromeritics 2020 surface area analyzer. Freeze-dried samples were weighted into sample cells and outgassed under vacuum (10-3 mbar) at 298 K. The SSA was determined by the Brunauer–Emmett–Teller (BET) equation (Brunauer et al., 1938).

4.2.5. Attenuated total reflectance Fourier transform infrared spectroscopy

The ATR-FTIR spectra of reacted and unreacted samples were recorded after freeze drying with a Bruker Tensor 27. Samples were scanned over the 4000-600 cm^{-1} range, with a resolution of 2 cm^{-1} and 64 scans min^{-1}. Automatic baseline correction and normalization was applied to all spectra. Spectral analysis was performed using the Igor Pro 7 software.

4.3. Results and discussion

4.3.1. Physical and chemical characteristics of unreacted SOM fractions

For CF and GL, the OCs content in the FSa fraction (110 g kg^{-1}) is higher than that in FSi+Cl (54 and 85 g kg^{-1}, respectively), whereas for AG, the OC_s concentration in FSi+Cl is 5 times higher than that in FSa (18.1 vs. 3.6 g kg^{-1}) (Table 4.2). Therefore, the FSa fraction accounts for 9 (in AG) to 33% (in GL) of total organic C (TOC), whereas the FSi+Cl contains 11 (in CF) to 46% (in AG) of TOC. The different distribution and concentration of organic C among SOM pools mirrors differences in terms of inputs and mineralization rates across ecosystems (Oades, 1988). In the AG soil, an increased aggregate disruption and aeration due to tillage probably resulted in a preferential SOM accumulation in the FSi+Cl fraction (*e.g.,* Weismeier et al., 2014); conversely, forest and grassland soils accumulated more organic C in the sand size fractions, as also found in previous studies (Christensen, 1992; Hassink, 1997).

As expected, FSi+Cl fractions show much higher SSA than FSa, with values ranging from 3.4 (GL) to 20.8 m^2 g^{-1} (CF) and from 0.1 (GL) to 1.8 m^2 g^{-1} (CF), respectively (Fig. 4.1). This is due to the different mineralogy characterizing both fractions.

The ATR-FTIR spectra of the unreacted FSi+Cl fractions of GL and CF show a predominant broad band centered around 1420 cm^{-1}, which reveals the presence of symmetric COO^- stretching (Chorover and Amistadi, 2001) (Fig. 4.2). Udvardi et al. (2014) attributed the band at 1428 cm^{-1} to calcite asymmetric CO_3^{2-} stretching, paired with the calcite CO_3^{2-} out of plane bending mode at 874 and 714 cm^{-1}. The simultaneous occurrence of these peaks represents a common feature for GL and CF spectra. The dominant broad band at 1000-1100 cm^{-1}, found in all spectra, may be indicative of stretching of carbohydrate and polysaccharides-like substances (Fu and Quan, 2006). Several other studies have suggested that thermally labile, microbial derived materials and easily metabolizable compounds (e.g., carbohydrates, amino acids, nucleic acids) occur in significant proportions in the mineral-associated organic matter fraction (Kleber et al. 2011; Hatton et al. 2012; Keiluweit et al. 2012; Plaza et al. 2013, 2016; Zaccone et al., 2018). At the same time, however, Si-O-Fe and Al-Al-OH bonds of several (alumino)silicates may also cause absorption between 900 and 1000 cm^{-1} (*e.g.,* Nguyen et al., 1991; Fritzsche et al., 2015).

The ATR-FTIR spectra of the FSa fractions reveal differences due to the presence of symmetric carboxylate group peaks around 1640 cm^{-1} in CF and GL. Unlike the spectra of the FSi+Cl fractions, those of the FSa fractions exhibit a peak at 1420 cm^{-1} for CF and GL. The lower intensity of carbohydrate peaks suggests the comparatively scarce presence of labile organic materials in coarse fractions (Ladd et al., 1996; Paul, 2016 and refs. therein), where they act as binding agents in stable aggregates (Tisdall and Oades, 1982). Peaks at 796 and 777 cm^{-1} are generally ascribed to symmetric stretching of Si-O of quartz (Udvardi et al., 2014), being quartz one of the main mineral characterizing the sand.

4.3.2. Sorption experiments

After the sorption experiments, from 99.6 to 100% of Fe(III) added was removed from solution (Table 4.2). The percent of organic C remaining in solution (OC_{aq}) after Fe(III) sorption decreased with increasing amounts of added Fe ($R = -0.729$; $p=0.040$) and, consequently, with increasing OC_s contents in the fractions ($R = -0.727$; $p=0.041$).

In CF and GL, the Fe ions stabilizing effect is more evident for FSa than for FSi+Cl, with OC_s values in the latter fraction that are almost twice as large; an opposite trend is observed for AG, where three times more organic C from the FSa fraction remained in

solution after reaction with Fe ions as compared to the corresponding FSi+Cl fraction (Table 4.2). Moreover, although the SSA of AG FSa is 0.3 and 7 times that of CF and GL FSa, respectively (Fig. 4.1), the OC_{aq} is 15 times higher (Table 4.2). According to the soil C saturation concept, soil C storage efficiency decreases as a soil approaches C saturation (Stewart et al., 2007). Chen et al. (2014) hypothesized that organic C can be better protected in soils with a low rather than high SOM content, i.e., that SOM adsorbed in excess is not efficiently protected. Thus, the stability of organic C bound onto mineral surfaces decreases with increasing of C loading as the organo-mineral bonding strength becomes weaker (Feng et al., 2014). This would indicate that soils with lower initial TOC should be able to sorb C stronger than soils with higher initial TOC; however, our results suggest that the AG soil, with the lowest TOC content (11.8 g kg^{-1}; Table 4.1), has the least C storage efficiency (Table 4.2), which might be attributed to differences in mineralogical properties and/or land use.

4.3.3. Properties of sorption complexes

The reaction with Fe(III) possibly causes two opposite effects on SSA, *i.e.,* either a considerable decrease of SSA, mainly occurring in the FSi+Cl fractions (with the exception of GL soil), or an increase of SSA values, mainly occurring in the FSa fractions (with the exception of AG soil) (Fig. 4.1). The decrease of SSA is probably due to the flocculation induced by precipitated Fe(III) which adsorbed onto clay surfaces. For example, Shanmuganathan and Oades (1982) described Fe(III) adsorption on clay negative charges causing the flocculation of fine particle into microaggregates (50-250 μm) with a consequent decrease in SSA. The formation of ternary SOM-Fe oxides-clay associations (Oades, 1984) and the aggregation of nanoparticles in DOM-ferrihydrite precipitates causing the inaccessibility of the surface to N_2 adsorption (Schwertmann et al., 2005) could also explain this phenomenon. On the other hand, the increase of SSA could be ascribed to a coating process. Penn et al. (2001), for example, provided evidence for the sorption of Fe(III) onto quartz surfaces in near-neutral pH and the formation of Fe oxide minerals, where coatings dominated the reactive SSA. Scheidegger et al. (1993) reported increased SSA in FSa after reaction of silica sand with Fe(III) oxides, suggesting that almost the whole surface of Fe(III) oxides could be available for N_2 adsorption. The binding of Fe oxides on sand (silica) surfaces appeared irreversible (Scheidegger et al., 1993) and not due simply to electrostatic forces.

Therefore, our results suggest that samples with higher organic C content can be stabilized by added Fe(III), probably through the formation of bonds between surface hydroxyl groups of precipitated Fe(III) oxides and the acidic functional groups of SOM fractions. However, in the fractions characterized by lower OCs contents (*i.e.,* AG FSa and AG FSi+Cl), the percentage of organic C released in the solution was higher, thus suggesting a lower Fe stabilizing effect. The main SOM functional groups involved in Fe binding seem to be related to carbohydrates (Eusterhues et al., 2011, 2014; Karlsson and Persson, 2012; ThomasArrigo et al., 2014); small differences in carbohydrates peaks in AG can be indicative of labile SOM already associated with minerals as well as of mononuclear Fe-SOM complexes (Karlsson and Persson, 2012). Conversely, for GL and CF, in both FSi+Cl and FSa fractions, an increase in the carbohydrates band relative intensity (1000-1100 cm^{-1}) is observed after the reaction. This indicates the possible formation of inner-sphere surface complexes between the carbohydrates OH functional groups and the Fe atoms (Eusterhues et al., 2011; 2014). Karlsson and Persson (2012) found major spectral changes in the carbohydrate region around 1080 cm^{-1}, whereas carboxylate groups seemed marginally involved in the formation of ferrihydrite (very small ferrihydrite particles can be stabilized by an encapsulating layer of polysaccharides).

In our study, in both FSi+Cl and FSa of GL and CF, the absence of shifts in the asymmetric carboxylate peak correlated to changes in carbohydrate stretching, which suggests the formation of surface complexes between carbohydrates with ferrihydrite of neo-formation. Many other studies (*e.g.,* Kaiser et al, 1997; Wagai and Mayer, 2007) proposed a ligand exchange mechanism for sorption of SOM through the Fe(III) oxides hydroxyl groups to carboxylic groups of SOM. However, the role of Fe oxides (*e.g.,* ferrihydrite) on carbohydrates decomposition is already known; for example, Miltner and Zech (1998) showed that ferrihydrite reduced SOM decomposition by 12% and carbohydrate decomposition by 15%, whereas Nuclear Magnetic Resonance spectroscopy studies conducted by Schwertmann et al. (2005) suggested the involvement of functional groups from carbohydrates in the interaction with Fe. Furthermore, Gu et al. (1994) obtained for hematite a strong absorption peak at 1000-1100 cm^{-1}, indicating sorption of carboxylate C-O groups, possibly via H-bonds.

4.3.4. Desorption experiments

Most of the organic C release occurs at the first desorption step (Fig. 4.3a). After the first desorption (i.e., reaction with NaH_2PO_4), the organic C released ranged from 0.5% (in the FSa fraction of both CF and GL) to 4.9% (in AG FSi+Cl). Lower amounts of organic C were released from the second desorption step, i.e., from 0% (in GL FSi+Cl) to 3.5% (in AG FSa) (Fig. 4.3a). The occurrence of SOM that is not desorbed during the first step indicates a continuum in the strength of the association with Fe forms, i.e., weakly complexed SOM is removed during the first desorption step, while more tightly bound SOM is removed during the second desorption step.

With respect to the organic C released after both desorption steps (OC_{des}), the highest loss was observed for the AG FSa fraction (8%), characterized by the lowest OCs content, and AG FSi+Cl fraction (5.7%) (Table 4.2). Desorption data confirm Fe-mediated stabilization of organic C in the FSa fraction of CF and GL, with losses of C in the solution being 0.7 and 0.6% of the total, respectively (Table 4.2). For the FSa fraction of CF and GL, the much lower organic C desorption from the reacted samples may be ascribed to a stronger sorption extent for polysaccharide-associated C with Fe. Thus, sorption of SOM to precipitated Fe(III) in the reacted samples, either via adsorption or coprecipitation, can explain the decrease in SOM release.

With an increase in Fe(III) added, there is also a decrease in organic C released from samples. This is particularly evident after the second round of desorption (Fig. 4.3b). Samples reacted with more Fe(III) tend to have more organic C retained on their surfaces. The percentage of organic C in solution after reaction with Fe(III) (*i.e.,* OC_{aq}) is significantly ($p < 0.001$) correlated to that released after the second desorption step (Fig. 4.4); this also indicates that organic C with higher added Fe(III) content is also more strongly bound to the solid phase and, therefore, resistant to release. Small changes between adsorption and desorption indicate irreversible binding of SOM to the mineral solid phase. In ATR-FTIR spectra of AG FSi+Cl, small changes in carbohydrate stretching after desorption seem to indicate that carbohydrates are already strongly bound to clays and not reactive to Fe stabilization (Fig. 4.2). Our data are in agreement with Kaiser and Guggenberger (2000) who reported strong bonding between organic C and hydrous oxides by ligand exchange, resulting in a negligible desorption of organic molecules. The same authors ascribed the low release of SOM from Fe oxyhydroxides to

multiple ligands involved in bonding to the sorbent surface. Irreversible sorption has been also reported by Kaiser and Guggenberger (2007) and Mikutta et al. (2007).

4.4. Conclusions

Both sorption and desorption experiments provide evidence that SOM in the FSa fraction is generally more strongly stabilized by Fe(III) addition than in the FSi+Cl fraction. Organic C retained after Fe-mediated stabilization is also less sensitive to desorption, and this stabilization effect is more evident with higher Fe concentration added. The reaction with Fe(III) caused two opposite effects on SSA, *i.e.,* either a decrease in SSA mainly occurring in the FSi+Cl fractions and probably due to flocculation, or an increase of SSA values, probably due to coating. Interestingly, the AG soil often constitutes an exception, probably because of the nature of its SOM. Additional studies need to be performed to understand the stability of proposed Fe-organic C complexes, unraveling the role played by different land uses and/or mineralogical properties, as well as to elucidate the proposed mechanisms. Improvements in our mechanistic knowledge of SOM stabilization like this will be useful to better understand land degradation processes related to the decline of SOM, and to develop strategies to fight against it.

The ATR-FTIR data suggest that carbohydrates are associated to Fe(III) oxides by surface complexation, possibly by an inner-sphere ligand exchange mechanism, as suggested in the literature (Kaiser and Guggenberger, 2000) (this was observed mainly in FSa). The formation of coprecipitated SOM with Fe-oxides is also possible. The irreversible nature of this complexation is confirmed by the reaction with Fe(III), where increasing added Fe(III) correlated to a decrease in OC_{des}. Sorption and desorption data paired with SSA and ATR-FTIR demonstrate that in the AG soil the absence of the involvement of carbohydrate functional groups in ligand exchange bonds with Fe leads to higher organic C release after sorption and desorption experiments.

References

Amundson, R., 2001. The carbon budget in soils. Annual Review of Earth and Planetary Sciences 29, 535-562.

Brunauer, S., Emmet, P.H., Teller, E., 1938. Adsorption of Gases in Multimolecular Layers. Journal of the American Chemical Society 60, 309-319.

Campbell, G.S., Nielsen, D.R., Jackson, R.D., Mortland, M.M., Klute, A., 1986. Methods of Soil Analysis Part 1-Physical and Mineralogical Methods (2nd ed.) SSSA Book Series 5.1 SSSA-ASA, Madison, WI.

Chen C., Kukkadapu, R.K., Lazareva, O., Sparks, D.L., 2017. Solid-Phase Fe Speciation along the Vertical Redox Gradients in Floodplains using XAS and Mössbauer Spectroscopies. Environmental Science and Technology 51, 7903−7912.

Chen, C., Dynes, J.J., Wang, J., Sparks, D.L., 2014. Properties of Fe-Organic Matter Associations via Coprecipitation versus Adsorption. Environmental Science and Technology 48, 13751-13759.

Chen, C., Sparks, D.L., 2015. Multi-elemental scanning transmission X-ray microscopy–near edge X-ray absorption fine structure spectroscopy assessment of organo–mineral associations in soils from reduced environments. Environmental Chemistry 12, 64-73.

Chorover, J., Amistadi, M.K., 2001. Reaction of forest floor organic matter at goethite, birnessite and smectite surfaces. Geochimica et Cosmochimica Acta 65, 95-109.

Christensen, B. T., 1992. Physical fractionation of soil and organic matter in primary particle size and density separates. Advances in Soil Science 20, 1–90.

Eusterhues, K., Neidhardt, J., Hädrich, A., Küsel, K., Totsche, K.U., 2014. Biodegradation of ferrihydrite-associated organic matter. Biogeochemistry 119, 45-50.

Eusterhues, K., Rennert, T., Knicker, H., Kögel-Knabner, I., Totsche, K.U., Schwertmann, U., 2011. Fractionation of Organic Matter Due to Reaction with Ferrihydrite: Coprecipitation versus Adsorption. Environmental Science and Technology 45, 527-533.

Eusterhues, K., Rumpel, C., Kögel-Knabner, I., 2005. Organo-mineral associations in sandy acid forest soils: Importance of specific surface area and iron oxides and micropores. European Journal of Soil Science 56, 753-763.

Eusterhues, K., Wagner, F.E., Häusler, W., Hanzlik, M., Knicker, H., Totsche, K.U., Kögel-Knabner, I., Schwertmann, U., 2008. Characterization of Ferrihydrite-Soil Organic Matter Coprecipitates by X-ray Diffraction and Mössabuer Spectroscopy. Environmental Science and Technology 42, 7891-7897.

FAO, ITPS, 2015. Status of the World's Soil Resources (SWSR) – Main Report. Food and Agriculture Organization of the United Nations and Intergovernmental Technical Panel on Soils, Rome, Italy.

Feng, W., Plante, A.F., Aufdenkampe, A.K., Six, J., 2014. Soil organic matter stability in organo-mineral complexes as a function of increasing C loading. Soil Biology and Biochemistry 69, 398-405.

Feng, W., Plante, A.F., Six, J., 2013. Improving estimates of maximal organic carbon stabilization by fine soil particles. Biogeochemistry 112, 81-93.

Fritzsche, A., Schröder, C., Wieczorek, A.K., Händel, M., Ritschel, T., Totsche, K.U., 2015. Structure and composition of Fe-OM co-precipitates that form in soil-derived solutions. Geochimica et Cosmochimica Acta 269, 167-183.

Fu, H., Quan, X., 2006. Complexes of fulvic acid on the surface of hematite, goethite, and akaganeite: FTIR observation. Chemosphere 63, 403-410.

Giannetta, B., Plaza, C., Vischetti, C., Cotrufo, M.F., Zaccone, C., 2018. Distribution and thermal stability of physically and chemically protected organic matter fractions in soils across different ecosystems. Biology and Fertility of Soils 54, 671-681.

Gu, B., Schmitt, J., Chen, Z., Liang, L., McCArty, J.F., 1994. Adsorption and Desorption of Natural Organic Matter on Iron Oxide: Mechanisms and Models. Environmental Science and Technology 28, 38-46.

Harris, D., Horwath, W.R., van Kessel, C., 2001. Acid fumigation of soils to remove carbonates prior to total organic carbon or carbon-13 isotopic analysis. Soil Science Society of America Journal 65, 1853–1856.

Hassink, J., 1997. The capacity of soils to preserve organic C and N by their association with clay and silt particles. Plant and Soil 191, 77–87.

Hatton, P.-J., Kleber, M., Zeller, B., Moni, C., Plante, A.F., Townsend, K., Gelhaye, L., Lajtha, K., Derrien, D., 2012. Transfer of litter-derived N to soil mineral–organic associations: Evidence from decadal 15N tracer experiments. Organic Geochemistry 42, 1489-1501.

Henneberry, Y.K., Kraus, T.E.C., Nico, P.S., Horwath, W.R., 2012. Structural stability of coprecipitated natural organic matter and ferric iron under reducing conditions. Organic Geochemistry 48, 81-89.

Kaiser, K., Guggenberger, G., 2000. The role of DOM sorption to mineral surfaces in the preservation of organic matter in soils. Organic Geochemistry 31, 711-725.

Kaiser, K., Guggenberger, G., 2007. Sorptive stabilization of organic matter by microporous goethite: sorption into small pores vs. surface complexation. European Journal of Soil Science 58, 45-59.

Kappler, A., Straub, K.L., 2005. Geomicrobiological Cycling of Iron. Reviews in

Mineralogy and Geochemistry 59, 85-108.

Karlsson, T., Persson, P., 2010. Coordination chemistry and hydrolysis of Fe (III) in a peat humic acid studied by X-ray absorption spectroscopy. Geochimica et Cosmochimica Acta 74, 30-40.

Karlsson, T., Persson, P., 2012. Complexes with organic matter suppress hydrolysis and precipitation of Fe(III). Chemical Geology 322-323, 19-27.

Keiluweit, M., Bougoure, J.J., Zeglin, L., Myrold, D.D., Weber, P.K., Pett-Ridge, J., Kleber, M., Nico, P.S., 2012. Nano-scale investigation of the association of microbial nitrogen residues with iron (hydr)oxides in a forest soil O-horizon. Geochimica et Cosmochimica Acta 95, 213-226.

Kleber, M., Nico, P.S., Plante, A., Filley, T., Kramer, M., Swanston, C., Sollins, P., 2011. Old and stable soil organic matter is not necessarily chemically recalcitrant: implication for modeling concepts and temperature sensitivity. Global Change Biology 17, 1097-1107.

Kögel-Knabner, I., Guggenberger G., Kleber M., Kandeler, E., Kalbitz, K., Scheu, S., Eusterhues, K., Leiweber, P., 2008. Organo-mineral associations in temperate soils: integrating biology, mineralogy, and organic matter chemistry. Journal of Plant Nutrition and Soil Science 171, 61-82.

Ladd, J.N., Foster, R.C., Nannipieri, P., Oades, J.M., 1996. Soil structure and biological activity. In: Stotzky G and Bollag J-M (eds) Soil Biochemistry, vol 9. Marcel Dekker, New York, pp 23-78.

Lalonde, K., Mucci, A., Ouellet, A., Gélinas, Y., 2012. Preservation of organic matter in sediments promoted by iron. Nature 483, 198-200.

Lopez-Sangil, L., Rovira, P., 2013. Sequential chemical extractions of the mineralassociated soil organic matter: An integrated approach for the fractionation of organomineral complexes. Soil Biology and Biochemistry 62, 57-67.

Mayer, L.M., 1994. Surface area control of organic carbon accumulation in continental shelf sediments. Geochimica et Cosmochimica Acta 58, 1271–1284.

Matson, P.A., Parton, W.J., Power, A.G., Swift, M.J., 1997. Agricultural intensification and ecosystem properties. Science 277, 504-509.

Mikutta, C., Kretzschmar, R., 2011. Spectroscopic evidence for ternary complex formation between arsenate and ferric iron complexes of humic substances. Environmental Science and Technology 45, 9550-9557.

Mikutta, R., Mikutta, C., Kalbitz, K., Scheel, T., Kaiser, K., Jahn, R., 2007.

Biodegradation of forest floor organic matter bound to minerals via different binding mechanisms. Geochimica et Cosmochimica Acta 71, 2569-2590.

Miltner, A., Zech, W., 1998. Carbohydrate decomposition in beech litter as influenced by aluminium, iron and manganese oxides. Soil Biology and Biochemistry 30, 1-7.

Nguyen, T.T., Janik, L.J., Raupach, M., 1991. Diffuse reflectance infrared Fourier transform (DRIFT) spectroscopy in soil studies. Australian Journal of Soil Research 29, 49–67.

Nierop, K.G.J., Jansen, B., Verstraten, J.M., 2002. Dissolved organic matter, aluminum and iron interactions: precipitation induced by metal/carbon ratio, pH and competition. Science of the Total Environment 300, 201-211.

Oades, J.M., 1984. Soil organic matter and structural stability: mechanisms and implications for management. Plant and Soil 76, 319-337.

Oades, J.M., 1988. The retention of organic matter in soils. Biogeochemistry 5, 35-70.

Paul, E.A., 2016. The nature and dynamics of soil organic matter: Plant inputs, microbial transformations, and organic matter stabilization. Soil Biology and Biochemistry 98, 109–126.

Penn, R.L., Zhu, C., Xu, H., Veblen, D.R., 2001. Iron oxide coatings on sand grains from the Atlantic coastal plain: High-resolution transmission electron microscopy characterization. Geology 29, 843-646.

Plaza, C., Gascó, G., Méndez, A.M., Zaccone, C., Maestre, F.T., 2018a. Soil organic matter in dryland ecosystems. In: García, C., Nannipieri, P., Hernández, T. (Eds.). The Future of Soil Carbon. Its conservation and formation, Elsevier, pp. 39-70 (doi: 10.1016/B978-0-12-811687-6.00002-X).

Plaza, C., Giannetta, B., Fernández, J.M., López-de-Sá, E.G., Polo, A., Gascó, G., Méndez, A., Zaccone, C., 2016. Response of different soil organic matter pools to biochar and organic fertilizers. Agriculture, Ecosystems and Environment 225, 150-159.

Plaza, C., Zaccone, C., Sawicka, K., Méndez, A.M., Tarquis, A., Gascó, G., Heuvelink, G.B.M., Schuur, E.A.G., Maestre, F.T., 2018b. Soil resources and element stocks in drylands to face global issues. Scientific Reports 8, 13788.

Post, W.M., Kwon, K.C., 2000. Soil carbon sequestration and land-use change: processes and potential. Global Change Biology 6, 317-327.

Rhoades, J.D., 1996. Salinity: Electrical Conductivity and Total Dissolved Solids. In: Sparks DL (ed) Methods of Soil Analysis, Part 3-Chemical methods. SSSA Book

Series 5.3 SSSA-ASA, Madison, WI, pp 417-435.

Scheidegger, A., Borkovec, M., Sticher, H., 1993. Coating of silica sand with goethite: preparation and analytical identification. Geoderma 58, 43-65.

Schmidt, M.W.I., Torn, M.S., Abiven, S., Dittmar, T., Guggenberger, G., Janssens, I.A., Kleber, M., Kögel-Knabner, I., Lehmann, J., Manning, D.A.C., Nannipieri, P., Rasse, D.P., Weiner, S., Trumbore, S.E., 2011. Persistence of soil organic matter as an ecosystem property. Nature 478, 49-56.

Schmizu, M., Zhou, J., Schröder, C., Obst, M., Kappler, A., Borch, T., 2013. Dissimilatory Reduction and Transformation of Ferrihydrite-Humic Acid Coprecipitates. Environmental Science and Technology 47, 13375-13384.

Schwertmann, U., 1966. Inhibitory effect of soil organic matter on the crystallization of amorphous ferric hydroxide. Nature 212, 645-646.

Schwertmann, U., Wagner, F., Knicker, H., 2005. Ferrihydrite-Humic Associations: Magnetic Hyperfine Interactions. Soil Science Society of America Journal 69, 1009-1015.

Shanmuganathan, R.T., Oades, J.M., 1982. Modification of soil physical properties by manipulating the net surface charge on colloids through addition of Fe (III) polycations. Journal of Soil Science 33, 451-465.

Six, J., Callewaert, P., Lenders, S., De Gryze, S., Morris, S.J., Gregorich, E.G., Paul, E.A., Paustian, K., 2002. Measuring and Understanding Carbon Storage in Afforested Soils by Physical Fractionation. Soil Science Society of America Journal 66, 1981-1987.

Sparks, D.L., Chen, C., 2013. The Role of Mineral Complexation and Metal Redox Coupling in Carbon Cycling and Stabilization. Functions of Natural Organic Matter in Changing Environment in Xu, J., Wu, J., He, Y., (Eds.), Functions of Natural Organic Matter in Changing Environment. Zhejiang University Press and Springer Science+Business Media, Dordrecht, pp. 7-12.

Stevenson, F.J., 1994. Humus chemistry. Genesis, composition, reactions, second ed. Wiley, New York.

Stewart, C.E., Paustian, K., Conant, R.T., Plante, A.F., Six, J., 2007. Soil carbon saturation: concept, evidence and evaluation. Biogeochemistry 86, 18-31.

Thomas, G.W., 1996. Soil pH and Soil Acidity. In: Sparks DL (ed) Methods of Soil Analysis, Part 3-Chemical methods. SSSA Book Series 5.3 SSSA-ASA, Madison, WI, pp 475-490.

ThomasArrigo, L.K., Mikutta, C., Byrne, J., Barmettler, K., Kappler, A., Kretzschmar,

R., 2014. Iron and Arsenic Speciation and Distribution in Organic Flocs from Streambeds of an Arsenic-Enriched Peatland. Environmental Science and Technology 48, 13218- 13228.

Tisdall, J.M., Oades, J.M., 1982. Organic matter and water-stable aggregates in soils. Journal of Soil Science 33, 141-163.

Udvardi, B., Kovács, I.J., Kónya, P., Földvári, M., Füri, J., Budai, F., Falus, G., Fancsik, T., Szabó, C., Szalai, Z., Mihály, J., 2014. Application of attenuated total reflectance Fourier transform infrared spectroscopy in the mineralogical study of a landslide area, Hungary. Sedimentary Geoogy. 313, 1-14.

von Lützow, M., Kögel-Knabner, I., Ekschmitt, K., Matzner, E., Guggenberger, G., Marschner, B., Flessa, H., 2006. Stabilization of organic matter in temperate soils: mechanisms and their relevance under different soil conditions-a review. European Journal of Soil Science 57, 426-445.

Wagai, R., Mayer, L.M., 2007. Sorptive stabilization of organic matter in soils by hydrous iron oxides. Geochimica et Cosmochimica Acta 71. 25-35.

Wiesmeier, M., Schad, P., von Lützow, M., Poeplau, C., Spörlein, P., Geuß, U., Hangen, E., Reischl, A., Schilling, B., Kögel-Knabner, I., (2014). Quantification of functional soil organic carbon pools for major soil units and land uses in southeast Germany (Bavaria). Agriculture, Ecosystems and Environment 185, 208-220.

Yang, J., Liu, J., Hu, Y., Rumpel, C., Bolan, N., Sparks, D.L., 2017. Molecular-level understanding of malic acid retention mechanisms in ternary kaolinite-Fe(III)-malic acid systems: The importance of Fe speciation. Chemical Geology 464, 69-75.

Zaccone, C., Beneduce, L., Lotti, C., Martino, G., Plaza, C., 2018. DNA occurrence in organic matter fractions isolated from amended, agricultural soils. Applied Soil Ecology 130, 134-142.

Table 4.1 Classification, sampling depth and main physical and chemical properties of bulk soils collected from a coniferous forest (CF), grassland (GL) and agricultural (AG) field. Data are from Giannetta et al. (2018).

Soil	**Site**	**Depth** *(cm)*	**Soil Taxonomy**	**Texture ($g \cdot kg^{-1}$)** *Sand*	*Silt*	*Clay*	**EC** *($\mu S \cdot cm^{-1}$)*	**pH**	**Organic C** *($g \cdot kg^{-1}$)*	**Total N** *($g \cdot kg^{-1}$)*	**C/N**
CF	San Lorenzo (San Severino Marche, Italy)	0-25	Lithic Rendoll	527	212	261	113.1	7.9	78.0	4.6	17.4
GL	Forcatura (Fiuminata, Italy)	0-15	Typic Haplustoll	631	202	167	68.9	7.6	93.0	7.7	12.0
AG	Arganda del Rey (Madrid, Spain)	0-15	Xerofluvent	339	471	190	102.6	8.8	11.8	1.1	10.7

Table 4.2 Initial organic C concentration in the solid phase (OC_s), organic C remaining in solution after sorption (OC_{aq}), sum of organic C released to solution after two desorption steps (OC_{des}), and Fe remaining in solid phase (Fes) following sorption and after two desorption steps, in fine silt and clay (FSi+Cl) and fine sand (FSa) fractions of coniferous forest soil (CF), grassland soil (GL) and agricultural soil (AG).

	OC_s	**OC_{aq}**	**OC_{des}**	**Fe_s**	**Fe_s**
				After sorption	After desorption
	($g \cdot kg^{-1}$)	*(%)*	*(%)*	*(%)*	*(%)*
CF FSi+Cl	54.1	1.6±0.2	1.6	99.8±0.2	99.8±0.1
GL FSi+Cl	84.8	1.8±0.9	4.3	99.9±0.1	99.9±0.1
AG FSi+Cl	18.1	4.6±1.7	5.7	99.6±0.3	99.7±0.2
CF FSa	110	0.7±0.1	0.7	99.7±0.3	92.1 ±7.1
GL FSa	110	1.0±0.2	0.6	99.6±0.4	96.5±0.9
AG FSa	3.6	15.5±2.4	8.0	100.0±0.0	100.0±0.0

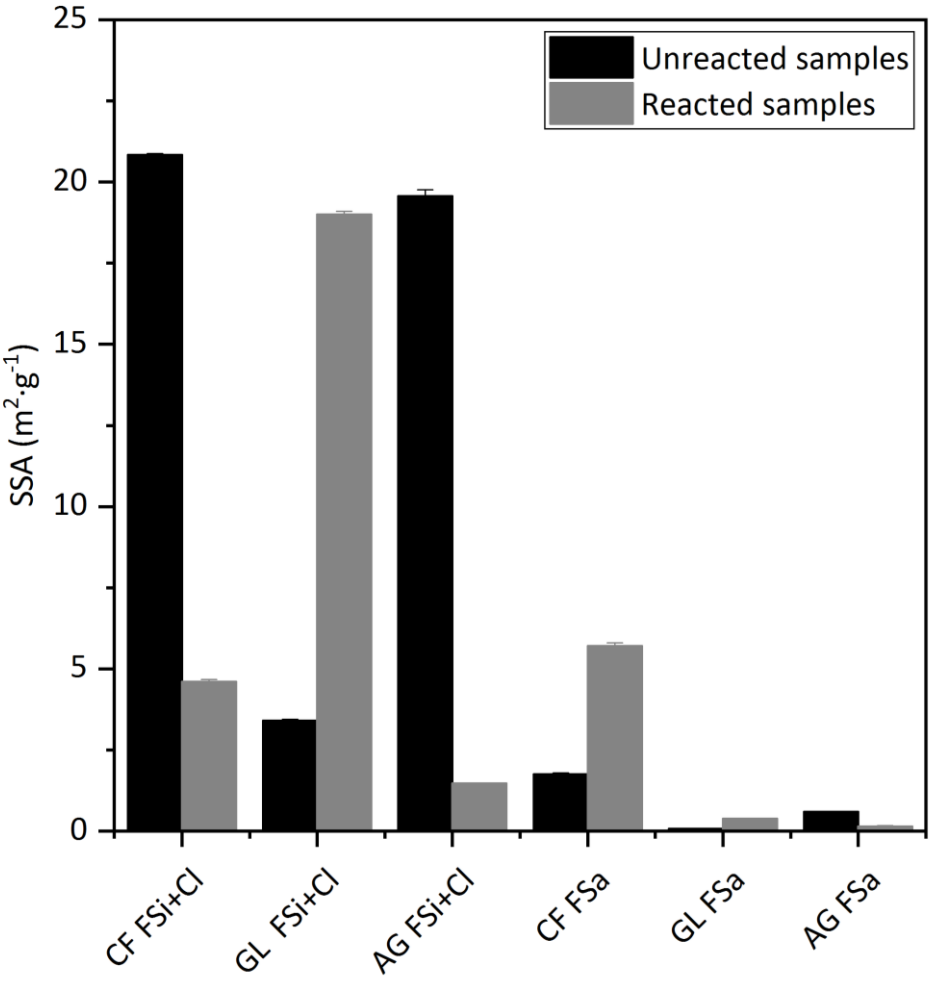

Figure 4.1 Specific surface area (SSA) values before and after reaction with Fe(III) of fine silt and clay (FSi+Cl) and fine sand (FSa) fractions from coniferous forest soil (CF), grassland soil (GL) and agricultural soil (AG). Bars represent the standard error of the measurement.

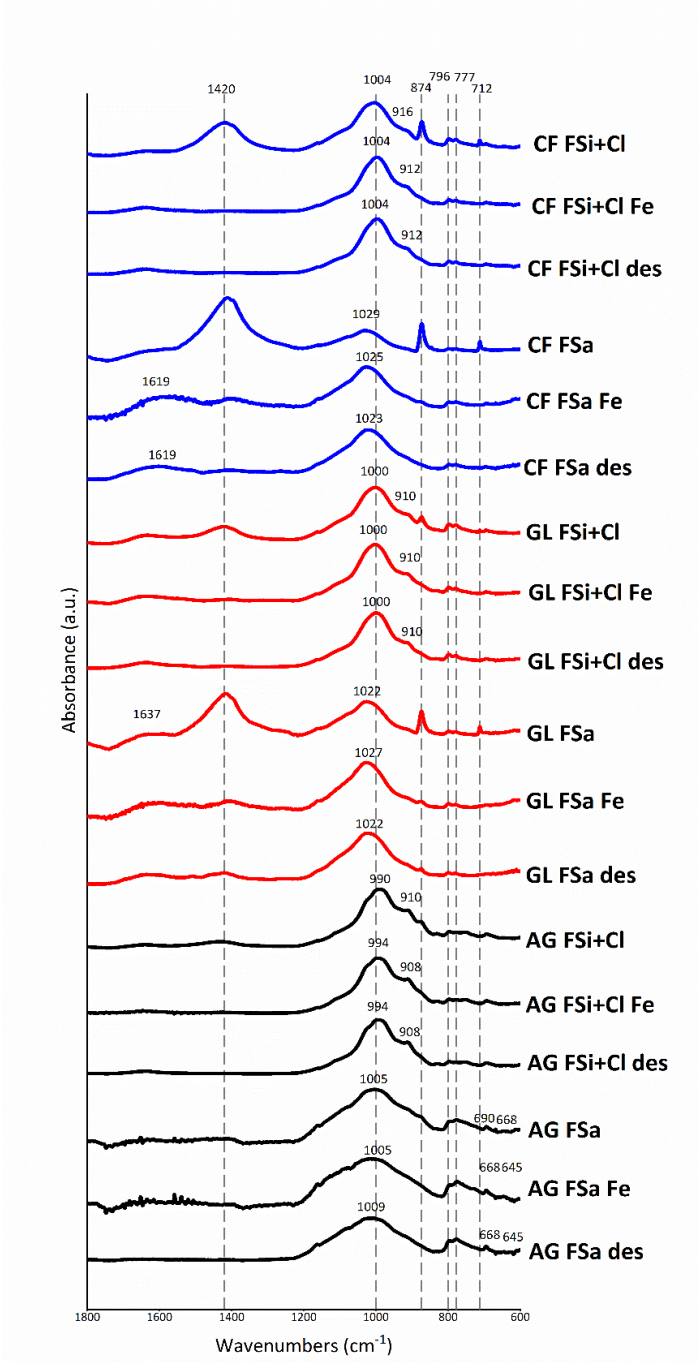

Figure 4.2 ATR-FTIR spectra of the fine silt and clay (FSi+Cl) and fine sand (FSa) fractions before reaction with Fe, after reaction with Fe(III) and after desorption (des) reactions (CF = coniferous forest soil; GL = grassland soil; AG = agricultural soil). In both FSi+Cl and FSa fractions, ATR-FTIR spectra collected after the sorption reaction show the disappearance of the band at 1420 cm^{-1}, as well as of peaks at 874 and 712 cm^{-1}; this is due to the removal of carbonates when the acidic Fe nitrate stock solution was added (pH<2). On the bottom right corner, a zoom of the region 1500-1300 cm^{-1} is reported for AG spectra.

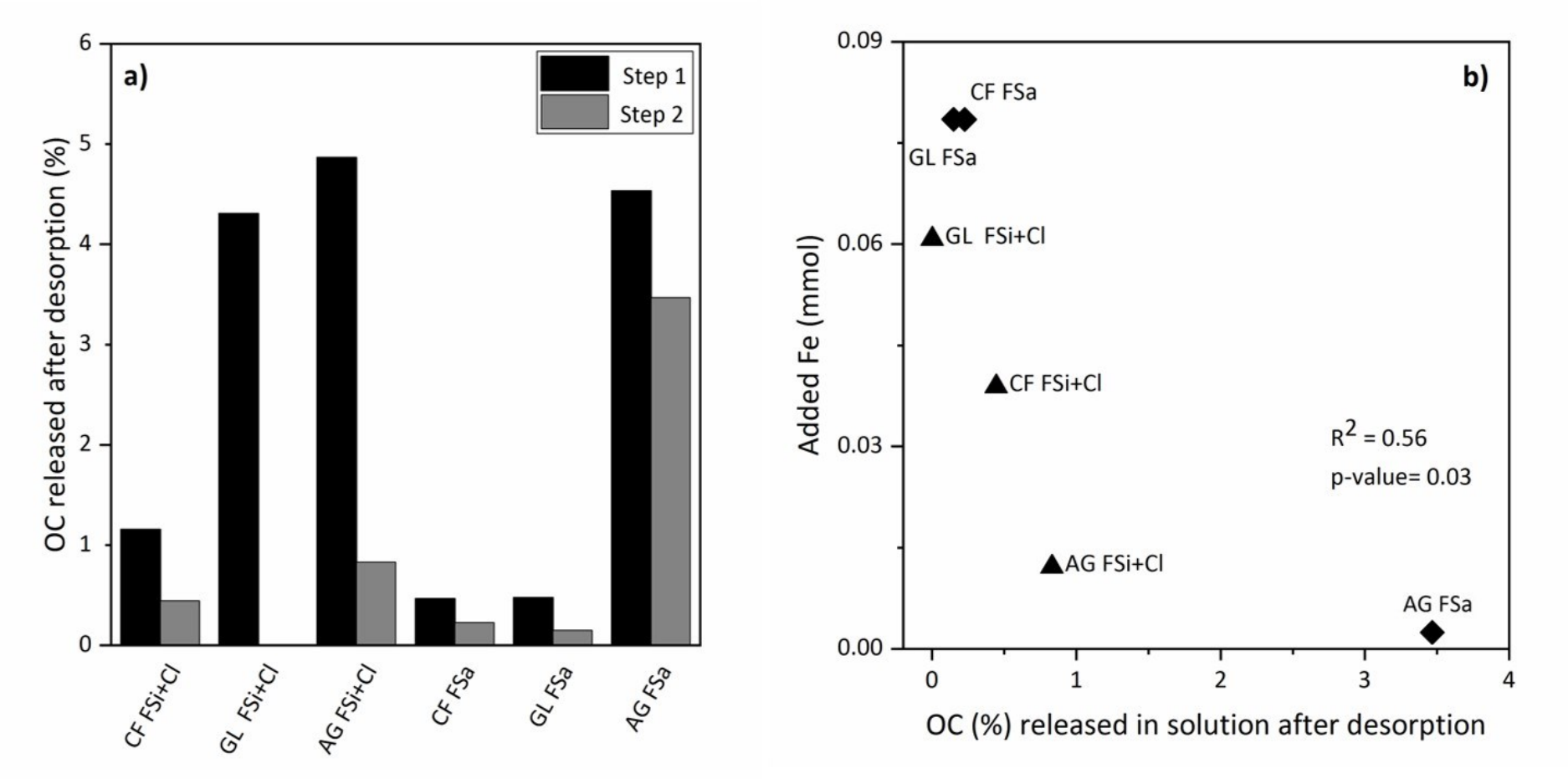

Figure 4.3 Percentages of organic C (OC) released to solution after desorption experiments (a), and after the second desorption reaction (b) related to Fe (mmol) added in the sorption experiment.

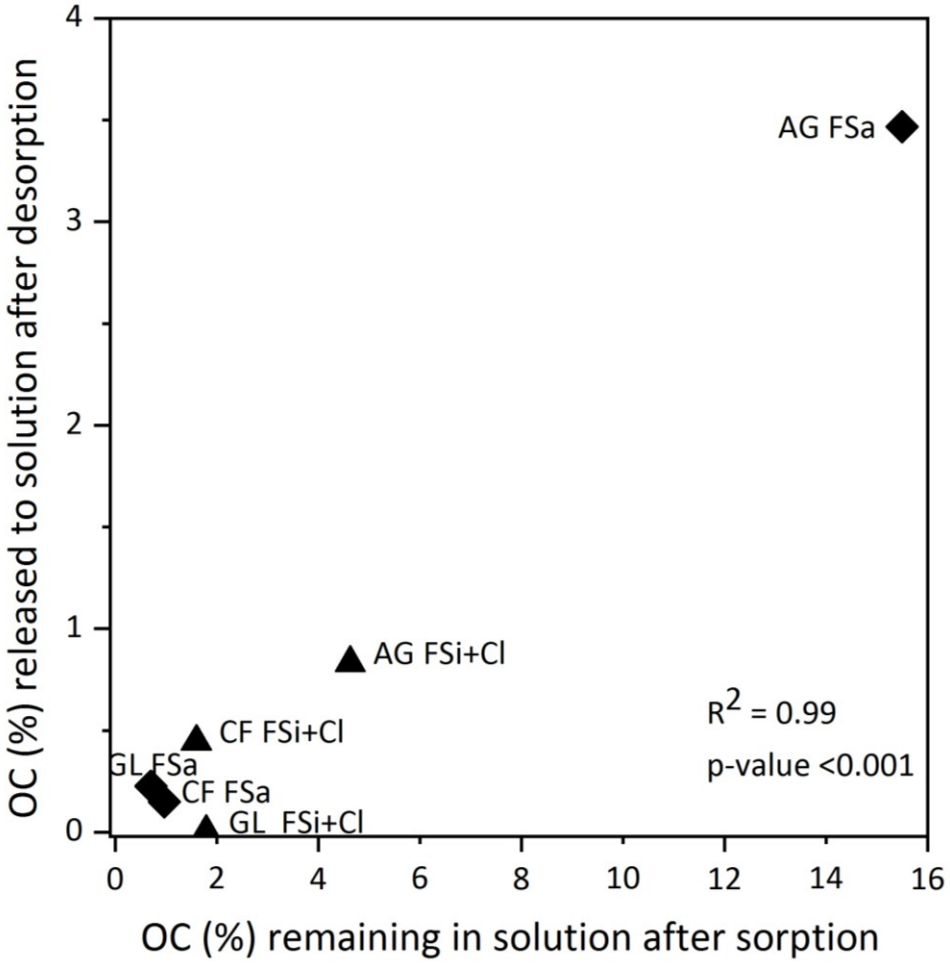

Figure 4.4 Correlation between organic C (OC, in %) remaining in solution after Fe(III) precipitation and OC (%) released to solution after the second desorption step.

5. Fe(III) fate after complexation with SOM in fine silt and clay fractions: an EXAFS spectroscopic approach

(Giannetta, B., Siebecker, M.G., Zaccone, C., Plaza, C., Vischetti, C., Sparks, D.L., Submitted)

Abstract

Iron (Fe) oxides have been suggested as key regulators in the soil carbon (C) cycle, and Fe speciation in soils is highly dependent on environmental conditions, mineralogy, and chemical interactions with soil organic matter (SOM). The behavior of organic C bound to Fe minerals in soils represents a critical knowledge gap for understanding the biogeochemical cycles of organic C and Fe at a global scale.

In this study, soil fractions, consisting of the fine silt/clay (FSi+Cl) particle size, reacted with Fe(III) at pH 7; unreacted and reacted samples were then studied by means of X-ray absorption spectroscopy.

Results show that the fractions consisted of Fe phyllosilicates, Fe (hydr)oxides, and Fe complexed by SOM in different proportions among samples. The analysis of Fe K-edge extended X-ray absorption fine structure (EXAFS) spectra suggested the formation Fe(III)-SOM complexes in the reacted sample. We hypothesize that this complexation can inhibit the hydrolysis and polymerization of Fe (III), due to the presence of C inputs from plant litter and root exudation that offers a constant supply of SOM from the litter surface, with a consequent production of soluble organic compounds that precipitate with the added Fe(III). At the same time, labile molecules (*e.g.,* sugars, amino acids, proteins) can be preferentially associated with mineral surfaces (*e.g.,* Fe(III) hydroxides of new formation), allowing these low molecular weight compounds to be stored in relatively passive pools.

5.1. Introduction

Soil organic carbon (SOC), representing the largest C stock on the Earth's surface contains 3000 Pg of C (Köchy et al., 2015), plays a pivotal role in regulating the global C cycle (Amundson, 2001; Blanco-Canqui, 2004; Lal, 2004; Lehmann et al., 2007).

Knowledge of SOC dynamics, as affected by soil management, is critical to accurately understand C cycling and its response to climate change (Schmidt et al., 2011), and is tightly linked to the comprehension of the formation of protective associations between soil minerals and soil organic matter (SOM). Soil clay fraction contains a mixture of mineral phases with highly contrasting surface properties (Barré et al., 2014) and mineral surface areas (Feng et al., 2013; Barré et al., 2014; Chen et al., 2014). The soil clay-size fraction (Kögel-Knabner et al., 2008) has been considered as the main driver of C sequestration potential in soils.

Soils are characterized by the presence of multiple iron (Fe) phases, ranging from Fe(II)/Fe(III) phyllosilicate clay minerals to poorly and highly crystalline Fe-oxides, hydroxides, and oxyhydroxides. Fe (hydr)oxide minerals are ubiquitous in soils (Schwertmann, 1991) and represent an important phase for the stabilization of SOC (Jambor and Dutrizac, 1998; Eusterhues et al., 2005; Lalonde et al., 2012). Fe(III) oxides are characterized by low solubility at extremely acidic conditions (Emerson et al., 2012). After its dissolution Fe(III) precipitates as Fe(III) (hydr)oxides in near-neutral pH environments and more than 99% of oceanic Fe(III) is organically complexed (Rue and Bruland, 1995).

SOM nature plays an important role in Fe-SOM interactions (Rose et al., 1998). In particular, Fe-OM complexation represents a challenge because it influences long-term C sequestration and can modify reactivity and structure of Fe (hydr) oxides (Eusterhues et al., 2008, 2014). Fe oxide crystal structure is affected by coprecipitation with humics, which inhibits their transformation into more stable forms (*e.g.,* ferrihydrite to goethite) (Schwertmann, 1966; Schwertmann et al., 2005). Being Fe speciation in soils highly dependent on environmental conditions and chemical interactions with SOM (Karlsson and Persson, 2012), improving our understanding about the molecular structure and hydrolysis of Fe species formed in association with SOM and the mechanisms and stability of SOM-metal coprecipitates under different environments is fundamental to predict the response of soil Fe and C to changes in global climate and land use (Post and Kwon, 2000).

Recently, state-of-the-art synchrotron-based techniques, such as Extended X-ray Absorption Fine Structure (EXAFS) spectroscopy, have been used for the speciation of model metal (hydr)oxide systems (pure Fe (hydr)oxides) and Fe(III) complexation with different types of SOM, dissolved organic matter (DOM) (Nierop et al., 2002; Eusterhues et al., 2008; Eusterhues et al., 2011; Henneberry et al., 2012; Chen et al., 2014a), peats

(Karlsson and Persson, 2010), humic substances (Mikutta and Kretzschmar, 2011; Shimizu et al., 2013), small organic acids (Mikutta, 2011; Yang et al., 2016), or bulk soils and waters (Sundman et al., 2014). In contrast, the chemical interactions between Fe species and physically-fractionated SOM pools from different ecologically important land uses have not been investigated. Thus, it is less clear how Fe-mediated stabilization of SOM in natural systems (rather than model systems) can control the persistence of C.

Here we investigated the dynamics of solid phase Fe speciation in order to define how Fe reacts with minerals and SOM contained in the fine silt and clay fraction of different soils collected from a coniferous forest (CF), a grassland (GL), a technosol (TS) and an agricultural (AG) soil.

The main objectives of this study were: (1) to test the role of SOM in the fine silt_ clay fraction in the formation of Fe(III)-SOM complexes or Fe(III) precipitation in Fe(III) oxides by coprecipitation experiments; (2) to determine Fe speciation before and after reactions by Fe K-edge X-ray absorption spectroscopy (EXAFS).

Our approach using LCF and WT helps to identify which SOM pools can influence Fe(III) speciation and demonstrate how both Fe(III)-SOM complexes and Fe(III) polymerization can affect SOM reactivity, with a consequent improve of the understanding of SOM mean residence time in fine silt and clay fractions.

Considering the gap between modeled and natural systems in understanding the possible SOM stabilization mechanisms as a function of land use, this research provides unique information relevant to global terrestrial SOC cycling.

5.2. Experimental section

5.2.1. Soil samples collection

The soil samples were collected from a coniferous forest (CF), a grassland (GL), a technosol (TS) and an agricultural field (AG). Mean annual temperature of sampling sites ranged from 9.7±6.1 and 14.8±6.9°C, whereas mean annual precipitation ranged between 440 and 980 mm. The main physical and chemical properties of soils included in this study are summarized in Table 5.1 and already reported in Giannetta et al. (2018).

5.2.2. Physical fractionation

A physical size fractionation by ultrasonic dispersion and wet sieving was performed, allowing for separation of particles into four different size fractions: coarse sand (CSa: 2000-200 µm diameter), fine sand (FSa: 200-50 µm), coarse silt (CSi: 50-20 µm) and fine silt and clay (FSi+Cl: <20 µm) (Lopez-Sangil and Rovira, 2013). 15 g of each sample were put into 50 mL vials and filled with deionized water to 3/4 of their volume. Samples were then subjected to vertical agitation (20 rpm) for 60 minutes and to ultrasonic dispersion of the soil particles for 10 minutes at 60% of the total amplitude (100W output) using a Branson 45 sonifier. The derived suspensions were then wet-sieved through a set of three sieves (200 µm, 50 µm and 20 µm) splitting particles into four different size fractions. The fractions retained by sieves (CSa, FSa, CSi) were directly recovered from the sieves, quantitatively transferred to pre-weighted vials and dried at 60 ºC to constant weight. The particles passing through the last sieve (<20 µm: FSi+Cl) were brought to ca. 1 L and left to stand refrigerated for 2 days; overlying water was then carefully siphoned off and discarded. The sediment was transferred into 250 mL polypropylene vials and centrifuged for 15 min at 2500 g. In this research, we used the FSi+Cl fractions (Table 5.2).

5.2.3. Sorption Experiments

Fe(III)-SOM complexation was conducted following the methods proposed by Karlsson and Persson (2010) and Mikutta and Kretzschmar (2011). The methods were modified to react Fe(III) with our soil fractions. An aliquot (200 mg) of each fraction was weighted into a 50 mL polypropylene vial. Acidified Fe(III) nitrate stock solution (12.15 mM) was added to each sample to reach a loading of 200 mg Fe /g C. The pH of the slurry was immediately raised to 7 and monitored during the next 24 hours and adjusted to 7±0.5 with 0.1 M KOH. The suspensions were shaken at 60 rpm at room temperature for 24 hours and then centrifuged at 10,000 rpm for 20 minutes. The supernatant was removed and filtered through a 0.2 µm polysulfone membrane filters and acidified with 2% HNO3 (trace metal grade). Filtrates were analyzed for both dissolved organic C (DOC), using a Vario TOC cube analyzer, and Fe concentration, by inductively coupled plasma mass spectrometry (ICP-MS) (Agilent 7500 Series). Sorption experiments were conducted in duplicate at room temperature and the results of the batch experiment are described in Giannetta et al (2019).

5.2.4. Organic C and total N analyses Iron K-edge Extended X-ray Adsorption Fine Structure Spectroscopy (EXAFS)

Complementary to our previous batch experimental study (Giannetta et al., 2019), the speciation of Fe before and after reactions was analyzed by X ray absorption spectroscopy (XAS).

X-ray absorption spectroscopic analyses of unreacted and Fe(III) reacted samples were conducted at Beamlines 4-1 and 4-3 at the Stanford Synchrotron Radiation Lightsource (SSRL) in Menlo Park, CA. Fe K-edge X-ray absorption fine structure (EXAFS) were collected in transmission mode. X-ray energy energy was maintained by a crystal Si (222) 4-1 monochromator at 4-1 and Si (111) at 4-3. The monochromator was detuned 50% to reduce higher order harmonics.

Ground samples (15-30 mg) were prepared as pressed pellets between Kapton® tape. Sample thickness and homogeneity were optimized. Two to six replicate scans were collected, in order to obtain satisfactory data quality, with energy calibrated against an Fe (0) foil to the inflection point of the first derivative (7112 eV).

5.2.5. Data analysis

Spectral data processing was performed in Athena (Ravel and Newville, 2005). Scans were averaged using Athena program. Athena was also used for background removal, using linear pre-edge line between -200 and -800 before the edge step. The frequency cutoff parameter, Rbkg, was set to 1 for Fe. The k weight in the background function determination was set to three.

Principal Components Analysis (PCA), Target Transformation (TT), SPOIL values, LCF and F-test were also carried out. Sixpack software was used to carry out PCA of the EXAFS data, in order to determine the appropriate number of components to use for LCF. Moreover, Sixpack was also used to perform TT of standards in order to generate the SPOIL values that were coupled with Chi-squares and R-values, to evaluate each standard. R-values of the LCF represent a measure of the percent misfit and chi-square values are the sum of the squared differentials.

LCF of the EXAFS spectra was performed using the Athena XAS data processing software to evaluate different contributions from different Fe forms in the complexation reactions (Siebecker et al., 2017). The fitting was performed on k^3-weighted spectra. In addition to a scree plot and the visual inspection of components, the exact number of

standards enough to account for the structure in the EXAFS spectra was accurately determined using the F-test (Hamilton test), varying the number of standards and evaluating if adding new components statistically improved the LCF (Calvin, 2013). A regularized lower incomplete beta function calculator was used to perform F-tests. Siebecker et al. (2017) underlined the importance of the application of R-factor values in LCF, since the latter is sensitive to the specific number of standards used in each fit. LCF results are summarized in table 5.3.

A large spectra reference library of model Fe minerals and related compounds (O'Day et al., 2004) has been used to represent the typical Fe phases, such as phyllosilicates: with high Fe(II) / Fe (III) ratios: chlorite ($Ca_{0.5}$) ($Mg^{4.44}$, $Fe[III]_{3.47}$, $Fe[II]_{3.02}Al_{0,60}$, $Mn_{0.01}$,$Ti_{0.06}$), and with low Fe(II)/Fe(III) in the structure: illite ($K_{1.37}$,$Mg_{0.09}$,$Ca_{0.06}$)($Al_{2.69}$,$Fe[III]_{0.67}$,$Fe[II]_{0.06}Mg_{0.43}$,$Ti_{0.06}$)($Si_{6.77}$,$Al_{1.23}$)$O_{20}(OH)_4$ and vermiculite ($Ca_{2.92}$,$Mg_{2.27}$, $K_{0.01}$)($Mg_{5.98}$,$Mn_{0.01}$,$Ti_{0.02}$)($Si_{7.71}$, $Al_{0.13}$, $Fe_{0.16}$)$O_{20}(OH)_4$; smectite ($Ca_{0.39}$, $Na_{0.36}$, $K_{0.02}$,)($Al_{2.71}$, $Fe_{0.12}$, $Mg_{1.11}$, $Mn_{0.01}$, $Ti_{0.03}$)($Si_{8.0}$)$O_{20}(OH)_4$; carbonates siderite ($FeCO_3$); oxides and hydroxides: ferrihydrite $Fe(OH)_3$, goethite FeOOH, lepidocrocite FeOOH, magnetite Fe_3O_4, hematite Fe_2O_3, and some analog for the Fe(III) complexation to low molecular weight OC: Fe(III)citrate hydrate $C_6H_5FeO_7$; Fe(III)ACAC $C_{15}H_{21}FeO_6$.

WT analysis was performed following the methods reported in Mikutta and Kretzschmar (2011), Karlsson and Persson (2012) and Siebecker and Sparks (2017). k^3-weighted spectra were used to create wavelet transform using the HAMA program written for Igor Pro wavelet transform script developed by Funke et al. 2005 and applied for a qualitative analysis of the nature of backscattering atoms in the higher coordination shells. The aim of this method is to resolve the data in both k- and r- space, separating more than one type of backscatter located at the same interatomic distance from the central adsorbing atom. The WT plots of each sample were systematically compared to the suite of standards to evaluate the number and type of backscattering components in EXAFS spectra.

WT has been particularly useful to investigate the qualitative elemental discrimination of signal contributions from backscattering neighboring atoms in the FT peaks occurring between 2.2 and 4.0 Å R+ΔR. WT allows the discrimination of the nature of atoms beyond the first coordination shell, using a two-dimensional plot created from the k-weighted EXAFS spectrum and the corresponding Fourier transform to determine the distance and intensity of atoms. A combination of two adjustable parameters η=from

9 to 4 and σ= 1 was used for an appropriate resolution in R- and k- space, allowing the discrimination of the atomic contributions in the Fourier transforms of the Fe K-edge EXAFS spectra. In detail, η= 8 and 6 and σ= 1 have been used for a detailed WT. For the WT of the second shell, the optimal resolution in k and r space is twice the distance of interest in R-space (r) obtained adjusting the resolution of η and σ values.

5.3. Results and discussion

5.3.1. Synchrotron-based data acquisition and analysis: PCA, TT and F-test

The results of PCA are summarized in Table B1 and Figure B1. In a first step, the Factor Indicator Function (Malinowski, 1977), *i.e.,* the IND value obtained from the PCA analysis, reached a minimum at four components, indicating that four components were adequately able to reconstruct the EXAFS data. Moreover, the scree plot represented in Figure B1 indicates a break in the slope at two components, indicating the minimum number of components able to reproduce the data. In the second step, appropriate model compound spectra were selected by TT. The EXAFS spectra of model compounds with a SPOIL value below 6 were considered during fitting (Malinowski, 1978). Although the SPOIL values were <1.5 and most of the models classified as excellent model compounds; the best fit of unreacted and reacted samples was obtained using three fitting components. The application of the F-test provided complementary information about the number of standards able to statistically improve the fit. The results obtained from the F-test are labeled as "I" in Table 5.3 and confirmed the need to use three standards for LCF. The confidence level of the F-test was 95% to avoid a fit caused by random variation or noise in the data. Fit improvement was not significant adding the fourth standard. The entire list of standards used for LCF are described in table B2 and their LCF and FT plots in figures B2 and B3, respectively. Chi-square, R-values, and SPOIL and chi-square are also reported. All of the standards have been described in O' Day et al. (2004).

5.3.2. LCF

LCF results are reported in table 5.4, revealing the standards that best reconstruct the sample data. Although Fe EXAFS provides a good estimation of the relative contribution from different mineral classes (*e.g.,* discrimination of Fe oxyhydroxides and Fe-organic

complexes), it is well stated that differentiating among specific Fe(III) oxyhydroxides (e.g., ferrihydrite, goethite and hematite) can be difficult (O'Day et al., 2004; Prietzel et al., 2007). Thus, for modeling simplicity, ferrihydrite was selected to represent pedogenic Fe(III)-minerals, and Fe(III)-citrate as model compound for organically bound Fe. In detail, Fe(III)-citrate has been chosen to represent low-molecular weight organic acids, being one of the major constituents in microbial metabolites and root exudates (Yang et al., 2016) and assuming that organically bound Fe is mainly bound to carboxylate groups of deprotonized low-molecular weight acids (Pohlman and McColl, 1988; Prietzel et al., 2007). Moreover, low molecular weight acids represent a common soil constituent, are partly redox-active, and their interaction with Fe(III)-hydroxydes is comparable to that with SOM (Evanko and Dzombak, 1998).

The Fe EXAFS data fitting of untreated soils revealed that ferrihydrite fits varied from 23% in CF to 48% in GL and AG. The lowest value in CF is possibly explained by its organic C impoverishment in the organo-mineral complex. Coniferous needles are rich in recalcitrant compounds (lignin, suberin, lipidic polymers) which confer to litter a low decomposition rate and microbial use efficiency, thus leading to a relatively higher C accumulation in coarse fractions. Conversely, soils richer in microbial-derived SOM contain also abundant SRO.

Fe(III)-silicates are represented by illite (39%) in CF, smectite (31%) in GL, and chlorite in TS and AG (26 and 22%, respectively). The illite reference sample contains 7.32 wt % Fe_2O_3 and 0.55 wt % FeO substituted in the octahedral layer for Al. Smectite is a low-Fe standard with 1.42% Fe_2O_3 and 0.88 wt % FeO that also contains Al and Mg in the octahedral layer (O'Day et al., 2004). Fe(III)–organic complexes (*i.e.,* Fe(III)-citrate) range from 18% in GL to 41% in CF.

After the reaction, a slight increase in ferrihydrite percentage is noticeable in CF (30%) and TS (52%). Conversely, the Fe(III)-citrate percentage increases in GL (23%) and AG (46%), and decreases in CF (35%) and TS (28%).

LCF results are shown in Figure 5.1 and the fit of each sample, in dotted lines, is labeled with the R factor. Fe K-edge EXAFS spectra of unreacted samples show similar features at ~4.0 $Å^{-1}$ (peak 1), ~6.5 $Å^{-1}$ (peak 2), ~7.5 $Å^{-1}$ (peak 3), ~8.5 $Å^{-1}$ (peak 4). The peak at 4.0 $Å^{-1}$ remained basically unchanged after reaction with Fe(III). Conversely, the peak at 7.5 $Å^{-1}$, characteristic of ferrihydrite (Mikutta, 2011), becomes less evident in GL and AG. The predominance of Fe(III)-citrate in AG is demonstrated by the shift of the peak at 8.5 $Å^{-1}$ towards the characteristic peak at 8 $Å^{-1}$ typical of Fe III citrate (Figure

B2) (Yang et al., 2016). Ligand-promoted dissolution at neutral pH can have a large impact on Fe speciation in soils because they affect ferrihydrite formation and can exert a strong influence on its structure (Mikutta et al., 2008). Mikutta et al. (2010) reported that organic chelates such as hydroxybenzoic acids control the kinetics of ferrihydrite formation via Fe(III) complexation thereby effectively lowering the solution saturation state of inorganic Fe(III) species, leaving less Fe(III) available for ferrihydrite precipitation. Although this has been demonstrated in laboratory systems, it still needs to be proven in soils. In GL and AG the complexation of Fe(III) by organic ligands may be responsible of the decreasing of Fe(III) activity in solution, consequently inhibiting the Fe ions precipitation as ferrihydrite. Increasing amounts of organic Fe(III) complexes identified in the LCF of the solid phase suggest that low molecular weight organic acids can affect Fe(III) availability for ferrihydrite polymerization reactions in SOM-rich environments. In both GL and AG the presence of C inputs from plant litter and root exudation offers a constant supply of SOM, with a consequent production of soluble organic compounds that complex with Fe(III).

Conversely, TS are mainly composed by new molecules resulting from a common microbial transformation rather than highly degraded litter inputs. As reported in Giannetta et al. (2018) technosols seem to be enriched in labile molecules (*e.g.,* sugars, amino acids, proteins) that can associate with mineral surfaces (*e.g.,* Fe(III) that precipitates as Fe(III) hydroxides), allowing low molecular weight metabolic compounds to be stored as organo-mineral complexes.

In the CF sample, the precipitation of Fe(III) seems to lead to the preferential formation of ferrihydrite. This finding is in agreement with previous results obtained by Giannetta et al. (2019) who observed an increase in the carbohydrates band relative intensity in ATR spectra after the reaction with Fe(III); this was ascribed to the possible formation of inner-sphere surface complexes between the carbohydrates OH functional groups and the Fe atoms (Eusterhues et al., 2011; 2014), *i.e.,* the formation of surface complexes between carbohydrates with newly formed ferrihydrite. It has been shown that ferrihydrite particles can be stabilized by an encapsulating layer of polysaccharides (Karlsson and Persson, 2012). Our LCF also indicate a slight increase in the contribution of ferrihydrite to the reacted sample fit. For the AG soil, we hypothesized that small differences in carbohydrates peaks reaction can be indicative of labile SOM already associated with minerals as well as of the formation of Fe-SOM complexes, as previously proven also by Karlsson and Persson (2012). These results have been then confirmed by

the LCF results.

Although linear combination fitting (LCF) is widespread in EXAFS studies, applying F-test (Hamilton test) to determine an appropriate number of standards was a useful tool for accurately choose the standards, since the increase and decrease of only one standard heavily influence the calculated percentage of each component (Siebecker et al., 2017).

LCF remains still a difficult tool to quantify different Fe phases in soils and different particle size fractions because often natural constituents can be only partially represented by Fe minerals synthesized in the laboratory. For this reason, the LCF values often do not sum to 100%. Conversely, in model systems, shell fitting analysis of the second-shell can be carried out because the systems are simpler. The Fe–C and Fe–Fe distances in those model systems describe the coordination modes of the organic Fe complexes and the polymeric Fe (hydr)oxides, respectively. Gustafsson et al. (2005) reported that Fe(III) in organic soils (pH 4) occurred either as Fe (hydr)oxides or organically complexed likely as a mixture of di- and trinuclear $(O_5Fe)_2O$ and $(O_5Fe)_3O$ complexes. Rose et al. (1998) determined the speciation of Fe in natural organic matter (NOM) from natural freshwaters (pH 5.5–7.5) and found that Fe was poorly polymerized due to complexation with NOM. These results suggest that Fe-SOM interactions influence Fe speciation in organic rich soils, but the role of SOM in Fe hydrolysis and in the formation of various hydrolyzed species in soils under different ecosystems is still very much unknown.

5.3.3. Wavelet transformation

As in EXAFS studies on Fe associated with SOM the application of traditional EXAFS analyses (*e.g.,* shell fitting of the Fourier transform (FT)) can be challenging, we also employed WT. This challenge is due to the need to separate contributions from different backscattering atoms in coordination shells at similar interatomic distances from the central absorbing Fe atom. WT can provide useful information resolving simultaneously data in both k-space ($Å^{-1}$) and interatomic distance (R-space), helping to differentiate lighter backscattering elements when they are in the same coordination shell from the central adsorbing atom (Funke et al., 2007; Siebecker et al., 2017) *e.g*. Fe. WT represents an analog to the FT and reveals at which energies the backscattering components are most significant in addition to the distances of the backscattering atoms, like FT. WT *k*-R maps are helpful in improving the fitting model and understanding local atomic structure (Xia et al., 2018).

WT analysis has been used to qualitatively test for the presence of Fe back-scatterers in the second coordination shell of the Fe K-edge EXAFS data. We calculated the Morlet wavelet transforms of k^3-weighted Fe K-edge EXAFS spectra of the samples over a R + ΔR-range of 2.2-4.0 Å and compared the resulting wavelet plots with those of Fe(III) reference compounds (ferrihydrite, Fe(III)-citrate, illite, smectite, chlorite). Figure 5.3 contains the WT plots of the standards. In the ferrihydrite plot, the Fe shell contributes a strong feature at 7-8 $Å^{-1}$ and 2.75 Å (Daugherty et al., 2017). In Fe(III)citrate-SOM complexes there is no significant Fe backscattering but features at 2.0–2.5 Å and 3.1–3.7 Å and indicate back-scattering from lighter atoms. These features are in agreement with single and multiple backscattering from C/O in the second and third coordination shells of trisoxalatoiron(III) (Daugherty et al., 2017; Karlsson and Persson, 2008; Persson and Axe, 2005). Moreover, these features appear at lower energies (3–4 $Å^{-1}$) than those of Fe. In general, phyllosilicate clay minerals can be described by three atomic backscattering shells: the first-neighbor O, second-neighbor octahedral Fe, Al, or Mg; and tetrahedral Si. In many Fe oxyhydroxides and phyllosilicates the Fe-Fe neighbor distances overlap, and cannot be used a diagnostic in EXAFS.

WT of the EXAFS data from the samples showed that both the intensity caused by light back-scatterers at low k-values and by heavier atoms at higher k varied among the samples and between unreacted and Fe(III) reacted samples (Figure 5.4). The WT results support the LCF analysis, which indicated that EXAFS spectra of the soil samples could be described roughly as a mixture of Fe-bearing clay minerals, Fe (hydr)oxides and organically complexed Fe. The WT plots of the unreacted CF sample indicate a Fe-Fe second shell contribution possibly from both ferrihydrite and illite. A contribution from Fe(III)-citrate at above 2.2 Å and 2–4 $Å^{-1}$ is also evident. After the reaction, the Fe-Fe shell appears at lower R-values (2.75 Å), indicating a slight increase in ferrihydrite percentage, as also reported in the LCF results. Unreacted GL is mainly composed of ferrihydrite and the Fe-Fe feature exactly appears at distance in both k- and R-space ascribed to ferrihydrite. Differences are small in the reacted sample plot, with perhaps a minor component appearing at low $Å^{-1}$ and attributed to the minor increase in Fe(III)-OM compounds after reaction, as also reported in the LCF results. The predominant feature in the unreacted TS WT plots show a clear indication of heavy back- scattering atoms, followed by a minor feature from C backscattering. Noticeable differences are not reported in the reacted plot. In AG, the presence of 37% of Fe(III)-OM from LCF is

supported by the presence of the feature in agreement with Fe(III)-OM compounds. After the reaction this feature increases, in agreement with the results reported in LCF.

Modifying η from 9 to 4, at η=9 the resolution in R-space is high while resolution in k-space is low, reaching the best spatial resolution in R-space at η= 6. The third component maximum is clearly resolved at η=6. At 6, the maximum starts to separate into separate peaks (Figure B5), indicating the splitting of the major component in two minor components. These features can be possibly attributed to phyllosilicate clay minerals can be described by the second-neighbor octahedral Fe, Al, or Mg; and tetrahedral Si, being the splitting in two different components a common feature of illite and smectite (Figure B4). In the agricultural soil, characterized by the presence of chlorite, the splitting into separate peaks at η= 6 is not evident like in the other samples. This also confirms that WT analysis is challenging due to the overlapping of the Fe-Fe neighbor distances in many Fe oxyhydroxides and phyllosilicate.

Our data show that the formation of Fe(III)-OM complexes suppresses the hydrolysis and polymerization of Fe(III) and that in oxic environments, the fate of Fe is with large extent controlled by the properties of the organic Fe(III) complexes. The variation in contribution from Fe oxides and Fe-OM complexes is controlled by the total concentration of SOM. These complexes most certainly have different reactivities as compared to Fe(III) in (hydr)oxide phases or other Fe(III)-bearing minerals. The combination of Fe EXAFS with size-fractioned samples represents an important approach to further study the Fe dynamics in natural environments as it could provide connections between Fe origin, mechanisms and structures.

5.4. Conclusions

Here we unraveled the role of SOM and minerals present in the FSi+Cl size fraction on the Fe speciation when Fe(III) was added to the system using EXAFS. We underline the importance of WT in providing information to resolve data in both k-space (k-) and interatomic distance (R-space), helping to differentiate lighter backscattering elements when they are in the same coordination shell from the central adsorbing Fe atom.

Batch sorption data from our past work have been used to probe the effect of different natural ecosystems on Fe(III) precipitation mechanisms. Both LCF and WT results indicated that the soil samples can be described as a mixture of Fe-bearing phyllosilicate

clay minerals, Fe (hydr)oxides, and organically complexed Fe.

Increasing amounts of organic Fe(III)-complexes in the solid phase of grassland and agricultural soils suggest that low molecular weight organic acids affect Fe(III) availability for ferrihydrite polymerization reactions in SOM-rich environments. In the silt/clay fraction of the coniferous forest soil, the precipitation of Fe(III) seem to lead to the preferential formation of ferrihydrite, which is also supported by the ATR results described in our previous study.

This study shows that Fe speciation varied strongly with organic C concentration and most likely by the chemical properties of SOM, although more research is needed in this regard. The analysis of Fe EXAFS spectra suggested the formation Fe(III)-OM complexes, inhibiting the hydrolysis and polymerization of Fe (III) in GL and AG. Conversely, in CF and TS, the percentage of ferrihydrite-like polymeric Fe(III) oxides increased after the reaction.

In the current literature, the role of SOM controlling Fe speciation is mostly discussed in terms of speciation of model metal (hydr)oxide systems, such as pure Fe (hydr)oxides) and Fe(III) complexation with different types of SOM, dissolved organic DOM, peats, humic substances, small organic acids, or bulk soils and waters. Thus, considering the knowledge and research gap between model and natural systems in understanding the possible SOM stabilization mechanisms as a function of ecosystems, physical fractionation methods coupled with synchrotron-based characterization provide unique information relevant to regulation of global terrestrial SOC cycling. Additional experiments need to be performed to understand the influence of SOM on Fe speciation and complexation during changing environmental conditions (*e.g.,* redox, pH, and temperature).

This study provides a partial picture of the Fe speciation in different ecosystems. Future studies should include more samples where Fe species can be determined at different Fe/SOM ratios. The combination of Fe EXAFS with size-fractioned samples represents an important approach to further study the Fe dynamics in natural environments as it could provide connections between Fe origin, mechanisms and structures.

References

Amundson, R., 2001. The carbon budget in soils. Annual Review of Earth and Planetary Sciences 29, 535-562.

Barré, P., Fernandez-Ugalde, O.,Virto, I., Velde, B., Chenu, C., 2014. Impact of phyllosilicate mineralogy on organic carbon stabilization in soils: Incomplete knowledge and exciting prospects. Geoderma 235–236, 382-395.

Blanco-Canqui, H., Lal, R., 2004. Mechanisms of carbon sequestration in soil aggregates. CRC. Critical Reviews in Plant Sciences 23, 481-504.

Calvin, S., 2013. XAFS for Everyone. CRC Press.

Chen, C., Dynes, J.J., Wang, J., Karunakaran, C., Sparks, D., 2014. L. Soft X-ray spectromicroscopy study of mineral-organic matter associations in pasture soil clay fractions. Environmental Science and Technology 48, 6678-6686.

Chen, C., Dynes, J.J., Wang, J., Sparks, D.L., 2014. Properties of Fe-organic matter associations via coprecipitation versus adsorption. Environmental Science and Technology 48, 13751-13759.

Daugherty, E.E., Gilbert, B., Nico, P.S., Borch, T., 2017. Complexation and Redox Buffering of Iron(II) by Dissolved Organic Matter. Environmental Science and Technology 51, 11096-11104.

Emerson, D., Roden, E., Twining, B.S., 2012. The microbial ferrous wheel: Iron cycling in terrestrial, freshwater, and marine environments. Frontiers in Microbiology 3, 1-2.

Eusterhues, K., Rennert, T., Knicker, H., Kögel-Knabner, I., Totsche, K.U., Schwertmann, U., 2011. Fractionation of organic matter due to reaction with ferrihydrite: Coprecipitation versus adsorption. Environmental Science and Technology 45, 527-533.

Eusterhues, K., Rumpel, C., Kögel-Knabner, I., 2005. Stabilization of soil organic matter isolated via oxidative degradation. Organic Geochemistry 36, 1567-1575.

Eusterhues, K., Wagner, F.E., Ha, W., Hanzlik, M., Knicker, H., Totsche, K.U., Ko, I., Schwertmann, U., 2008. Characterization of Ferrihydrite-Soil Organic Matter Coprecipitates by X-ray Diffraction and Mössbauer Spectroscopy. Environmental Science and Technology 42, 7891-7897.

Eusterhues, K.; Hädrich, A.; Neidhardt, J.; Küsel, K.; Keller, T. F.; Jandt, K. D.; Totsche, K. U. Reduction of ferrihydrite with adsorbed and coprecipitated organic matter: Microbial reduction by Geobacter bremensis vs. abiotic reduction by Na-dithionite.

Biogeosciences 2014, 11 (18), 4953–4966.

Evanko, C.R., Dzombak, D.A., 1998. Influence of structural features on sorption of NOM-analogue organic acids to goethite. Environmental Science and Technology 32, 2846-2855.

Feng, W., Plante, A.F., Six, J., 2013. Improving estimates of maximal organic carbon stabilization by fine soil particles. Biogeochemistry 112, 81-93.

Funke, H., Chukalina, M., Scheinost, A.C.A., 2007. A new FEFF-based wavelet for EXAFS data analysis. Journal of Synchrotron Radiation 14, 426-432.

Funke, H., Scheinost, A.C., Chukalina, M., 2005. Wavelet analysis of extended x-ray absorption fine structure data. Physical Review B 71, 094110.

Giannetta, B., Plaza, C., Vischetti, C., Cotrufo, M.F., Zaccone, C., 2018. Distribution and thermal stability of physically and chemically protected organic matter fractions in soils across different ecosystems. Biology and Fertility of Soils 54, 671-681.

Gustafsson, J.P., Persson, I., Kleja, D.B., Van Schaik, J.W.J., 2007. Binding of iron(III) to organic soils: EXAFS spectroscopy and chemical equilibrium modeling. Environmental Science and Technology 41, 1232-1237.

Harris, D., Horwath, W.R., van Kessel, C., 2001. Acid fumigation of soils to remove carbonates prior to total organic carbon or carbon-13 isotopic analysis. Soil Science Society of America Journal 65, 1853–1856.

Henneberry, Y.K., Kraus, T.E.C., Nico, P.S., Horwath, W.R., 2012. Structural stability of coprecipitated natural organic matter and ferric iron under reducing conditions. Organic Geochemistry 48, 81-89.

Jambor, J.L., Dutrizac, J.E., 1998. Occurrence and Constitution of Natural and Synthetic Ferrihydrite, a Widespread Iron Oxyhydroxide. Chemical Reviews 98, 2549-2586.

Karlsson, T., Persson, P., 2010. Coordination chemistry and hydrolysis of Fe(III) in a peat humic acid studied by X-ray absorption spectroscopy. Geochimica et Cosmochimica Acta 74, 30-40.

Karlsson, T., Persson, P., 2012. Complexes with aquatic organic matter suppress hydrolysis and precipitation of Fe(III). Chemical Geology 322-323, 19-27.

Karlsson, T., Persson, P., Skyllberg, U., Mörth, C.-M., Giesler, R., 2008. Characterization of Iron(III) in Organic Soils Using Extended X-ray Absorption Fine Structure Spectroscopy. Environmental Science and Technology 42, 5449-5454.

Köchy, M, Hiederer, R., Freibauer, A., 2015. Global distribution of soil organic carbon – Part 1: Masses and frequency distributions of SOC stocks for the tropics, permafrost

regions, wetlands, and the world. Soil 1, 351-365.

Kögel-Knabner, I., Guggenberger, G., Kleber, M., Kandeler, E., Kalbitz, K., Scheu, S., Eusterhues, K., Leinweber, P., 2008. Organo-mineral associations in temperate soils: Integrating biology, mineralogy, and organic matter chemistry. Journal of Plant Nutrition and Soil Science 171, 61-82

Lal, R., 2004. Soil carbon sequestration to mitigate climate change. Geoderma 123, 1-22.

Lalonde, K., Mucci, A., Ouellet, A., Gélinas, Y., 2012. Preservation of organic matter in sediments promoted by iron. Nature 483, 198-200.

Lehmann, J., Kinyangi, J., Solomon, D., 2007. Organic matter stabilization in soil microaggregates: Implications from spatial heterogeneity of organic carbon contents and carbon forms. Biogeochemistry 85, 45-57.

Lopez-Sangil, L., Rovira, P., 2013. Sequential chemical extractions of the mineral-associated soil organic matter: An integrated approach for the fractionation of organo-mineral complexes. Soil Biology and Biochemistry 62, 57-67.

Malinowski, E.R., 1977. Determination of the Number of Factors and the Experimental Error in a Data Matrix. Analytical Chemistry 49, 612-617.

Malinowski, E.R., 1978. Theory of error for target factor analysis with applications to mass spectrometry and nuclear magnetic resonance spectrometry. Analytica Chimica Acta 103, 339-354.

Mikutta, C., 2011. X-ray absorption spectroscopy study on the effect of hydroxybenzoic acids on the formation and structure of ferrihydrite. Geochimica et Cosmochimica Acta 75, 5122-5139.

Mikutta, C., Kretzschmar, R., 2011. Spectroscopic evidence for ternary complex formation between arsenate and ferric iron complexes of humic substances. Environmental Science and Technology 45, 9550-9557.

Mikutta, C., Mikutta, R., Bonneville, S., Wagner, F., Voegelin, A., Christl, I.; Kretzschmar, R. Synthetic coprecipitates of exopolysaccharides and ferrihydrite. Part I: Characterization. Geochim. Cosmochim. Acta 2008, 72 (4), 1111–1127.

Mikutta, C.; Frommer, J.; Voegelin, A.; Kaegi, R.; Kretzschmar, R. Effect of citrate on the local Fe coordination in ferrihydrite, arsenate binding, and ternary arsenate complex formation. Geochim. Cosmochim. Acta 2010, 74 (19), 5574–5592.

Nierop, K.G.J., Jansen, B., Verstraten, J.M., 2002. Dissolved organic matter, aluminium and iron interactions: Precipitation induced by metal/carbon ratio, pH and competition. Science of the Total Environment 300, 201-211.

O'Day, P.A., Rivera, N., Root, R., Carroll, S.A., 2004. X-ray absorption spectroscopic study of Fe reference compounds for the analysis of natural sediments. American Mineralogist 89, 572-585.

Persson, P., Axe, K., 2005. Adsorption of oxalate and malonate at the water-goethite interface: Molecular surface speciation from IR spectroscopy. Geochimica et Cosmochimica Acta 69, 541-552.

Plaza, C., Giannetta, B., Fernández, J.M., López-de-Sá, E.G., Polo, A., Gascó, G., Méndez, A., Zaccone, C., 2016. Response of different soil organic matter pools to biochar and organic fertilizers. Agriculture, Ecosystems and Environment 225, 150-159.

Pohlman, A. A., McColl, J.G., 1988. Soluble Organics from Forest Litter and their Role in Metal Dissolution. Soil Science Society of America Journal 52, 265-271.

Post, W.M., Kwon, K.C., 2000. Soil carbon sequestration and land-use change : processes and potential. Global Change Biology 6, 317-327.

Prietzel, J., Thieme, J., Eusterhues, K., Eichert, D., 2007. Iron speciation in soils and soil aggregates by synchrotron-based X-ray microspectroscopy (XANES, μ-XANES). European Journal of Soil Science 58, 1027-1041.

Ravel, B., Newville, M., 2005. ATHENA, ARTEMIS, HEPHAESTUS: Data analysis for X-ray absorption spectroscopy using IFEFFIT. Journal of Synchrotron Radiation 12, 537-541.

Rose, J., Vilge, A., Olivie-Lauquet, G., Masion, A., Frechou, C., Bottero, J.Y., 1998. Iron speciation in natural organic matter colloids. Colloids and Surfaces A: Physicochemical and Engineering Aspects 136, 11-19.

Rue, E. L., Bruland, K.W., 1995. Complexation of iron(III) by natural organic ligands in the Central North Pacific as determined by a new competitive ligand equilibration/adsorptive cathodic stripping voltammetric method. Marine Chemistry 50, 117-138.

Schmidt, M.W.I., Torn, M.S., Abiven, S., Dittmar, T., Guggenberger, G., Janssens, I.A., Kleber, M., Kögel-Knabner, I., Lehmann, J., Manning, D.A.C., et al., 2011. Persistence of soil organic matter as an ecosystem property. Nature 478, 49-56.

Schwertmann, U., 1966. Inhibitory effect of soil organic matter on the crystallization of amorphous ferric hydroxide. Nature 209, 694-696.

Schwertmann, U., 1991. Solubility and dissolution of iron oxides. Plant and Soil 1991, 3-27.

Schwertmann, U., Wagner, F., Knicker, H., 2005. Ferrihydrite–Humic Associations. Soil Science Society of America Journal 69, 1009.

Shen, Q., Suarez-Abelenda, M., Camps-Arbestain, M., Calvelo Pereira, R., McNally, S. R., Kelliher, F.M., 2018. An investigation of organic matter quality and quantity in acid soils as influenced by soil type and land use. Geoderma 328, 44-55.

Shimizu, M., Zhou, J., Schröder, C., Obst, M., Kappler, A., Borch, T., 2013. Dissimilatory reduction and transformation of ferrihydrite-humic acid coprecipitates. Environmental Science and Technology 47 13375-13384.

Siebecker, M.G., Chaney, R.L., Sparks, D.L., 2017. Nickel speciation in several serpentine (ultramafic) topsoils via bulk synchrotron-based techniques. Geoderma, 298, 35-45.

Siebecker, M.G., Sparks, D.L., 2017. Structural Differentiation between Layered Single (Ni) and Double Metal Hydroxides (Ni-Al LDHs) Using Wavelet Transformation. The Journal of Physical Chemistry A 121, 6992-6999.

Sundman, A., Karlsson, T., Laudon, H., Persson, P., 2014. XAS study of iron speciation in soils and waters from a boreal catchment. Chemical Geology 364, 93-102.

Xia, Z., Zhang, H., Shen, K., Qu, Y., Jiang, Z., 2018. Wavelet analysis of extended X-ray absorption fine structure data: Theory, application. Physica B: Condensed Matter 542, 12-19.

Yang, J., Wang, J., Pan, W., Regier, T., Hu, Y., Rumpel, C., Bolan, N., Sparks, D.L., 2016. Retention Mechanisms of Citric Acid in Ternary Kaolinite-Fe(III)-Citrate Acid Systems Using Fe K-edge EXAFS and $L_{3,2}$-edge XANES Spectroscopy. Scientific Reports 6, 1-9.

Table 5.1 Main physical and chemical properties of coniferous forest soils (CF), broadleaved forest soils (BF), grassland soils (GL), technosols (TS) and agricultural soils (AG). Data are from Giannetta et al. (2018).

Land use	**EC** *($\mu S \cdot cm^{-1}$)*	**pH**	**Sand** *($g \cdot kg^{-1}$)*	**Silt** *($g \cdot kg^{-1}$)*	**Clay** *($g \cdot kg^{-1}$)*	**Organic C** *($g \cdot kg^{-1}$)*	**Total N** *($g \cdot kg^{-1}$)*	**C/N**	**Fe** *($mg \cdot kg^{-1}$)*	**CEC** *(meq/100g)*	**Exch. Mg** *($mg \cdot kg^{-1}$)*	**Exch. Na** *($mg \cdot kg^{-1}$)*	**Exch. K** *($mg \cdot kg^{-1}$)*	**Exch. Ca** *($mg \cdot kg^{-1}$)*
CF	113	7.9	527	212	261	77.9	4.5	17.4	30927	44.2	170	66	132	10851
GL	69	7.6	631	202	167	93	7.7	12	27461	36.1	108	43	289	8956
TS	51	8.5	142	452	406	7.5	0.8	9	21181	20.8	458	42	202	3250
AG	103	8.4	339	471	190	11.8	1.1	10.7	22111					

Table 5.2 Chemical properties of the fine silt and clay (FSi+Cl) coniferous forest soils (CF), broadleaved forest soils (BF), grassland soils (GL), technosols (TS) and agricultural soils (AG).

Land use	**Organic C** *(g/100g)*	**Total N** *(g/100g)*	**C/N**	**Mg** *(%)*	**Al** *(%)*	**Si** *(%)*	**P** *(%)*	**K** *(%)*	**Ca** *(%)*	**Ti** *(%)*	**Mn** *(%)*	**Fe** *(%)*
CF	5.41	0.42	12.9	2.2	16.9	38.3	0.1	5	26.5	0.86	0.7	9
GL	8.5	0.76	11.1	2.5	18.3	47	0.4	6.7	12.7	0.9	0.7	10.3
TS	0.7	0.08	8.2	4.1	14.9	37	0.2	4.5	31	0.7	na	7.4
AG	1.8	0.19	9.5	3.8	23.6	47.7	0.3	7.6	6.6	1.3	0.1	8.5

Table 5.3 Summary of EXAFS linear combination fitting over the *k* range 2.5-10 Å. F-test has been calculated and is reported in the third column.

Sample	k range fit	I	Measurements	R-factor	Component 1		Component 2		Component 3		Sum
CF U	2.5-9	0.248	13.414	0.0086	Illite	39%	Ferrihydrite	23%	Fe(III)-citrate	41%	102%
CF R	2.5-9.5	0.013	14.369	0.0178	Illite	25%	Ferrihydrite	30%	Fe(III)-citrate	35%	90%
GL U	2.5-10	0.002	15.324	0.0266	Smectite	31%	Ferrihydrite	48%	Fe(III)-citrate	18%	97%
GL R	2.5-10	0.001	15.324	0.0387	Smectite	21%	Ferrihydrite	43%	Fe(III)-citrate	23%	86%
TS U	2.5-10	0.050	15.324	0.0729	Chlorite	26%	Ferrihydrite	47%	Fe(III)-citrate	33%	105%
TS R	2.5-10	0.025	15.324	0.0959	Chlorite	33%	Ferrihydrite	52%	Fe(III)-citrate	28%	112%
AG U	2.5-10	0.002	15.324	0.0320	Chlorite	22%	Ferrihydrite	48%	Fe(III-)citrate	37%	107%
AG R	2.5-10	0.021	15.324	0.0604	Chlorite	14%	Ferrihydrite	41%	Fe(III)-citrate	46%	102%

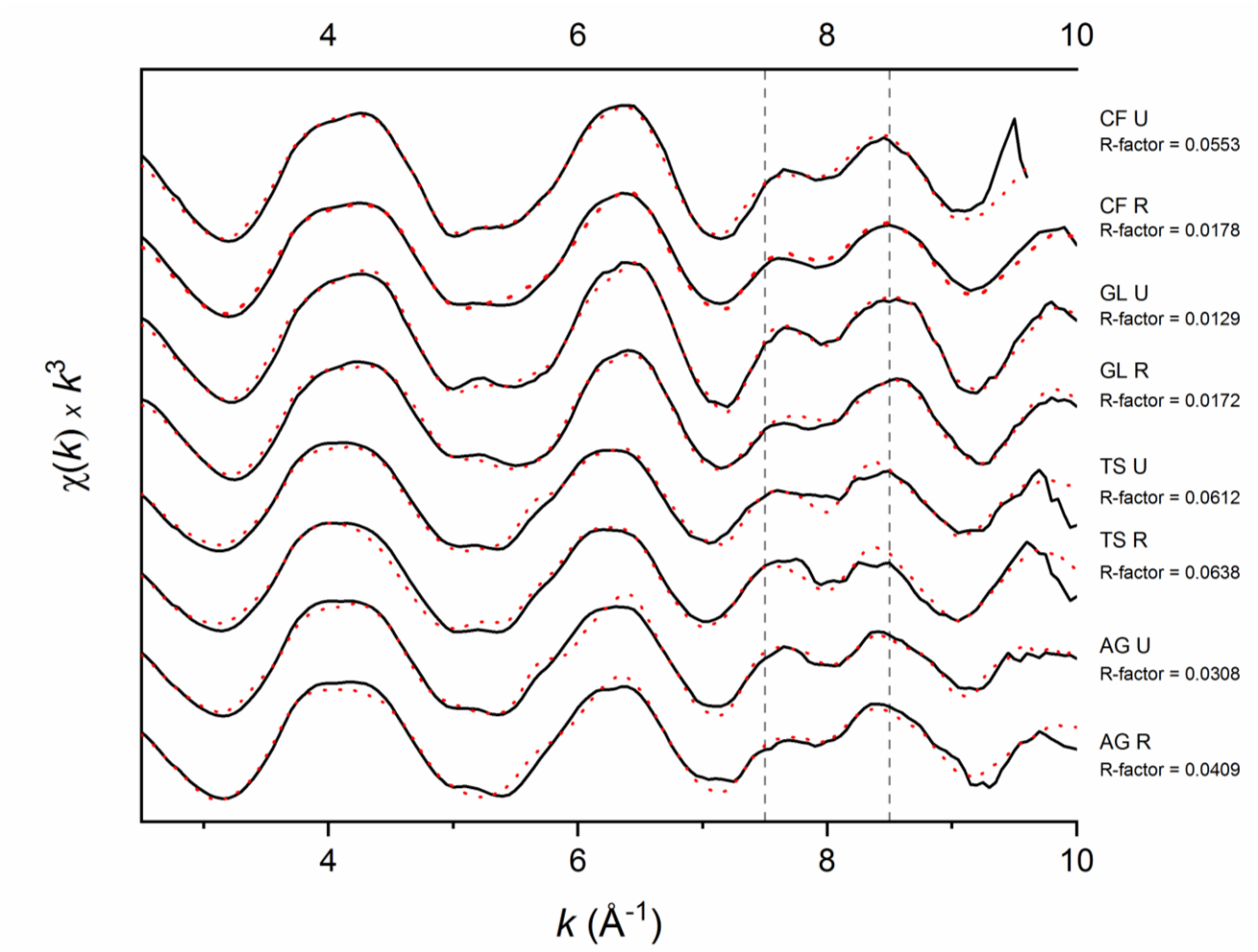

Figure 5.1 k^3–weighted EXAFS spectra of fine silt and clay (FSi+Cl) fraction from coniferous forest (CF), grassland (GL), technosol (TS) and agricultural (AG) soils before and after reaction with Fe(III). Solid lines indicate the sample data, whereas red dotted lines represent the LCF fit. R-factors are also displayed.

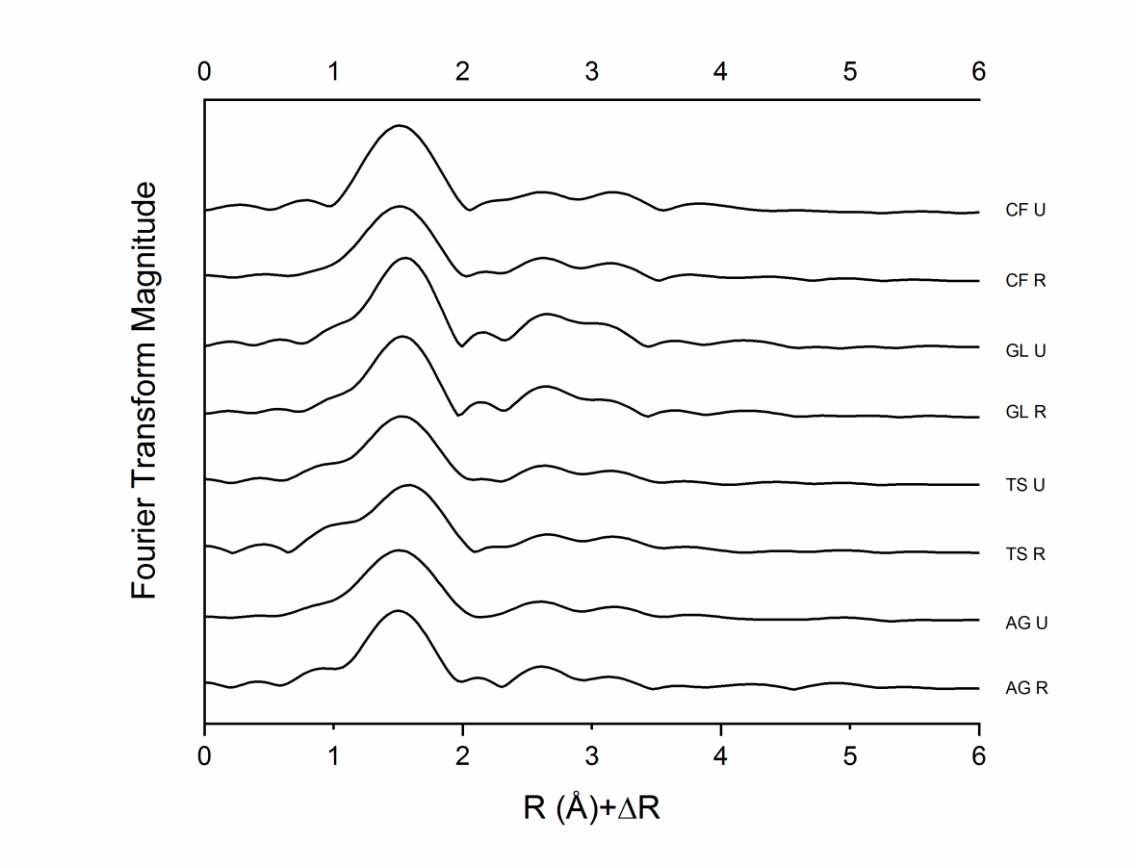

Figure 5.2 FT spectra of fine silt and clay (FSi+Cl) fractions from coniferous forest (CF), grassland (GL), technosol (TS) and agricultural (AG) soils before (U) and after reaction with Fe(III) (R).

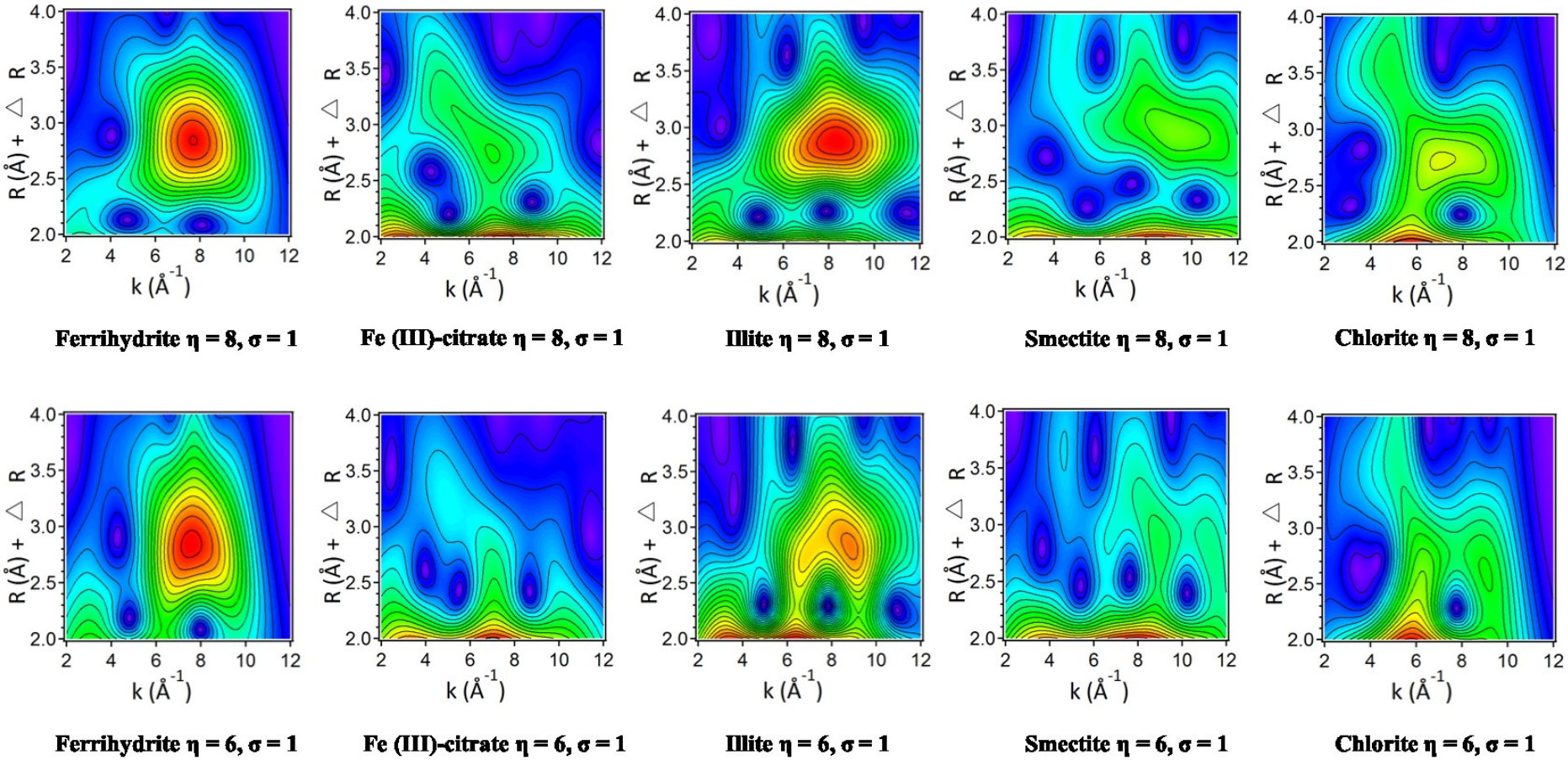

Figure 5.3 High resolution WT plots of standards displaying the second coordination shell. Data are plotted as a function of k (Å-1) on the x axis and R (Å) on the y axis in the range 2.0-4.0 (Å).

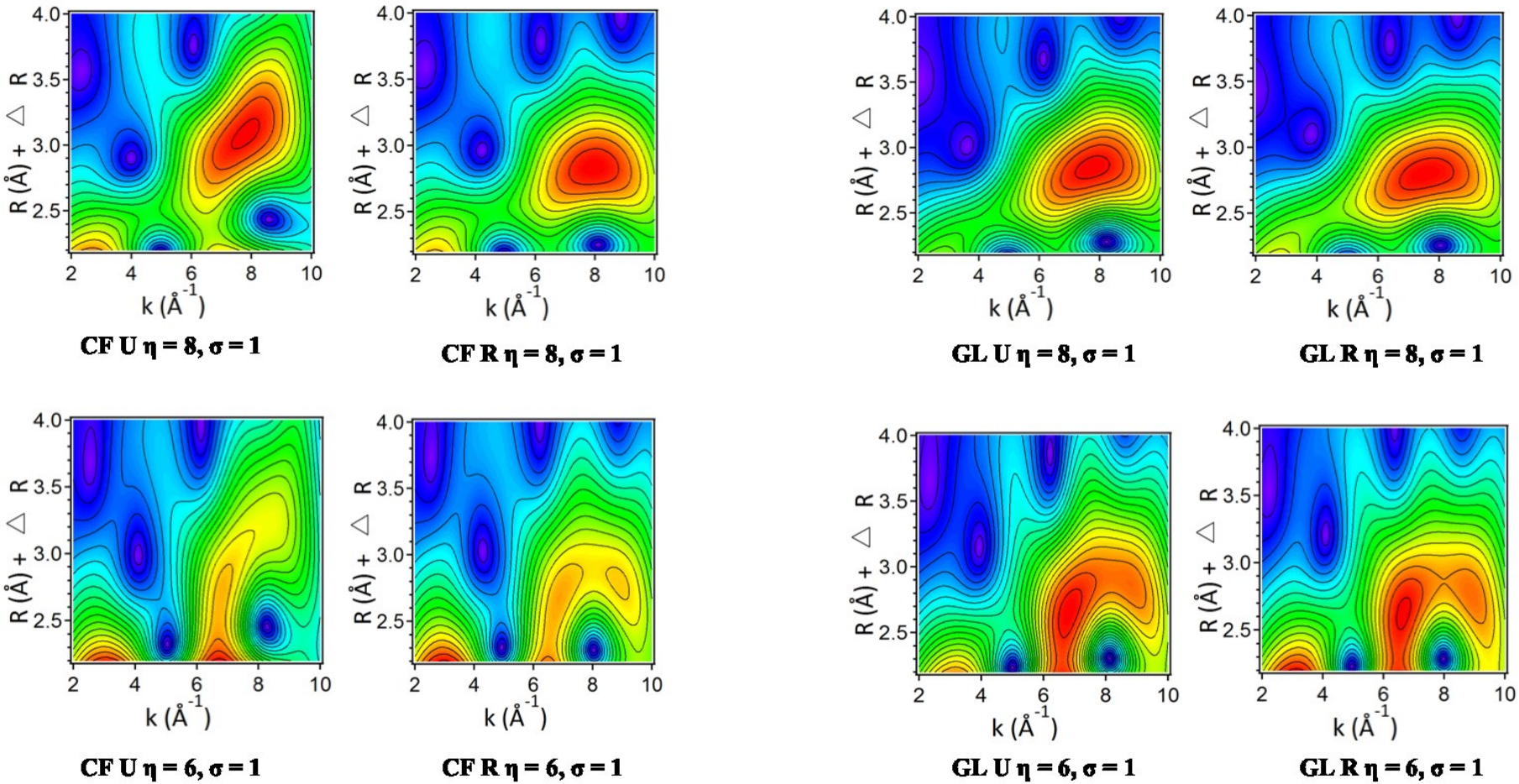

Figure 5.4 High resolution WT plots of fine silt and clay (FSi+Cl) fractions from coniferous forest (CF), grassland (GL), technosol (TS) and agricultural (AG) soils before (U) and after (R) reaction with Fe(III) displaying the second shell. Data are plotted as a function of k ($Å^{-1}$) on the x axis and R (Å) on the y axis in the range 2.2-4.0 (Å)

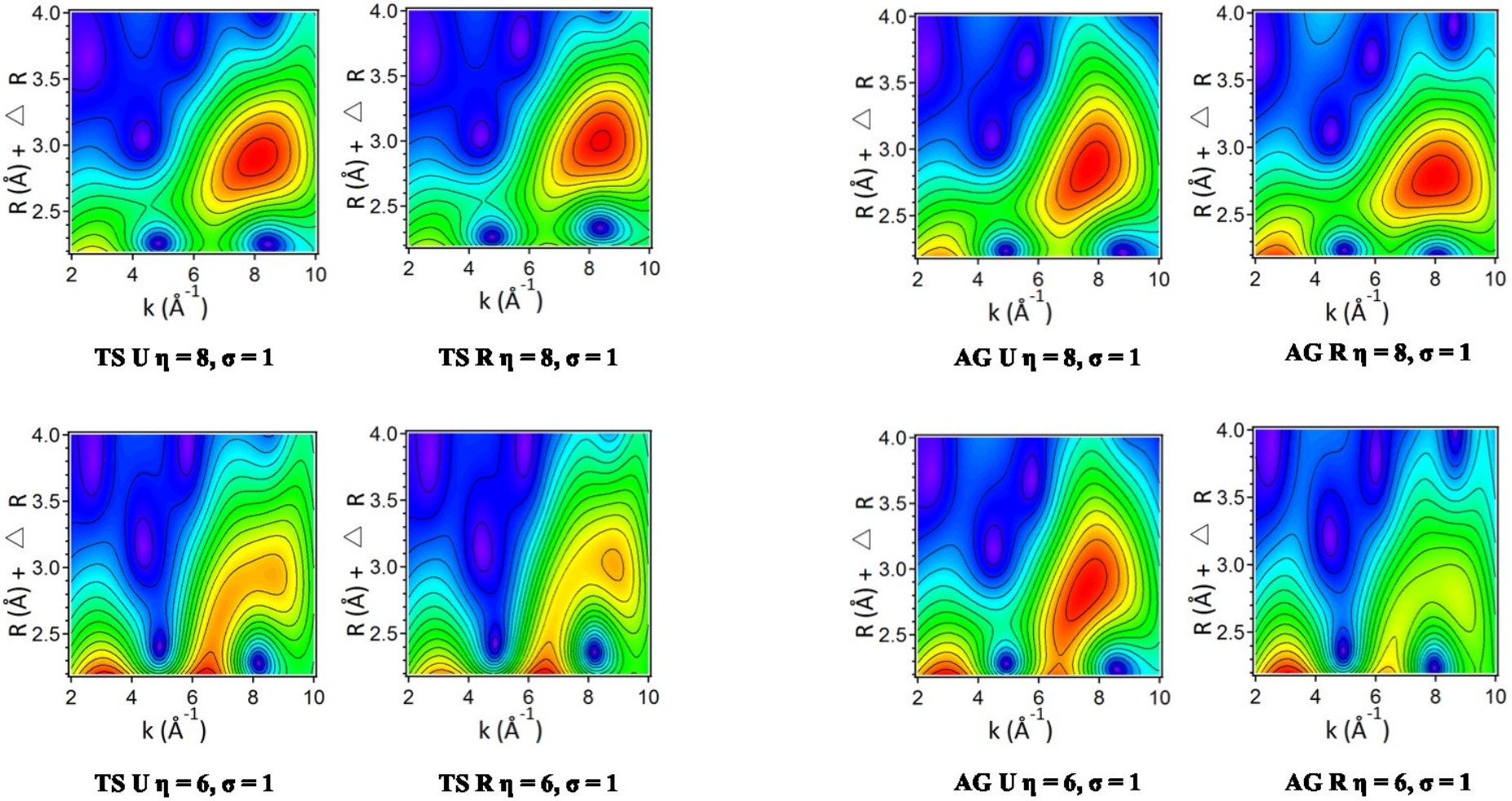

Figure 5.4 (continues)

6. Fe speciation changes induced by biochar and organic fertilizers amendments in SOM pools under agricultural soils

(Giannetta, B., Siebecker, M.G., Plaza, C., Zaccone, C., Aquilanti., G., Vischetti, C., Sparks., D.L., Submitted)

Abstract

Biochar, as well as of its interactions with other organic amendments co-applied to the soil, represents an agronomic and environmental potential as a carbon (C) sequestration strategy Although is well-known how different fertilization practices affect organo-mineral associations and aggregation, their role in regulating iron (Fe) speciation remains less clear. Due to the growing environmental interest related to a sustainable agriculture, we aimed in this study to identify and quantify the Fe phases present in different agricultural soil fractions: fine sand (FSa) and fine silt and clay (FSi+Cl). We employed Fe Extended X-ray Adsorption Fine Structure Spectroscopy (EXAFS) to analyze an agricultural soil with added organic amendments (*i.e.,* biochar (BC), compost (MC) and the simultaneous application of both BC+MC.

The application of linear combination fitting (LCF) and wavelet transform (WT) revealed noticeable differences between unamended FSa and FSi+Cl fractions. The fine fraction was mainly characterized by ferrihydrite (48%) and Fe(III)–organic complexes (*i.e.,* Fe(III)-citrate) (37%), whereas in the coarse fraction ferrihydrite still represented the main phase (44%), with less significant contribution from Fe(III)-OM (18%). The increase in Fe-OM complexation after amendment indicated that the introduction of organic amendments can hinder the transformation of Fe(III) complexed by organic ligands in the soil solution into ferrihydrite. In the FSi+Cl fraction the interaction between freshly added organic matter (OM) can eventually lead to surface site blockage and to the formation of more aggregated particles and consequently to a less dissolution rate. Our results provide evidence that reactive Fe mineral species and their association with C are affected by the type of fertilization and particle size.

6.1. Introduction

Understanding soil organic carbon (SOC) cycling and its response to climate change

(Amundson, 2001; Lal, 2004; Blanco-Canqui and Lal, 2004; Schmidt et al., 2011) requires a full comprehension of the mechanisms involved in the buildup of soil organic matter (SOM) pools with long residence time (Kögel-Knabner et al., 2008; Dungait et al., 2012).

Soil scientists are recently asked to provide concrete answers to two major questions with regard to global issues concerning greenhouse gas and atmospheric CO_2: (1) can agricultural soils sustainably increase their total sequestrated organic carbon (C) contents (Lal, 2004) and (2) how will soils respond to the expected global warming trend (Bellamy et al., 2005). These issues are a challenge because "Sustainable agriculture is not a luxury" (Rasmussen et al., 1998) and many C sequestration strategies have been recently proposed for a long-term CO_2 withdrawal. Among them, the main purposes of biochar, a C-rich product made by the pyrolysis of biomass (*e.g.,* plant-derived biomass), application are well documented (Lehmann, 2007; Bolan et al., 2012; Singh and Cowie, 2014) for soil quality enhancement and climate change mitigation. Moreover, due to the ability of biochar to accept and donate electrons, it plays and important role in abiotic redox reactions (Keiluweit et al., 2010; Klüpfel et al., 2014; Kappler et al., 2014; Zhou et al., 2017), thus transferring the accepted electrons to iron (Fe)(III) minerals, known as electron acceptors (Kappler et al., 2014).

Reactive mineral surfaces including Al and Fe minerals drive C stabilization (Solomon et al., 2012; Lalonde et al., 2012; Kleber et al., 2015) and SOM is supposed to increase with the low crystallinity short-range-order (SRO) minerals (Torn et al., 1997; Kleber et al., 2007). Cultivation practices modify physicochemical conditions which propose soil stability, leading to the dissolution of already existing minerals and the formation of others (Basile-Doelsh et al., 2009). For example, the application of organic amendments in soils can influence the reactive surfaces of organo-mineral complexes, leading to the conclusion that Fe composition relates to SOM composition (Hall et al., 2018).

Soil systems characterized by a broad range of Fe mineral species (*e.g.,* clay minerals, Fe-SOM complexes, and polymeric Fe (hydr)oxydes, the possibility to quantify species in different particle size fractions of soils using advanced spectroscopic techniques can constitute a rapid and nondestructive addition to sequential extraction methods. Extended X-ray absorption fine structure spectroscopy (EXAFS) has been used to study local bonding and local structure of metal complexes, but its use for the characterization of Fe species present in SOM is limited. Regarding Fe association with natural organic matter

(NOM), it found its main application to characterize Fe(III) in organic soils under different pH ranges and with varying natural Fe content (*i.e.,* Gustafsson et al. 2007, Karlsson et al. 2008).

Although the relationship between Fe and C abundance is well-known, limited research has been performed to clarify the complex interdependence between Fe phases and amount and chemical composition of SOM (Hall et al., 2018) at an atomic scale using advanced spectroscopic techniques. In detail, although the biochar association with other organic amendments has been described as a C sequestration mechanism (Bolan et al., 2012; Agegnehu et al., 2016; Plaza et al., 2016), less is known about the role of biochar and different amendments on the association between OM and Fe-bearing minerals in naturally occurring fractions at the submicron scale.

The application of Fe EXAFS in structurally and elementally complex soils and fractions can represent a challenging step, although this method should allow Fe speciation in soil particles and aggregates (Prietzel et al., 2007). More recently Fe EXAFS has enabled the identification of fertilization practices on Fe speciation, but it was limited to soil colloids (Xiao et al., 2016; Huang et al., 2016; Wen et al., 2018). Xiao et al. (2016) demonstrated the effect of organic inputs (*i.e.,* manure application) on the composition of reactive Fe minerals in soil colloids. Fe speciation in soils, soil horizons and aggregates and the Fe spatial distribution in the aggregates is determined by soil pH, redox potential, organic ligands activity (Blume et al., 1969; Prietzel et al., 2007). Moreover, the complexity of particle size can affect both SOM storage mechanisms and Fe speciation, and thus, the role of Fe-bearing minerals in organic C retention and thus pairing traditional size particle fractionation with advanced spectroscopic investigation has never been more needed. To the best of our knowledge, only Asano et al. (2018) used soft X-ray scanning transmission microscopy (STXM) coupled with near edge X-ray adsorption fine structure (NEXAFS) in size fractions.

In natural soils and soil fractions the possibility to discriminate the contributions from different backscattering atoms in higher coordination shells at similar bonding distances from the central Fe atom received an advantage pairing the traditional EXAFS analyses (*e.g.,* shell fitting of the Fourier transform (FT)) with Wavelet transformation (WT). WT provides useful information resolving simultaneously data in both wave space (k-) and interatomic distance uncorrected for phase shifts (R-) space and *k*-R maps are helpful in improving the fitting model and understanding the local structure (Xia et al., 2018).

We tested the effect of (1) different amendments (*i.e.,* biochar (BC), compost (MC)

and the simultaneous application of both (BC+MC)) and (2) of size fractions (*i.e,* fine sand (FSa) and fine silt plus clay (FSi+Cl)) on the quantity and composition of Fe minerals.

6.2. Materials and methods

6.2.1. Soil samples collection and physical fractionation

The site selected for this research was located in the experimental farm "La Poveda" (Spanish National Research Council, CSIC), Arganda del Rey, Madrid, Spain (40190 N, 3290 W, 534 m above sea level). The site was characterized by a Mediterranean climate, with an average annual rainfall of 436 mm and average annual temperature of 14 ºC. The soil showed a clay loam texture and was classified as a Xerofluvent. The biochar used in this study was produced in a pyrolysis plant from holm oak (*Quercus ilex L.*) chips through a slow pyrolysis process at 600 C. The municipal solid waste compost was produced using a conventional windrow composting system at a waste treatment plant. The main properties of the top soil (0–15 cm), biochar, and conventional amendments, as also the detailed description of the experiment, were reported in Fernández et al. (2014) and Plaza et al. (2016) and are summarized here in Table 6.1 and table 6.2.

A physical size fractionation by ultrasonic dispersion and wet sieving was performed, allowing for splitting particles into four different size fractions (Lopz-Sangil and Rovira, 2013): coarse sand (CSa: 2000-200 µm diameter), fine sand (FSa: 200-50 µm), coarse silt (CSi: 50-20 µm) and fine silt and clay (FSi+Cl: <20 µm). 15 g of each sample were put into 50 mL vials and filled with deionized water to 3/4 of their volume. Samples were then subjected to vertical agitation (20 rpm) for 60 minutes and to ultrasonic dispersion of the soil particles for 10 minutes at 60% of the total amplitude (100 W output) using a Branson 45 sonifier. The derived suspensions were then wet-sieved through a set of three sieves (200 µm, 50 µm and 20 µm hole) splitting particles into four different size fractions. The fractions retained by sieves (CSa, FSa, CSi) were directly recovered from the sieves, quantitatively transferred to pre-weighted vials and dried at 60 ºC to constant weight. The particles passing through the last sieve (<20 µm: FSi+Cl) were brought to *ca.* 1 L and left to stand refrigerated for 2 days; overlying water was then carefully siphoned off and discarded. The sediment was transferred into 250 mL polypropylene

vials and centrifuged for 15 min at 2500 g. In this research, we used the FSa and FSi+Cl fractions (Table 6.3).

6.2.2. Organic C, total N and Fe analyses

Total C and N contents of both bulk soil samples and SOM fractions were determined by dry combustion using a Thermo Flash 2000 NC Soil Analyzer. Before analysis, an aliquot of each sample was ground with a ball mill. For organic C determination, the whole soil samples and mineral-associated OM fractions were subjected to acid acid fumigation before the analysis (Harris et al., 2001) to remove carbonates.

6.2.3. Iron K-edge Extended X-ray Adsorption Fine Structure Spectroscopy (EXAFS)

X-ray absorption spectroscopic analyses of FSa and FSi+Cl fractions were conducted at the XAFS beamline at Elettra Sincrotrone Trieste. Fe EXAFS spectra were collected in transmission mode using Si (111) monochromator, which was calibrated to the first-derivative maximum of the K-edge absorption spectrum of a metallic Fe foil (7112 eV). The monochromator was detuned 40% to reduce higher order harmonics. Samples were prepared as pressed powders between Kapton® tape and mounted in a sample chamber at room temperature. Two to six replicates were collected and averaged.

6.3. Results and discussion

6.3.1. Organic C and total N contents

A summary of organic C and total N contents of the examined fractions is shown in table 6.2. Total soil organic C content ranges from 3.5 to 9.1 g kg^{-1} in FSa and from 18.1 to 28.2 g kg^{-1} in FSi+Cl, whereas total N varies between 0.26 and 0.41 g kg^{-1} in FSa and between 1.9 and 2.3 g kg^{-1} in FSi+Cl. The main organic C and total N accumulation in the FSi+Cl fraction can be the consequence of an increased aggregate disruption and aeration due to tillage with a consequent preferential storage in the finer fraction. Biochar-treated soils have significantly greater total organic C contents than biochar-untreated soils, while compost fertilization increases not only soil organic C but also N content.

This is in agreement with our previous work (Plaza et al., 2016), showing that biochar and compost can increase SOM content and that can the mechanism through which they promote C stabilization is the formation of organo-mineral complexes by intimate interaction between organic inputs and mineral particles.

6.3.2. PCA, TT and F-test

The results of PCA are summarized in table C1 and figure C1. In a first step, the Factor Indicator Function (Malinowski, 1977), the IND value obtained from the PCA analysis, reached the minimum for four components, indicating that four was the ideal number of structurally meaningful components. Moreover, the scree plot represented in figure C1 indicates a break in the slope at two components, indicating that the components before the break are more likely to be structural.

In the second step, the number of components that should be included in the fitting were selected by TT, using the SPOIL function (Malinowski, 1978). The SPOIL values were <1.5 (Table C2) and most of the models classified as excellent model compounds, the best fit of unamended and amended samples was obtained using three fitting components. The description of the standards used for LCF is reported in table C2. All of them have been previously described in O'Day et al. (2004). Chi-square, R-values, and SPOIL and chi-square are also reported.

6.3.3. LCF

LCF results are reported in table 6.3, revealing the dominant types of species identified as major components by the fit. The Fe EXAFS data fitting revealed that Fe phases in unamended FSa and FSi+Cl fractions are noticeably different. In the coarse fraction (C FSa) ferrihydrite represented the main phase (44%), followed by chlorite (26%) and with less significant contribution from Fe(III)- organic complexes (*i.e.,* Fe(III)-citrate) (18%). The fine fraction was mainly characterized by ferrihydrite (48%) and Fe(III)–OM (37%), Low molecular weight organic acids constitute an important part of labile C and can be subjected to minerals and metal cations binding mechanisms (Mikutta et al., 2010; Yang et al., 2016). Among them, citric acid is the main constituent of microbial metabolites and root exudates (Gunina et al., 2014) and represents in this study an analog model compound for Fe-OM complexes. Our results agree with Asano and Wagai (2014), proposing that larger size fractions are increasingly dominated by primary mineral

crystals and smaller size fractions are more dominated by the micron- and submicron-sized composites enriched in low crystallinity short-range-order (SRO) minerals and organo-metal associations.

Ferrihydrite was prominent in all the FSi+Cl fractions, with similar values, 48% in the unamended and 45% in the compost amended soil. The remaining Fe phases were composed of clay minerals and Fe(III)-silicate, represented by chlorite. The percentage of Fe(III)-OM was the similar under biochar amendment (44%), followed by compost (43%) and both biochar and compost (41%), compared to the control soil (37%) (Table 6.3).

When compared to the fine fraction, the coarse SOM fraction was characterized by higher chlorite contents (25-36%) and lower contents in poor crystalline high surface area Fe minerals (ferrihydrite), ranging from ca. 28% in all the amended soils to 44% in the control soil. Conversely, Fe phases in amended FSa fractions were represented by higher Fe-OM contents.

The common increase in Fe-OM complexation after the amendment, in both FSa and FSi+Cl fractions, suggests that the introduction of organic amendments can hinder the transformation of Fe(III) complexed by organic ligands in the soil solution into ferrihydrite (Rose et al., 1998; Karlsson and Persson, 2012) It is well-known that dissolved organics can retard ferrihydrite transformation (Schwertmann, 1966; Kodama and Schnitzer, 1977; Cornell and Schwertmann, 1979; Schwertmann et al., 1982, 2005). Specifically, the sorption of SOM and some organic acids (*i.e.,* citric) on the ferrihydrite surface inhibits the crystallization of further Fe oxide phases. Fe speciation has been studied to evaluate contrasting organic-inorganic amendments systems. Xiao et al. (2016) found an increase in ferrihydrite minerals after organic amendments and agrees with the results reported in Xu et al. (2010). The latter indicated that the presence of low molecular weight organic acids was responsible of the inhibition and thus of the further growth of the SRO minerals. Huang et al. (2016) added oxalic acid to soil colloids, confirming the role of organic inputs in the formation of reactive minerals through the increasing in ferrihydrite instead of goethite. The effectiveness in suppressing crystallization can depend on whether and how strongly the acid adsorbs onto ferrihydrite and how strongly it complexes with Fe(III) in solution. Additionally, the extent by which the adsorption of organic molecules prevents the dissolution of ferrihydrite depends on the degree of surface coverage. For example, Fe(III) oxides exhibit a large specific surface area and contribute to the overall surface area of soils. This is important in view of the fact that the

dissolution rate is usually a function of surface area (Schwertmann, 1991) and that mineral nanoparticles behave differently as a function of their particle size (Hochella et al., 2008). As the surface area decreases, the particle size increases, and the surface reactivity of the particles increases (Villacís-García et al., 2015). Although controversial, this might constitute an explanation for the higher OM complexation to ferrihydrite in the FSa fraction. Organic ligands are known, through surface adsorption, to either accelerate or retard dissolution. The dissolution acceleration depends on the weakening the Fe-O bond operated by organic ligands (Schwertmann, 1991).

Mikutta et al. (2008) found that the coprecipitation of polysaccharides with Fe(III) (hydr)oxides can increase the ligand-accessible surface area of ferrihydrite, enhancing the dissolution of ferrihydrite by low molecular weight ligands. This can explain the increasing in ferrihydrite dissolution in the amended samples, in the FSa fraction. In the FSi+Cl fraction, the interaction between freshly added OM can lead to surface site blockage and to the formation of more aggregated particles and consequently to a lower dissolution rate. Mikutta et al. (2010) reported that organic chelates such as hydroxybenzoic acids control the kinetics of ferrihydrite formation via Fe(III) complexation thereby effectively lowering the solution saturation state of inorganic Fe(III) species, leaving less Fe(III) available for ferrihydrite precipitation., Mikutta et al. (2010) proved the citrate decreased ferrihydrite particle size impairing the polymerization of the octahedral via edge and corner linkages. Organic ligands surface adsorption may accelerate dissolution, weakening the Fe-O bond. Thus, Fe released might give rise to Fe-OM complexes. Citrate reduced the static disorder of Fe-O bonds, with a consequent octahedral distortion in ferrihydrite. Citrate stabilized ferrihydrite colloidal suspensions, reducing ferrihydrite formation at the expense of soluble Fe(III)-citrate complexes.

The hypothesis of an increased ferrihydrite dissolution rates after amendments in FSa rather than in FSi+Cl needs to be confirmed over time. Following ferrihydrite transformation dynamics, proving these mechanisms overtime (*i.e.,* after three consecutive years of amendment) can support the hindering role played by organics in ferrihydrite and application of the modeled knowledge in natural systems. Moreover, biochar can accept and donate electrons, influencing ferrihydrite microbial reduction (Kappler et al., 2014) and a next step of this research can involve the evaluation of field aging on the long-term electron shuttling capability of biochar.

Fe EXAFS can be also used for qualitative analysis of the composition of Fe minerals. LCF results are drawn in figure 6.1 and the fit of each sample, in dotted lines, is labeled

with the R factor. Fe K-edge EXAFS spectra show similar features at ~4.0 $Å^{-1}$ (peak 1), ~6.5 $Å^{-1}$ (peak 2), ~7.5 $Å^{-1}$ (peak 3), ~8.5 $Å^{-1}$ (peak 4). The peak at 7.5 $Å^{-1}$ is characteristic of ferrihydrite (Fig. C2) and become less evident in all the FSa samples compared to FSi+Cl, although is more pronounced in the control. The role of OM in hindering the formation of ferrihydrite is confirmed in the FSi+Cl spectra.

Compared to the control, organic amendment is responsible of the shift of the peak at 8.5 $Å^{-1}$ towards the characteristic peak at 8 $Å^{-1}$ typical of Fe (III) citrate, indicating the role of OM in promoting Fe-OM complexation. This is noticeable in FSa samples and not in FSi+Cl, in which the difference in Fe(III) compounds ranged only from 37% in the control to 44% in the biochar amended soil. The peak at 4.0 $Å^{-1}$ remained basically unchanged, and the its lower intensity in FSa confirms the lower percentage in crystalline oxides.

Moreover, since the SOM composition dictates the aggregation dynamics and the surface coverage, influencing the ligand-promoted dissolution we underline the importance of consider the surface-controlled processes driving dissolution rates.

6.3.4. Wavelet transformation

WT analysis has been used to qualitatively test for the presence of Fe back-scatterers in the second coordination shell of Fe. We calculated the Morlet wavelet transforms of k^3-weighted Fe K-edge EXAFS spectra of the samples over a R + ΔR-range of 2.2-4.0 Å and compared the resulting wavelet plots with those of Fe(III) reference compounds (ferrihydrite, Fe(III)-citrate, chlorite). Figure 6.2 contains the WT plots of the standards. In the ferrihydrite plot, the Fe shell contributes a strong feature at 7-8 $Å^{-1}$ and 2.75 Å, as as supported by the FT plots in figure C3. In Fe(III)-SOM complexes the absence in Fe backscattering is accompanied by new features at distances of 2.0–2.5 Å and 3.1–3.7 Å and indicates back-scattering from lighter atoms, in agreement with single and multiple backscattering from C/O in the second and third coordination shells of trisoxalatoiron(III) (Persson and Axe, 2005; Karlsson and Persson, 2010; Daugherty et al., 2017). Moreover, these features appear at lower energies (3–4 $Å^{-1}$) than those of Fe. In general clay minerals can be described by three atomic backscattering shells: the first-neighbor O, second-neighbor octahedral Fe, Al, or Mg; and tetrahedral Si. In many Fe oxyhydroxides and phyllosilicate the Fe-Fe neighbor distances overlap, and cannot be used a diagnostic in EXAFS.

WT of the EXAFS data (η=8, σ=1) showed that both the intensity caused by light back-scatterers at low k-values and by heavier atoms at higher k varied among the samples (Figure 6.3). The WT results support the LCF analysis, which indicated that EXAFS spectra of the soil samples can be described as a mixture of Fe-bearing clay minerals, Fe (hydr)oxides and organically complexed Fe. The WT (Fig. 6.3) and the FT (Figure C4) plots of the unamended FSi+Cl and FS samples indicate a Fe-Fe second shell contribution from ferrihydrite and chlorite. A contribution from Fe(III)-citrate at above 2.2 Å and 2–4 $Å^{-1}$ is also evident. After the biochar amendment, the Fe-Fe signal remains the main feature in the FSi+Cl fraction, and is also evident a slight increase in the Fe-OM signal contribution, as also reported in the LCF results. Fe-Fe backscatters in the second shell of FSi+Cl samples (Fig. 6.3) are in agreement with the results reported in LCF.

In the biochar amended FSa fraction, the signal from the Fe-Fe second shell disappears, mirroring the decrease in the ferrihydrite percentage from 44 to 29%, whereas the increase of the feature from C backscattering is evident, related to the increase of Fe(III)-OM from 18 to 31%. The same trend is reported in the compost and biochar plus compost reacted samples: the predominant feature in the second shell of FSa samples (Fig. 6.3) is from C backscattering.

Modifying η from 9 to 4, at η=9 the resolution in R-space is high while resolution in k-space is low, reaching the best spatial resolution in R-space at η= 7 (Figures C5 and C6). The scattering path from different elements between 6 and 10 $Å^{-1}$ starts to be more clearly resolved at η= 7, with the best resolution at η=6. At 7 the maximum starts to discrete into separate peaks, for both standards (Figure C5) and samples (Figure C6), indicating the splitting of the major component in two minor components. In all the amended FSi+Cl fraction, the peak resolution over the η range considered is similar to the one in ferrihydrite sample (Figure C5). Conversely, in FSa, the plots present clear similarity with the WT plots of Fe(III)-citrate (Figure C5).

Our data indicate that the formation of Fe(III)-OM complexes is occurring in amended FSa fractions. The formation of Fe(III)-OM complexes seems to strongly suppress the hydrolysis and polymerization of Fe(III) and that in oxic environments, the fate of Fe is with large extent controlled by the properties of the organic Fe(III) complexes.

Due to the wide variability of physicochemical properties, Fe-OM complexation mechanisms are difficult to assess and leave opened a lot a possible interpretation

scenarios.

6.4. Environmental implications

Fe-organic associations need to be evaluated in the complexity and heterogeneity of soils instead of model compounds. Although the relationship between Fe and C abundance is well-known, limited research has been performed to clarify the complex interdependence between Fe phases and amount and chemical composition of SOM at an atomic scale using advanced spectroscopic techniques. In detail, although the BC association with other organic amendments has been described as a C sequestration mechanism, less is known about their role on the association between OM and Fe-bearing minerals in naturally occurring fractions at the submicron scale.

The results show that unamended FSa and FSi+Cl fractions are noticeably different, being the fine fraction mainly characterized by ferrihydrite and Fe(III)–organic complexes whereas the coarse fraction by similar ferrihydrite content and lower Fe(III)-OM.

After the amendment, the LCF results revealed a more marked decrease in ferrihydrite percentage in FSa than in FSi+Cl. In the FSi+Cl fraction the interaction between freshly added OM can lead to surface site blockage and to the formation of more aggregated particles and consequently to a less dissolution rate. We underline the importance of consider the surface-controlled processes driving dissolution rates. This is important in view of the fact that the dissolution rate is usually a function of surface area and that mineral nanoparticles behave differently as a function of their particle size. As the surface area decreases, the particle size increases, and the surface reactivity of the particles increases. Although controversial, this might constitute an explanation for the higher reactivity of ferrihydrite in FSa fraction to OM complexation.

Future studies should address the possibility of an increased ferrihydrite dissolution rates and its transformation dynamics after amendments in FSa rather than in FSi+Cl over time. This can confirm the hindering role played by organics in ferrihydrite transformation, applying the modeled knowledge to natural systems.

References

Amundson, R., 2001. The carbon budget in soils. Annual Review of Earth and Planetary Sciences 29, 535-562.

Agegnehu, G., Bass, A.M., Nelson, P.N., Bird, M.I., 2016. Benefits of biochar, compost and biochar-compost for soil quality, maize yield and greenhouse gas emissions in a tropical agricultural soil. Science of the Total Environment 543, 295-306.

Asano, M., Wagai, R., 2014. Evidence of aggregate hierarchy at micro- to submicron scales in an allophanic andisol. Geoderma 216, 62-74.

Asano, M., Wagai, R., Yamaguchi, N., Takeichi, Y., Maeda, M., Suga, H., Takahashi, Y., 2018. In Search of a Binding Agent: Nano-Scale Evidence of Preferential Carbon Associations with Poorly-Crystalline Mineral Phases in Physically-Stable, Clay-Sized Aggregates. Soil Systems, 2, 32.

Basile-Doelsch, I., Brun, T., Borschneck, D., Masion, A., Marol, C., Balesdent, J., 2009. Effect of landuse on organic matter stabilized in organomineral complexes: A study combining density fractionation, mineralogy and $\delta^{13}C$. Geoderma 151, 77-86.

Bellamy, P. H., Loveland, P.J., Bradley, R.I., Lark, R.M., Kirk, G.J.D., 2005. Carbon losses from all soils across England and Wales 1978-2003. Nature 437, 245-248.

Blanco-Canqui, H., Lal, R., 2004. Mechanisms of carbon sequestration in soil aggregates. CRC. Critical Reviews in Plant Sciences 23, 481-504.

Blume, H. P., Schwertmann, U., 1969. Genetic Evaluation of Profile Distribution of Aluminum, Iron, and Manganese Oxides1. Soil Science Society of America Journal 33, 439-444.

Bolan, N.S., Kunhikrishnan, A., Choppala, G.K., Thangarajan, R., Chung, J.W., 2012. Stabilization of carbon in composts and biochars in relation to carbon sequestration and soil fertility. Science of the Total Environment 424, 264-270.

Cornell, R.M., Schwertmann, U., 1979. Influence of Organic Anions on the Crystallization of Ferrihydrite. Clays and Clay Minerals 27, 402-410.

Daugherty, E.E., Gilbert, B., Nico, P.S., Borch, T., 2017. Complexation and Redox Buffering of Iron(II) by Dissolved Organic Matter. Environmental Science and Technology 51, 11096-11104.

Dungait, J.A.J., Hopkins, D.W., Gregory, A.S., Whitmore, A.P., Soil organic matter turnover is governed by accessibility not recalcitrance. Global Change Biology 18, 1781-1796.

Fernández, J.M., Nieto, M.A., López-de-Sá, E.G, Gascó, G., Méndez, A., Plaza, C., 2014. Carbon dioxide emissions from semi-arid soils amended with biochar alone or combined with mineral and organic fertilizers. Science of the Total Environment, 482-483, 1-7.

Gunina, A., Dippold, M.A., Glaser, B., Kuzyakov, Y., 2014. Fate of low molecular weight organic substances in an arable soil: From microbial uptake to utilisation and stabilisation. Soil Biology and Biochemistry 77, 304-313.

Gustafsson, J.P., Persson, I., Kleja, D.B., Van Schaik, J.W.J., 2007. Binding of iron(III) to organic soils: EXAFS spectroscopy and chemical equilibrium modeling. Environmental Science and Technology 41, 1232-1237.

Hall, S.J., Berhe, A.A., Thompson, A., 2018. Order from disorder: do soil organic matter composition and turnover co-vary with iron phase crystallinity? Biogeochemistry 2018, 4.

Harris, D., Horwath, W.R., van Kessel, C., 2001. Acid fumigation of soils to remove carbonates prior to total organic carbon or carbon-13 isotopic analysis. Soil Science Society of America Journal 65, 1853-1856.

Hochella, M.F., Lower, S.K., Maurice, P.A., Penn, R.L., Sahai, N., Sparks, D.L., Twining, B.S., 2008. Nanominerals, mineral nanoparticles, and earth systems. Science 319, 1631-1635.

Huang, C., Liu, S., Li, R., Sun, F., Zhou, Y., Yu, G., 2016. Spectroscopic evidence of the improvement of reactive iron mineral content in red soil by long-term application of swine manure. PLoS One 11, 1-15.

Huang, C., Liu, S., Li, R., Sun, F., Zhou, Y., Yu, G., 2016. Spectroscopic evidence of the improvement of reactive iron mineral content in red soil by long-term application of swine manure. PLoS One 11, 1-15.

Kappler A., Wuestner, M.L., Ruecker, A., Harter, J., Halama, M., Behrens, S., 2014. Biochar as an Electron Shuttle between Bacteria and Fe(III) Minerals. Environmental Science and Technology Letters 1, 339-344.

Karlsson, T., Persson, P., 2010. Coordination chemistry and hydrolysis of Fe(III) in a peat humic acid studied by X-ray absorption spectroscopy. Geochimica et Cosmochimica Acta 74, 30-40.

Karlsson, T., Persson, P., 2012. Complexes with aquatic organic matter suppress hydrolysis and precipitation of Fe(III). Chemical Geology 322-323, 19-27.

Karlsson, T., Persson, P., Skyllberg, U., Mörth, C.-M., Giesler, R., 2008. Characterization

of Iron(III) in Organic Soils Using Extended X-ray Absorption Fine Structure Spectroscopy. Environmental Science and Technology 2008, 42, 5449-5454.

Keiluweit, M., Nico, P.S., Johnson, M.G., 2010. Dynamic Molecular Structure of Plant Biomass-Derived Black Carbon (Biochar). Environmental Science and Technology 44, 1247-1253.

Kleber, M., Eusterhues, K., Keiluweit, M., Mikutta, C., Mikutta, R., Nico, P.S., 2015. Mineral-organic associations: formation, properties, and relevance in soil environments. Advances in Agronomy 130, 1-140.

Kleber, M., Sollins, P., Sutton, R., 2007. A conceptual model of organo-mineral interactions in soils: Self-assembly of organic molecular fragments into zonal structures on mineral surfaces. Biogeochemistry 85, 9-24.

Klüpfel, L., Keiluweit, M., Kleber, M., Sander, M., 2014. Redox properties of plant biomass-derived black carbon (biochar). Environmental Science and Technology 48, 5601-5611.

Kodama, H., Schnitzer, M., 1977. Effect of fulvic acid on the crystallization of Fe(III) oxides. Geoderma 19, 279-291.

Kögel-Knabner, I., Guggenberger, G., Kleber, M., Kandeler, E., Kalbitz, K., Scheu, S., Eusterhues, K., Leinweber, P., 2008. Organo-mineral associations in temperate soils: Integrating biology, mineralogy, and organic matter chemistry. Journal of Plant Nutrition and Soil Science 171, 61-82

Lal, R., 2004. Soil carbon sequestration to mitigate climate change. Geoderma 123, 1-22.

Lalonde, K., Mucci, A., Ouellet, A., Gélinas, Y., 2012. Preservation of organic matter in sediments promoted by iron. Nature 483, 198-200.

Lehmann, J.A., 2007.A handful of carbon. Nature 447 143-144.

Lopez-Sangil, L., Rovira, P., 2013. Sequential chemical extractions of the mineral-associated soil organic matter: An integrated approach for the fractionation of organo-mineral complexes. Soil Biology and Biochemistry 62, 57-67.

Malinowski, E.R., 1977. Determination of the Number of Factors and the Experimental Error in a Data Matrix. Analytical Chemistry 49, 612-617.

Malinowski, E.R., 1978. Theory of error for target factor analysis with applications to mass spectrometry and nuclear magnetic resonance spectrometry. Analytica Chimica Acta 103, 339-354.

Mikutta, C., Frommer, J., Voegelin, A., Kaegi, R., Kretzschmar, R., 2010. Effect of citrate on the local Fe coordination in ferrihydrite, arsenate binding, and ternary arsenate

complex formation. Geochimica et Cosmochimica Acta 74, 5574-5592.

Mikutta, C., Frommer, J., Voegelin, A., Kaegi, R., Kretzschmar, R., 2010. Effect of citrate on the local Fe coordination in ferrihydrite, arsenate binding, and ternary arsenate complex formation. Geochimica et Cosmochimica Acta 74, 5574-5592.

Mikutta, C., Mikutta, R., Bonneville, S., Wagner, F., Voegelin, A., Christl, I., Kretzschmar, R., 2008. Synthetic coprecipitates of exopolysaccharides and ferrihydrite. Part I: Characterization. Geochimica et Cosmochimica Acta 72, 1111-1127.

O'Day, P.A., Rivera, N., Root, R., Carroll, S.A., 2004. X-ray absorption spectroscopic study of Fe reference compounds for the analysis of natural sediments. American Mineralogist 89, 572-585.

Persson, P., Axe, K., 2005. Adsorption of oxalate and malonate at the water-goethite interface: Molecular surface speciation from IR spectroscopy. Geochimica et Cosmochimica Acta 69, 541-552.

Plaza, C., Giannetta, B., Fernández, J. M., López-de-Sá, E.G., Polo, A., Gascó, G., Méndez, A., Zaccone, C., 2016. Response of different soil organic matter pools to biochar and organic fertilizers. Agriculture, Ecosystems and Environment 225, 150-159.

Prietzel, J., Thieme, J., Eusterhues, K., Eichert, D., 2007. Iron speciation in soils and soil aggregates by synchrotron-based X-ray microspectroscopy (XANES, μ-XANES). European Journal of Soil Science 58, 1027-1041.

Rasmussen, P. E., Goulding, K. W. T.; Brown, J. R.; Grace, P. R.; Janzen, H.; Korschens, M. Long-Term Agroecosystem Experiments: Assessing Agricultural Sustainability and Global Change. Science 828, 893-896.

Rose, J., Vilge, A., Olivie-Lauquet, G., Masion, A., Frechou, C., Bottero, J.Y., 1998. Iron speciation in natural organic matter colloids. Colloids and Surfaces A: Physicochemical and Engineering Aspects 136, 11-19.

Schmidt, M.W.I., Torn, M.S., Abiven, S., Dittmar, T., Guggenberger, G., Janssens, I.A., Kleber, M., Kögel-Knabner, I., Lehmann, J., Manning, D.A.C., et al., 2011. Persistence of soil organic matter as an ecosystem property. Nature 478, 49-56.

Schwertmann, U., 1966. Inhibitory effect of soil organic matter on the crystallization of amorphous ferric hydroxide. Nature 209, 694-696.

Schwertmann, U., 1991. Solubility and dissolution of iron oxides. Plant and Soil 130, 1-25.

Schwertmann, U., Schulze, D.G., Murad, E., 1982. Identification of ferrihydrite in soils by dissolution kinetics, differential X-ray diffraction, and Mossbauer spectroscopy. Soil Science Society of America Journal 46, 869-875.

Schwertmann, U., Wagner, F., Knicker, H., 2005. Ferrihydrite–Humic Associations. Soil Science Society of America Journal 69, 1009-1015.

Singh, B.P., Cowie, A.L., 2014. Long-term influence of biochar on native organic carbon mineralisation in a low-carbon clayey soil. Scientific Reports 4 ,3687.

Solomon, D., Lehmann, J., Harden, J., Wang, J., Kinyangi, J., Heymann, K., Karunakaran, C., Lu, Y., Wirick, S., Jacobsen, C., 2012. Micro- and nano-environments of carbon sequestration: Multi-element STXM-NEXAFS spectromicroscopy assessment of microbial carbon and mineral associations. Chemical Geology 329, 53-73.

Torn, M.S., Trumbore, S.E., Chadwick, O.A., Vitousek, P.M., Hendricks, D.M., 1997. Mineral control of soil organic carbon storage and turnover content were measured by horizon down to the depth at which. Nature 389, 3601-3603.

Villacís-García, M., Ugalde-Arzate, M., Vaca-Escobar, K., Villalobos, M., Zanella, R., Martínez-Villegas, N., 2015. Laboratory synthesis of goethite and ferrihydrite of controlled particle sizes. Boletín de la Societad Geológica Mexicana 2015, 67, 433-446.

Wen, Y., Xiao, J., Liu, F., Goodman, B.A., Li, W., Jia, Z., Ran, W., Zhang, R., Shen, Q., Yu, G, 2018. Contrasting effects of inorganic and organic fertilisation regimes on shifts in Fe redox bacterial communities in red soils. Soil Biology and Biochemistry 117, 56-67.

Xia, Z., Zhang, H., Shen, K., Qu, Y., Jiang, Z., 2018. Wavelet analysis of extended X-ray absorption fine structure data: Theory, application. Physica B: Condensed Matter 542, 12-19.

Xiao, J., He, X., Hao, J., Zhou, Y., Zheng, L., Ran, W., Shen, Q., Yu, G., 2016. New strategies for submicron characterization the carbon binding of reactive minerals in long-term contrasting fertilized soils: Implications for soil carbon storage. Biogeosciences 13, 3607-3618.

Xu, R.K., Hu, Y.F., Dynes, J.J., Zhao, A.Z., Blyth, R.I.R., Kozak, L.M., Huang, P.M., 2010. Coordination nature of aluminum (oxy)hydroxides formed under the influence of low molecular weight organic acids and a soil humic acid studied by X-ray absorption spectroscopy. Geochimica et Cosmochimica Acta 74, 6422-6435.

Yang, J., Wang, J., Pan, W., Regier, T., Hu, Y., Rumpel, C., Bolan, N., Sparks, D.L., 2016. Retention Mechanisms of Citric Acid in Ternary Kaolinite-Fe(III)-Citrate Acid Systems Using Fe K-edge EXAFS and $L_{3,2}$-edge XANES Spectroscopy. Scientific Reports 6, 1-9.

Zhou, G.W., Yang, X.R., Marshall, C.W., Li, H., Zheng, B.X., Yan, Y., Su, J.Q.; Zhu, Y. G., 2017. Biochar addition increases the rates of dissimilatory iron reduction and methanogenesis in ferrihydrite enrichments. Frontiers in Microbiology 8, 1-14.

Table 6.1 Site details, sampling depth, classification, total organic C content, total N, C/N ration (mean ± pooled standard error) of agricultural soils either unfertilized (C), amended with biochar (BC), municipal solid waste compost (MC) and with both of them (BC+MC). Data from Plaza et al. (2016).

Soil	Depth (cm)	Soil Taxonomy †	Land use	Total organic C ($g \cdot kg^{-1}$)	Total N ($g \cdot kg^{-1}$)	C/N	Fe ($mg \cdot kg^{-1}$)
C	0-15	Xerofluvent	Agricultural soil, unamended planted with *Hordeum vulgare*	11.8±0.7 d	1.10±0.05 c	10.7±0.6 c	22112±279
MC	0-15	Xerofluvent	Agricultural soil, amended with municipal solid waste compost	14.2±0.7 c	1.31±0.05 ab	10.8±0.6 c	21930±986
BC	0-15	Xerofluvent	Agricultural soil, amended with biochar	19.8±0.7 b	1.08±0.05 c	18.6±0.6 a	22102±629
BC+MC	0-15	Xerofluvent	Agricultural soil, amended with biochar and municipal solid waste compost	22.6±0.7 b	1.42±0.05 a	15.9±0.6 b	22731±461

Different letters indicate statistically significant differences according to Fischer's LSD test at 0.05 level.

† Soil Survey Staff (2014)

Table 6.2 Organic C and N concentrations of fine sand (FSa) and fine silt and clay (FSi+Cl) pools of agricultural soils either unfertilized (C), amended with biochar (BC), municipal solid waste compost (MC) and with both of them (BC+MC).

Land use	**Total OC FSa** *($g \cdot kg^{-1}$)*	**Total N FSa** *($g \cdot kg^{-1}$)*	**Total OC FSi+Cl** *($g \cdot kg^{-1}$)*	**Total N FSi+Cl** *($g \cdot kg^{-1}$)*
C	3.5	0.26	18.1	1.9
MC	4.6	0.37	20.8	2.2
BC	8.2	0.33	25.1	2.1
BC+MC	9.1	0.41	28.2	2.3

Table 6.3 Summary of Fe mineralogy of samples based on EXAFS linear combination fitting over the *k* range 2.5-10 Å.

Sample	k range fit	Mesurements	R-factor	Component 1		Component 2		Component 3		Sum
C FSa	2.5-10	15.324	0.124	Chlorite	26%	Ferrihydrite	44%	Fe(III)-citrate	18%	89%
BC FSa	2.5-10	15.324	0.079	Chlorite	36%	Ferrihydrite	29%	Fe(III)-citrate	31%	96%
MC FSa	2.5-10	15.324	0.077	Chlorite	31%	Ferrihydrite	28%	Fe(III)-citrate	31%	90%
BC+MC FSa	2.5-10	15.324	0.060	Chlorite	25%	Ferrihydrite	28%	Fe(III)-citrate	35%	88%
C FSi+Cl	2.5-10	15.324	0.032	Chlorite	22%	Ferrihydrite	48%	Fe(III)-citrate	37%	107%
BC FSi+Cl	2.5-10	15.324	0.039	Chlorite	21%	Ferrihydrite	47%	Fe(III)-citrate	44%	112%
MC FSi+Cl	2.5-10	15.324	0.021	Chlorite	18%	Ferrihydrite	45%	Fe(III)-citrate	43%	105%
BC+MC FSi+Cl	2.5-10	15.324	0.040	Chlorite	19%	Ferrihydrite	46%	Fe(III)-citrate	41%	107%

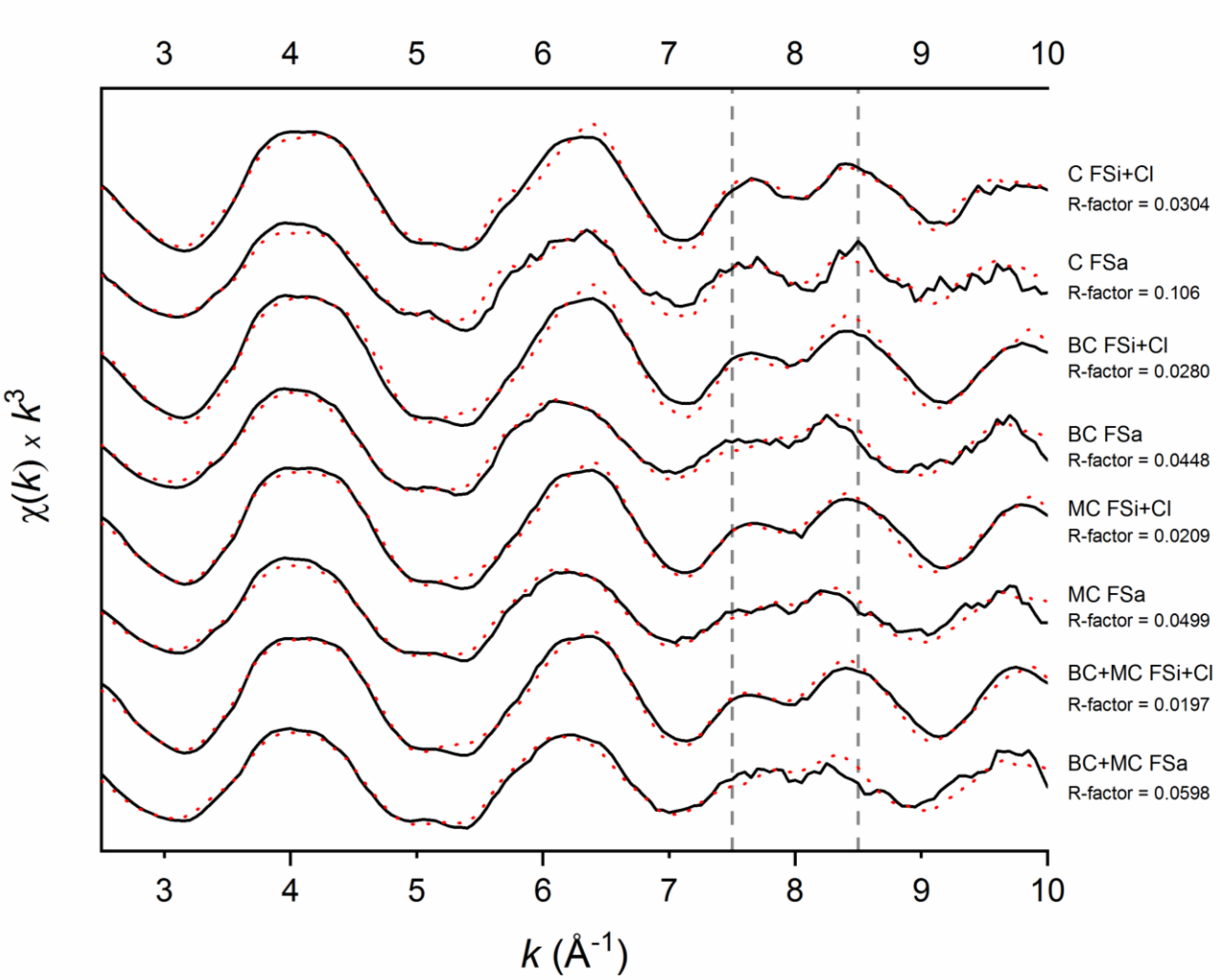

Figure 6.1 k^3 –weighted spectra of fine silt and clay (FSi+Cl) and fine sand (FSa) fractions of agricultural soils either unfertilized (C), amended with biochar (BC), municipal solid waste compost (MC) and with both of them (BC+MC). Solid lines indicate the sample data, whereas dotted lines represent the fit. R-factors are also displayed.

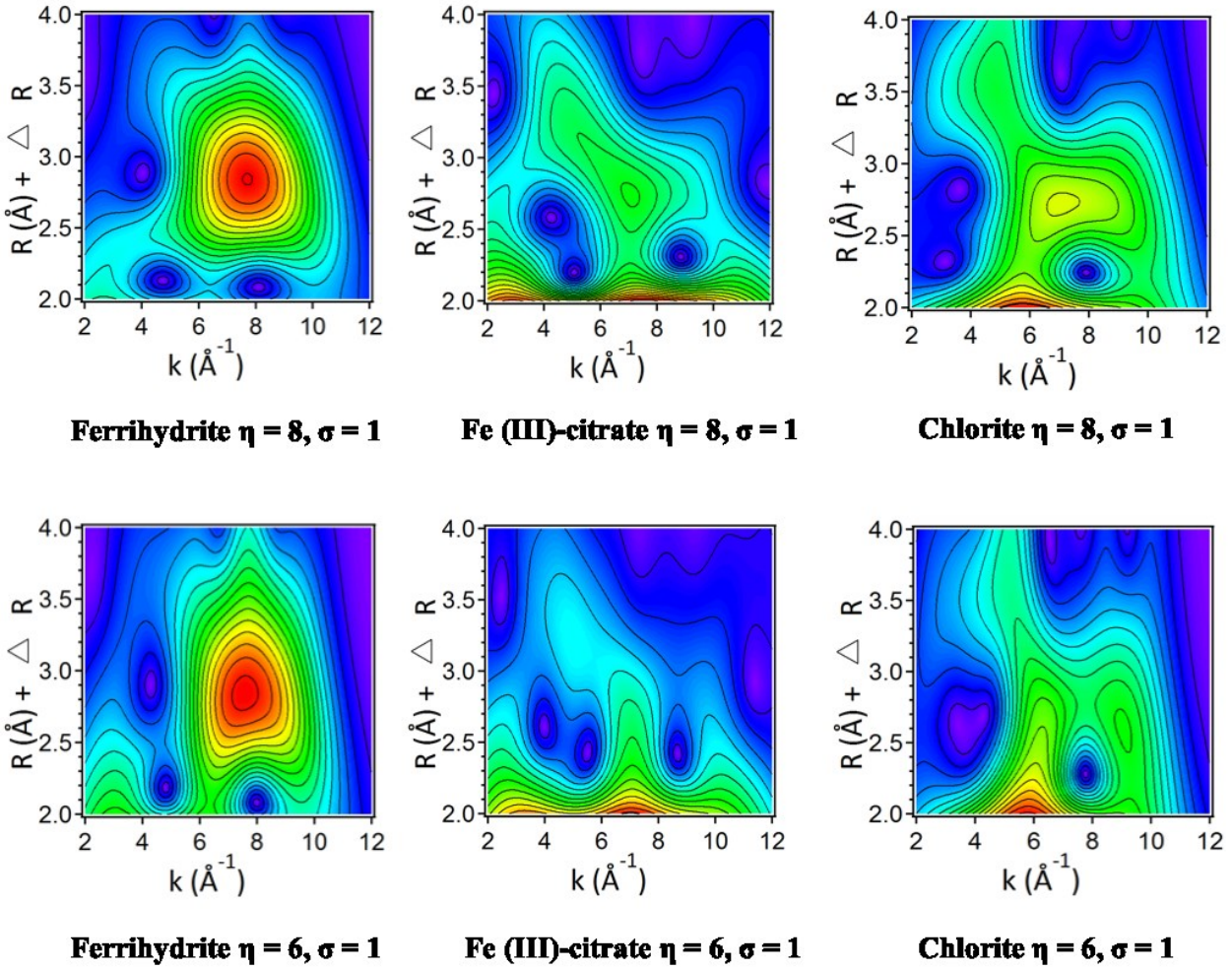

Figure 6.2 High resolution WT plots of standards displaying the second and third coordination shell. Data are plotted as a function of k ($Å^{-1}$) on the x axis and R (Å) on the y axis in the range 2.0-4.0 (Å)

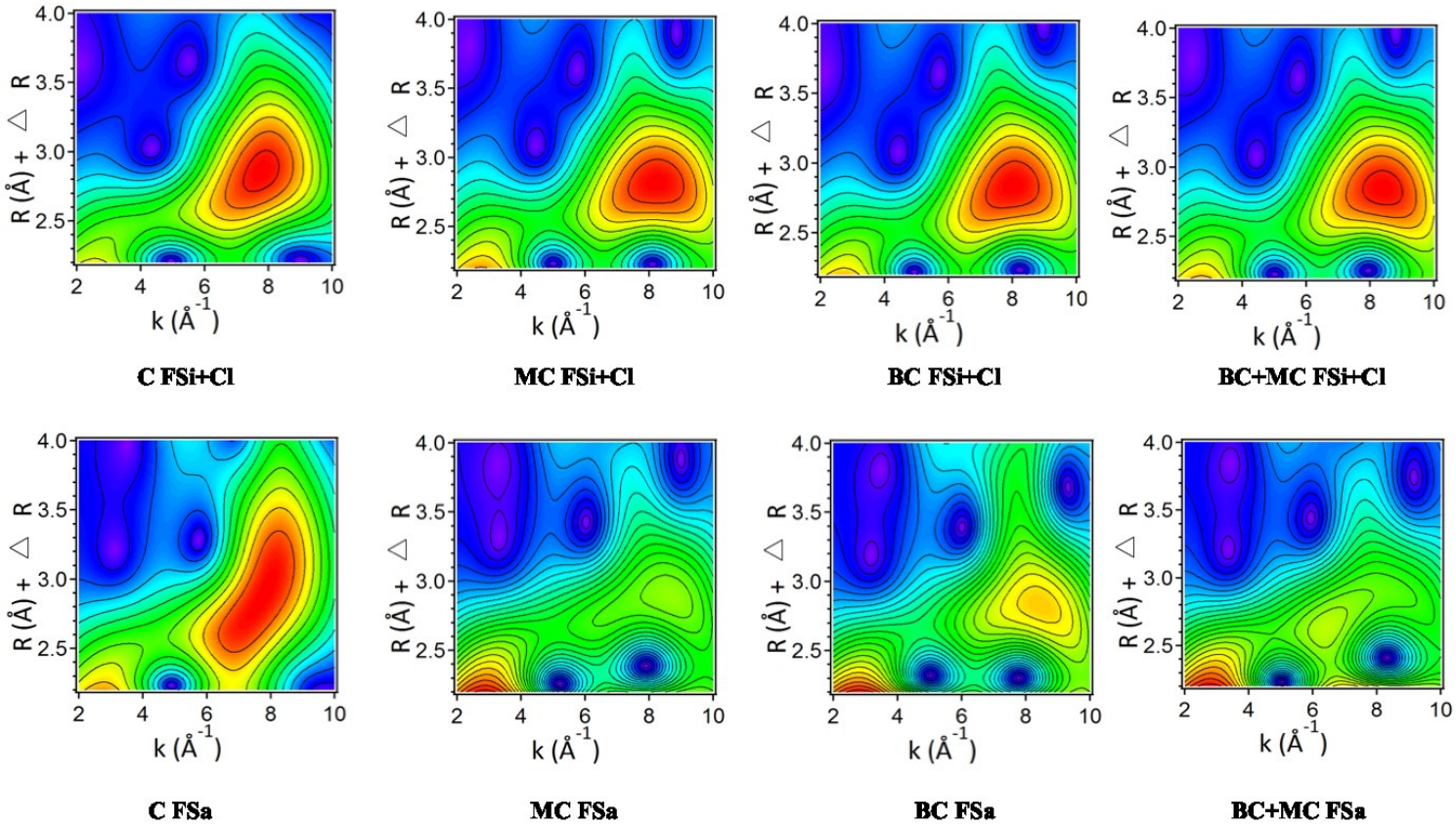

Figure 6.3 High resolution WT plots of fine silt and clay (FSi+Cl) and fine sand (FSa) fractions from agricultural soil unamended (C), amended with biochar (BC), compost (MC) and biochar and compost (BC+MC) displaying the second and third coordination shells (η= 8, σ= 1). Data are plotted as a function of k ($Å^{-1}$) on the x axis and R (Å) on the y axis in the range 2.2-4.0 (Å).

.

7. Conclusions

Accrual of C in soil is a significant and realizable management option to mitigate the relentless increase in atmospheric CO_2. OC bound to minerals is considered relatively stable (Torn et al., 1997; Kalbitz et al., 2005; Mikutta et al., 2006), thus driving the long-term sequestration of OM in soils. SOM stabilization by minerals has been envisioned as a combined effect of the mineralogical properties (surface area and charge) and the composition of the OM involved (Kalbitz et al., 2005; Mikutta et al., 2007). A clear understanding of the mechanisms controlling the persistence of C in SOM, and how they are affected by land use, has never been more needed. SOC accrual requires N; thus understanding of N distribution in soil is equally important.

In the first step of this thesis (chapter 2), SOM physical and chemical stabilization mechanisms under a variety of land uses have been investigated. Using elemental and thermal analyses, we examined changes in the quantity and quality of physically-fractionated SOM pools characterized by different mechanisms of protection from decomposition. Independently of land use, the majority of the OC and total N were found in the mineral-associated SOM pool, mainly protected by chemical mechanisms. Indexes of thermal stability and C/N ratio of this heavy SOM fraction were lower (especially in agricultural soils) compared to light SOM fractions found free or occluded in aggregates, and suggested a marked presence of inherently labile compounds. As a whole, different land uses may differ in terms of absolute SOM content among fractions; however, the results suggest a common mechanism of SOM dynamics, where plant input and their inherent recalcitrance control LF quality and distribution, while microbial by-products, largely independent of land use, govern SOM accumulation in the MAOM fraction.

Physical fractionations by particle size coupled with an extensive set of chemical extractions allowed obtaining new insights about SOM sequestration in mineral soils characterized by different land use (chapter 3). Organo-mineral interactions in soils under different land uses widely differing in their SOM content were studied by a double approach: (i) a size fractionation by wet sieving after sonication, to isolate the particulate organic matter (POM, >20 μm) from the organo-mineral complex (OMC, <20 μm), and (ii) a characterization of the OMC by sequential extractions with different chemicals, each one disrupting a specific kind of bond between SOM and active mineral surfaces. More than 60% of TOC and >75% of total N were found in the OMC. Differences in land uses affected the total amount of SOM, but barely its distribution between POM and OMC. The sequential extractions showed that a

substantial amount of the OM in the OMC (20-30%) was loosely bound through electrostatic, van der Waals, or metallic bonds. However, the main pool of the OMC occurred by far in the final residue remaining after removing all the active mineral components causing insolubility. Because the unextractability of the final residue can be due only to its own chemical characteristics (*i.e.,* solubility), and because this residue accounts for 34-48% of the TOC in OMC, 38-69% of the total N in the OMC and has a low C/N ratio, we suggest that the biochemical evolution from plant-derived material towards insoluble microbial forms is a relevant path for SOM stabilization.

SOM protection, stability and long-term accumulation are controlled by several factors, including sorption onto mineral surfaces. Fe has been suggested as a key regulator of SOM stability, both in acidic conditions, where Fe(III) is soluble, and in near neutral pH environments, where it precipitates as Fe(III) (hydr)oxides. The study described in chapter 4 aimed to probe, by sorption/desorption experiments in which Fe was added to the system, the mechanisms controlling Fe(III)-mediated OC stabilization; FSi+Cl and FSa SOM fractions of three soils under different land uses were tested. Fe(III) addition caused a decrease in the OC remaining in solution after reaction, indicating an Fe-mediated OC stabilization effect. This effect was two times larger for FSa than for FSi+Cl, the former fraction being characterized by both low specific surface area and high OC content. The reaction with Fe(III) caused two opposite effects on SSA, *i.e.,* either a decrease in SSA mainly occurring in the FSi+Cl fractions and probably due to flocculation, or an increase of SSA values, probably due to coating. The ATR-FTIR data suggested that carbohydrates are association to Fe(III) oxides by surface complexation, possibly by an inner-sphere ligand exchange mechanism, as suggested in the literature (this was observed mainly in FSa). The formation of coprecipitated SOM with Fe-oxides is also possible. The irreversible nature of this complexation is confirmed by the reaction with Fe(III), where increasing added Fe(III) correlated to a decrease in OC desorbed. These results demonstrated that the binding of labile SOM compounds to Fe(III) contributes to its preservation, and that the mechanisms involved (flocculation *vs.* coating) depend on the size fractions.

In the current literature, the role of SOM controlling Fe speciation is mostly discussed in terms of speciation of model metal (hydr)oxide systems, such as pure Fe (hydr)oxides) and Fe(III) complexation with different types of SOM, dissolved organic DOM, peats, humic substances, small organic acids, or bulk soils and waters. Thus, considering the knowledge and research gap between model and natural systems in understanding the possible SOM stabilization mechanisms as a function of ecosystems, physical fractionation methods coupled

with synchrotron-based characterization provide unique information relevant to regulation of global terrestrial SOC cycling. In the chapter 5 the dynamics of Fe across different soils ecosystems were studied, considering the influence of added Fe(III) on the variation of Fe speciation in FSi+Cl fractions. The data compared Fe speciation and reactions with different soil components such as SOM, Fe metal oxides, and phyllosilicates under a variety of ecosystems including coniferous forest, grassland, technosols, and agricultural soils. The analysis of Fe EXAFS spectra suggested that the formation Fe(III)-OM complexes inhibited the hydrolysis and polymerization of Fe(III) in GL and AG. Conversely, in CF and TS, the percentage of ferrihydrite-like polymeric Fe(III) oxides increased after the reaction. We hypothesize that this complexation can inhibit the hydrolysis and polymerization of Fe (III) in GL and AG, due to the presence of C inputs from plant litter and root exudation that offers a constant supply of SOM from the litter surface, with a consequent production of soluble organic compounds that precipitate with the added Fe(III). Conversely, in CF and TS, labile molecules (*e.g.,* sugars, amino acids, proteins) were preferentially associated with mineral surfaces (*e.g.,* Fe(III) that precipitates as Fe(III) hydroxides).

Although is well-known how different fertilization practices affect organo-mineral associations and aggregation, their role in regulating Fe speciation remains less clear. Due to the growing environmental interest related to a sustainable agriculture we applied Fe EXAFS to identify and also quantify the Fe phases present in different mineral assemblages (*i.e.,* soil fractions: FSa and FSi+Cl) determined by added organic amendments (*i.e.,* biochar, compost and the simultaneous application of both) (chapter 6). The common increase in Fe-OM complexation after the amendment, in FSi+Cl, but more evidently in FSa fractions, confirmed that the introduction of organic amendments can hinder the transformation of Fe(III) complexed by organic ligands in the soil solution into ferrihydrite. In the FSi+Cl fraction the interaction between freshly added OM can lead to surface site blockage and to the formation of more aggregated particles and consequently to a less dissolution rate. Future studies should address the possibility of an increased ferrihydrite dissolution rates and its transformation dynamics after amendments in FSa rather than in FSi+Cl over time. This can confirm the role of SOM amount and quality on the hindrance of Fe hydrolysis, crystallization and transformation processes, extending the application of the modeled knowledge to complex natural systems.

7.1. Future research: SOM composition and Fe crystallinity changes induced by dynamic redox conditions in complex natural soil systems

Fe redox cycling between oxidized and reduced forms regulates soil SOM preservation and aggregation (Lalonde et al., 2012; Sparks and Chen, 2013; Thompson et al., 2006). An array of Fe phases, ranging from Fe(II)/Fe(III) phyllosilicates to poorly and highly crystalline Fe(III) oxides, hydroxides, and oxyhydroxides coexists in the soil system. They dynamically evolve in response to environmental and geochemical conditions that drive Fe precipitation and reductive dissolution, with a consequent technical difficulty in analyzing mechanisms dictating organic C sequestration. For example, during rainfall, soils can be subjected to O_2 depletion and leaching of labile SOM during changes in the redox state of the soil.

The kinetics of Fe recrystallization and transformation processes under changing redox conditions have been mostly studied in SOM-ferrihydrite precipitates (Zhou et al., 2018), in freshwater flocs (ThomasArrigo et al., 2017) or soil slurries (Chen et al., 2018) reacted with Fe(II), but rarely in complex soils (Chen et al., 2017). However, it remains less clear how Fe phase composition and crystallinity relate to SOM chemical properties in natural systems (rather than in reductionist model systems). This is important because Fe crystallinity is redox sensitive and Fe species affect SOM and C turnover (Hall et al., 2018). The study of Fe-SOM cycling in natural soil systems represents a key factor in the long-term storage of OC and the global cycles of C and its response to global climate change.

LCF results of Fe K-edge EXAFS spectra previously collected on these natural soil fractions at suggested that Fe speciation is dependent on the fraction, type of ecosystem, and C concentration. The fractions include the FSi+Cl and fine sand FSa pools. Fe solid phases are dominated by Fe(III)-oxyhydroxides, represented by ferrihydrite, that fits to varying degrees, from 20% in coniferous forest soils to 48% in agricultural soils in the fine silt and clay fraction. A less significant Fe component is represented by ferrihydrite in the coarse sand fraction. Conversely, Fe(III)–organic references complexes (*i.e.,* Fe(III) citrate) constitute the main Fe phase in broadleaved forest soils.

The hypothesis of this future research is that the nature/composition of SOM stabilized in different pools dictates solid phase Fe speciation under different redox conditions. Specifically, the presence of organic ligands and environmental conditions can affect Fe(II) interaction with soil fractions to produce either short-range-order (SRO) Fe(III) oxides such as ferrihydrite and organic Fe(III) complexes or more well-ordered Fe oxides will be investigated.

The interactions between Fe(II) and physically fractionated soils, comparing Fe(II)-catalyzed mineralogical changes in bulk and fractionated soils under different ecosystems will be studied. Complementary to the redox experimental studies, selective dissolution procedures to extract Fe-C associations, and other cutting-edge spectroscopic and micro-scale characterizations, the speciation of Fe before and after the fractionation will be analyzed by X-ray absorption spectroscopy.

The solid phase Fe transformation and kinetics using Fe(II) and conducting the experiment in triplicates in a glovebox using similar reported methods (ThomasArrigo et al., 2017). 500 mg of dried samples, previously placed in serum bottles and equilibrated for 16 h in 250 mL of anoxic 50 mM 3-(N-morpholino) propanesulfonic acid (MOPS) or 2-(N-morpholino) ethanesulfonic acid (MES) buffer adjusted to pH 7 (MOPS) or pH 5.5 (MES) will be reacted with Fe(II). The Fe(II) stock solution of 100 mM Fe(II) will be prepared. The samples will be equilibrated with 0.1 and 1.0 mM Fe(II) in serum bottles and horizontally shaken (150 rpm) for 1 week, adjusting the pH at 7.0 ±0.1 or 5.5 ±0.1.

Bulk soils and SOM pools (*i.e.*, the fine silt/clay and fine sand fractions) characterized by different initial organic C contents will be obtained using a particle size physical fractionation method (Lopez-Sangil and Rovira, 2013) and used as model OC. The soils, sampled in Marche region (Italy) compare stabilization processes of SOM under a variety of ecosystems (*i.e.*, coniferous and broadleaved forest soils, and agricultural soils).

The speciation of Fe will be analyzed using synchrotron-based techniques so study changes over time (kinetics). We will analyze both the K-edge X-ray absorption near edge structure (XANES) and extended X-ray absorption fine structure (EXAFS) data for Fe. Solid-phase material previously collected on 0.22 μm cellulose filters, washed with DDI water and dried in the glovebox. Samples will be finely ground, diluted with boron nitride, pressed into a pellet and sealed between Kapton® tape inside of a glovebox. They will be prepared for transport to beamline by packing within heat-sealed aluminized mylar bags and placed in secondary air-tight hard-walled containment vessels inside of glovebox. The samples will be kept anoxic until the end of the XAS experiment using a liquid-N_2 cryostat. The fractions of different Fe mineral phases will also be determined by principle component analysis and LCF using a suite of Fe reference spectra. Statistical methods will be used to determine goodness-of-fit parameters for LCF of synchrotron-based XAS data. Wavelet transformation analysis will be applied for a qualitative analysis of the nature of backscattering atoms in the higher coordination shells. Finally, we will correlate the speciation of Fe with the amount and nature of OC. In addition to synchrotron-based analysis, we will use thermogravimetric analyses (TGA) and

scanning/transmission electron microscopy(SEM/TEM) analysis to characterize SOM composition. Selective dissolution procedures (*i.e.,* pyrophosphate (PP) to isolate colloidal or dispersable Fe, HCl-hydroxylamine (HH) and ammonium oxalate (AO) to isolate SRO Fe, and inorganic dithionite-HCl (DH) to isolate more crystalline pedogenic Fe), X-ray diffraction and cold temperature Mössbauer spectroscopy will be applied for Fe phases characterization.

This approach will help reveal the mechanisms by which SOM pools and organic C chemical composition can control Fe dynamics in redox environments under different ecosystems, consequently improving our understanding of SOM mean residence time on a large scale. The protection of solid-phase OC in soils is of utmost importance with respect to global C cycling and climate change because soils are a critical sink for C that can potentially be released into the atmosphere. Thus, this study of Fe-OM complexation under redox conditions and in different ecosystems can provide useful insights into storage and sequestration of C and thus towards the achievement of sustainable soil management. Because redox interfaces are ubiquitous in the environment, pairing Fe cycling with the chemical composition and aggregation of OC will provide information about the fate of C in the natural environment and the results are applicable to soil ecosystems such as agricultural and forest soils.

Considering the gap between model and natural systems in understanding the possible SOM stabilization mechanisms as a function of ecosystem, synchrotron-based characterization of our soils will not only provide unique solid phase information relevant to global terrestrial SOC cycling extend the current reductionist-based knowledge from simplified modeled systems to complex natural systems.

References

Chen, C., Kukkadapu, R.K., Lazareva, O., Sparks, D.L., 2017. Solid-phase Fe speciation along the vertical redox gradients in floodplains using XAS and Mössbauer spectroscopies. Environmental Science and Technology 51, 7903-7912.

Chen, C., Maile, C., Wilmoth, J., Barcellos, D., Thompson, A., 2018. Influence of pO2 on iron redox cycling and anaerobic organic carbon mineralization in a humid tropical forest soil. Environmental Science and Technology 52, 7709-7719.

Giannetta, B., Plaza, C., Vischetti, C., Cotrufo, M. F., Zaccone, C., 2018. Distribution and thermal stability of physically and chemically protected organic matter fractions in soils across different ecosystems. Biology and Fertility of Soils 54, 671-681.

Hall, S.J., Berhe, A.A., Thompson, A., 2018. Order from disorder: do soil organic matter composition and turnover co-vary with iron phase crystallinity? Biogeochemistry 140, 93.

Kalbitz, K., Schwesig, D., Rethemeyer, J., Matzner, E., 2005. Stabilization of dissolved organic matter by sorption to the mineral soil. Soil Biology and Biochemistry 37, 1319-1331.

Lalonde, K., Mucci, A., Ouellet, A., Gélinas, Y., 2012. Preservation of organic matter in sediments promoted by iron. Nature 483, 198-200.

Lopez-Sangil, L., Rovira, P., 2013. Sequential chemical extractions of the mineral-associated soil organic matter: An integrated approach for the fractionation of organo-mineral complexes. Soil Biology and Biochemistry 62, 57-67.

Mikutta, R., Kleber, M., Torn, M.S., Jahn, R., 2006. Stabilization of soil organic matter: Association with minerals or chemical recalcitrance? Biogeochemistry 77, 25-56.

Mikutta, R., Mikutta, C., Kalbitz, K., Scheel, T., Kaiser, K., Jahn, R., 2007. Biodegradation of forest floor organic matter bound to minerals via different binding mechanisms. Geochimica et Cosmochimica Acta 71, 2569-2590.

Sparks, D.L., Chen, C., 2013. The Role of Mineral Complexation and Metal Redox Coupling in Carbon Cycling and Stabilization. Functions of Natural Organic Matter in Changing Environment in Xu, J., Wu, J., He, Y., (Eds.), Functions of Natural Organic Matter in Changing Environment. Zhejiang University Press and Springer Science+Business Media, Dordrecht, pp. 7-12.

ThomasArrigo, L.K., Mikutta, C., Byrne, J., Barmettler, K., Kappler, A., Kretzschmar, R., 2017. Iron and Arsenic Speciation and Distribution in Organic Flocs from Streambeds of an Arsenic-Enriched Peatland. Environmental Science and Technology 48, 13218-13228.

Thompson, A., Chadwick, O.A., Rancourt, D.G., Chorover, J., 2006. Iron-oxide crystallinity increases during soil redox oscillations. Geochimica et Cosmochimica Acta 70, 1710-1727.

Torn, M.S., Trumbore, S.E., Chadwick, O.A., Vitousek, P.M., Hendricks, D.M., 1997. Mineral control of soil organic carbon storage and turnover content were measured by horizon down to the depth at which. Nature 389, 3601-3603.

Zhou, Z., Latta, D.E., Noor, N., Thompson, A., Borch, T., Scherer, M.M., 2018. Fe(II)-catalyzed transformation of organic matter-ferrihydrite coprecipitates: a closer look using Fe isotopes. Just accepted manuscript. DOI 10.1021/acs.est.8b03407.

Appendix

A. Density-based fractionation of soil organic matter: effects of heavy liquid and heavy fraction washing

(Plaza, C., Giannetta, B., Benavente, I., Vischetti, C., Zaccone, C., Under review. Scientific Reports*)*

Abstract

Physical fractionation methods used in soil organic matter (SOM) research commonly include density-based procedures with heavy liquids to separate SOM pools with varying turnover rates and functions. Once separated, the heavy SOM pools are often thoroughly rinsed with water to wash off any residues of the heavy liquids. Using four soils with contrasting properties, we investigated the effects of using either sodium polytungstate (SPT) or sodium iodide (NaI), two of the most commonly used heavy liquids, on the distribution of organic carbon (C) and total nitrogen (N) in light free, light intra-aggregate, and heavy mineral-associated SOM pools isolated by a common fractionation scheme. We also determined the effects of washing the heavy mineral-associated SOM fractions on the recovery of organic C and total N after separation. Because of its smaller viscosity compared to that of NaI, SPT consistently yielded greater intra-aggregate and smaller mineral-associated soil organic C contents. We also found that commercial SPT, such as the one used here, can adversely contaminate heavy organo-mineral pools with N during density-based fractionation procedures. We do not recommend the repeated washing of heavy fractions separated with Na-based heavy liquids, as this can mobilize SOM.

A.1. Introduction

Soil organic matter (SOM) is a key component of terrestrial ecosystems, contributing to the support of natural vegetation and agricultural production, filtering and holding water, and storing carbon (C) (Lal, 2009; Paul, 2016). The preservation of SOM is of paramount importance because of the need to maintain these ecosystem functions and services to face major global issues, such as food security, desertification, and climate change (Schmidt et al., 2011; Plaza et al., 2018). Key mechanisms controlling the persistence of SOM include

occlusion within soil aggregates and sorption onto mineral surfaces, which cause disconnection and therefore inaccessibility of SOM to decomposer microorganisms and enzymes (Von Lützow et al., 2006; Schmidt et al., 2011; Plaza et al., 2013; Lehmann and Kleber, 2015).

The acknowledge of the importance of these preservation mechanisms has led to the increased use of physical fractionation methods to isolate SOM pools of distinct location within the soil mineral matrix (Von Lützow et al., 2006; Crow et al., 2007; Poeplau et al., 2018). Among the large number of physical fractionation methods available in the literature (see Poeplau et al., 2018 for a recent comparative description of many of them), the density-based separation scheme developed by Golchin et al. (1994) is one of the most commonly used and has constituted the basis for the development of other fractionation methods (Sohi et al., 2001; Plaza et al., 2012, 2013). This scheme is intended to separate three fractions: a light, free SOM fraction not physically disconnected from microorganisms and enzymes; a light, occluded SOM fraction located within aggregates, which forms a physical barrier that limits O_2 diffusion and the accessibility of microorganisms and enzymes; and a heavy fraction consisting of SOM intimately associated with minerals, which decreases microbial and enzymatic capacity to decompose organic substrates (Golchin et al., 1994). Briefly, the free SOM fraction is isolated by an initial density separation, and the intra-aggregate SOM is then separated from the mineral-associated pool by a second density separation after ultrasonic disruption of stable aggregates (Golchin et al., 1994).

Sodium polytungstate (SPT, $Na_6[H_2W_{12}O_{40}]$) and sodium iodide (NaI) are the chemical reagents most commonly used to prepare the heavy liquids for density-based fractionation of SOM (Golchin et al., 1994; Sohi et al., 2001; Plaza et al., 2012, 2013; Courtier-Murias et al., 2013; Poeplau et al., 2018). After separating the light SOM fractions, the heavy mineral-associated SOM fractions are commonly washed with deionized water to eliminate the remaining SPT and NaI (*e.g.,* protocols for density-based separations in Poeplau et al., 2018, Supplementary data). Having different properties, these heavy liquids may interact differently with the soil and therefore yield different fractionation results. Similarly, the washing intended to eliminate SPT and NaI may arguably cause losses of mineral-associated SOM, thus affecting the recovery of SOM after fractionation. In spite of the potential importance of these effects, there are no studies in the literature specifically and systematically addressing these issues, which may seriously compromise meaningful interpretations of SOM dynamics.

The objectives of this study were to (a) investigate comparatively the effects of the heavy liquid, SPT versus NaI, on the distribution of organic C and total N in free, intra-aggregate, and mineral-associated pools separated by common density-based procedures; (b) determine

the effects of washing the heavy mineral-associated SOM fraction isolated using either SPT or NaI on its organic C and total N contents; and (c) evaluate the influence of soil properties on the potential effects of the heavy liquid and washing. The final purpose of this study was to provide general recommendations to prevent misinterpretation of fractionation results in SOM research.

A.2. Materials and methods

A.2.1. Soil samples

We collected four samples (SOIL 1 to 4) from the surface layer of four contrasting soils, with the aim of covering a wide range of textures. The samples were air dried, gently crushed, and sieved to 2 mm. Table A.1 shows the origin and main physical and chemical properties of the samples used in this work.

A.2.2. Soil organic matter fractionation

The prepared soil samples (dried and 2-mm sieved) were subjected to the physical fractionation scheme developed by Golchin et al. (1994) to isolate free, intra-aggregate, and mineral-associated SOM. The fractionation was conducted using a solution of either SPT or NaI as heavy liquid and either not washing or washing the isolated mineral-associated SOM fraction. Specifically, 80 mL of either SPT (purum p.a., for the preparation of heavy liquid, for sink-float analysis, ≥85% WO_3 basis, Fluka, Sigma-Aldrich, St. Luois, MO) or NaI (ACS reagent, ≥99.5%, Sigma-Aldrich, St. Luois, MO) at a density of 1.85 g mL^{-1} was added to 10 g of soil in a 100-mL centrifuge tube. The centrifuge tube was rotated at 1 revolution s^{-1} for 30 s in an overhead shaker to allow free SOM outside aggregates to float. After centrifugation at 2500 g for 30 min, the floating light fraction (free SOM) was separated from the heavy fraction by suction and filtration through a glass fiber filter (GF/A, Whatman, UK) and washed thoroughly with deionized water. The heavy fraction in the centrifuge tube was resuspended and dispersed in the SPT or NaI solution by sonication at an energy input of 1500 J g^{-1}. The floating light fraction (intra-aggregate SOM) was separated from the heavy fraction (mineral-associated SOM) by centrifugation at 2500 g for 60 min, suction, and filtration through a glass fiber filter, and washed thoroughly with deionized water. The fractionation procedure was repeated six times for each soil and heavy liquid. Three of the six replicates of the isolated mineral-

associated SOM were not washed, and the other three replicates were thoroughly washed three times by adding 80 mL of deionized water, shaking for 10 min, and centrifuging at 2500 g for 30 min.

A.2.3. Chemical and physicochemical analysis

The whole soil samples and SOM fractions were analyzed for organic C and total N content by dry combustion using a Thermo Flash 2000 NC Soil Analyzer. Prior to organic C analysis, the whole soil samples and mineral-associated SOM fractions were subjected to acid fumigation to remove carbonates (Harris et al., 2001). The SPT and NaI reagents (powders) used to prepare the solutions for density fractionations were analyzed for total C and N by dry combustion, as described above for soils samples and SOM fractions. The prepared heavy liquids were analyzed for viscosity, pH, and electrical conductivity at 20 ºC using a capillary viscometer, a pH meter, and a conductivity meter, respectively.

A.2.4. Data analysis

We used two-way analysis of variance (ANOVA) tests to evaluate the main and interaction effects of heavy liquid and soil on free and intra-aggregate organic C and total N, and three-way ANOVA tests to evaluate the effects of heavy liquid, washing, and soil on mineral-associated organic C and total N and on the recovery of each element after fractionation. When assumptions of normality and homoscedasticity were not met, we used nonparametric ANOVA on aligned rank transformed data. Post hoc pairwise comparisons within each soil were conducted using t or Wilcoxon rank-sum tests at the 0.05 level. All data analyses were performed using R statistical software version 3.5.1 (R Core Team, 2018).

A.3. Results

The ANOVA tests reveal significant main and interaction effects ($P < 0.001$) of the heavy liquid and soil on free organic C and total N contents (Table AS.1). Post hoc pairwise tests, however, being more conservative, failed to detect significant differences between the effects of SPT and NaI on free organic C and total N contents for any of the soils examined (Figs. A1 and A2). Nonetheless, compared to SPT, NaI tended to yield slightly smaller free organic C

and total N contents for the soils with the largest total organic C and total N contents, SOIL 1 and SOIL 3 (Table A.1).

Intra-aggregate organic C and N contents and C/N ratio were significantly affected ($P < 0.001$) by the heavy liquid and soil factors and their interaction (Tables AS 1). Compared to SPT, NaI resulted in significantly smaller intra-aggregate organic C and total N contents for the four soils examined, with the magnitude of the differences slightly depending on the soil (Figs. A1 and A2).

We also found significant two-way interaction effects of the heavy liquid and soil ($P < 0.001$) and washing and soil ($P < 0.01$) on mineral-associated organic C content, and significant three-way interaction effects of the heavy liquid, washing, and soil on mineral-associated N content ($P< 0.01$) (Table AS 1). Specifically, with respect to SPT, NaI resulted in significantly larger mineral-associated organic C content for the four soils, especially for SOIL 1 and SOIL 3, regardless of the washing treatment (Fig. A1). Independently of the heavy liquid used, washing decreased mineral-associated organic C content, especially for SOIL 1 and SOIL 3. Compared to NaI, SPT yields larger mineral-associated N content (Fig. A2). The size and significance of these differences depended on the soil. For SPT treated soils, washing decreased mineral-associated N content, but had a negligible effect for NaI treated soils (Fig.A2).

Total organic C recovery after fractionation was significantly affected by the interaction of washing and soil ($P < 0.05$) (Table AS 1). In particular, washing decreased organic C recovery by 0.2 for SOIL 1 to 21% for SOIL 3 (Table A2). We also found significant interaction effects of washing and soil ($P < 0.05$) and heavy liquid and washing ($P < 0.001$) on total N recovery (Table AS 1). Specifically, N recovery after SOM separation with SPT and without washing the mineral-associated fraction ranged from 106 to 143%, increasing with soil clay content (SOIL 1 to 4) (Table A2). With washing, N recovery after SOM separation with SPT decreased (especially for SOIL 3 and SOIL 4), ranging from 88 to 110%. Total N recovery with NaI was markedly smaller and not significantly affected by the washing treatment (Table A2).

The SPT powder used to prepare the solution for density fractionations contained no C but 0.646 g kg^{-1} of total N. The NaI powder had no detectable amounts of total C and N. The SPT solution had a viscosity of 1.1 mPa s, a pH of 3.3, and an electrical conductivity of 61 dS m^{-1} whereas the NaI liquid has a viscosity of 1.7 mPa s, a pH of 8.0, and an electrical conductivity of 154 dS m^{-1}.

A.4. Discussion

Our research highlights substantial differences between the heavy liquids in SOM fractionation results. These differences may be mainly related to the significantly different physicochemical and chemical properties of the heavy liquids, while only secondarily depend on the specific properties of the soil under study.

The greater intra-aggregate and smaller mineral-associated organic C contents obtained after fractionation with SPT, compared to NaI, may be attributed to the smaller viscosity of the SPT solution. In fact, a smaller viscosity favors the propagation of the ultrasonic pulses and the cavitation process (Santos et al., 2009). This may increase the effectiveness of the ultrasonic disruption treatment to break up aggregates and the release of intra-aggregate SOM, which in turn decreases the amount of SOM recovered in the mineral-associated pool.

Because of the lower viscosity and higher efficacy of sonication, SPT also results in greater intra-aggregate N compared to NaI, but not in smaller mineral-associated N. This is because, unlike NaI, the SPT powder used to prepared the heavy solution is contaminated with N as supplied. Some of the N in SPT inevitably ends up in the heavy fraction remaining after the last density separation, thus adding up to the mineral-associated N pool. The concentration of N in the SPT used here are within the range detected in commercially available SPT for the preparation of heavy liquid in a previous study (Kramer et al., 2009). As opposed to those obtained with commercially available SPT, results obtained by Kramer et al. (2009) using low N content SPT (0.05 mg kg^{-1}; specially requested to a manufacturer) show no adverse contamination of soils after density fractionation. To the best of our knowledge, commercial production of SPT with low N levels has not been developed yet.

To remove SPT and NaI residues, the heavy organo-mineral fractions remaining after density-based separations are often thoroughly rinsed with water (*e.g.,* protocols for density-based separations in Poeplau et al., 2018, Supplementary data). Our results show that this procedure may result in significant losses of organic C from the mineral-associated SOM fraction, thus hampering the meaningful interpretation of fractionation results. These C losses, which tend to become more evident with increasing the number of washes and the soil organic C content (Supplementary Fig. AS 1), can be attributed to soil dispersion and organic matter solubilization induced by the high amounts of Na added with the SPT and NaI solutions. Initially, the high electrolyte concentration in the heavy solutions helps maintain soil aggregated during density fractionation (Sparks, 2003). With washing, this coagulation effect of a high electrolyte concentration disappears (Supplementary Fig. AS 2), and soil particles

disperse. Washing the Na-saturated soils causes hydrolysis reactions and increased pH (Supplementary Fig. AS 3). This rise in pH may also cause the disruption of bonds between organic matter and minerals and the conversion of acidic organic components to their soluble salt forms (Sparks, 2003).

As a whole, our results reveal substantial effects of the heavy liquid used for density fractionation on the distribution of organic C and total N in intra-aggregate and mineral associated pools. These effects are largely independent of the soil and has several implications that need to be accounted for when applying SOM fractionation methods and interpreting SOM fractionation data. First, to facilitate the comparison of results across studies, ultrasonic energy has to be properly calibrated not only for the soil under study but also for the heavy liquid and applied to an extent to completely disrupt aggregates. Our results also highlight the need of determining C and N levels in the heavy liquids used for density-based SOM separations, particularly N in SPT, to prevent or account for potential contamination effects. Finally, we do not recommend repeated washing of the heavy soil organo-mineral fractions separated with Na-based heavy liquids, as this can lead to mobilization of SOM.

References

Courtier-Murias, D., Simpson, A.J., Marzadori, C., Baldoni, G., Ciavatta, C., Fernández, J.M., López-de-Sá, E.G., Plaza, C., 2013. Unraveling the long-term stabilization mechanisms of organic materials in soils by physical fractionation and NMR spectroscopy. Agriculture Ecosystems Environment 171, 9-18.

Crow, S.E., Swanston, C.W., Lajtha, K., Brooks, J.R., Keirstead, H., 2007. Density fractionation of forest soils: methodological questions and interpretation of incubation results and turnover time in an ecosystem context. Biogeochemistry 85, 69-90.

Giannetta, B., Plaza, C., Vischetti, C., Cotrufo, M.F., Zaccone, C., 2018. Distribution and thermal stability of physically and chemically protected organic matter fractions in soils across different ecosystems. Biology and Fertility of Soils 54, 671-681.

Golchin, A., Oades, J.M., Skjemstad, J.O., Clarke, P., 1994. Soil structure and carbon cycling. Australian Journal of Soil Research 32, 1043-1068.

Harris, D., Horwath, W.R., van Kessel, C., 2001. Acid fumigation of soils to remove carbonates prior to total organic carbon or carbon-13 isotopic analysis. Soil Science Society of America Journal 65, 1853-1856.

IUSS Working Group WRB, 2015. World Reference Base for Soil Resources 2014, update 2015. International soil classification system for naming soils and creating legends for soil maps. World Soil Resources Reports No. 106. FAO, Rome, Italy.

Jiménez-González, M.A., Álvarez, A.M., Carral, P., González-Vila, F.J., Almendros, G., 2017. The diversity of methoxyphenols released by pyrolysis-gas chromatography as predictor of soil carbon storage. Journal of Chromatography A 1508, 130-137.

Jiménez-González, M.A., Álvarez, A.M., Hernández, Z., Almendros, G., 2018. Soil carbon storage predicted from the diversity of pyrolytic alkanes. Biology and Fertility of Soils 54, 617-629.

Kramer, M.G., Lajtha, K., Thomas, G., Sollins, P., 2009. Contamination effects on soil density fractions from high N or C content sodium polytungstate. Biogeochemistry 92, 177-181.

Lal, R., 2009. Challenges and opportunities in soil organic matter research. European Journal of Soil Science 60, 158-169.

Lehmann, J., Kleber, M., 2015. The contentious nature of soil organic matter. Nature 528, 60-68.

Paul, E.A., 2016. The nature and dynamics of soil organic matter: plant inputs, microbial transformations, and organic matter stabilization. Soil Biology and Biochemistry 98, 109-126.

Plaza, C., Courtier-Murias, D., Fernández, J.M., Polo, A., Simpson, A.J., 2013. Physical, chemical, and biochemical mechanisms of soil organic matter stabilization under conservation tillage systems: a central role for microbes and microbial by-products in C sequestration. Soil Biology and Biochemistry 57, 124-134.

Plaza, C., Fernández, J.M., Pereira, E.I.P., Polo, A., 2012. A comprehensive method for fractionating soil organic matter not protected and protected from decomposition by physical and chemical mechanisms. CLEAN-Soil Air Water 40, 134-139.

Plaza, C., Zaccone, C., Sawicka, K., Méndez, A.M., Tarquis, A., Gascó, G., Heuvelink, G.B.M., Schuur, E.A.G., Maestre, F.T., 2018. Soil resources and element stocks in drylands to face global issues. Scientific Reports 8, 13788.

Poeplau, C., Don, A., Six, J., Kaiser, M., Benbi, D., Chenu, C., Cotrufo, M.F., Derrien, D., Gioacchini, P., Grand, S., Gregorich, E., Griepentrog, M., Gunina, A., Haddix, M., Kuzyakov, Y., Kühnel, A., Macdonald, L.M., Soong, J., Trigalet, S., Vermeire, M.L., Rovira, P., van Wesemael, B., Wiesmeier, M., Yeasmin, S., Yevdokimov, I., Nieder, R., 2018. Isolating organic carbon fractions with varying turnover rates in temperate

agricultural soils – A comprehensive method comparison. Soil Biology and Biochemistry 125, 10-26.

R Core Team, 2018. R: A language and environment for statistical computing. R Foundation for Statistical Computing. Vienna, Austria, https://www.R-project.org.

Santos, H.M., Lodeiro, C., Capello-Martínez, J.L., 2009. The power of ultrasound, in: Capello-Martínez, J.L. (Eds.), Ultrasound in Chemistry: Analytical Applications. Wiley-Vch, Verlag GmbH & Co. KGaA, Weinheim, Germany.

Schmidt, M.W.I., Torn, M.S., Abiven, S., Dittmar, T., Guggenberger, G., Janssens, I.A., Kleber, M., Kogel-Knabner, I., Lehmann, J., Manning, D.A.C., Nannipieri, P., Rasse, D.P., Weiner, S., Trumbore, S.E., 2011. Persistence of soil organic matter as an ecosystem property. Nature 478, 49-56.

Sohi, S.P., Mahieu, N., Arah, J.R.M., Powlson, D.S., Madari, B., Gaunt, J.L., 2001. A procedure for isolating soil organic matter fractions suitable for modeling. Soil Science Society of America Journal 65, 1121-1128.

Sparks, D.L., 2003. Environmental Soil Chemistry, 2nd Edition. Academic Press, London, UK.

Von Lützow, M., Kögel-Knabner, I., Ekschmitt, K., Matzner, E., Guggenberger, G., Marschner, B., Flessa, H., 2006. Stabilization of organic matter in temperate soils: mechanisms and their relevance under different soil conditions – a review. European Journal of Soil Science 57, 426-445.

Table A.1 Location, vegetation, class (IUSS Working Group WRB, 2015), sampling depth, and main physical and chemical properties of the soils used in this study.

Soil	Location	Vegetation	Class	Depth (cm)	Texture	Sand (g kg^{-1})	Silt (g kg^{-1})	Clay (g kg^{-1})	pH	EC [a] (dS m^{-1})	CEC [b] ($cmol_c$ kg^{-1})	Organic C (g kg^{-1})	Total N (g kg^{-1})
SOIL 1 [c]	El Berrueco, Madrid, Spain	*Paeonia coriacea*	Dystric Cambisol	0-10	Sandy loam	522	352	126	5.3	0.418	14.4	45	3.7
SOIL 2 [d]	Foresta Cesane, Fossombrone, Italy	*Pinus nigra*	Rendzic Leptosol	0-10	Loam	379	481	140	8.3	0.064	22.1	31	2.2
SOIL 3 [d]	Chiaserna, Cantiano, Italy	*Pinus nigra*	Haplic Cambisol	0-20	Clay loam	380	232	388	8.0	0.059	49.6	57	4.6
SOIL 4 [d]	Castelluccio, Castelsantangelo sul Nera, Italy	*Fagus sylvatica*	Haplic Cambisol	0-20	Clay	265	312	423	8.1	0.082	35.9	35	2.4

[a] Electrical conductivity.
[b] Cation exchange capacity.
[c] Jiménez-González et al. (2017, 2018).
[d] Giannetta et al. (2018).

Table A.2 Organic C and total N recovery (mean ± standard error) for each soil (SOIL 1 to 4) after fractionation, as affected by the heavy liquid used for separation (sodium polytungstate, SPT, vs. sodium iodide, NaI) and washing.

Recovery	Heavy liquid	Washing	SOIL 1	SOIL 2	SOIL 3	SOIL 4
Organic C	SPT	Unwashed	85.2 ± 6.3 a A	92.5 ± 0.9 a A	98.1 ± 0.1 a A	87.8 ± 3.3 a A
(%)	SPT	Washed	85.0 ± 7.3 a A	82.3 ± 3.2 a A	77.3 ± 3.2 a B	86.3 ± 2.3 a A
	NaI	Unwashed	89.9 ± 1.0 a A	98.3 ± 3.4 a A	97.5 ± 1.9 a A	96.4 ± 1.2 a A
	NaI	Washed	82.5 ± 1.2 a B	83.8 ± 3.2 a B	85.3 ± 2.1 a B	87.7 ± 1.0 a A
Total N	SPT	Unwashed	105.5 ± 9.1 a A	107.1 ± 12.8 a A	131.4 ± 1.1 a A	143.1 ± 25.2 a A
(%)	SPT	Washed	104.7 ± 6.2 a A	92.2 ± 7.9 a A	87.8 ± 2.5 a B	110.4 ± 3.8 a A
	NaI	Unwashed	76.2 ± 1.8 a A	51.5 ± 10.7 b A	77.1 ± 3.8 b A	73.5 ± 18.5 a A
	NaI	Washed	79.7 ± 1.6 b A	75.4 ± 4.8 a A	80.5 ± 5.5 a A	71.5 ± 2.6 b A

Within the same soil and washing treatment, different lowercase letters indicate statistically significant differences at the 0.05 level. Within the same soil and heavy liquid, different uppercase letters indicate statistically significant differences at the 0.05 level.

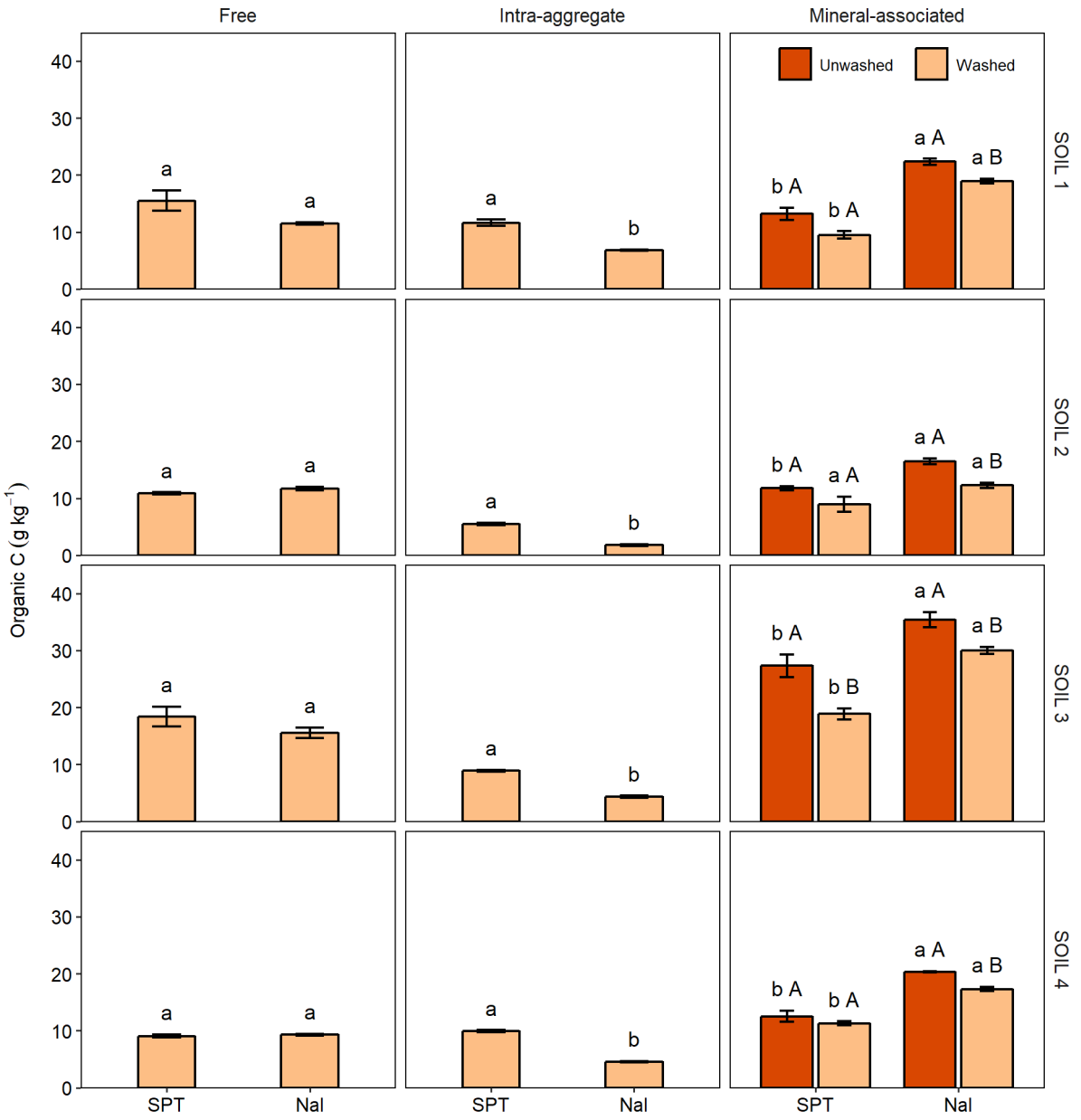

Figure A.1 Free, intra-aggregate, and mineral-associated organic C content (mean ± standard error) of soils (SOIL 1 to 4) as affected by the heavy liquid used for separation (sodium polytungstate, SPT, vs. sodium iodide, NaI) and washing. Within the same soil, fraction, and washing treatment, different lowercase letters indicate statistically significant differences at the 0.05 level. Within the same soil and heavy liquid, different uppercase letters indicate statistically significant differences at the 0.05 level.

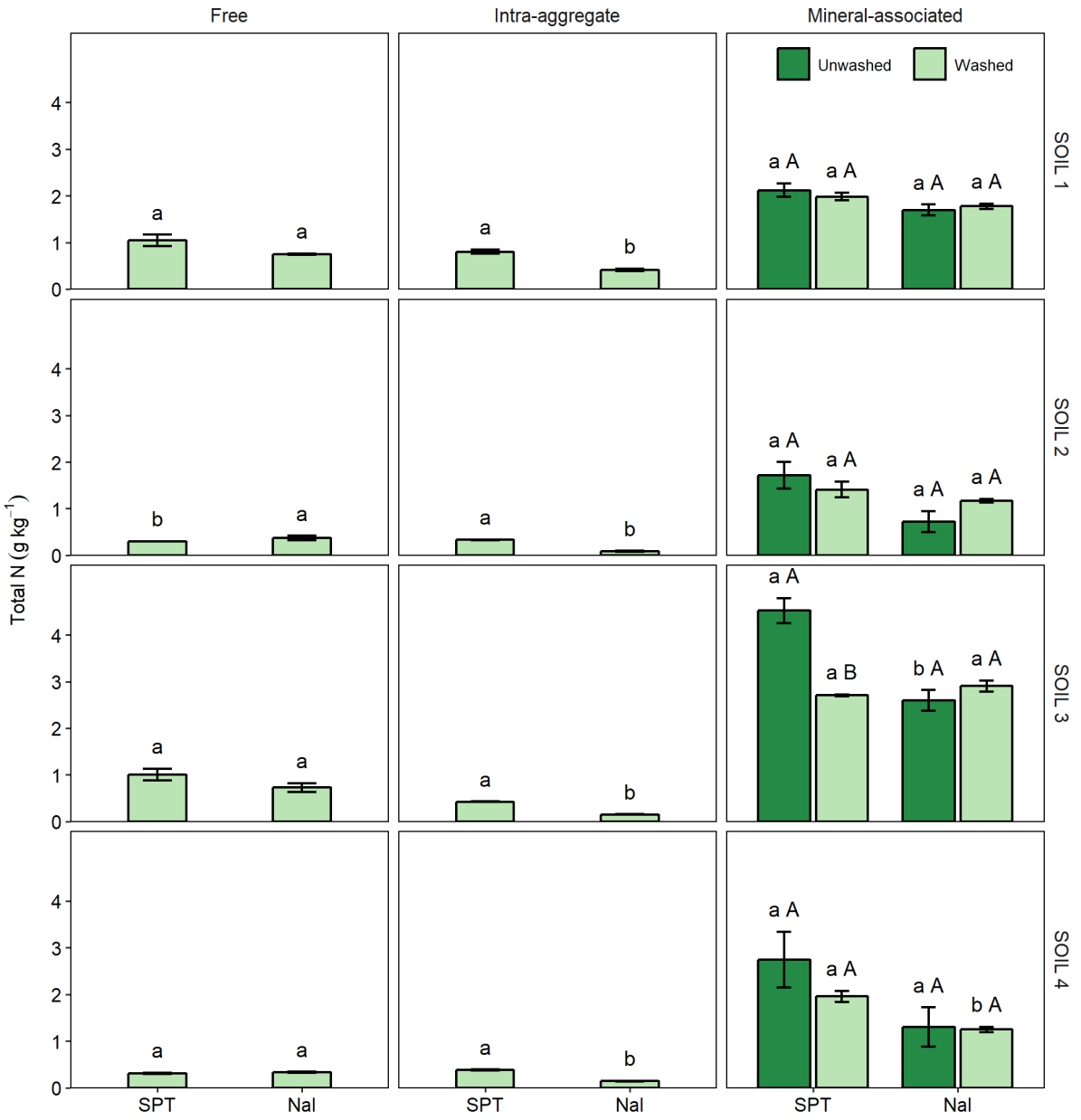

Figure A.2 Free, intra-aggregate, and mineral-associated N content (mean ± standard error) of soils (SOIL 1 to 4) as affected by the heavy liquid used for separation (sodium polytungstate, SPT, vs. sodium iodide, NaI) and washing. Within the same soil, fraction, and washing treatment, different lowercase letters indicate statistically significant differences at the 0.05 level. Within the same soil and heavy liquid, different uppercase letters indicate statistically significant differences at the 0.05.

Supplementary Information

Table AS.1 Analysis of variance for free, intra-aggregate, and mineral-associated organic C and total N content and total recovery, as affected by heavy liquid (HL), washing (WA), and soil type (SO).

	Free organic C	Intra-aggregate organic C	Mineral-associated organic C	Free N	Intra-aggregate N	Mineral-associated N	Recovery of organic C	Recovery of N
HL	***	***	***	***	***	***	*	***
WA	-	-	***	-	-	*	***	*
SO	***	***	***	***	***	***	NS	NS
HL × WA	-	-	NS	-	-	***	NS	***
HL × SO	***	***	***	***	***	*	NS	NS
WA × SO	-	-	**	-	-	*	*	*
HL × WA × SO	-	-	NS	-	-	**	NS	NS

NS $P > 0.05$; * $P < 0.05$; ** $P < 0.01$; *** $P < 0.001$.

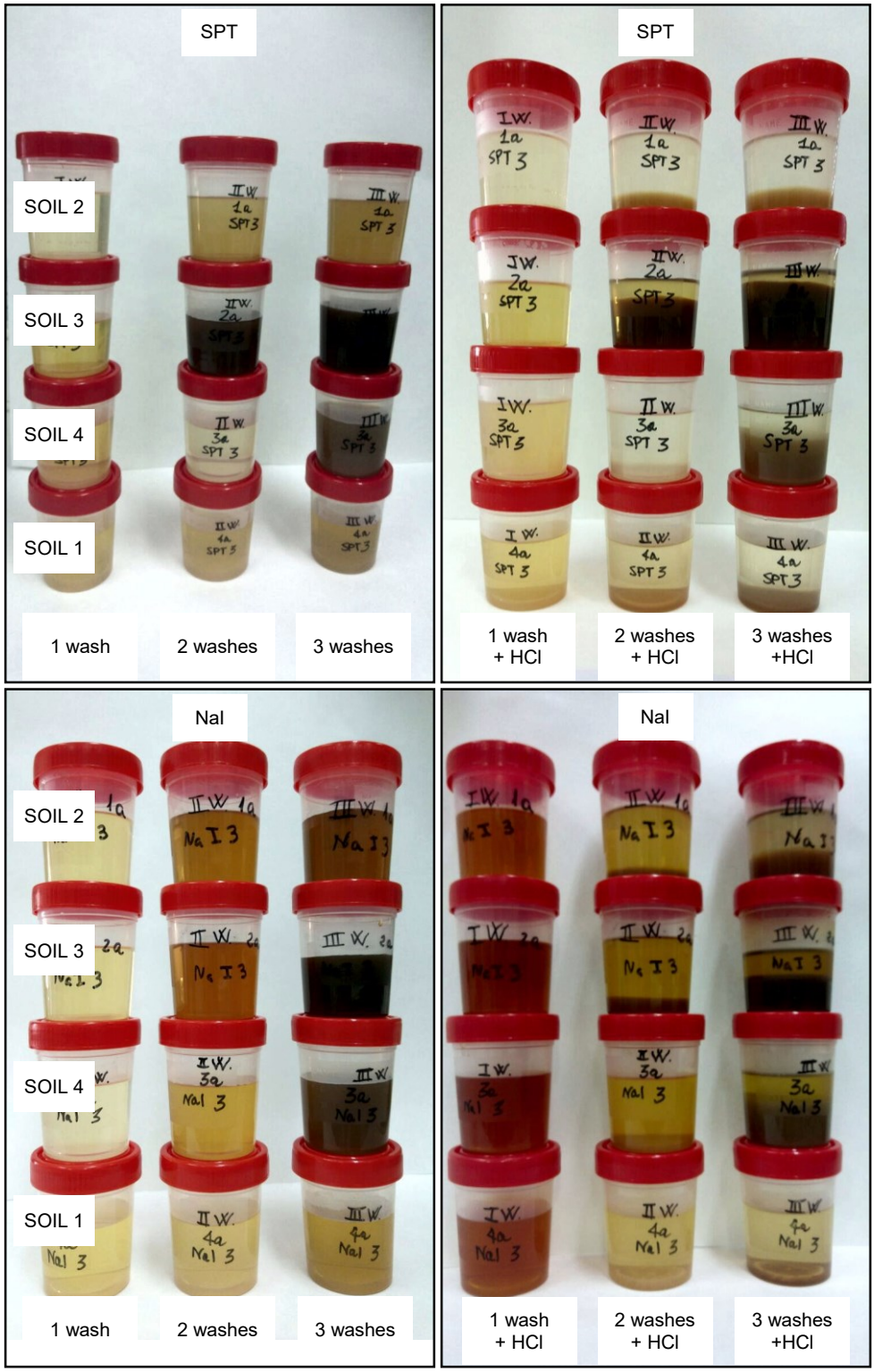

Figure AS.1 Wash water after 1, 2, and 3 washes of the mineral-associated organic matter fraction separated with either sodium polytungstate (SPT) or sodium iodide (NaI) of the soils used in this study (SOIL 1 to 4) before and after acidification with HCl**.**

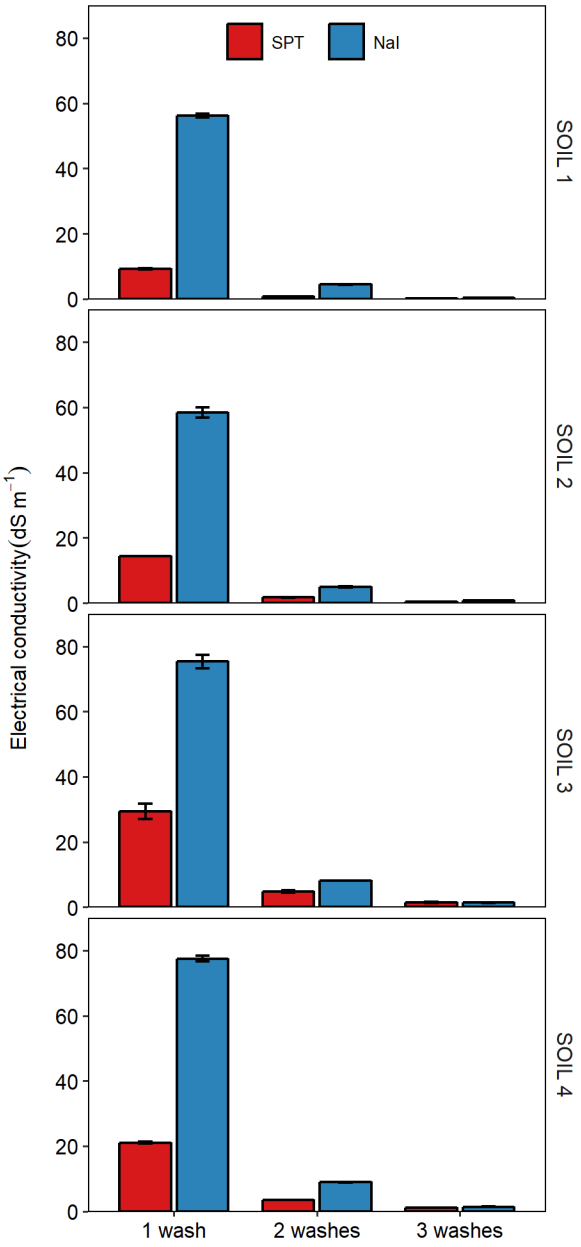

Figure AS.2 Electrical conductivity of wash water after 1, 2, and 3 washes of the mineral-associated organic matter fraction of the soils used in this study (SOIL 1 to 4), as affected by the heavy liquid used for separation (sodium polytungstate, SPT, vs. sodium iodide, NaI). Within the same soil and wash, differences between SPT and NaI are all statistically significant at the 0.05 level (except for the third wash).

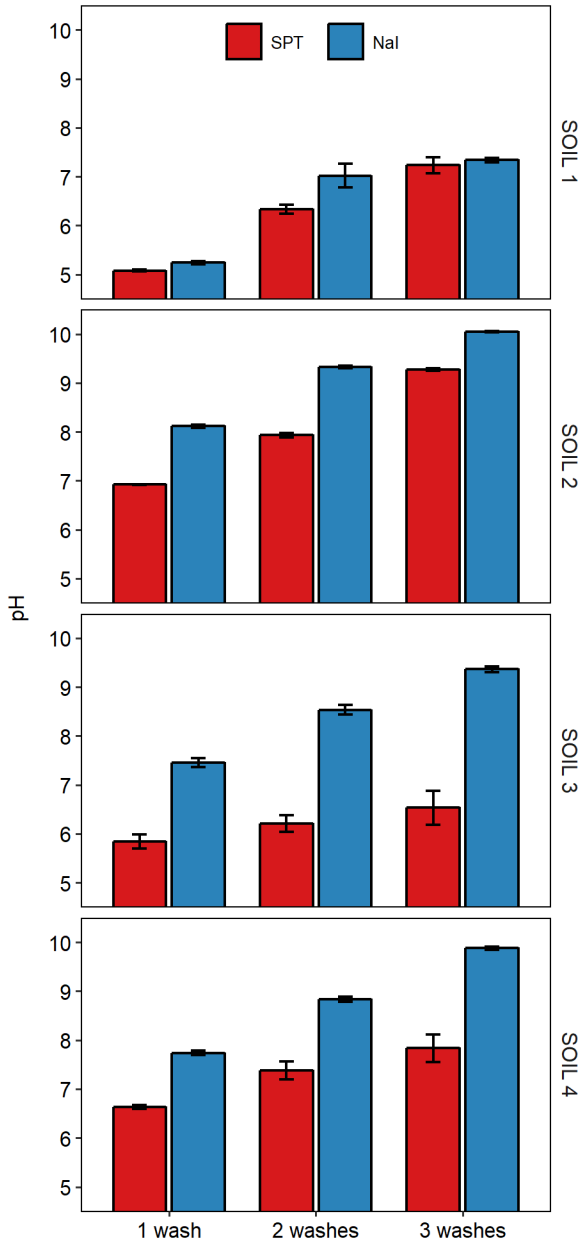

Figure AS.3 pH of wash water after 1, 2, and 3 washes of the mineral-associated organic matter fraction of the soils used in this study (SOIL 1 to 4), as affected by the heavy liquid used for separation (sodium polytungstate, SPT, vs. sodium iodide, NaI). Within the same soil and wash, differences between SPT and NaI are all statistically significant at the 0.05 level (except for the third wash of SOIL 1).

B. Supplementary information for Chapter 5

Table B.1 Results of the Principal Component Analysis (PCA) performed on the EXAFS spectra from the 8 samples analyzed.

Component	Eigenvalues	Variance	Cum. Var.[a]	IND[b]
1	55.771	0.949	0.949	0.01468
2	1.766	0.030	0.979	0.00803
3	0.615	0.010	0.990	0.00629
4	0.325	0.005	0.995	0.00420
5	0.097	0.001	0.997	0.00594
6	0.078	0.001	0.998	0.00874
7	0.039	0.000	0.990	0.02939
8	0.029	0.000	1.0	NA

[a] Cumulative variance.

[b] Indicator function (Malinowski, 1997).

Table B.2 EXAFS standard used for LCF. Target transformation was applied to determine SPOIL values, chi square and R-values of each standard considered. More in detail, chi square and R-values and SOIL values were performed in a k-range of 2.5-10, with 3 components, with the exception of CF (k-range 2.5-9.5). k-range of 2.5-10, with 2 and 4 components were also tested. The source and description of each standards are also reported in the table.

Standard	Chi sq	R	SPOIL[a]	Source
Fe (III) citrate	162.37	0.1	0.44	O'Day et al. 2004
Fe (III) ACAC	348.77	0.14	0.48	O'Day et al. 2004
Ferrihydrite	165.81	0.15	0.46	O'Day et al. 2004
Goethite	296.95	0.19	1.09	O'Day et al. 2004
Hematite	1397.66	0.53	0.83	O'Day et al. 2004
Magnetite	962.75	0.59	2.3	O'Day et al. 2004
Siderite	701.31	0.74	0.76	O'Day et al. 2004
Illite	76.39	0.62	0.82	O'Day et al. 2004
Nontronite	203.87	0.09	1.4	O'Day et al. 2004
Smectite	200.05	0.08	0.38	O'Day et al. 2004
Vermiculite	401.7	0.27	0.56	O'Day et al. 2004
Chlorite	354.93	0.26	0.06	O'Day et al. 2004

[a] SPOIL classification (Malinowski, 1978): 0-1.5, excellent; 1.5-3 good; 3-4.5, fair; 4.5-6, acceptable, and >6, unacceptable reference.

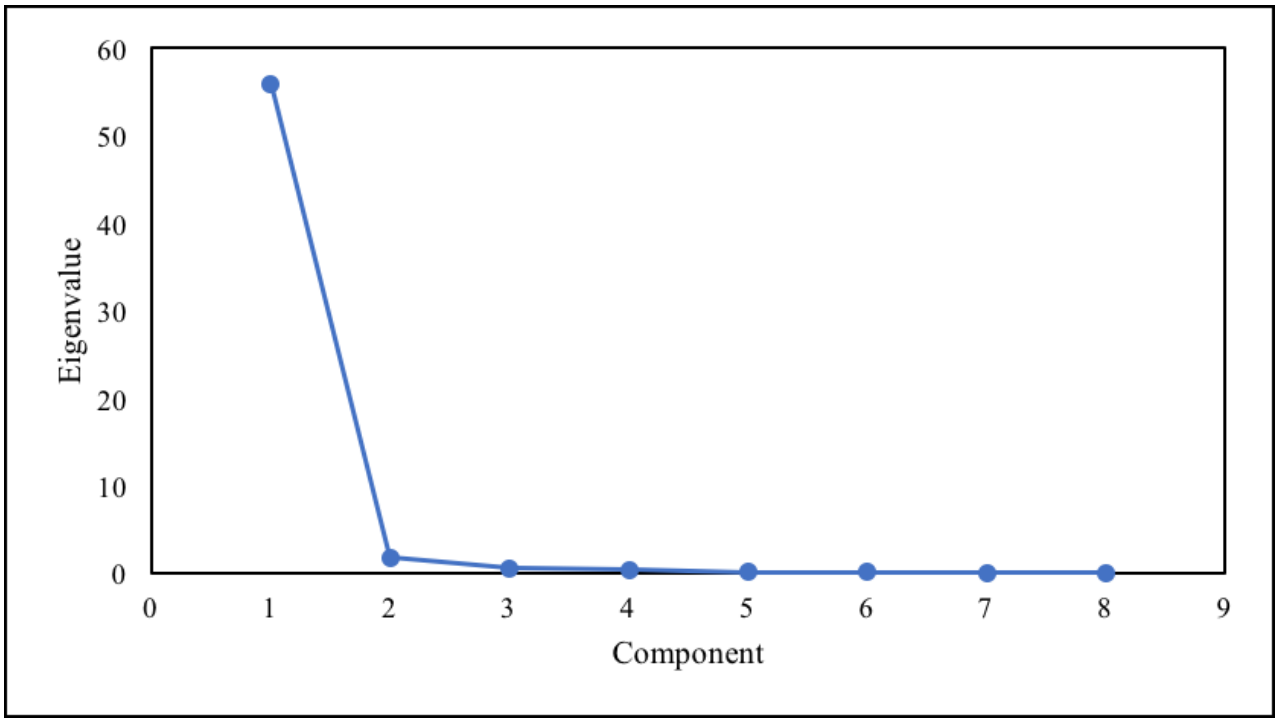

Figure B.1 Principal component analysis (PCA) results. The scree plot shows the first break in slope at two components.

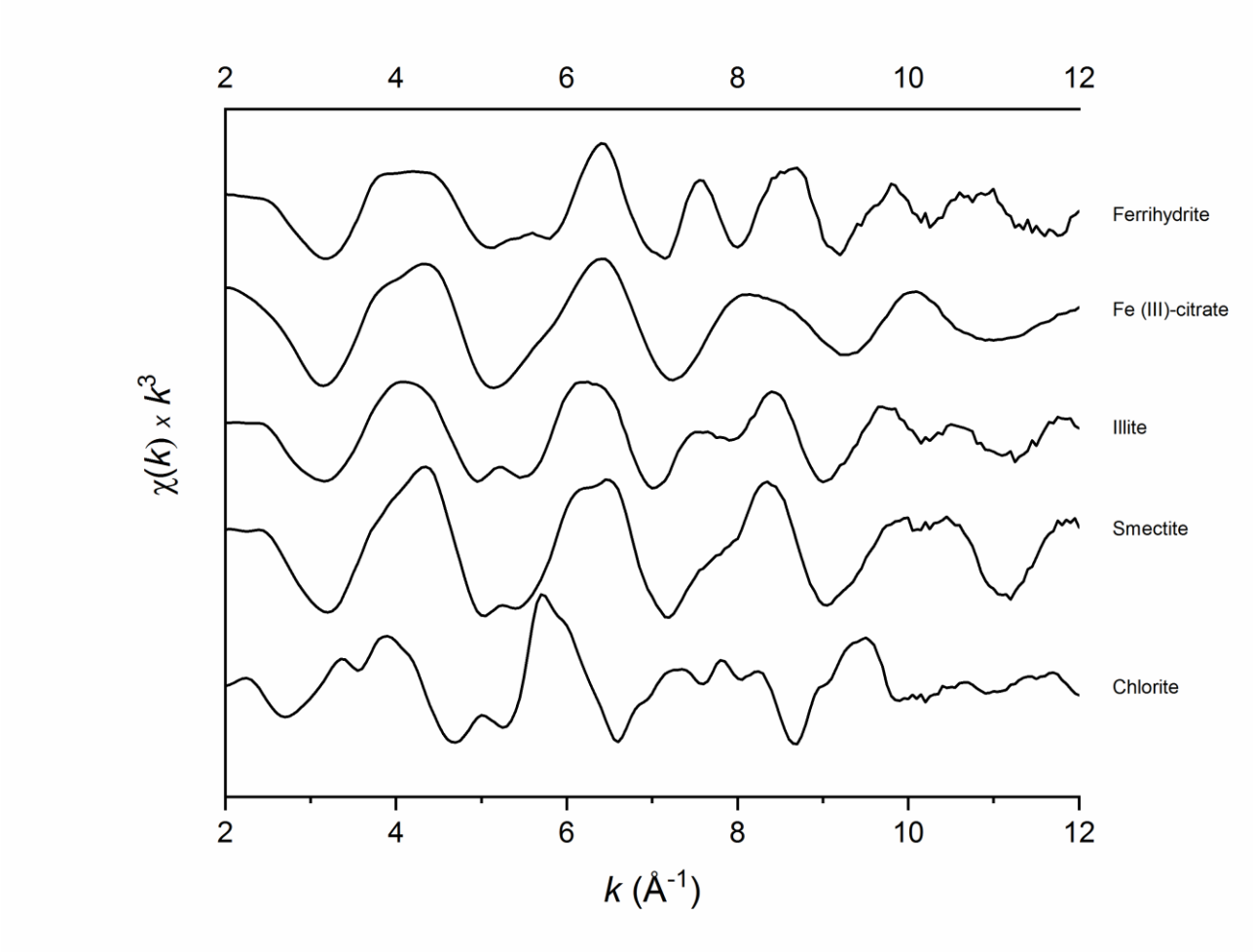

Figure B.2 EXAFS standards considered for LCF of the soil fractions. Sources and descriptions of each standard are indicated in Table B.2.

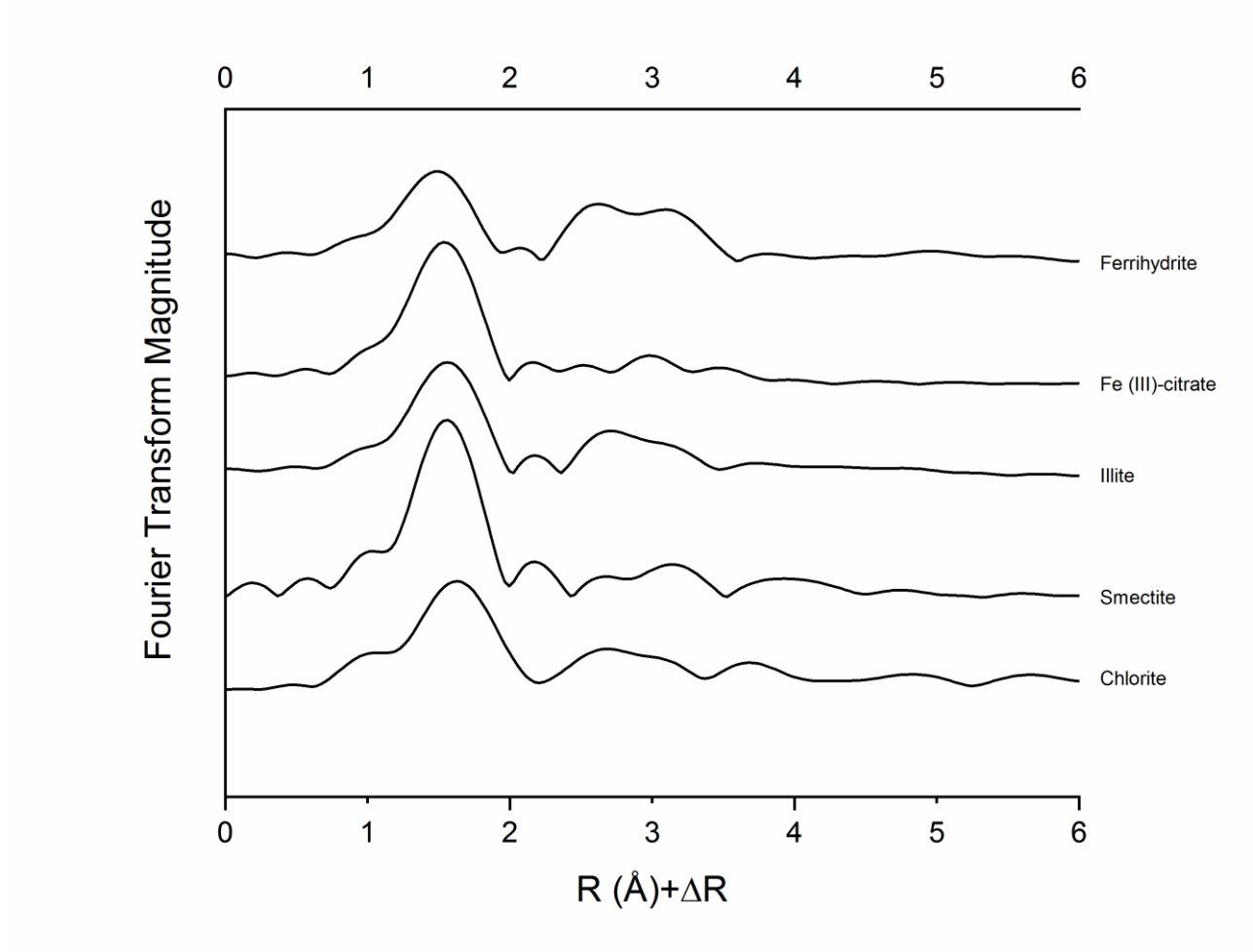

Figure B.3 FT spectra of the standards considered for LCF of the soil fractions. Sources and descriptions of each standard are indicated in Table B.2.

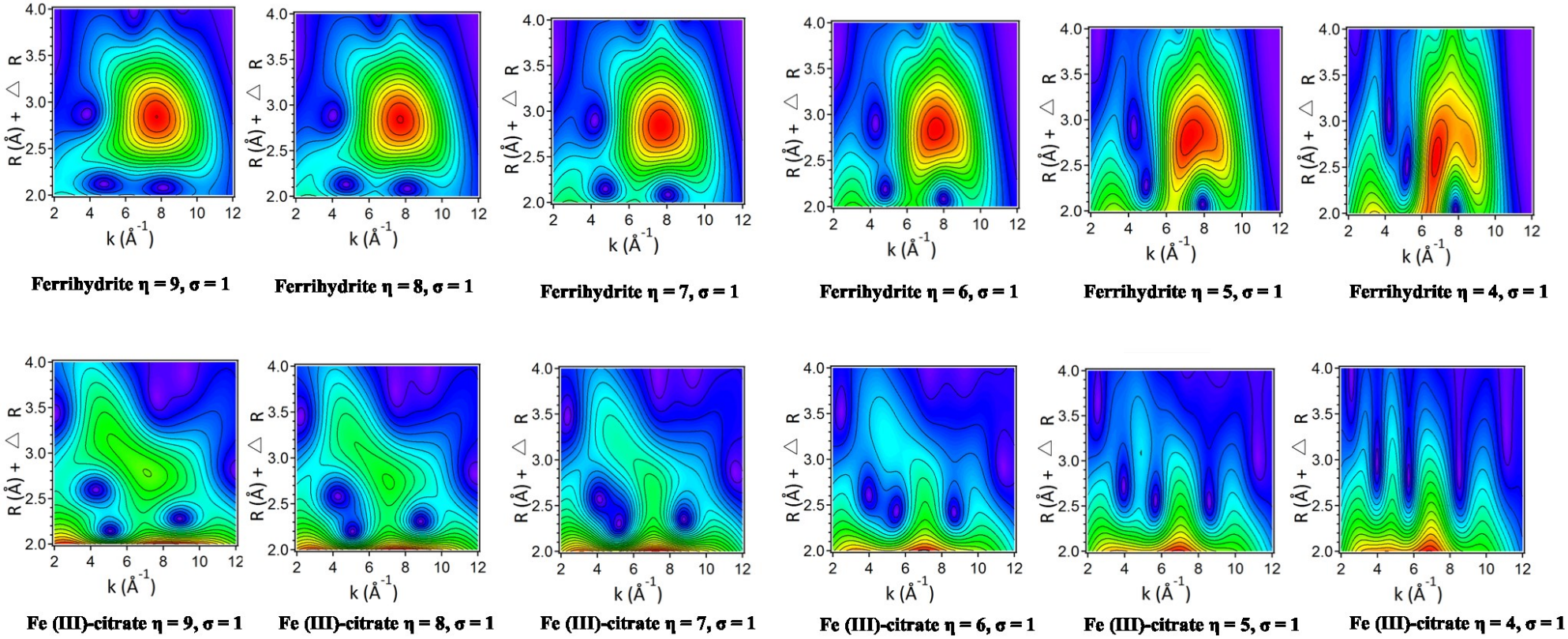

Figure B.4 WT plots illustrating the effect of changes to the eta (η) parameter on the second and third shells of the standards. In this series of plots, σ remains constant while η ranges from 9 to 4.

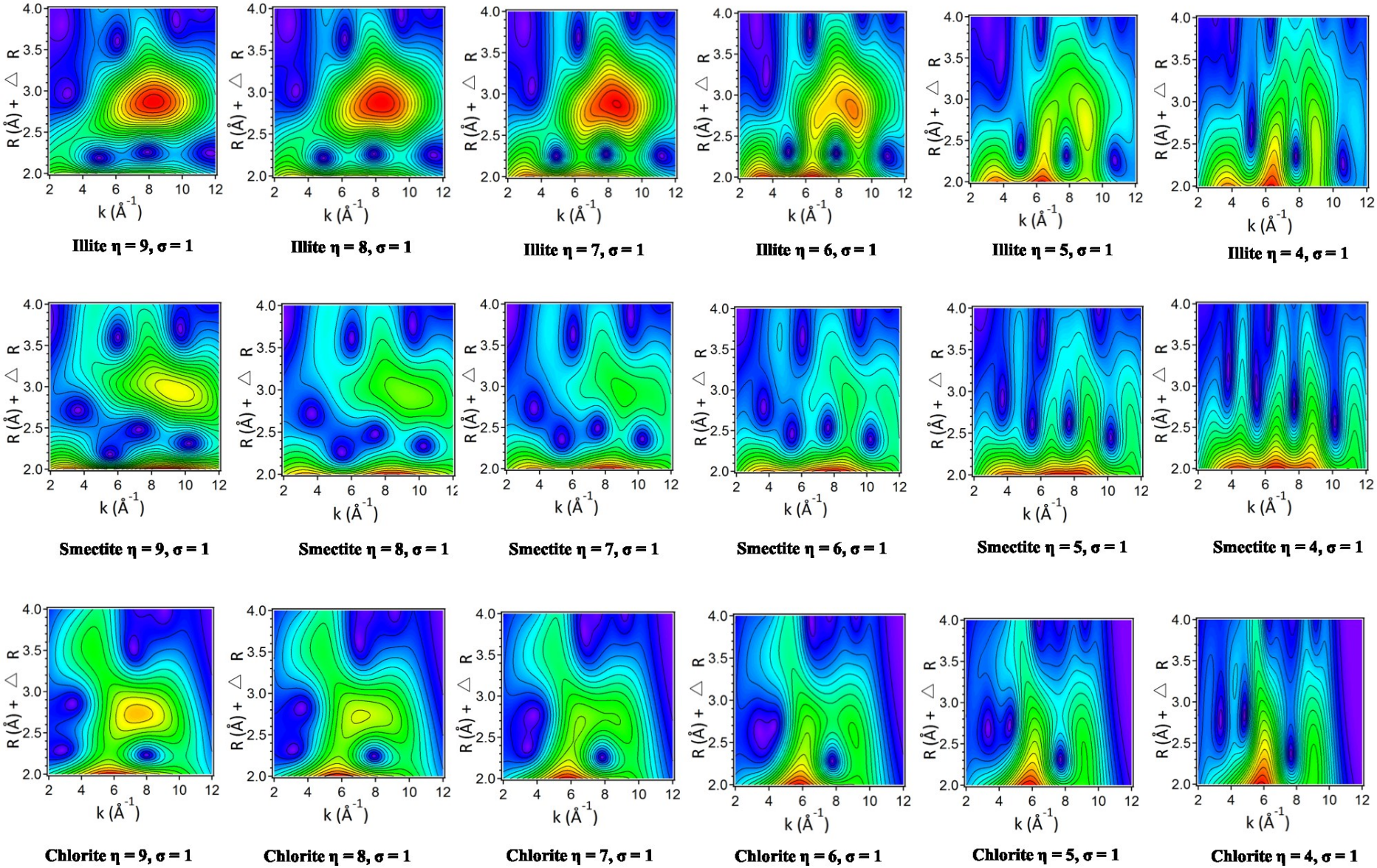

Figure B.4 (continues)

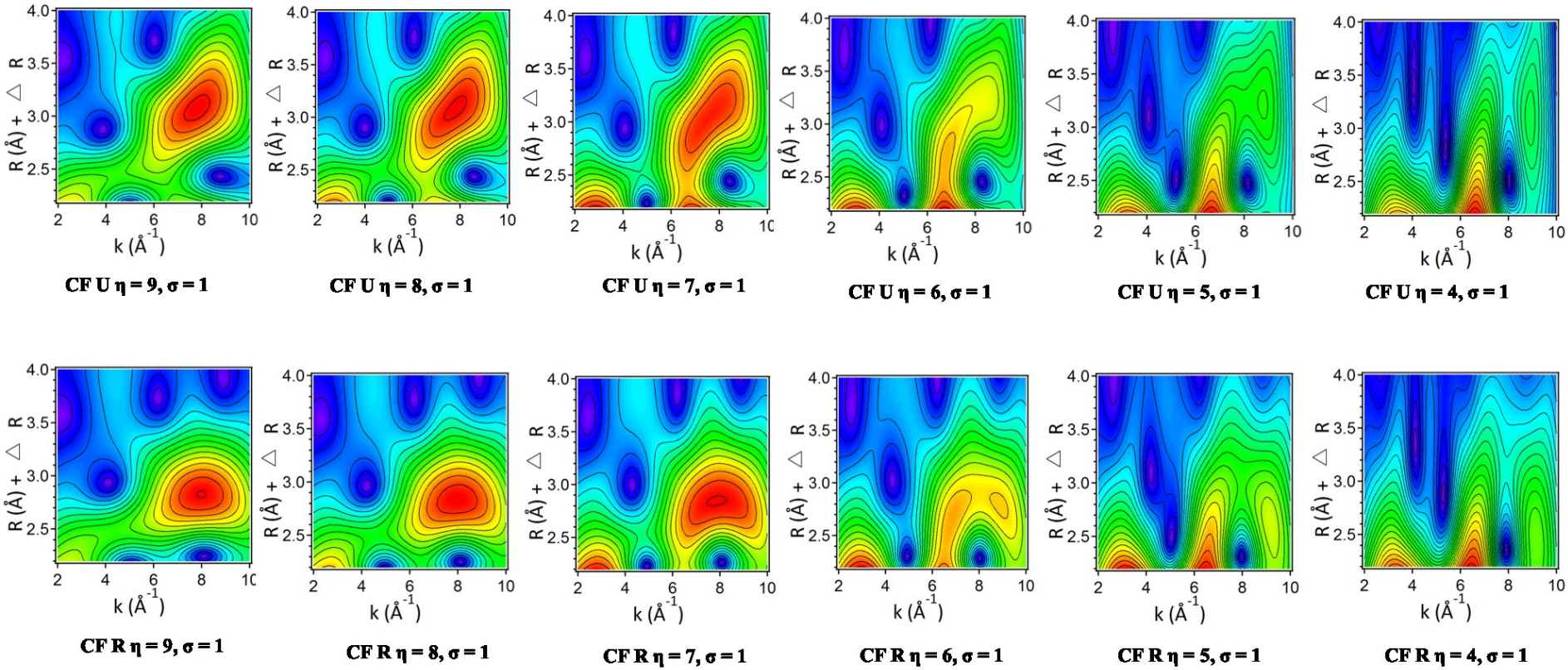

Figure B.5 WT plots illustrating the effect of changes to the eta (η) parameter on the second and third shells of the fine silt and clay samples. In this series of plots, σ remains constant while η ranges from 9 to 4.

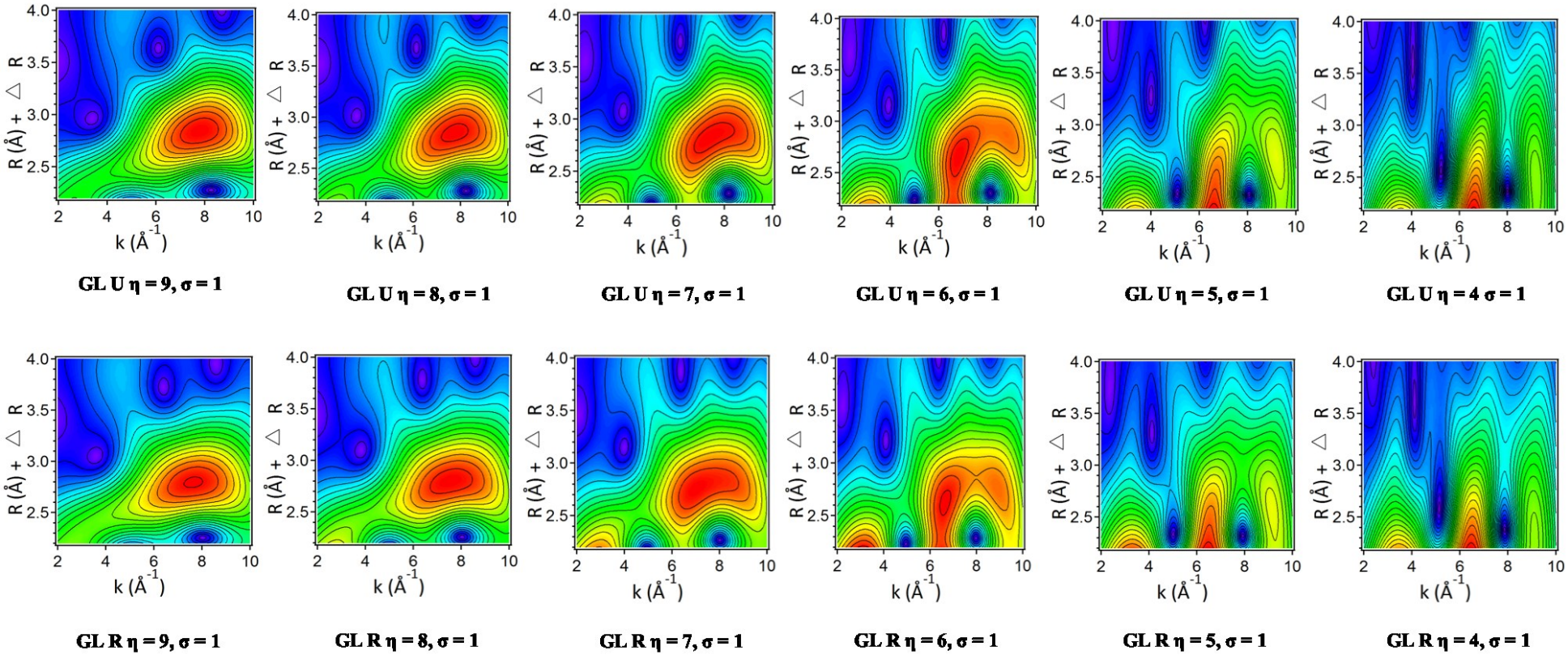

Figure B.5 (continues)

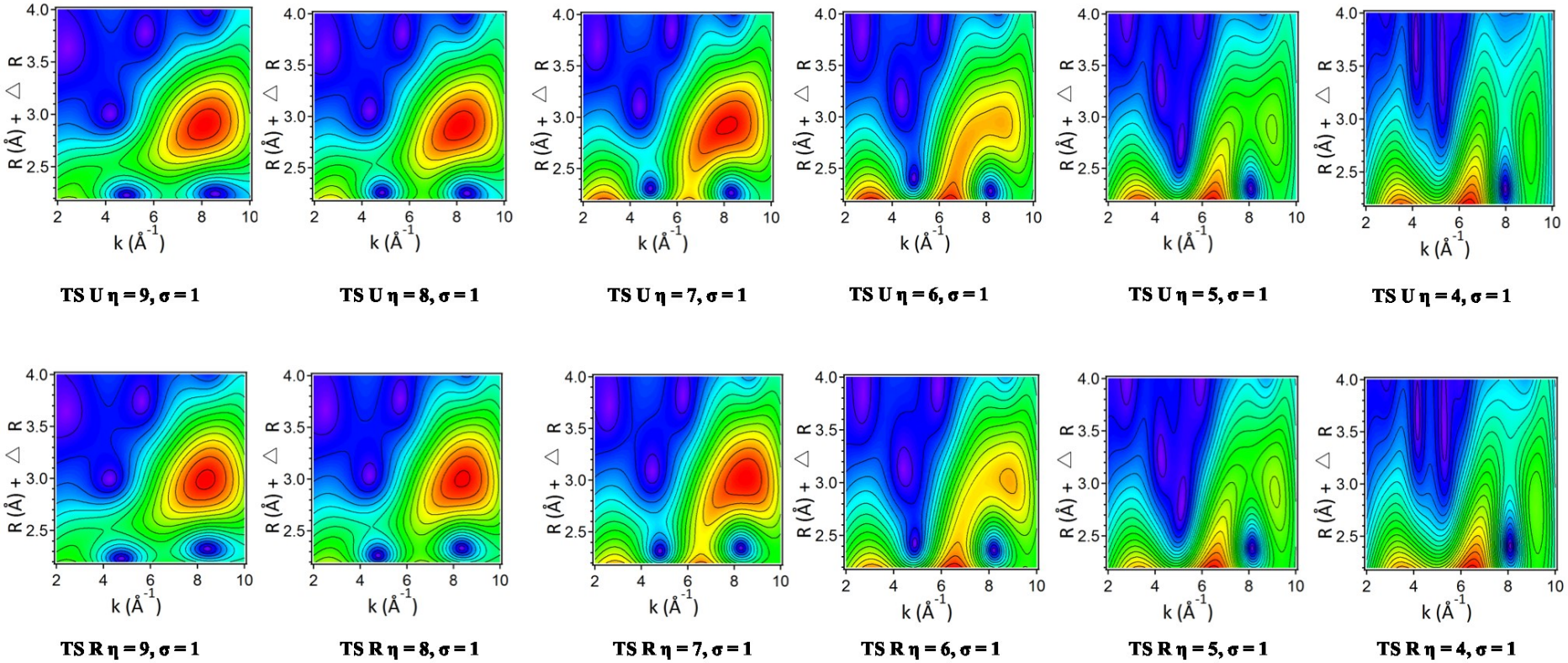

Figure B.5 (continues)

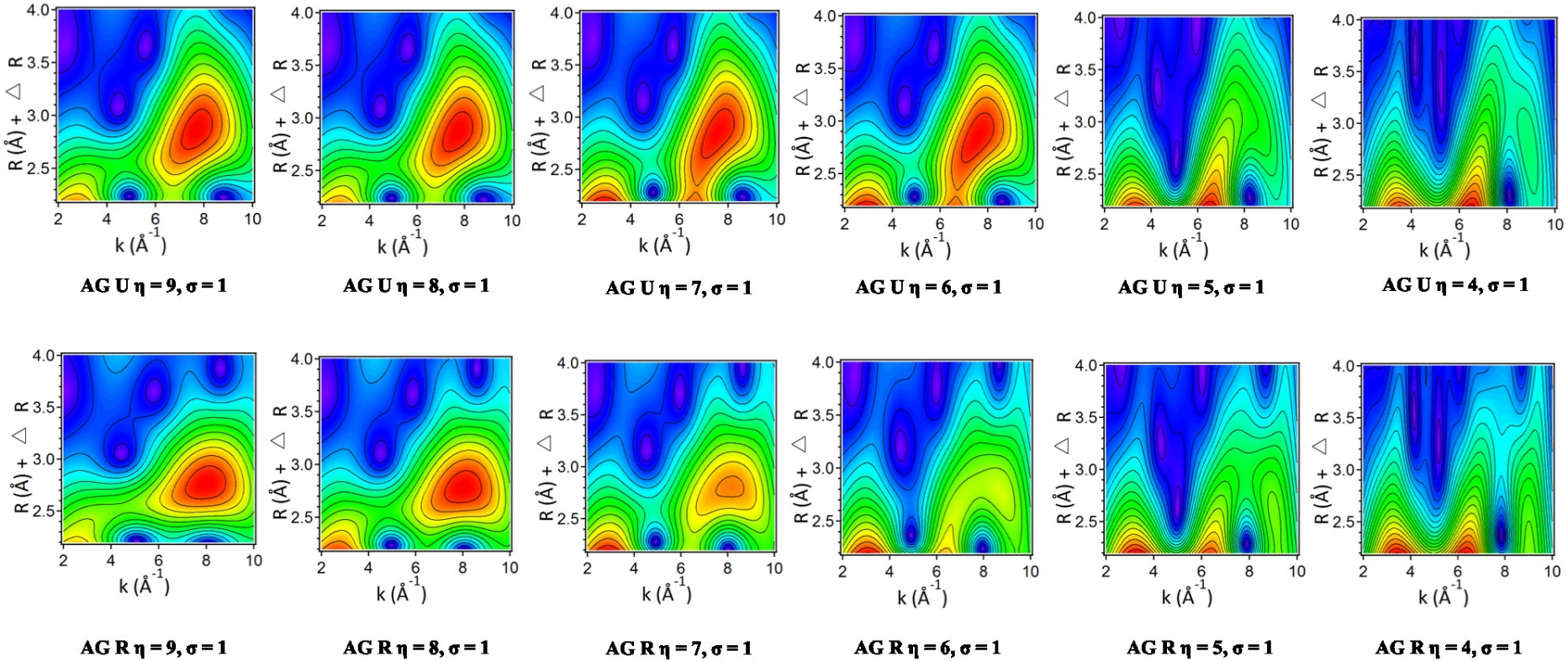

Figure B.5 (continues)

C. Supplementary information for Chapter 6

Table C.1 Results of the Principal Component Analysis (PCA) performed on the EXAFS spectra from the 8 samples analyzed.

Component	Eingenvalue	Variance	Cum. Var.[a]	IND[b]
1	55.771	0.949	0.949	0.01468
2	1.766	0.030	0.979	0.00803
3	0.615	0.010	0.990	0.00629
4	0.325	0.005	0.995	0.00420
5	0.097	0.001	0.997	0.00594
6	0.078	0.001	0.998	0.00874
7	0.039	0.000	0.990	0.02939
8	0.029	0.000	1.0	NA

[a] Cumulative variance.

[b] Indicator function (Malinowski, 1997).

Table C.2 EXAFS standard used for LCF. Target transformation was applied to determine SPOIL values, chi square and R-values of each standard considered. More in detail, chi square and R-values and SOIL values were performed in a k-range of 2.5-10, with 3 components, with the exception of CF (k-range 2.5-9.5). k-range of 2.5-10, with 2 and 4 components were also tested. The source and description of each standards are also reported in the table.

Standard	Chi sq	R	SPOIL[a]	Source
Fe (III) citrate	162.37	0.1	0.44	O'Day et al. 2004
Fe (III) ACAC	348.77	0.14	0.48	O'Day et al. 2004
Ferrihydrite	165.81	0.15	0.46	O'Day et al. 2004
Goethite	296.95	0.19	1.09	O'Day et al. 2004
Hematite	1397.66	0.53	0.83	O'Day et al. 2004
Magnetite	962.75	0.59	2.3	O'Day et al. 2004
Siderite	701.31	0.74	0.76	O'Day et al. 2004
Illite	76.39	0.62	0.82	O'Day et al. 2004
Nontronite	203.87	0.09	1.4	O'Day et al. 2004
Smectite	200.05	0.08	0.38	O'Day et al. 2004
Vermiculite	401.7	0.27	0.56	O'Day et al. 2004
Chlorite	354.93	0.26	0.06	O'Day et al. 2004

[a] SPOIL classification (Malinowski, 1978): 0-1.5, excellent; 1.5-3 good; 3-4.5, fair; 4.5-6, acceptable, and >6, unacceptable reference.

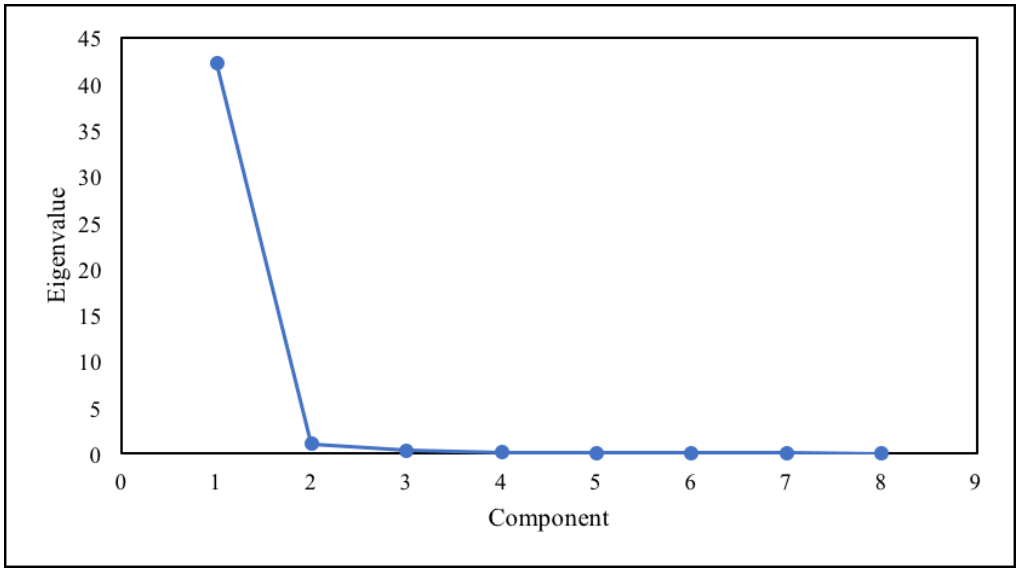

Figure C.1 Principal component analysis (PCA) results. The scree plot shows a break in slope at two components.

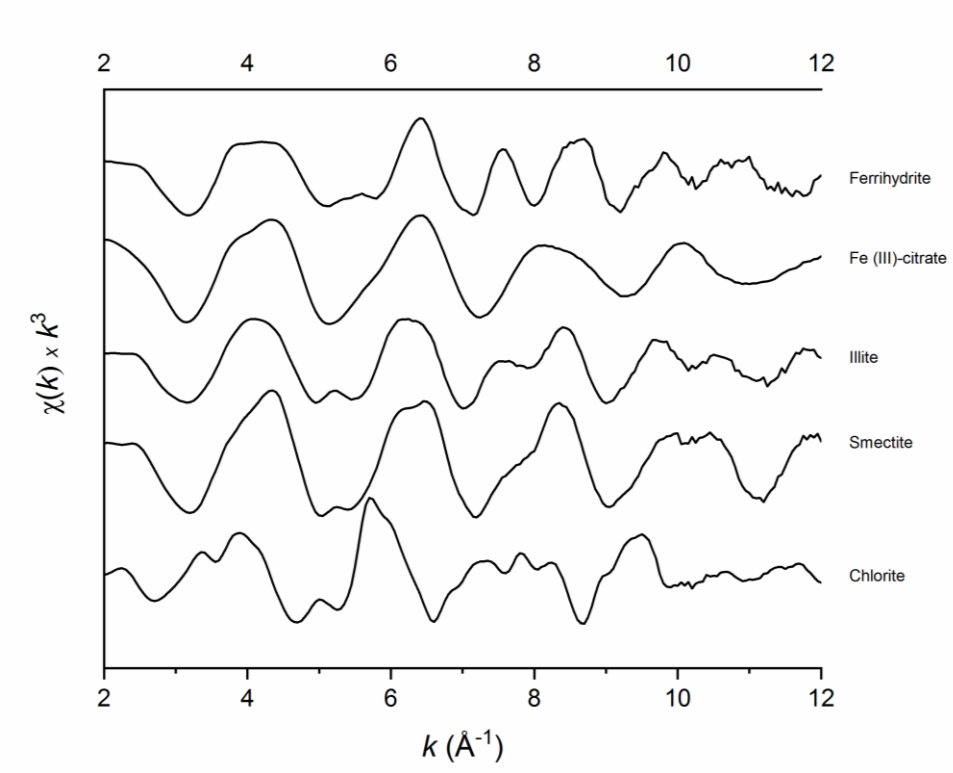

Figure C.2 EXAFS standards considered for LCF of the soil fractions. Sources and descriptions of each standard are indicated in Table C

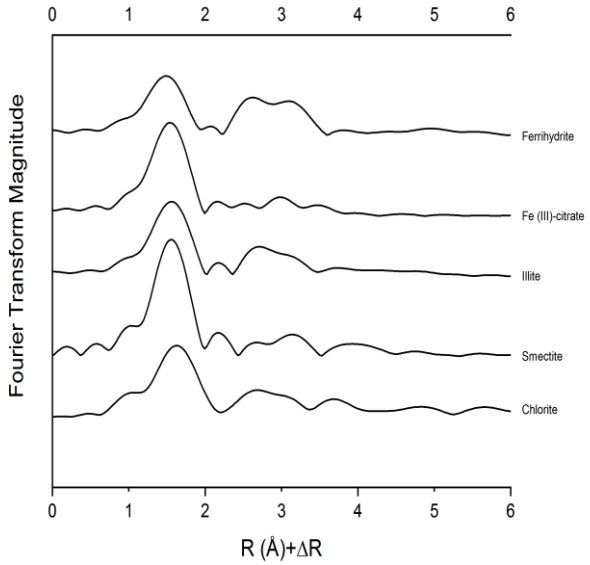

Figure C.3 FT spectra of the standards considered for LCF of the soil fractions. Sources and descriptions of each standard are indicated in Table C2.

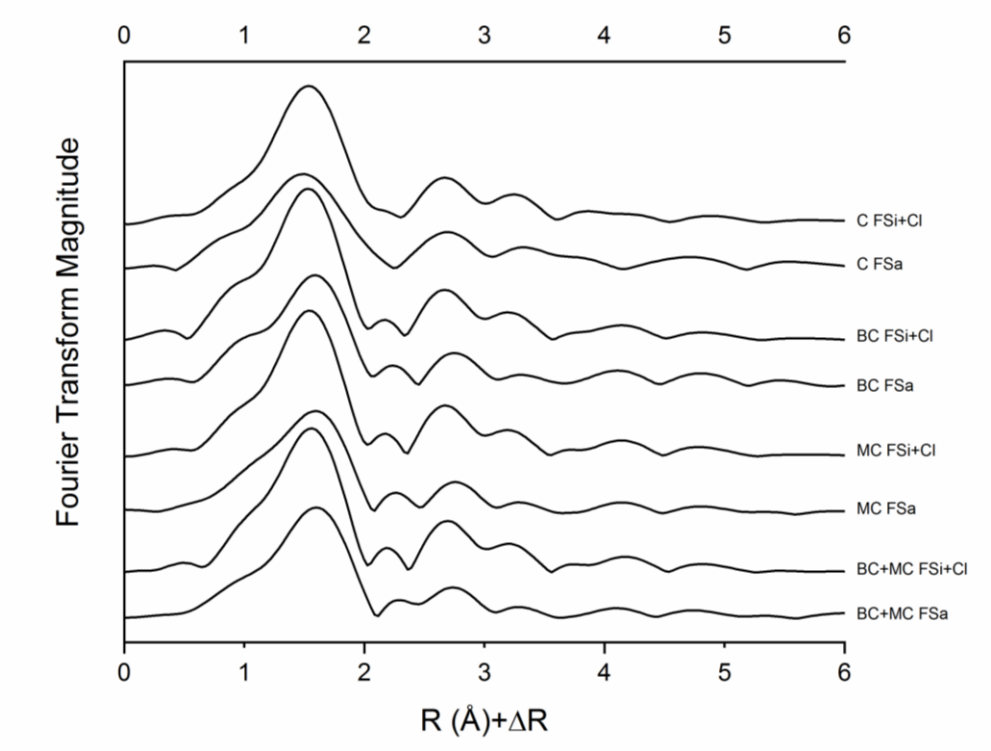

Figure C.4 FT spectra of the fine silt and clay (FSi+Cl) and fine sand (FSa) fractions of agricultural soils either unfertilized (C), amended with biochar (BC), municipal solid waste compost (MC) and with both of them (BC+MC).

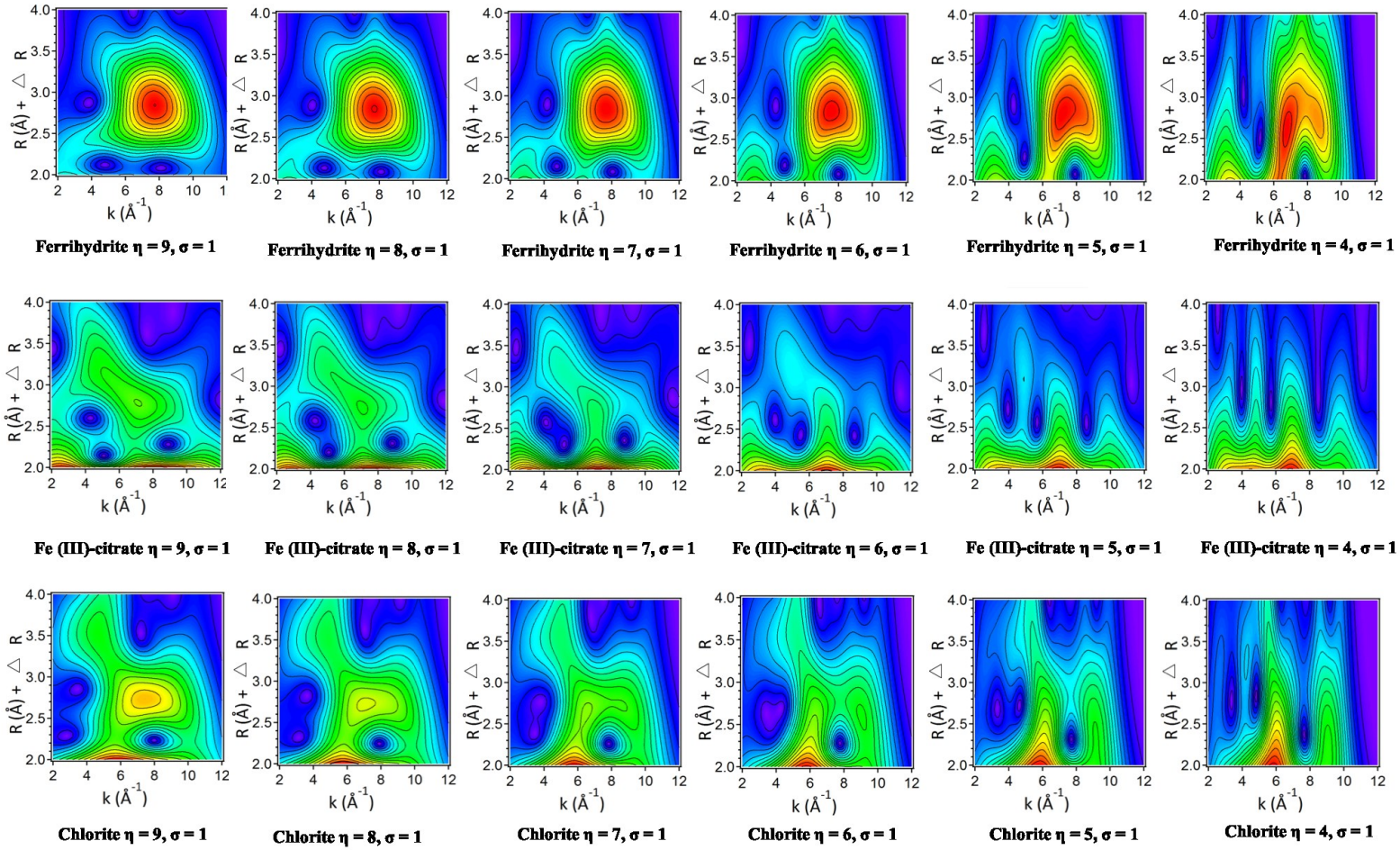

Figure C.5 WT plots illustrating the effect of changes to the eta (η) parameter on the second and third shells of the standards. In this series of plots, σ remains constant while η ranges from 9 to 4.

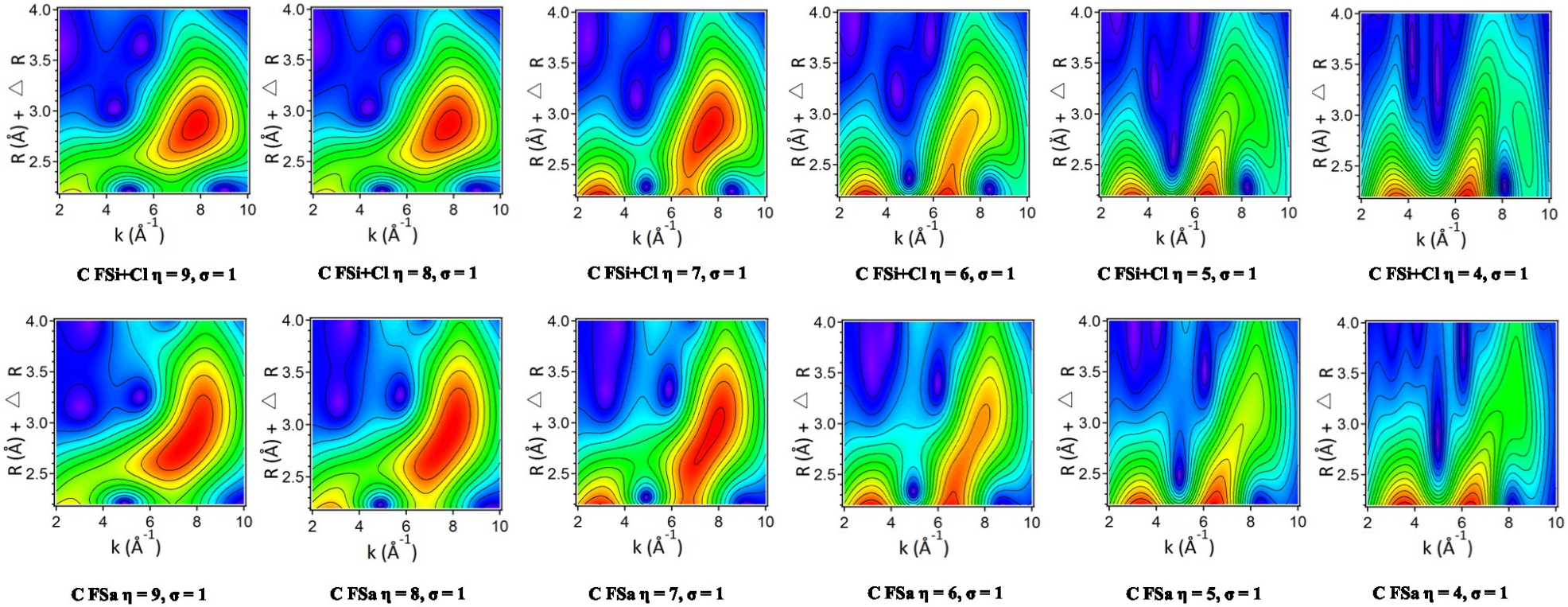

Figure C.6 WT plots illustrating the effect of changes to the eta (η) parameter on the second and third shells of the fine silt and clay samples. In this series of plots, σ remains constant while η ranges from 9 to 4.

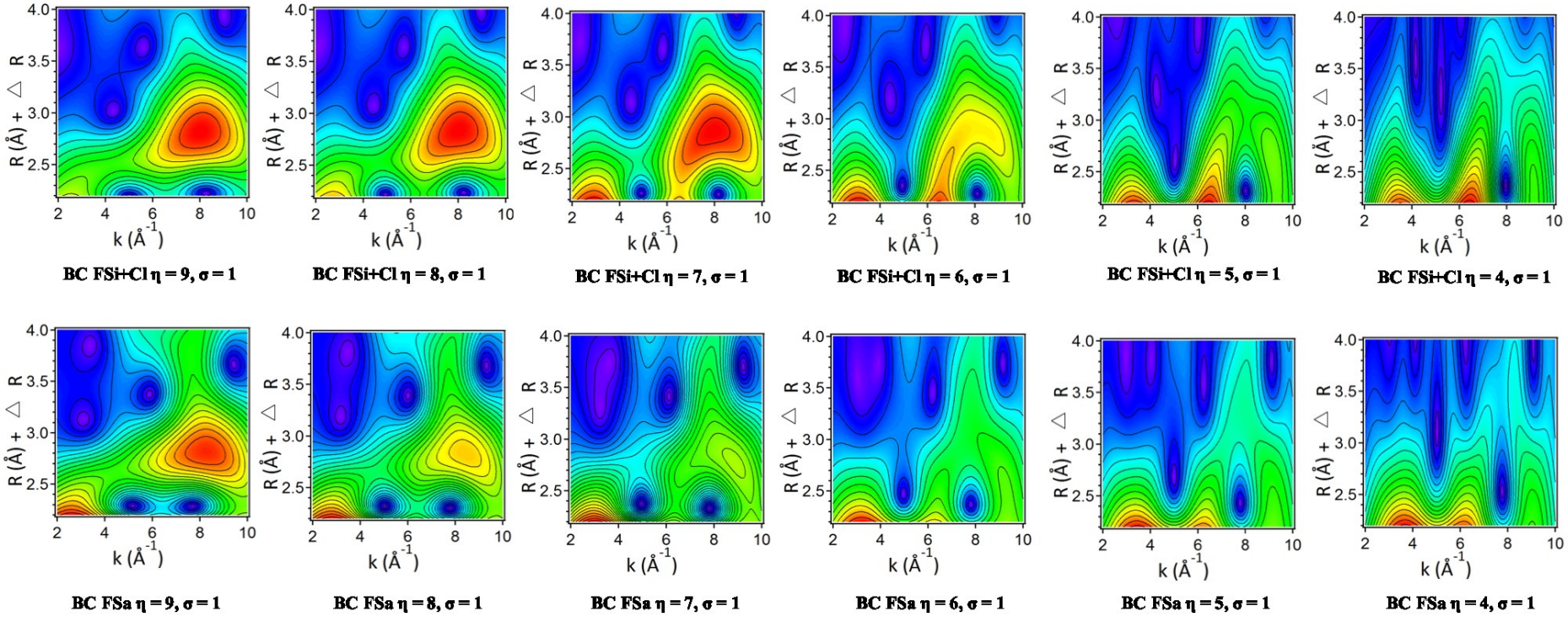

Figure C.6 (continues)

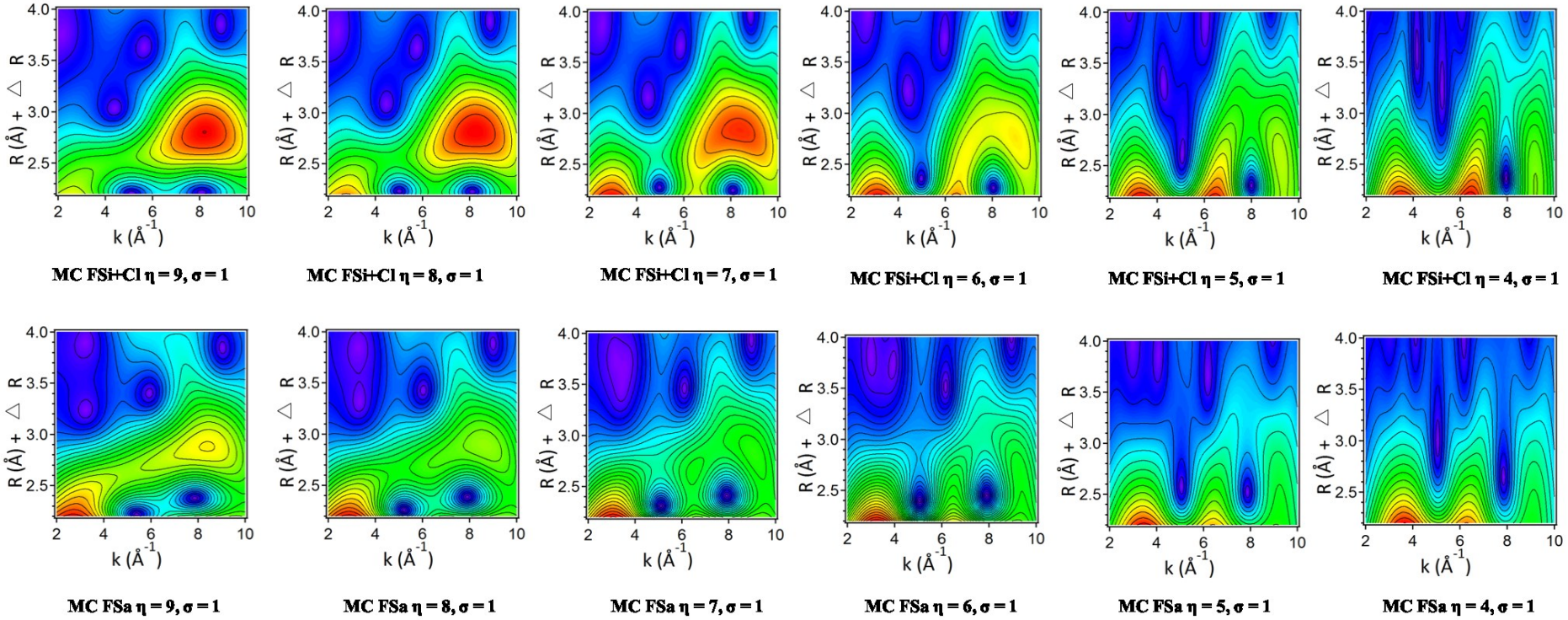

Figure C.6 (continues)

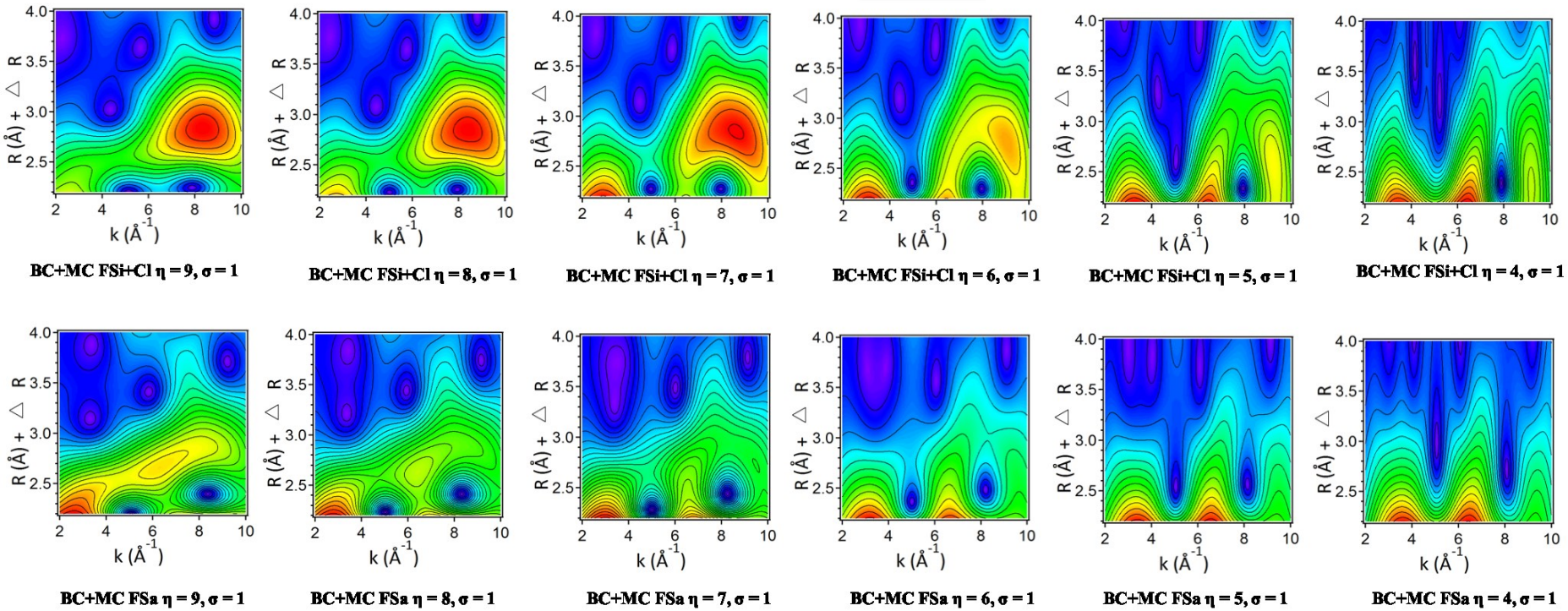

Figure C.6 (continues)

Acknowledgments

The collaboration, support, encouragement of many great scientists made this Ph.D. possible, enriching my doctoral experience.

I would like to express my gratitude to my advisor, Prof. Costantino Vischetti, for giving me the opportunity to earn my Ph.D. in Soil Chemistry and for being a supporter of my independent thinking, my co-advisor Dr. César Plaza (CSIC ICA, Madrid), for hosting me in his research group, for providing the resources, generosity and support to carry out this research, and Prof. Claudio Zaccone (University of Foggia) for contributing his ideas, time, encouragement and propositive behavior, and for showing, also in this step of my career, a genuine interest in my success. You are great mentors!

I would like to acknowledge "Fondazione Cariverona" for providing the fellowship that supported me during my Ph.D. studies and the "Servizio Suoli Regione Marche" for the help in field sites selection and sampling.

I have had the opportunity and pleasure to work in different research groups, in Europe and in USA and I would like to thank all the collaborators that helped me in collecting, understanding, and interpreting my data. I would like to thank Dr. Ester López-de-Sá and all the Dr. Plaza's group (CSIC ICA, Madrid) for the great help during the physical fractionation lab activities, and I express sincere gratitude to Dr. Pere Rovira (CTFC, Solsona) for hosting me in his research group, for his valuable advice and enlightening discussions.

A significant part of my research has been conducted at University of Delaware. I owe so much to Prof. Donald L. Sparks for his guidance and leadership during my stay at UD. I sincerely thank Prof. Matt Siebecker for his patience, help, and willingness to share his knowledge about XAFS data collection and interpretation. Additionally, I appreciate the helpful work of Jerry Hendricks, Karen Rodalunas, Jerry Poirier, Caroline Golt and the UD Soil Testing Lab. I thank all the Environmental Soil Chemistry group members at UD, for their scientific feedbacks and for their friendship.

I am particularly grateful to Dr. Giuliana Aquilanti and all the staff members of the XAFS beamline at Elettra Sincrotrone Trieste for providing guidance and support during the beamtrips.

I am grateful for the use of DOE national labs in USA: Stanford Synchrotron Radiation Lightsource (SSRL) and Brookhaven National Lab.

I owe thanks to Prof. Alain Plante (University of Pennsylvania), Dr. Daniel Said Pullicino and Dr. Ramona Balint (University of Torino) for the help and support while performing experiments at their laboratories during the final steps of my Ph.D. program.

Finally, I am thankful to Soil, for being the Foundation of Life…